MOLECULAR MECHANISMS OF NUCLEAR HORMONE RECEPTOR TRANSCRIPTIONAL SYNERGY AND AUTOINDUCTION

by

Pia D. Bagamasbad

A dissertation submitted in partial fulfillment
of the requirements for the degree of
Doctor of Philosophy
(Molecular, Cellular and Developmental Biology)
in the University of Michigan
2012

Doctoral Committee:

Professor Robert J. Denver, Chair
Professor Kenneth M. Cadigan
Professor Cunming Duan
Professor Audrey F. Seasholtz

To my father whose last wish was for me to pursue and finish my doctoral degree

To my mother for her endless, unconditional love and support, and for teaching me the value of a good education and hardwork

ACKNOWLEDGEMENTS

I would like to thank my thesis advisor Dr. Robert J. Denver for his guidance, support and patience, not only in science but also through the personal obstacles that I have encountered through graduate school. He has been an excellent mentor and has greatly influenced my scientific growth and outlook.

I thank my committee members, Dr. Kenneth Cadigan, Dr. Cunming Duan and Dr. Audrey Seasholtz for their insight and guidance. Their expertise in the different disciplines of biology was of significant importance in shaping my dissertation research.

I thank the MCDB administrative staff, particularly Mary Carr and Kelly Campbell, for consistently helping me out with administrative paper works and concerns.

I am grateful for the funding support provided by the Rackham Predoctoral Fellowship and the Edwin H. Edwards Scholarship given by the Department of Molecular, Cellular and Developmental Biology.

I am lucky to have worked with people like Chris, Yoshi, Melissa, Joe and Rose who are always willing to help in experiments and have provided an intellectually stimulating and friendly lab environment. I am also grateful to Keith Williamson for his guidance in experimental techniques, and to Fang Hu and Ron Bonett for their contributions in my dissertation research.

I thank Gizem Kalay, Anita Guidea and Karishma Collete for the friendship and emotional support through the past seven years

I am grateful to Roche de Guzman for encouraging me to pursue my doctoral studies; Katrina Mae Carbreros and Ian Dinar Cuenco for the friendship and laughter; Papa family, Ng family, Ninna Yuson, Robert Diaz and especially Jomart and Gianna Rodriguez, Jeffrey Wesolowski and Gari Romano Vargas for the emotional support through the final stages of graduate school and for the sense of family they have provided for me in Ann Arbor.

I would also like to thank Peng Ponce, Maya Medalla, Andre Ochoa, Angel Prudente, Notnot Gonzales and Frank Montano for the fun conversations, encouragement and friendship they provided through time and distance.

Lastly, I thank Chito Fulgencio for his love, patience, understanding, and for being a source of inspiration.

TABLE OF CONTENTS

LIST OF TABLES

LIST OF FIGURES

LIST OF APPENDICES

APPENDIX

A. Supplemental Methods, Tables and Figures for Chapter 2

B. Supplemental Figures for Chapter 3

C. Supplemental Tables for Chapter 4

D. Supplemental Table for Chapter 5

ABSTRACT

Thyroid hormone (TH) and glucocorticoid (GC) play critical roles in animal development and physiology, particularly the development and function of the central nervous system (CNS). These hormones exert their actions by binding to nuclear hormone receptors (NRs) that function as ligand-activated transcription factors. Cooperative, synergistic gene regulation by NRs is an important mechanism to amplify gene expression cascades initiated by hormones during animal development. A good example of synergy between TH and GC in development is the acceleration of tadpole metamorphosis caused by the synergistic actions of these two hormones. In my dissertation work I studied the regulation by TH and GC of Krüppel like factor 9 (*Klf9*/Basic Transcription Element Binding Protein 1; *Bteb1*), a transcription factor expressed in the CNS that plays an important role in neuronal development and plasticity. The protein product of the *Klf9* gene is a member of the Sp1/KLF family of zinc finger transcription factors that bind to short genomic sequences that are rich in guanine and cytosine nucleotides. In prior work *Klf9* was found to be a direct TH receptor (TR) target gene. I showed that *Klf9* is also directly targeted by the GC receptor (GR), and that together TH and GCs cause synergistic induction of *Klf9*. I also found that this form of regulation is phylogenetically ancient; that it was likely present in the earliest tetrapods and has been evolutionarily conserved from frogs to mammals. I identified a genomic region in the 5' flanking region of the *Klf9* gene that confers synergistic gene regulation

by TH and GC (I named this region the '*Klf9* synergy module'). The *Klf9* synergy module contains five hexanucleotide NR binding sites, three of which form a composite TR/GR response element required for synergistic gene activation. The synergistic effect of TH and GC on *Klf9* is explained, in part, by a TR-dependent increase in the recruitment of the GR and enhanced association of stalled RNA polymerase II at the *Klf9* synergy module, and an interaction between the synergy module and the *Klf9* promoter by chromosomal looping. I also conducted a genome-wide microarray analysis to identify genes that are synergistically regulated by TH and GC in mouse hippocampus-derived neurons. This is the first study to investigate transcriptional targets that are coordinately regulated by TH and GC in the brain.

Lastly, my work demonstrated a role for KLF9 in regulating expression of TRβ during tadpole development. I found that KLF9 acts as an accessory transcription factor to support TH-dependent expression of TRβ (autoinduction), a gene regulation process that is necessary for the progression of amphibian metamorphosis, and normal mammalian brain development. Given the synergistic regulation of the *Klf9* gene by TR and GR, and its role in TRβ autoinduction, my findings support that KLF9 is an important intermediate that functions to integrate TH and GC actions, in part by enhancing the sensitivity of a cell to hormonal signals. Taken together, my thesis broadens our understanding of the molecular mechanisms of NR cooperativity and autoinduction, with important implications for animal development.

Chapter 1

INTRODUCTION TO THESIS

1. Introduction

Thyroid and steroid hormones are powerful signaling molecules that play crucial roles in animal development, particularly development of the nervous system. One of the first discovered developmental actions of thyroid hormone (TH) was its role in controlling amphibian metamorphosis. Thyroid hormone has been shown to play a role in the development of all chordates that have been studied thus far. In the developing brain, TH shapes neuronal morphology and function, influencing dendritic arborization, neuronal differentiation, cell migration, cell proliferation, myelination, and synaptogenesis (Rami, Patel et al. 1986; Rami, Rabie et al. 1986; Gould, Allan et al. 1990; Rami and Rabie 1990; Madeira and Paula-Barbosa 1993; Gilbert and Paczkowski 2003). Lack of TH during critical periods of early human development leads to a condition of severe mental and growth retardation known as cretinism (Porterfield and Hendrich 1993).

A version of parts of this chapter was published in Bagamasbad, P. and R.J. Denver, *Mechanisms and significance of nuclear receptor auto- and cross-regulation.* Gen Comp Endocrinol, 2011. **170**(1): p. 3-17.

Glucocorticoids (GCs) are steroid hormones produced in response to stress. Glucocorticoids play central roles in an organism's survival, and in physiological and behavioral responses to stress. Stress hormones can either accelerate or retard development depending on the developmental stage at which they become elevated, and are known to be important for determining the timing of birth, and hatching and metamorphosis in diverse vertebrate species (Amiel-Tison, Cabrol et al. 2004; Crespi and Denver 2005; Denver 2009). The brain is a primary target of GCs during development, where they alter neuronal morphology and function, and strongly impact learning and memory in adults (McEwen 2008). In juveniles and adults, stress hormones can have both positive and negative effects on the brain depending on the type and context of the stressor (Joels 2008). Chronic stress leads to atrophy of neurons and impairs performance in cognitive tasks, while acute stress may enhance memory consolidation and reconsolidation (Watanabe, Gould et al. 1992; Roozendaal and McGaugh 1996; Roozendaal, Portillo-Marquez et al. 1996; Magarinos, Verdugo et al. 1997; Magarinos, Orchinik et al. 1998; McEwen 1999; Shors 2001; Shors, Chua et al. 2001; Beylin and Shors 2003).

Glucocorticoids and TH exert their actions on animal development by binding to their cognate nuclear hormone receptors (NR) which function as ligand-activated transcription factors to induce gene regulation programs. A gene that we found to be a common target of GC (GR) and TH (TR) receptor is *Krüppel-like factor 9* (*Klf9*; a.k.a. *basic transcription element binding protein 1* - *Bteb1*) ((Denver, Ouellet et al. 1999; Hoopfer, Huang et al. 2002; Bonett, Hu et al. 2009), Chapter 2). Krüppel-like factor 9 functions in

neuronal process formation in the developing frog and rodent brain, and may integrate GC and TH-dependent signaling pathways to influence neuronal morphogenesis (Denver, Ouellet et al. 1999; Cayrou, Denver et al. 2002; Morita, Kobayashi et al. 2003; Bonett, Hu et al. 2009; Scobie, Hall et al. 2009).

The following thesis introduction focuses on the molecular mechanisms of NR action in animal development and physiology. Emphasis is placed on the modulation of GC and TH signaling through autoregulation of their cognate NRs, and cooperativity between NRs and other constitutively active transcription factors in the regulation of common target genes. Portions that focus on NR autoregulation have been published as part of a review paper by Bagamasbad and Denver, 2011 (Bagamasbad and Denver 2011).

2. Nuclear Hormone Receptor Superfamily

The NR superfamily can be divided into two types based on evolutionary relatedness, cellular localization and receptor function. Type I NRs include the steroid hormone receptors: androgen (AR), estrogen (ER), GR, mineralocorticoid (MR) and progesterone (PR) receptor. In the unliganded form, type I NRs are localized to the cytoplasm associated with molecular chaperones (e.g., heat shock proteins- HSP90, 70, 40) that keep the receptors in an inactive but ligand-binding conformation. Upon hormone binding, type I NRs change conformation and are released from the chaperone complex. They then associate with co-chaperones (FKBP52, PP5) that facilitate translocation to the nucleus (Pratt, Galigniana et al. 2004) where they associate with DNA at hormone response elements (HRE) (Fig. 1.1A) (Mangelsdorf, Thummel et al. 1995; Germain, Staels et al. 2006). Type II NRs include TR, Vitamin D (VDR), retinoic acid (RAR),

peroxisome proliferator-activated (PPAR) and retinoid X (RXR) receptor. In contrast to type I NRs, type II NRs are located in the nucleus constitutively bound to DNA, and they usually act as transcriptional repressors in the absence of hormone (Fig. 1.1B). There are other types of NRs called orphan nuclear receptors since only candidate ligands or no ligands have been identified thus far (Mangelsdorf, Thummel et al. 1995; Ribeiro, Kushner et al. 1995; Aranda and Pascual 2001; Germain, Staels et al. 2006)) .

All NRs exhibit a modular structure composed of different functional domains. A typical NR has six functional domains, designated A-F from the amino to the carboxy end of the protein (Fig.1.2). The A/B domain is highly variable in sequence and size, and has both ligand- dependent and independent activation function (AF-1). The C domain is the DNA binding domain (DBD) composed of two highly conserved zinc finger motifs that enables the NRs to bind to HREs. The D domain is highly variable among NRs and functions as a hinge between the DBD and ligand binding domain (LBD). The LBD is located in the E domain which is also responsible for NR dimerization, ligand- dependent transactivation function (AF-2) and association with heat-shock proteins (for Type I NRs) (Germain, Staels et al. 2006). The AF-2 domain of NRs is responsible for interaction with coactivators that have a NR box (LXXLL motif, where X is any amino acid). Domain F, which is highly variable, has yet unknown functions and is not present in some NRs such as PR, PPAR, RAR and RXR.

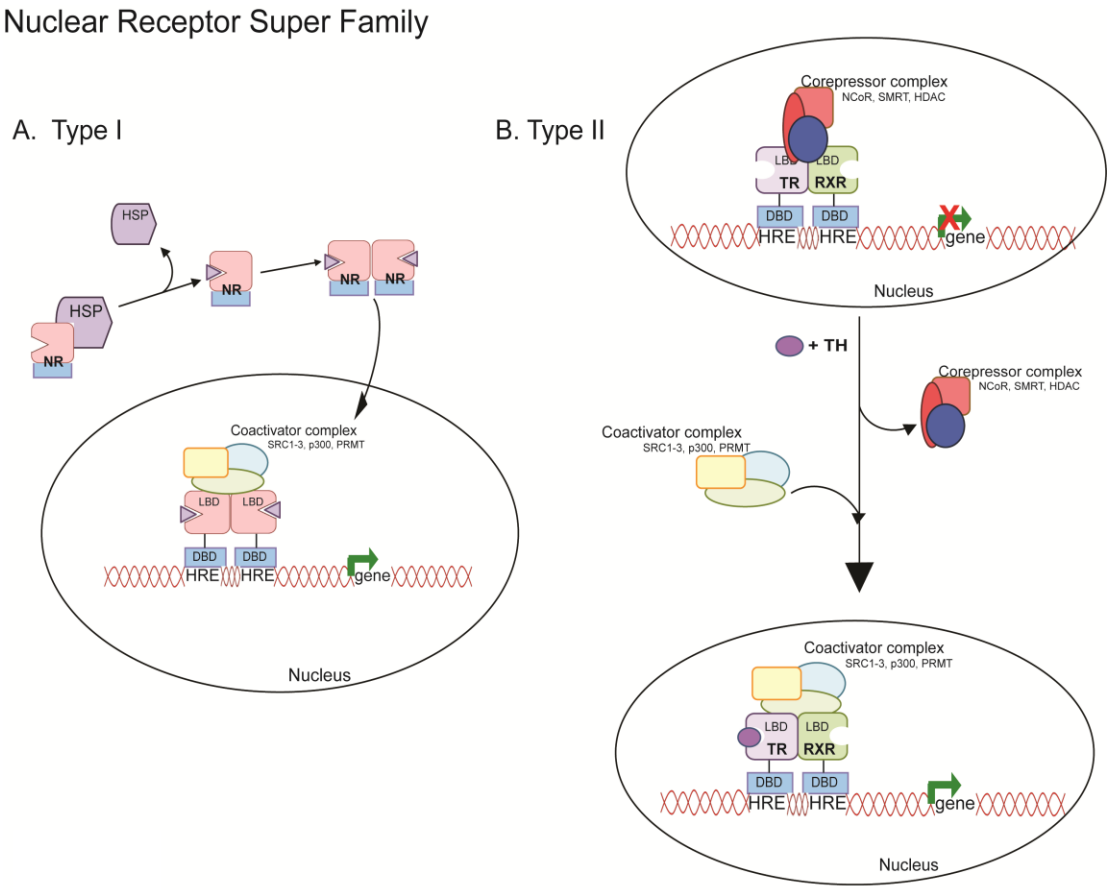

Fig.1.1. Nuclear hormone receptor superfamily. **(A)** Type I NRs include the steroid hormone receptors: androgen (AR), estrogen (ER), glucocorticoid (GR), mineralocorticoid (MR) and progesterone (PR) receptor. In the unliganded form, type I NRs are localized to the cytoplasm associated with molecular chaperones (e.g., heat shock proteins- HSP90, 70, 40) that keep the receptors in an inactive but ligand-binding conformation. Ligand binding induces allosteric changes that allow the Type I NRs to translocate into the nucleus and recognize specific hormone response elements (HREs) of their target genes. **(B)**Type II NRs include thyroid hormone (TR), Vitamin D (VDR), retinoic acid RAR), peroxisome proliferator-activated (PPAR) and retinoid X (RXR) receptor. Type II NRs are bound to DNA in the unliganded state and undergo an exchange in association of coregulators upon hormone binding. The ligand bound NRs recruit coactivators, some of which possess enzymatic activities to modify chromatin architecture to promote a transcriptionally active environment.

3. Transcriptional Regulation by Nuclear Hormone Receptors

Nuclear hormone receptors regulate gene transcription by directly binding to DNA or by protein-protein interactions, with direct DNA binding as a more common mechanism of gene targeting. The NRs activate gene regulation programs that include primary, secondary and tertiary responses. These responses are distinguished by the kinetics of gene regulation, with early responses generally representing direct regulation of a target gene by the NR. Secondary and tertiary responses are mostly due to the protein products of the primary response genes, many of which are transcription factors (TFs).

Transcriptional regulation by NRs is a multistep process that begins with binding of the hormone to its cognate NR. For Type I NRs, ligand binding induces allosteric changes that exposes the nuclear localization signal and allows the NR to translocate into the nucleus and recognize specific DNA sequences in target genes. In contrast, Type II NRs are bound to DNA in the unliganded state and undergo an exchange in association of coregulators upon hormone binding. The ligand bound NRs recruit coactivators, some of which possess enzymatic activities to modify chromatin architecture to promote a transcriptionally active environment. This ultimately results in the recruitment of RNA polymerase II (Pol II) and the general transcription factors (Roeder 2005; Wolf, Heitzer et al. 2008).

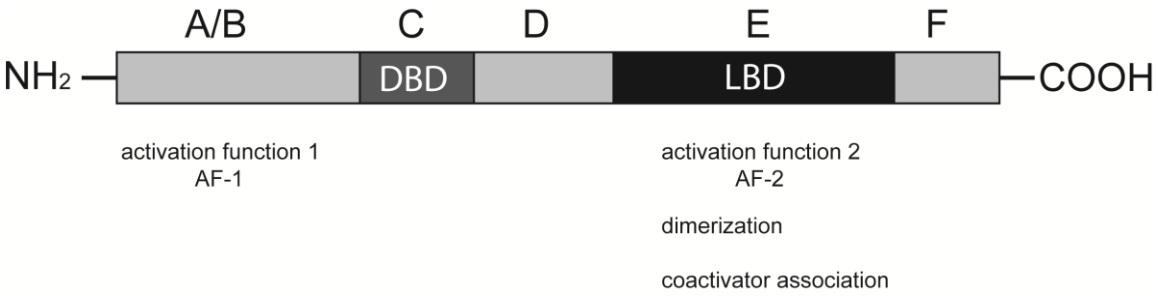

Fig 1.2. Nuclear hormone receptor functional domains . The A/B domain is highly variable in sequence and size and has both ligand dependent and independent activation function (AF-1). The C domain is the DNA binding domain (DBD) composed of two highly conserved zinc finger motifs that enables the NRs to bind to HREs. The D domain is highly variable among NRs and functions as a hinge between the DBD and ligand binding domain (LBD). The E domain is the LBD that mediates ligand binding, NR dimerization, transactivation function (AF-2) and association with heat-shock proteins (for Type I NRs) (Germain, Staels et al. 2006). The AF-2 domain of NRs is responsible for interaction with coactivators that have a NR box (LXXLL motif, where X is any amino acid). Domain F is highly variable, has yet unknown functions and is not present in some NRs such as PR, PPAR, RAR and RXR

3.1 Nuclear Hormone Receptor-DNA Interaction

Nuclear receptors bind as dimers to HREs of target genes which are composed of two hexanucleotide half sites separated by short spacers. Although more attention has been given to HREs that promote transcription upon ligand-NR activation, there are also well characterized negative HREs that repress transcription when associated with ligand-bound NR (Santos, Fairall et al. 2011). Hormone responsive elements are identified according to their sequence motif, orientation and length of spacer between half sites. Type I NRs mainly function as homodimers that recognize degenerate HREs with palindromic half sites separated by three nucleotide spacers. The GR, MR, AR and PR bind to half sites with the consensus sequence 5'AGGACA 3' while the ER recognizes a consensus sequence of 5'AGGTCA 3'. Type II NRs bind with higher affinity as heterodimers with RXR than as homodimers and recognize HREs of inverted, everted, palindromic and direct repeat (DR) half sites of 5'AGGTCA 3' separated by 1-5 nucleotide spacers (DR+ 1-5 repeats) (Mangelsdorf, Thummel et al. 1995). The length of the spacer between these DRs is an important determinant of which Type II NR is bound. For example, TR-RXR heterodimers preferentially bind DR+4 repeats (Naar, Boutin et al. 1991; Umesono, Murakami et al. 1991).

3.2 Transcriptional Activation by Nuclear Hormone Receptors

The NRs influence gene transcription by first binding NR target genes, then interacting with nuclear proteins leading to the recruitment of coregulators that promote posttranslational modifications of chromatin. Nuclear receptor coactivators can be classified into three general classes: histone modifying enzymes (e.g histone

acetyltransferases - HATs; histone methyltransferases - HMT; ATP-dependent chromatin remodelers - SWI/SNF family) and complexes that interact with the basal transcription machinery (Mediator complex, TRAP/DRIP) (Aranda and Pascual 2001).

3.2.1 Histone Modifying Coactivators.

The best characterized HAT coactivators, and the first to be recruited upon hormone binding of Type I and II NRs are members of the p160 family (Vo and Goodman 2001; McKenna and O'Malley 2002). Members of this protein family include the steroid receptor coactivator 1 (SRC-1), SRC-2 (also known as transcriptional mediator/intermediary factor 2 - TIF2) (Voegel, Heine et al. 1996) or GR interacting protein 1 (GRIP1 (Hong, Kohli et al. 1997)), SRC-3 (also known as receptor-associated coactivator 3 - RAC3) (Li, Gomes et al. 1997), ACTR (Chen, Lin et al. 1997), p300/CBP interacting protein (pCIP, (Torchia, Rose et al. 1997)) and TH receptor activator molecule (TRAM-1, (Takeshita, Cardona et al. 1997)). The p160 proteins interact with the ligand-bound NR LBD through a highly conserved LXXLL motif (NR box, where X is any amino acid) located within the NR interacting domain (RID) of the p160 proteins. The SRCs also have a highly conserved activation domain 1 that binds p300/CBP. Another conserved activation domain 2 has been shown to interact with the HMTs, coactivator associated arginine methyltransferase 1 (CARM1, (Koh, Chen et al. 2001)) and protein arginine methyltransferase (PRMT 1,(Bedford 2007)). SRC-1 and SRC-3 have also been shown to possess an intrinsic HAT activity (York and O'Malley 2010). SRC-1 may associate with the basal transcription machinery through TFIIB and TATA-binding protein (TBP) to promote transcription (Robyr, Wolffe et al. 2000).

Apart from the intrinsic HAT activity of some coactivators, a primary role for SRCs is to recruit other HATs, primarily p300/CBP and p300/CBP associated factor (PCAF) to hormone regulated genes. Both p300/CBP and PCAF have also been shown to directly interact with NRs in a ligand-dependent manner (Chakravarti, LaMorte et al. 1996). The HAT activity of these coactivators acetylates lysines in histone tails to neutralize their charge and weaken histone-DNA interactions leading to chromatin decompaction and greater accessibility of DNA sequences to other transcription factors and RNA Polymerase II (Grunstein 1997; Kurdistani and Grunstein 2003).

In addition to promoting histone acetylation, the SRCs recruit and interact with the HMTs, CARM1 and PRMT1. These HMTs catalyze the transfer of methyl group(s) from a methyl donor (S-andenosyl-L methionine) to arginine or lysine residues of histone 3 (H3) or 4 (H4). However, unlike histone acetylation that is associated with transcriptional activation, histone methylation can lead to activation or repression depending on which histone residues are methylated. For example, PRMT1- and CARM1-mediated methylation of H3 at arginine 2, 17 and 26, and lysine 4, 36 and 79 correlates with transcriptional activation; whereas, methylation of H3 at lysine 9 (dimethylation) or 27 (trimethylation) correlates with repression of transcription (Wu and Zhang 2009). The precise mechanisms by which histone methylation regulates NR-dependent transcription are poorly understood. One proposed mechanism was recently discovered in *Xenopus* where PRMT1 was found to be a coactivator for liganded TR that functions in enhancing TR binding, transcription of TR target genes and TH dependent- metamorphosis (Matsuda, Paul et al. 2009). Studies conducted *in vitro* showed that histone methylation promotes NR-dependent transcription through recruitment of p300 and subsequent H4

acetylation (Wang, Huang et al. 2001). Another study found CARM1 to be associated with the nucleosomal methylation activator complex (NUMAC) that includes the ATP-dependent chromatin remodeler BRG1 (Xu, Cho et al. 2004).

3.2.2 ATP-dependent Chromatin Remodeling Complex.

In addition to histone modifying enzymes, the SWI/SNF family of ATP-dependent remodeling complexes have been shown to be necessary for, and to promote NR-dependent transactivation (Trotter and Archer 2007). The vertebrate SWI/SNF complex is a multiprotein complex that uses energy derived from ATP hydrolysis to disrupt DNA-histone interactions, thereby promoting nucleosome eviction and disassembly, and enhanced transcription. The SWI/SNF complex includes a DNA-dependent ATPase called Brahma (BRM) or Brahma-related gene 1 (BRG-1) and its associated factors (BAFS) (Nie, Xue et al. 2000; Eberharter and Becker 2004). The role of BRG-1 in steroid-mediated transcription was established using the steroid responsive mouse mammary tumor virus (MMTV) promoter and the GR (Archer, Lefebvre et al. 1992). The MMTV promoter is a widely used model for steroid-dependent chromatin remodeling since, when integrated into chromatin, it acquires a highly organized structure where the long terminal repeats of the promoter are arranged into an array of 6 nucleosomes (A-F) (Richard-Foy and Hager 1987). Nucleosome A-B contains multiple GREs and binding sites for other transcription factors (e.g., nuclear factor-1 - NF-1, octamer transcription factor - OTF, TATA box binding protein - TBP) (Richard-Foy and Hager 1987; Archer, Lefebvre et al. 1992). Studies have shown the requirement for BRG-1 in GR-mediated remodeling of the MMTV promoter, and also for native promoters, such as the *11β hydroxysteroid dehydrogenase* promoter which is regulated by GCs and has binding sites

for the GR (Trotter and Archer 2004). BRG-1 was also found to play a role in AR, TR and PR-mediated chromatin remodeling of the MMTV promoter (Fryer and Archer 1998; Fryer, Nordeen et al. 1998; Huang, Li et al. 2003), and for ER-mediated transcriptional activity of a *vitellogenin* promoter containing an estrogen response element (Chiba, Muramatsu et al. 1994; Kinyamu and Archer 2004; Trotter and Archer 2007).

The SWI/SNF complex is also important for gene regulation by Type II NRs. For example in frogs, BRG-1 expression is increased during metamorphic climax and, together with its associated factor BAF57 was shown to enhance transcription of liganded TRs (Heimeier, Hsia et al. 2008). The SWI/SNF complex has also been shown to be necessary for RAR/RXR and VDR/RXR-dependent transcriptional activation (Trotter and Archer 2007).

3.2.3 Mediator Complex.

The final step in NR-mediated transcriptional activation is the recruitment of Pol II and the general transcription factors to form the preinitiation complex (PIC) at gene promoters. In NR-regulated genes, recruitment of Pol II depends on a protein complex known as the TR associated protein (TRAP) complex (also known as the SRB- and MED-containing cofactor complex - SMCCcomplex) (Ito, Yuan et al. 1999). The TRAP complex is a large multisubunit complex initially found to associate with TR at TH response element (T_3RE) in a ligand-dependent manner, and functions to enhance TR-dependent transcription (Fondell, Ge et al. 1996; Fondell, Guermah et al. 1999). A second TRAP-related complex was later identified to function with the VDR and was named the VDR-interacting complex (DRIP) (Rachez, Lemon et al. 1999). Both the TRAP and DRIP complexes are homologous to the yeast Mediator complex that is

known to directly recruit and interact with Pol II at gene promoters (Fig1.3; (Myers and Kornberg 2000)). In addition to being necessary for TR and VDR function, the TRAP/DRIP complexes have been shown to interact with RXR, PPARs, ER and GR in a ligand-dependent manner to enhance NR mediated transcription(Yuan, Ito et al. 1998; Hittelman, Burakov et al. 1999; Llopis, Westin et al. 2000; Chen and Roeder 2007). Among the many proteins that make up the TRAP complex, a 220 kDa subunit (TRAP220/DRIP205/MED1) contains two LXXLL motifs that directly associate with the AF2 domain of NRs in ligand-dependent manner. The physiological significance of the TRAP220/MED1 during development was shown in the TRAP220/MED1 knockout mouse that only survives until PND 11.5 and displays defects in NR mediated pathways (Ito, Yuan et al. 2000). The association of the TRAP/DRIP complexes with NRs is hypothesized to occur after the ligand-dependent recruitment of SRCs, p300/CBP and PCAF, and thus constitutes a final step in NR-mediated transcriptional activation (Fig. 1.3) (Ito and Roeder 2001).

Earlier studies in yeast showed that the Mediator complex is mostly recruited to gene promoters (Malik and Roeder 2010). More recent functional analyses conducted in mouse embryonic stem cells and fibroblasts from TRAP220/MED1 knockout mice demonstrate that the Mediator complex (i.e TRAP220/MED1 in TR dependent gene expression) plays a role in linking NR bound enhancers to gene promoters through chromosomal looping (Park, Li et al. 2005; Kagey, Newman et al. 2010).

3.3 Transcriptional Repression by Nuclear Hormone Receptors

Type II NRs are constitutively bound to HREs of target genes. In the absence of ligand, Type II NRs repress gene transcription by recruiting co-repressors. Type II NRs

can also regulate gene transcription in a ligand-dependent manner, although this is less common (discussed below). Therefore, Type II NRs have a dual function in that they repress or activate gene transcription in the absence or presence of ligand, respectively. Nuclear hormone receptor co-repressors, that were originally identified to interact with Type II NRs but have since been shown to also participate in type I NR function include the nuclear receptor corepressor (NCoR) and the silencing mediator of retinoic acid and TH receptor (SMRT). These proteins interact with NRs and recruit histone deacetylases (HDACs) that catalyze the deacetylation of lysine residues in histone tails, thereby promoting a compact chromatin structure that represses transcription (Germain, Staels et al. 2006)

A dual function model for Type II NRs, where the NR functions to repress or activate gene transcription during different developmental periods, was first proposed for TR actions in *Xenopus* and is hypothesized to play an important role in controlling tadpole metamorphosis. In this model, the unliganded TR represses expression of adult genes in the tadpole prior to the onset of metamorphosis, at which time TH production increases to activate gene regulation programs that drive organogenesis and tissue remodeling (Shi 2009). The repressor function of unliganded TR and its significance during developmental transitions is also observed in mice, where TRα was found to repress the expression of genes involved in controlling heart function during fetal development when TH levels are low. At birth and during early postnatal life when TH levels start to increase, TRα loses its repressive functions and activates the expression of some of the previously repressed genes in parallel with stimulation of heart rate, suggesting that TRα

may act as a molecular switch in controlling the development of the heart at or around the time of birth (Mai, Janier et al. 2004).

Type I and type II NRs can also repress transcription in a ligand-dependent manner. This can occur through direct binding of the NR to negative HREs (nHRE). For example, repression of the prolactin (PRL) gene by ligand-bound GR depends on a negative GRE (nGRE) in the PRL promoter (Sakai, Helms et al. 1988). Ligand-bound TR has also been shown to downregulate the expression of thyroid stimulating hormone α (TSHα) and beta subunit (TSHβ) through negative T_3REs located in the proximal promoters of these genes (Chatterjee, Lee et al. 1989; Wondisford, Farr et al. 1989). Ligand-bound NRs recruited to a nHRE repress transcription through several mechanisms that include competitive binding with other coactivators at the nHRE, or recruitment of corepressors rather than coactivators by the NR when ligand is bound (Santos, Fairall et al. 2011). Transcriptional repression by ligand-bound NRs can also occur independent of DNA binding through protein-protein interactions. For example, ligand-bound GR tethered to the NF-κB or AP1 transcription factors can confer negative regulation by GCs (De Bosscher, Vanden Berghe et al. 2003). Repression by the ligand-bound NR may also occur by squelching, whereby the positive actions of NRs on some genes causes sequestration of the limiting components of the transcriptional machinery, leading to downregulation of other non-NR regulated genes. Ligand-bound NRs can also repress gene transcription as a secondary effect of an upregulation of a repressive TF or corepressor protein (Santos, Fairall et al. 2011).

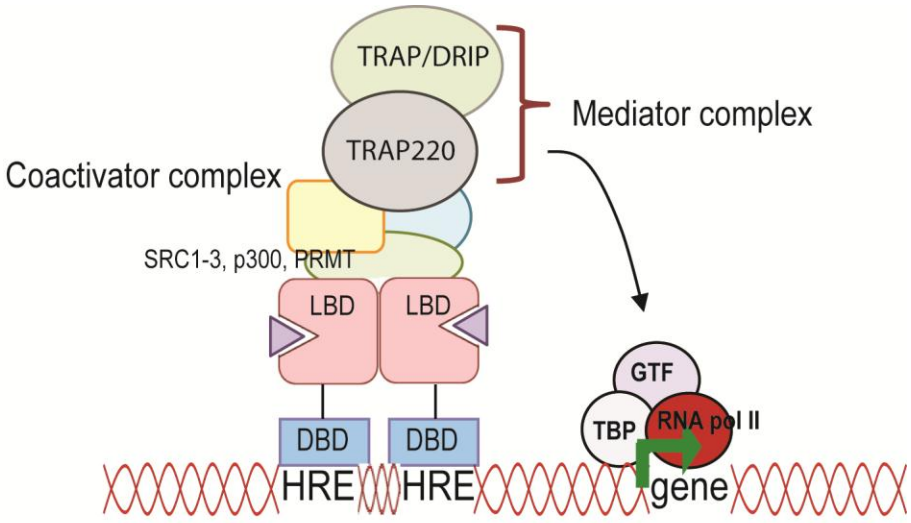

Fig. 1.3. TRAP/DRIP/ Mediator complex. The large multi subunit TR associated protein (TRAP)/ VDR-interacting complex (DRIP) complex (also known as the SRB- and MED-containing cofactor (SMCC)) is recruited to ligand- activated NR coactivator complex. Both the TRAP and DRIP complexes are homologous to the yeast Mediator complex that is known to directly recruit and interact with general transcription factors (GTF) and RNA Pol II at gene promoters. The association of the TRAP/DRIP complexes with NRs is hypothesized to occur after the ligand-dependent recruitment of SRCs, p300/CBP and PCAF, and constitutes a final step in NR-mediated transcriptional activation.

3.4 Other Modes of Transcriptional Regulation

In addition to directly binding to HREs, NRs can modulate gene transcription through cooperation with other TFs. A well-studied example is the interaction between TR, RAR or GR, and the TFs Fos/Jun at AP-1 binding sites, a highly-conserved enhancer-like element recognized by the Fos and Jun family of TFs (Zhang, Wills et al. 1991; Lopez, Schaufele et al. 1993; Wondisford, Steinfelder et al. 1993; Benkoussa, Brand et al. 2002; De Bosscher, Vanden Berghe et al. 2003; Kassel and Herrlich 2007). Ligand-bound NRs are able to repress AP-1 activity, and reciprocally, AP-1 complexes can act as transrepressors of NR function. Interaction between NRs and other TFs may involve: (1) composite DNA elements that bind both the NR and another TF; (2) overlapping response elements wherein the NR and another TF compete for the same binding site, and (3) protein-protein interactions where the NR directly or indirectly interacts with another TF without binding to DNA. The interaction that occurs between NRs and other TFs can lead to positive or negative gene regulation, and in some cases the actions may be synergistic such that the combined effect of the interacting TFs is greater than the additive effect (Ribeiro, Kushner et al. 1995; Aranda and Pascual 2001; Kassel and Herrlich 2007). The importance of interaction between NRs and other TFs is demonstrated by findings in a GR knock-in mouse where the wild type GR was replaced by a mutant GR incapable of receptor dimerization and DNA binding (Reichardt, Kaestner et al. 1998). Whereas, knocking out the GR was embryonic lethal, the GR dimerization/DNA binding mutant mice were viable, but with defective GC-dependent physiological functions (Reichardt, Kaestner et al. 1998). These findings suggest that the life-sustaining actions of GCs mediated by the GR do not depend on the DNA binding

function of the GR, but instead may reflect an important role for GR interactions with other nuclear proteins.

4. Nongenomic actions of Steroid and Thyroid Hormones

In addition to their nuclear actions, TH and steroid hormones have rapid effects on physiological processes that are too fast to be mediated by classical genomic mechanisms. Rapid signaling by steroid hormones, that occur within seconds to minutes, are mediated by membrane-associated Type I NRs and G-protein coupled receptors that activate several protein kinases (i.e MAPK, phosphotidylinositol 3-kinase [PI3K], and protein kinase C [PKC]), phosphatases, several cyclic amines (cAMP, cGMP) and the release of calcium from cells. The activation of these signaling cascades leads to posttranslational modification of nuclear proteins that include the classical NRs and NR coactivators (Hammes and Levin 2007). Posttranslational modification of NRs and their coactivators may augment the transcriptional function of the nuclear NRs and may account, at least in part, for the rapid hormone effects. Signaling from membrane localized NRs and GPCRs also occurs independent of the transcriptional activity of the nuclear NR (Losel, Falkenstein et al. 2003; Hammes and Levin 2007).

Another mechanism for the rapid effects of TH may be via the αvβ3 integrin plasma membrane receptor which has binding domains for TH. Hormone activated αvβ3 integrin can initiate TH-directed MAPK, PI3K and phospholipase C signaling. The hormone-activated kinase cascade also targets the TR for phosphorylation leading to enhanced transcriptional activity of the nuclear TR. Nongenomic TH actions may also be mediated by the TH-dependent modulation of ion channel function, membrane calcium ATPase

and protein kinase A activation. The TRβ was also detected in the cytoplasm in complex with TH, and has been shown to interact with PI3K signaling proteins leading to downstream gene transcription (Cheng, Leonard et al. 2010).

5. Modulation of Nuclear Hormone Receptor Signaling

Multiple extracellular signals and cellular factors determine whether, and to what extent a cell responds to a hormonal signal. First, the cell must express the NR at a sufficient level to mediate the hormone response. Variation in NR expression levels in part determines the responsiveness of a cell to a hormone. The presence of other hormones, or the degree of activation of other signaling pathways, and crosstalk between these pathways also play crucial roles in determining a cell's response to a hormone. Crosstalk is a general term that refers to one signaling pathway enhancing or opposing the activity of another signaling pathway. Although there are several mechanisms for crosstalk among different hormone signaling pathways (Bagamasbad and Denver 2011), the following section will primarily focus on the physiological significance and molecular mechanisms of three phenomena: (1) how hormones regulate the expression of their own receptor (autoregulation, Fig.1.4; in contrast to one NR regulating the expression of another NR, or cross-regulation; see Fig. 1.5), (2) how a NR cooperates with another NR to regulate a common target gene, and (3) how a NR cooperates with constitutively acting TFs to regulate gene expression. The interactions described in (2) and (3) are commonly referred to as 'cooperativity', and in some cases, these cooperative interactions lead to synergistic transcriptional activation. Transcriptional synergy between TFs can be defined as a greater than additive effect of two or more TFs in gene regulation (Bonett, Hoopfer et al. 2010). In the following section, emphasis will be

placed on mechanisms of signaling by GCs and TH; other hormone systems will be discussed based on their significance for understanding generalizable molecular mechanisms.

5.1 Nuclear Receptor Autoregulation

The regulation of the expression of a NR gene by the liganded NR (autoregulation) is an important means for modulating hormone action in developing animals, within the reproductive system of adult animals, and for maintaining homeostasis. Autoregulation of NR genes can be positive (autoinduction; i.e., homologous upregulation) or negative (autorepression; homologous down-regulation). Autoinduction leads to the biosynthesis of more NRs by the cell, thus enhancing cellular responsiveness to the hormone. Autorepression is a homeostatic mechanism to modulate hormone action by downregulating the receptor for the hormone.

Nuclear hormone receptor autorepression may function as a component of negative autoregulatory feedback loops to maintain homeostasis. For example, the GR is expressed in the brain in limbic structures involved with fear and anxiety (amygdala, bed nucleus of the stria terminalis), and learning and memory (hippocampus), and in neurosecretory neurons that regulate the hypothalamo-pituitary-adrenal (HPA) axis. The GR plays a central role in mediating negative feedback on the HPA axis, but also may facilitate stress-related behaviors through feed-forward actions on limbic structures. A physiological means to limit negative feedback of GCs on the HPA axis once the system has returned to baseline, and to ‘reign-in’ the facilitating effects of GCs on fear and anxiety is to downregulate GR expression in the hypothalamus and limbic structures, respectively. Downregulation of GR expression by GCs has been described in mammals

and in frogs, and may be a more common form of autoregulation of the GR than autoinduction. The GR plays a central role in mediating negative feedback by GCs on the activity of the hypothalamic-pituitary-adrenal (HPA) axis (reviewed by (De Kloet, Vreugdenhil et al. 1998)). It is expressed in the hypothalamus and limbic structures (e.g., amygdala, bed nucleus of the stria terminalis, hippocampus) of the brain, and in the anterior pituitary gland. The GR mediates the negative feedback by GCs on the synthesis and release of corticotropin-releasing factor (CRF) from the hypothalamus and adrenocorticotropic hormone (ACTH) from the anterior pituitary gland (reviewed by (Yao, Hu et al. 2008; Denver 2009; Denver 2009). Glucocorticoid receptor expressed in these tissues is predominantly negatively regulated by GCs. For example, administration of GCs decreased GR protein and/or mRNA throughout the brain of rats and frogs (Sapolsky, Krey et al. 1984; Reul, Pearce et al. 1989; Holmes, Yau et al. 1995; Chao, Ma et al. 1998; Ghosh, Wood et al. 2000; Spencer, Kalman et al. 2000; Hugin-Flores, Steimer et al. 2004; Han, Ozawa et al. 2007; Yao, Hu et al. 2008). In rats, adrenalectomy increased GR protein in the hippocampus, hypothalamus, and cortex (O'donnell, Francis et al. 1995; Spencer, Kalman et al. 2000; Kalman and Spencer 2002) and GR mRNA in the hippocampus; the latter could be reversed by supplementation with GCs (Tornello, Orti et al. 1982; Reul, Pearce et al. 1989; Okret, Dong et al. 1991; Holmes, Yau et al. 1995; Chao, Ma et al. 1998; Hugin-Flores, Steimer et al. 2004; Han, Ozawa et al. 2007).

Under physiological conditions, NR autoinduction is often observed when positive feedback within the neuroendocrine system increases hormone production, leading to a progressive rise in plasma hormone concentrations. Within hormone target tissues, NR autoinduction generates a feed-forward response that ends when the positive feedback on

hormone production is terminated. For example, during the mammalian ovarian cycle gonadotropins secreted by the pituitary gland stimulate estrogen production by the ovarian follicle, and rising plasma estrogen concentration causes positive feedback on the hypothalamo-pituitary axis. During the mid- to late follicular phase, when plasma estrogen titers increase, estrogen stimulates proliferation of uterine endometrial cells; estrogen action may be facilitated by the autoinduction of the ER in these cells, a feed-forward response. These actions are terminated, and plasma estrogen concentration drops upon ovulation induced by the surge in plasma luteinizing hormone caused by the positive feedback signal of estrogen. Nuclear receptor autoinduction is also seen during animal development where it serves as a feed-forward mechanism to drive the developmental process. The most studied example of this phenomenon is amphibian metamorphosis, where rising plasma TH titers cause autoinduction of TRs in target tissues (Tata 2000).

There are several mechanisms by which NR expression may be autoregulated that can be broadly described as transcriptional or posttranscriptional (Fig. 1.4). At the transcriptional level, regulation can be either direct, where the ligand-bound NR associates with its own gene to positively or negatively regulate transcription, or indirect, where the NR induces expression of a transcription factor(s) that regulates transcription of the NR gene (Fig. 1.4 A,B). Both direct and indirect regulation may also occur, where the NR binds to and regulates expression of its own gene (demonstrated for ER, GR and TR), but full transcriptional regulatory activity depends on the induction of a transcription factor(s) that regulates transcription of the NR gene (cooperative regulation; Fig. 1.4C). At the posttranscriptional level, the NR may induce expression of genes that

influence mRNA stability (i.e ER and GR) or protein stability via degradation (i.e GR) (Fig. 1.4 D,E,F; or perhaps also protein translation or protein bioactivity through posttranslational modifications).

One of the better understood examples of NR autoinduction and its biological significance is the autoinduction of the beta isoform of the TR (TRβ) that occurs during amphibian metamorphosis. The transformation of a tadpole into a frog is dependent on TH, and TH biosynthesis and secretion increases during metamorphosis reaching a peak at metamorphic climax (Denver 2009). The frog *X. laevis*, like all jawed vertebrates studied to date, has two TH receptor subtypes, TRα and TRβ encoded by four genes (TRαA and B, TRβA and B) owing to its pseudotetraploidy (Yaoita, Shi et al. 1990). The mRNAs for TR subtypes are detected at the time of hatching, and expression of TRα increases shortly thereafter to reach peak levels in the tadpole that are sustained through metamorphosis (Shi 2000). By contrast, after hatching TRβ mRNA expression is very low, but then rises in parallel with the elevation in plasma TH that occurs during metamorphosis, reaching a peak at metamorphic climax that coincides with maximal production of TH and a period of rapid tissue transformation (Shi 2000). Autoinduction of TRβ is also seen in *X. laevis* tissue culture cells (i.e XTC-2 and XL177), which has allowed for detailed investigations of response kinetics and molecular mechanisms of gene regulation (Kanamori and Brown 1992; Machuca and Tata 1992).

Fig. 1.4. Molecular mechanisms for regulation of nuclear receptor (NR) expression. The level of functional NRs in a cell can be regulated at transcriptional or posttranscriptional levels, or some combination of the two. **(A)** Direct transcriptional regulation involves the hormone (filled oval)–NR complex (NRA; shown as a homodimer, but type II NRs also function as heterodimers) directly binding to a hormone response element located within the *nra* gene that activates or represses its expression (for cross-regulation the NRA binds to and regulates a different NR gene). Some NRs may influence target genes through hormone response elements that are far upstream or downstream of the regulated locus. Also, some NRs regulate target genes through protein–protein interactions rather than by direct DNA binding. **(B)** Indirect transcriptional regulation involves the hormone–NRA complex inducing the expression of a gene that codes for a transcription factor (TF) that then positively or negatively regulates *nra* gene transcription (for cross-regulation the NRA regulates a TF that binds to and regulate a different NR gene). **(C)** Cooperative transcriptional regulation involves both direct and indirect transcriptional mechanisms shown in parts (A) and (B). **(D)** The NRA may regulate the expression of a gene that increases or decreases stability of the *nra* mRNA (for cross-regulation, the mRNA for a different NR gene). **(E)** Hormone binding to the NRA can stabilize it, thus increasing its half-life ($t_{½}$). **(F)** The NRA may induce expression of a ubiquitin ligase that ubiquitinates (Ub) NRs in the cell (either the NRA or a different NR) and targets it to the proteasome for degradation. NR protein stability and bioactivity may also be influenced through posttranslational modifications (e.g., phosphorylation).

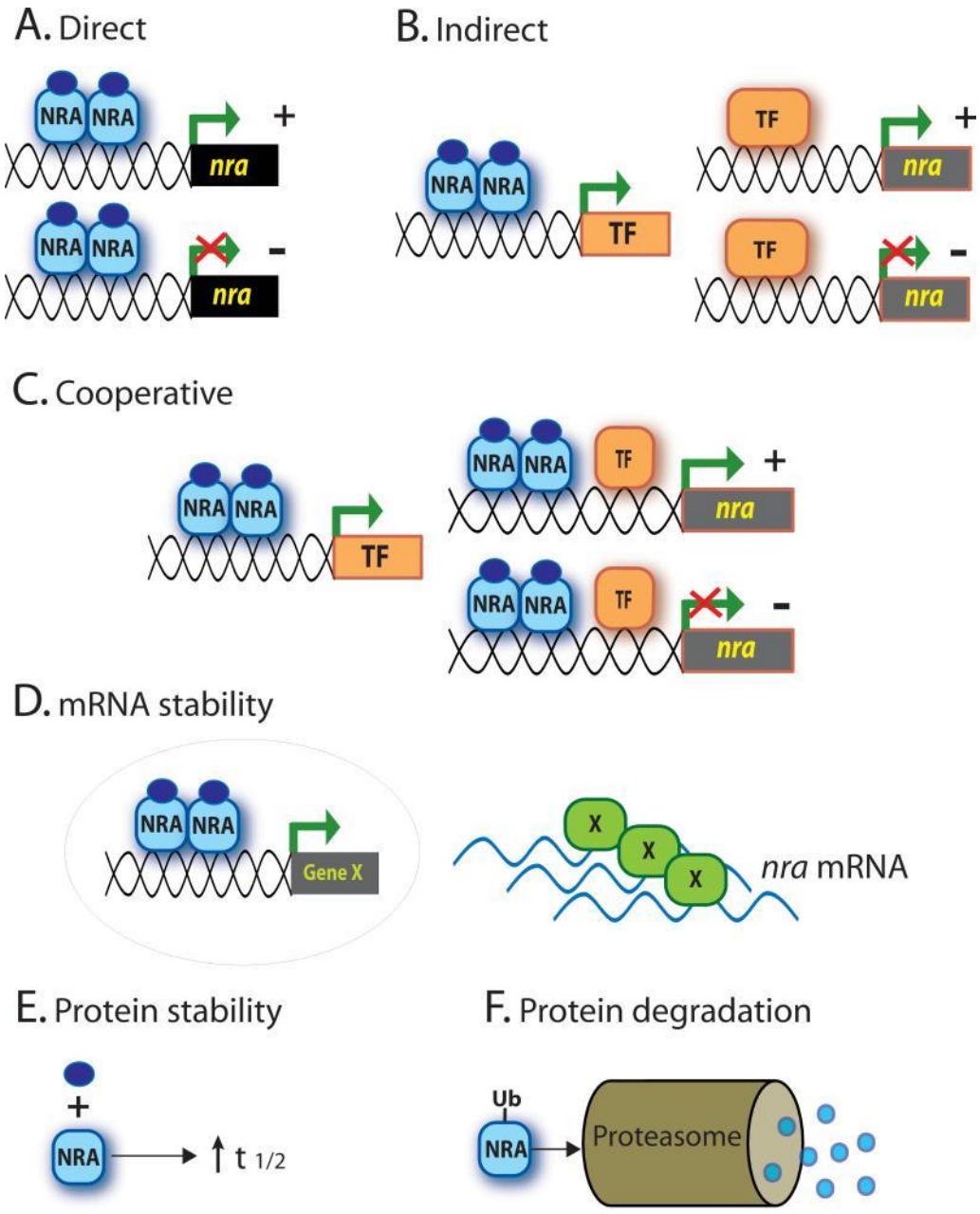
A. Direct
NRA
NRA
nra
+
NRA
NRA
nra
-
B. Indirect
NRA
NRA
TF
TF
nra
+
TF
nra
-
C. Cooperative
NRA
NRA
TF
NRA
NRA
TF
nra
+
NRA
NRA
TF
nra
-
D. mRNA stability
NRA
NRA
Gene X
X
X
X
nra mRNA
E. Protein stability
+
NRA
t 1/2
F. Protein degradation
Ub
NRA
Proteasome

The patterns of TRα and TRβ expression in rat brain parallel those seen in the tadpole during metamorphosis. For example, TRα expression is high and relatively constant throughout late fetal and neonatal periods; whereas, TRβ expression is low at birth and shows a dramatic increase during the first 2 weeks postnatally that is coincident with rising plasma TH concentrations (Strait, Schwartz et al. 1990). The human TRβ promoter has two functional TREs that mediate transactivation in transient transfection assays (Suzuki, Miyamoto et al. 1994) (discussed below), but to our knowledge, the occurrence and significance of TRβ autoinduction during mammalian development has not been investigated.

5.1.1 Molecular Mechanisms of TR Autoregulation.

Autoinduction of TRβ in the tadpole can be explained by the presence of TH response elements (TREs) located in the proximal promoter region of the gene (Ranjan, Wong et al. 1994); Machuca et al., 1995). The proximal TRβA promoter of *X. laevis* contains three putative TREs, two of which are near optimal direct repeat +4 (DR+4) TREs and are located just upstream or proximal to the transcription start site (Ranjan, Wong et al. 1994; Machuca, Esslemont et al. 1995). Transfection assays and mutational analysis have shown that both DR+4 T_3REs support TH-dependent transactivation, and also transrepression in the absence of TH. TR-RXR heterodimers, but not TR or RXR homodimers bound the DR+4 regions in a ligand-dependent manner (Ranjan, Wong et al. 1994; Machuca, Esslemont et al. 1995; Ulisse, Esslemont et al. 1996). The human TRβ gene has two functional T_3REs located in the 5' flanking region that mediate autoinduction in transient transfection assays using the rat pituitary tumor cell line GH3 (Sakurai, Miyamoto et al. 1992; Suzuki, Miyamoto et al. 1994).

Further support for the functionality of the proximal T_3RE in the *X. laevis* TRβA promoter was shown by studies using a promoter-reporter construct transfected into living tadpole tail muscle *in vivo* (Ulisse, Esslemont et al. 1996). Treatment with TH activated transcription of a TRβA promoter-reporter construct containing the proximal DR+4 T_3RE cotransfected with TRβ expression plasmids. This activity was abolished by cotransfection of a mutant TRβ capable of binding DNA but not hormone (Ulisse, Esslemont et al. 1996). Taken together, both *in vitro* and *in vivo* experiments support that the frog TRβA gene is a direct TR target. However, TH induction of TRβ was found to be partially sensitive to protein synthesis inhibition (Kanamori and Brown 1992; Machuca and Tata 1992), suggesting that the synthesis of proteins other than preexisting TRs may be required for full TRβ autoinduction.

Autoinduction of TRβ was originally thought to be the earliest TH response in premetamorphic tadpole tissues (Yaoita and Brown 1990), but it was subsequently discovered, through the use of gene expression screens, that other genes respond to TH more rapidly than TR (Shi 2000). One of the most rapidly responding TH-induced genes in tadpole tissues is the transcription factor Krüppel-like factor 9 (KLF9; also known as basic transcription element binding protein 1; BTEB1). In *X. laevis* tadpole tissues (brain, tail, intestine), *Klf9* is the most rapidly responding TH-induced gene, and its expression parallels the increase in plasma TH that occurs during tadpole metamorphosis (Wang and Brown 1993; Gomez, Lahmame et al. 1996; Denver 1997; Shi 2000; Furlow and Kanamori 2002; Hoopfer, Huang et al. 2002). *In my dissertation work I showed that KLF9 functions as an accessory transcription factor for TRβ autoinduction*

(Bagamasbad, Howdeshell et al. 2008). Evidence for this role, and the molecular mechanisms of KLF9 actions on TRβ autoinduction are described in chapter 5.

5.1.2 Physiological Significance of TR Autoinduction. The discovery that TRβ was autoinduced in tadpole tissues led to the hypothesis that the increase in TRβ is necessary for driving metamorphosis, whereas, the early expression of TRα was necessary to establish tissue competence to respond to the hormone (Tata 2000). There are at least two potential mechanisms by which TRβ autoinduction could function to promote metamorphosis: 1) Receptor autoinduction could cause a general increase in tissue sensitivity to TH, thereby amplifying gene expression responses to TH, or 2) TRα could regulate a set of genes/processes that are distinct from those regulated by TRβ. There are several lines of evidence that support a role for TRα in establishing tissue competence to respond to TH, and in the proliferative actions of the hormone, which are the earliest responses to TH that occur in target tissues. Studies of the temporal and spatial expression of the different TR subtypes, and the use of TR subtype-specific TH analogs support a role for TRα in cell proliferation in the hindlimb and brain. By contrast to TRα, the expression pattern of TRβ is dependent on the rise in plasma TH during metamorphosis, and findings using the TRβ specific TH analogs GC1 and GC24 support the hypothesis that TRβ functions in cell differentiation and apoptosis (reviewed by (Furlow and Neff 2006); (Denver, Hu et al. 2009))

Other lines of evidence support a role for TRβ autoinduction during metamorphosis. For example, treatment with prolactin, which blocked TH-induced tadpole limb bud growth and tail regression, decreased TRβ and completely blocked TRβ autoinduction (Tata, Kawahara et al. 1991; Baker and Tata 1992). These correlative data suggest that

one mechanism by which prolactin blocks metamorphosis is through inhibition of TRβ autoinduction, and therefore that TRβ autoinduction is necessary for tissue transformations.

Obligate paedomorphic salamanders (they attain reproductive maturity while retaining larval characteristics) do not respond to TH by initiating metamorphosis. Safi et al. (Safi, Begue et al. 1997) failed to find evidence for expression of TRβ mRNA in the mudpuppy *Necturus maculosus* using reverse transcriptase polymerase chain reaction, and suggested that this may be the reason that the animals do not respond to TH by metamorphosing. However, this species was found to have genes for both TR subtypes that are expressed in some tissues and code for functional proteins as evidenced by DNA binding, hormone binding, and transactivation of target genes in *in vitro* transfection assays (Safi, Vlaeminck-Guillem et al. 2006). Contrary to the initial report, Safi et al. (Safi, Vlaeminck-Guillem et al. 2006) have since found that both TRs are expressed in different tissues at low levels in *N. maculosus*, but TRβ shows no, or only modest responses to high doses of TH in gill and tail fin, two structures that undergo apoptosis in metamorphosing salamanders but not in *N. maculosus* (Safi, Vlaeminck-Guillem et al. 2006). However, TRβ may be induced in the brain of the mudpuppy where TH responses may have been retained to support neurological development (M. Miller and R.J. Denver, unpublished). Safi and colleagues suggested that loss of metamorphosis in the lineage of salamanders that includes *N. maculosus* may have depended on the loss of TH-dependent control of key genes required for tissue transformation. However, it is also possible that the failure to upregulate TRβ in organs that normally undergo metamorphic

transformation in metamorphosing species (e.g., the gill, tail, etc.) is responsible for the paedomorphic life history.

5.2 Nuclear Receptor Cross-regulation and Cooperativity

In addition to hormones autoregulating the expression of their receptors, the regulation of expression of other NRs (cross-regulation) and NR cooperativity in regulating common target genes are important means for modulating cellular responsiveness to different hormonal signals. Nuclear receptor cross-regulation allows for simultaneous crosstalk between hormonal signaling pathways, or can modulate in a temporal manner the responsiveness of a cell to a subsequent (different) hormonal signal. For example, during amphibian metamorphosis cross-regulation between GR/MR and TR sensitizes tissues to the TH signal, thereby accelerating metamorphosis.

In tadpole tail, corticosteroid treatment accelerated TH-induced tail shrinkage, a measure of metamorphic progression (reviewed by (Denver 2009)). Treatment of tadpole tail explants with corticosteroids increased nuclear binding capacity for TH (Kikuyama, Niki et al. 1983; Suzuki and Kikuyama 1983) and TR mRNAs; similar findings on corticosteroid actions on TR mRNA expression were observed in tadpole tail, intestine and brain *in vivo* (Krain and Denver 2004; Bonett, Hoopfer et al. 2010). These findings suggest that corticosteroids can enhance sensitivity of target tissues to TH by increasing the expression of TRs, thus accelerating metamorphosis. Corticosteroids have also been shown to increase expression of type 2 deiodinase in tadpole tissues, which catalyzes the conversion of thyroxine (T_4) to the more active form T_3 (Galton 1990; Bonett, Hoopfer et al. 2010). This would increase bioavailability of the ligand for TR, and thus facilitate TH action on target tissues.

There is also evidence that TH can regulate GR mRNA in some tadpole tissues. Treatment of tadpoles with T_3 downregulated GR mRNA in brain and intestine, but upregulated it in tail (Krain and Denver 2004; Bonett, Hoopfer et al. 2010). The synergistic actions of TH and corticosteroids on tadpole tail shrinkage may be explained, in part, by the reciprocal positive cross-regulation of TR and GR, which would sensitize the tissue to further hormone action.

The molecular basis for GR (or MR) regulation of TR gene expression has not been investigated. Therefore, it is not known whether this regulation is direct on TR gene transcription, or indirect through induction of other transcription factors, or through effects on mRNA transcript or protein stabilization. We recently found that *Klf9* is a direct GR target gene in frog and mouse brain ((Bonett, Hu et al. 2009); Chapter 2) and that it is synergistically induced by TH plus GC (Chapter 3). *Thus, in addition to GC-mediated increases in TR binding, TR expression and TH bioavailability, GCs may accelerate development through positive cooperativity between GR and TR on common target genes, leading to synergistic gene regulation that serves as a driver for the developmental process.*

In addition to amphibian metamorphosis, there are several examples from the mammalian literature of synergy between NRs and other TFs in the regulation of developmental and physiological processes. For example, synergy between GR and the signal transducer and activator of transcription (STAT) family of proteins is perhaps one of the better studied example of this type of synergy. The STAT proteins are phosphorylation targets for Janus kinases (JAK), which are in turn activated by ligand-bound cytokine receptors. Upon phosphorylation, STATs dimerize and translocate to the

nucleus where they bind to response elements in target genes (Pfitzner, Kliem et al. 2004). The synergy between GR and STAT5 seen in hepatocytes has been shown to play a critical role in GC-mediated postnatal growth and maturation (Tronche, Opherk et al. 2004; Engblom, Kornfeld et al. 2007). The cooperation between GR and cytokine signaling-activated STATs (STAT1-3) was also found to be important in the regulation of the HPA axis in response to infectious or inflammatory stimuli (Latchoumanin, Mynard et al. 2007). Conversely, GC-dependent negative feedback regulation of the HPA axis is also partially controlled by GR acting in synergy with the nuclear receptor steroidogenic factor-1(SF-1) (Gummow, Scheys et al. 2006).

The physiological significance of GR and STAT5 cooperativity is demonstrated in liver cells where GR directly interacts with growth hormone (GH)-activated STAT5 to induce the expression of genes important for GC-mediated postnatal growth and maturation (Tronche, Opherk et al. 2004; Engblom, Kornfeld et al. 2007). The interaction between GR and STAT5 is important for postnatal development, since GR also associates with STAT5-responsive regions of GH-induced genes (Tronche, Opherk et al. 2004). In addition, targeted deletion of GR or STAT5, or both in hepatocytes led to identical impairment of growth curves, and overlapping gene expression changes in single (GR or STAT5) and double (GR and STAT5) mutants (Engblom, Kornfeld et al. 2007). Deletion of the N-terminal domain of STAT5 that disrupts protein-protein interaction with GR lead to growth retardation and dyregulation of target genes, thus supporting that the interaction between GR and STAT5 plays a significant role in postnatal development (Engblom, Kornfeld et al. 2007).

Glucocorticoids are important modulators of the immune response where they mostly have potent immunosuppressive actions, and regulate inflammatory responses through crosstalk with cytokine signaling pathways. Glucocorticoids and CRH (which acts via a GPCR) act in synergy with cytokine signaling pathways to activate the HPA axis and accelerate inflammatory responses. For example, in a corticotropic cell line, the cytokine leukemic inhibitory factor (LIF)-mediated activation of STAT 1-3 stimulated *pro-opiomelanocortin (POMC)* gene transcription and ACTH secretion (Ray, Ren et al. 1996; Chesnokova and Melmed 2002). The GR and STAT 1-3 bound to the *POMC* promoter and cooperated to synergistically increase transactivation of the *POMC* promoter. These results suggest that although GR suppresses *POMC* expression, when the LIF pathway is activated GR loses its repressive actions on *POMC* transcription and instead facilitates STAT signaling (Latchoumanin, Mynard et al. 2007).

In contrast, GCs also act in synergy with SF-1, to suppress activation of the HPA axis. SF-1 is a monomeric nuclear receptor that regulates the expression of cytochrome P450 enzymes, which in turn catalyze the conversion of cholesterol to corticosteroids. In adrenocortical cells, GR and SF-1 synergistically activate the expression of *Dax-1* (Dose sensitive, adrenal hypoplasia congenital determining region on the X-chromosome-1). *Dax-1* codes for an orphan nuclear receptor that binds to the SF-1 promoter, and recruits nuclear receptor corepressors to inhibit SF-1 expression. Therefore, through the synergistic induction of *Dax-1* by GR and SF-1, a negative feedback loop is formed that results in GCs blocking further corticosteroid production (Gummow, Scheys et al. 2006).

5.2.1 Molecular Mechanisms that Underlie Transcriptional Synergy by Nuclear Hormone Receptors. Transcriptional synergy between TFs is defined as a greater than

additive effect of two or more TFs on gene regulation (Bonett, Hoopfer et al. 2010), or the nonlinear or sigmoidal response of a gene to increasing amounts of two or more activators (Carey 1998). Transcriptional synergy is an important means for the cell to use a limited number of TFs to link and integrate related signaling pathways (Bonett, Hoopfer et al. 2010). Synergy can occur between two NRs (ligand-inducible TFs), or between a NR and a constitutively acting TF. The transcriptional synergy between two TFs can take different forms. For example, each of the two TFs may individually induce the expression of a common target gene, and in combination lead to induction to levels significantly greater than their additive contributions. Another common example of synergy is when the activity of one or more TFs is insufficient to induce transcription, but when present together they induce or further enhance the induction of the target gene. Synergistic transrepression and thus downregulation is also observed, but for the present purposes I will focus only on synergistic transactivation.

One of the first and most extensively studied models of transcriptional synergy between NRs and other TFs is the synergy that occurs on the *MMTV LTR* promoter between GR, PR and other constitutively active TFs such as Specificity protein 1 (Sp1), CAAT-box binding factor, nuclear factor 1 (NF1) and octamer transcription factor (OTF) at the (Schule, Muller et al. 1988; Schule, Muller et al. 1988; Bruggemeier, Rogge et al. 1990). As mentioned earlier, the *MMTV LTR* promoter (-202 to -59 bp relative to transcriptions start site) is a useful model for investigating transcriptional regulation by steroid receptors since it contains four HRE half sites of the sequence 5'TGTTCT3', and binding sites for NF1, OTF and TATA binding protein (TBP) (Cato, Skroch et al. 1988; Cato and Weinmann 1988; Schule, Muller et al. 1988; Bruggemeier, Rogge et al. 1990).

More importantly, when integrated into chromatin it is arranged as an array of 6 nucleosomes (A-F), and therefore is widely used as a model to investigate NR-mediated chromatin remodeling (Pina, Bruggemeier et al. 1990; Archer, Lefebvre et al. 1992). Glucocorticoids, progestins and androgens are all capable of inducing *MMTV* transactivation by binding to the HREs present in the promoter, where all four HRE half sites contribute to give a maximal response in the presence of all three hormones (Cato, Skroch et al. 1988; Cato and Weinmann 1988). Using *MMTV* promoter-reporter assays, Schule and colleagues (Schule, Muller et al. 1988; Schule, Muller et al. 1988) showed that the spacing between the HRE half sites and the TF binding sites is a critical determinant for synergistic transactivation of the *MMTV* promoter. Greatest synergy was observed in the presence of two GRE/PRE elements (Schule, Muller et al. 1988). The presence of multiple HREs in close proximity has been found to be an important determinant in synergistic TH and steroid hormone action (Cato, Skroch et al. 1988; Klein-Hitpass, Kaling et al. 1988; Liu and Towle 1994). In addition to the steroid receptors, TR together with the pituitary-specific factor Pit-1 has also been found to have synergistic activity with Sp1, NF1, CP1, OTF-1 and CACC box binding protein in transactivation of the human placental lactogen B (hCS-B) promoter in rat pituitary cells (Voz, Peers et al. 1991; Voz, Peers et al. 1992). These observations suggest that the constitutive TFs, Sp1, NF-1, CP1, OTF-1 and CACC box binding protein may act with members of the ligand-inducible NR family to synergistically activate target genes.

There are several molecular mechanisms that may account for synergy between NRs/TFs. At the transcriptional level, this could be due to a combination of: 1) enhanced NR/TF expression by autoinduction (Fig. 1.5) or cross-regulation (Fig. 1.5), and thus

enhanced recruitment to genomic sites; 2) recruitment of an accessory transcription factor at regulatory regions that only occurs in the presence of the synergizing NRs/TFs (Fig. 1.6A); 3) unidirectional or reciprocal cooperative binding of the synergizing NRs/TFs that may be attributed to enhanced decompaction of chromatin, thereby allowing for greater DNA-protein contact (Fig. 1.6B); 4) interaction between two regulatory regions mediated by protein-protein interactions or chromosomal looping (Fig. 1.6C). Examples of mechanism no. 1 involving NR autoinduction and NR cross-regulation were described earlier (section 5.1 and 5.2). An example of mechanism no. 2 is the finding that ligand- bound PR and GR synergistically activate the *MMTV* promoter through the PR and GR-dependent recruitment of OTF-1, a TF known to interact with TFIID of the basal transcription machinery (Bruggemeier, Rogge et al. 1990). A similar mechanism may explain the synergy by GR, STAT5 and C/EBP β (CCAAT/ Enhancing Binding Protein β) in activating the *β-casein* gene expression since the recruitment of C/EBP β was dependent on GR and STAT5 binding to their respective response elements (Wyszomierski and Rosen 2001).

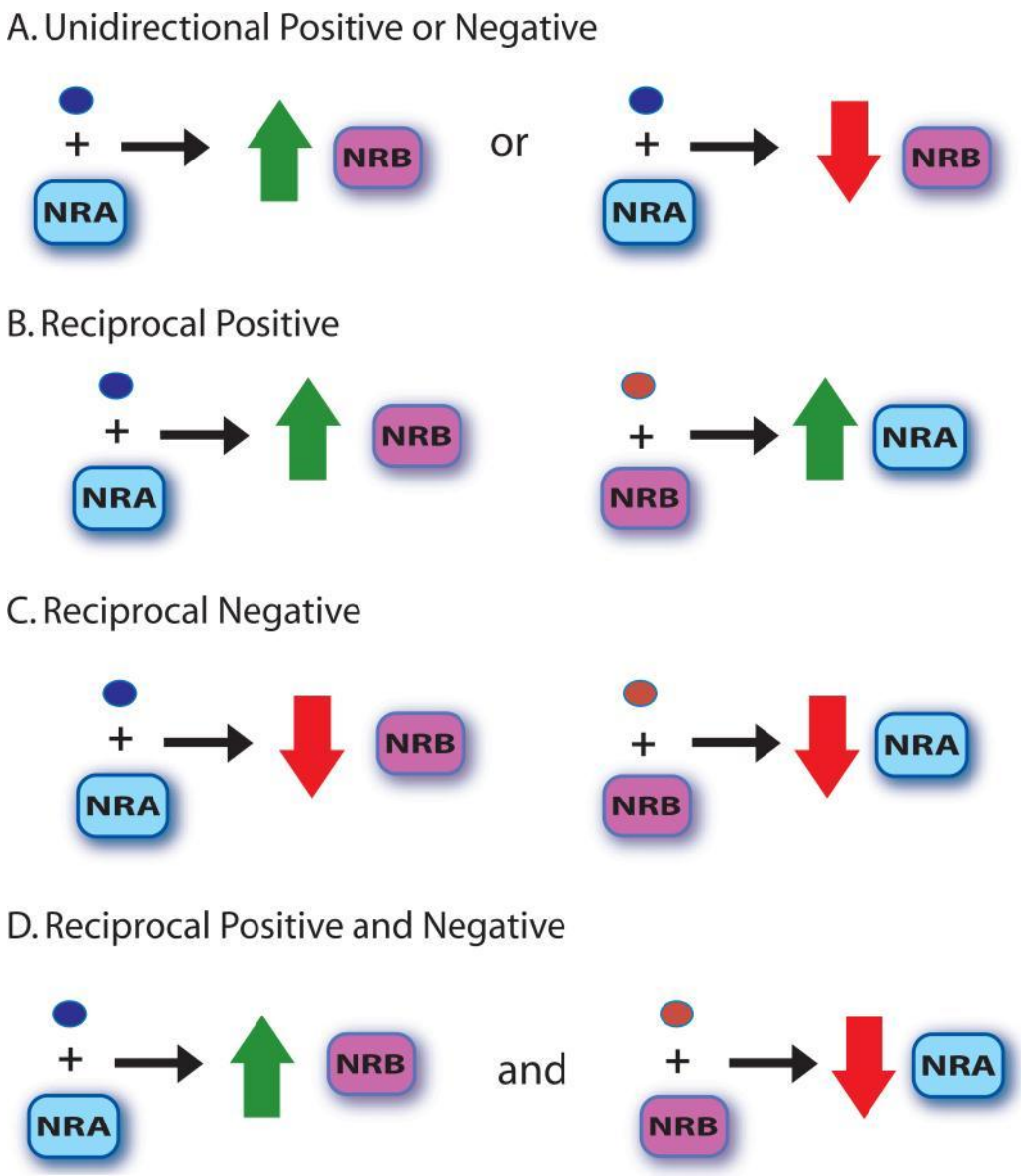

Fig. 1.5. Forms of nuclear receptor (NR) cross-regulation. Hormone-bound NRs can regulate the expression of other types of NRs, and NR cross-regulation can take several forms. (**A)** Unidirectional cross regulation involves a NR (NRA) regulating the expression of a different NR (NRB) while NRB does not affect the expression of NRA. (**B)** In reciprocal positive cross-regulation, the hormone-bound NR (NRA) positively regulates the expression of another type of NR (NRB) and at the same time, hormone-bound NRB upregulates the expression of NRA. (**C)** Reciprocal negative cross-regulation occurs when a hormone-bound NR (NRA) downregulates expression of another NR (NRB), and hormone-bound NRB negatively regulates expression of NRA. (**D)** In another form of cross-regulation, a hormone-bound NR (NRA) positive regulates the expression of another NR (NRB), while NRB downregulates expression of NRA.

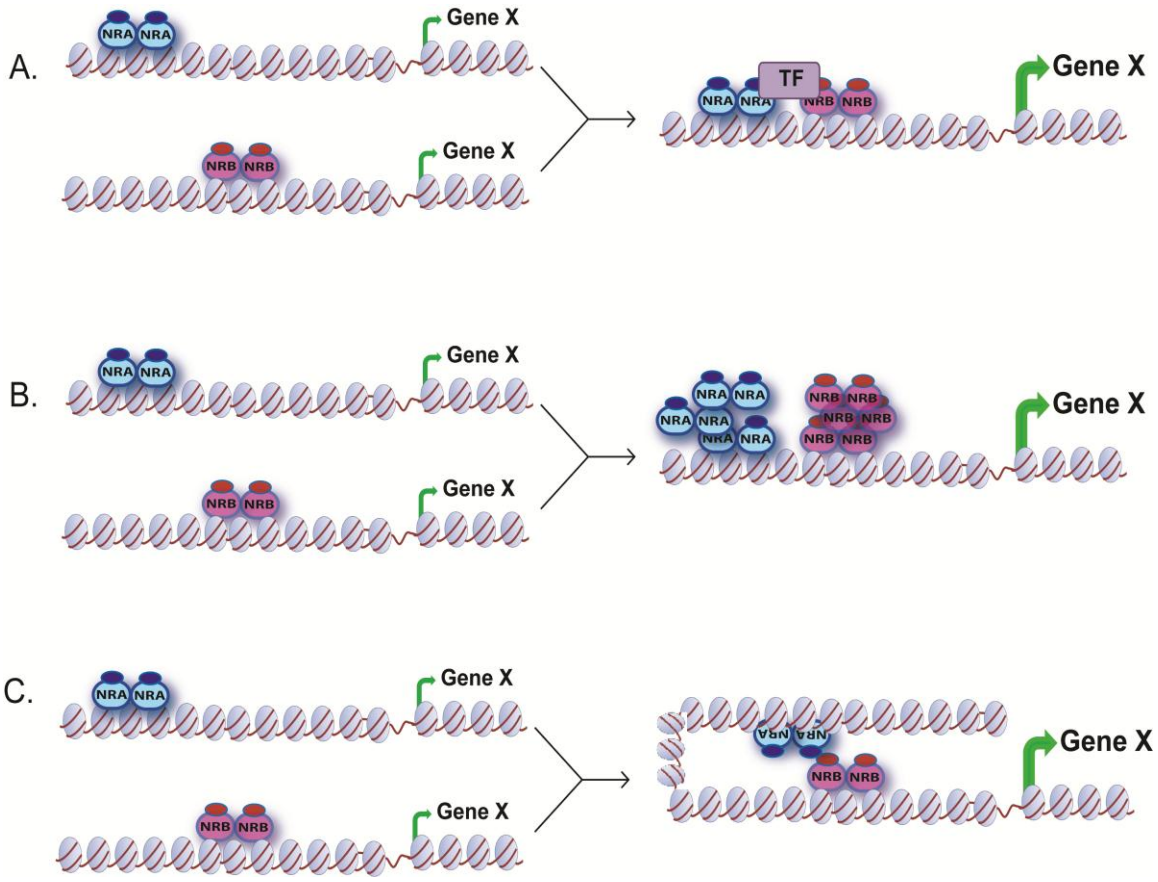

Fig. 1.6. Molecular mechanisms of transcriptional synergy between nuclear hormone receptors (NR) and/ or non-NR transcription factors (TFs.) Nuclear hormone receptor A or NRB regulates the expression of Gene X. Combined association of NRA and NRB at the Gene X regulatory regions leads to: **(A)** Recruitment of an accessory transcription factor (TF);
(B) Unidirectional or reciprocal cooperative binding of the synergizing NRA/NRB that may be attributed to enhanced decompaction of chromatin thereby allowing for greater DNA-protein contact and; **(C)** Interaction between two regulatory regions mediated by protein-protein interactions or chromosomal looping.

Mechanism no. 3, or cooperative DNA association, occurs when a NR/TF facilitates, enhances and/or stabilizes the association of the other TF/NR at gene regulatory regions. This is observed for the synergistic action of GR and NF-1 at the *11B-hydroxysteroid dehydrogenase* and *MMTV* promoters. The association of GR at the *MMTV* promoter led to NF-1, binding which in turn further increased GR association. Synergistic regulation by GR and NF-1 did not require protein-protein interactions between the two TFs. It is proposed that NF-1 binding facilitates changes that lead to a more open chromatin environment allowing for more GR to bind to the GRE (Hebbar and Archer 2007). A similar mechanism may account for the synergistic regulation of *Dax-1* by GR and SF-1, where GC was found to increase SF-1 recruitment to the *Dax-1* promoter (Gummow, Scheys et al. 2006).

Other examples of mechanism no. 3 include the synergistic effect of IL-6 and dexamethasone (DEX; a glucocorticoid) on *α2- macroglobulin* (*α2-M*) gene expression that may be explained by the cooperative DNA association of GR and IL-6-activated STAT3. Unlike IL-6- activated STAT3, ligand-bound GR does not induce *α2-M* expression. The *α2-M* gene has STAT3, AP-1 and OTF-1 binding sites at its promoter (-200 bp from TSS) but there is no GRE within this region. It is hypothesized that GR interaction with the *α2-M* gene occurs through protein-protein interactions at the AP-1 site. Combined treatment of IL-6 and DEX synergistically induced *α2-M* mRNA levels that may be attributed to the synergistic increase and the prolonged association of GR and STAT3 at the promoter (Lerner, Henriksen et al. 2003). This may be due to delayed STAT3 dephosphorylation and dissociation, which leads to a more stable protein complex to support synergistic transcription. This increase in GR and STAT3 association

at the *α2-M* promoter also correlated with an increased H3 acetylation and recruitment of Pol II (Takeda, Kurachi et al. 1998; Lerner, Henriksen et al. 2003). Cooperative DNA binding may also explain the synergistic action of GR and LIF-activated STAT1-3 on *POMC* induction, where combined treatment with LIF and DEX led to a prolonged association of both STAT3 and GR at the *POMC* promoter (Latchoumanin, Mynard et al. 2007).

An indirect contributing factor in the cooperative increase in NR/TF association at gene regulatory regions is the reciprocal enhancement of the nuclear translocation of the cooperating NRs/TFs. For example, androgens synergistically enhance STAT5-dependent activation of STAT5-response elements fused to luciferase (GAS-luciferase) and of the endogenous *β-casein* promoter in prostate cancer cells. Ligand-bound AR and active STAT5 led to reciprocal increases in the nuclear localization of AR and STAT5 (Tan, Dagvadorj et al. 2008). Therefore, cooperative DNA gene association between two NRs/TFs may be indirectly attributed to the enhanced, reciprocal increase in NR/TF nuclear translocation.

Transcriptional synergy that occurs by mechanism no. 4 is best exemplified by the interaction of GR and STAT5 in the regulation of the *β-casein* gene in mammary epithelial cells. The expression of the *β-casein* gene is induced by the cytokine PRL through STAT5-mediated transcription. The GR alone did not induce *β-casein* expression, but synergistically acted with STAT5 to enhance transcription (Lechner, Welte et al. 1997; Stoecklin, Wissler et al. 1997). The synergistic action between GR and STAT5 was attributed to two functional STAT5 response elements (STAT5REs) and seven GRE half sites at the proximal promoter region (-232 to -24 from TSS), and to two

STAT5REs at a distal enhancer region located -6.4 to -6 kb upstream of the TSS of the *β-casein* gene (Lechner, Welte et al. 1997; Stoecklin, Wissler et al. 1997; Wyszomierski, Yeh et al. 1999; Kabotyanski, Huetter et al. 2006). Mutation of the STAT5REs and GRE half sites abolished synergistic induction by GCs and PRL (Kabotyanski, Huetter et al. 2006).

Chromatin immunoprecipitation assays revealed that there is a GC-dependent recruitment of GR to the proximal promoter and distal enhancer of the *β-casein* gene that was not enhanced with combined GC and PRL treatment. The increase in GR association at the enhancer is of interest since there were no GREs identified in this region, suggesting that the association of GR at the enhancer may be due to indirect binding through protein-protein interactions, and/or through long range chromosomal interactions with the promoter. In contrast, there was a PRL-dependent increase in STAT5 association at the proximal promoter and enhancer that was synergistically increased in the presence of GC and PRL at both regulatory regions. Combined treatment with GC and PRL also led to an increase in Pol II association as well as an increase and prolonged p300 association at the promoter and enhancer of *β-casein* gene (Kabotyanski, Huetter et al. 2006).

The hormone-dependent increase in association of GR, p300 and Pol II at the enhancer favors a model for long range interactions between the enhancer and the promoter (Kabotyanski, Huetter et al. 2006). Studies of this model demonstrated that apart from cooperative DNA binding, NR/TFs can synergistically induce gene expression by the interaction of two distant regulatory regions that may be physically associated by long range chromosomal looping (Kabotyanski, Huetter et al. 2006). This model is

consistent with recent findings that regulatory functions of enhancers are relayed to the promoter by long range interactions mediated by chromosomal looping, tracking, cohesion and non-coding RNAs (Ong and Corces 2011).

6. Synergistic Transcriptional Regulation of the *Krüppel-like factor 9* Gene by Thyroid hormone and Glucocorticoids

A gene that we discovered to be independently and synergistically upregulated by GCs and TH in frogs and rodents is the transcription factor, *Klf9* (also known as *Basic Transcription Element Binding Protein 1*; *Bteb1*). We found that *Klf9* is a direct transcriptional target for TR and GR, and we identified an evolutionarily conserved enhancer element, we call the *Klf9* synergy module, that supports synergistic transactivation by TH and GCs (Chapter 3). Our analysis of the hormone-dependent transcriptional regulation of *Klf9* revealed that synergistic transcription of *Klf9* by TR and GR may be explained, in part, by several of the molecular mechanisms described above (see Chapter 3).

Krüppel-like factor 9 was first isolated from rat liver by its ability to bind to the basic transcription element (BTE), a GC rich sequence located in the promoter region of the cytochrome P450IA1 gene (Imataka, Sogawa et al. 1992). It belongs to the Sp1/Krüppel Like Factors (KLF) family of transcription factors. Members of this protein family are characterized by a highly conserved carboxy terminal DNA-binding domain composed of three tandem repeats of a Cys_2His_2 zinc finger motif that binds to GC and GT rich sequences (Kaczynski, Cook et al. 2003). In addition to the DNA-binding domain (DBD), the N-terminal region of KLF9 that contains two transcription activation domains

is also evolutionarily conserved, both in sequence and in transactivation function between the frog and mammalian KLF9 proteins (Kobayashi, Sogawa et al. 1995; Furlow and Kanamori 2002; Hoopfer, Huang et al. 2002; Bagamasbad, Howdeshell et al. 2007).

Analysis of *Klf9* expression in *X. laevis* throughout metamorphosis showed that *Klf9* is expressed in tadpole brain, tail and intestine, and its expression parallels the increase in plasma TH and tissue morphogenesis that occurs during metamorphosis (Hoopfer, Huang et al. 2002). Similar to *X. laevis*, the expression of rodent *Klf9* (rat – *rKlf9*; mouse – *mKlf9*) in the brain also parallels the postnatal rise in brain TRβ expression and plasma T_3 concentration (Porterfield and Hendrich 1993; Denver, Ouellet et al. 1999; Morita, Kobayashi et al. 2003; Denver and Williamson 2009). The expression of *Klf9* in the mouse hippocampus and cerebellum increased dramatically at postnatal day 7, a period that coincides with the critical window of TH action on the brain (Porterfield and Hendrich 1993; Denver, Ouellet et al. 1999; Morita, Kobayashi et al. 2003; Denver and Williamson 2009).

Consistent with its developmental expression that parallels the rise in TH during metamorphosis, gene expression screens in *X.laevis* identified *Klf9* (*xKlf9*) as one of the most rapidly responding, and strongly induced genes in TH-treated tadpole tissue (Shi and Brown 1993; Wang and Brown 1993; Brown, Wang et al. 1995; Brown, Wang et al. 1996; Denver, Pavgi et al. 1997; Shi 2000; Furlow and Kanamori 2002; Hoopfer, Huang et al. 2002). Thyroid hormone-dependent regulation of *xKlf9* has been attributed to a near perfect DR+4 T_3RE located ~6.0 kb upstream of the transcription start site of the frog gene (Furlow and Kanamori 2002). Two T_3REs have also been identified in the *mKlf9* gene to account for its TH-dependent regulation ((Denver and Williamson 2009), Chapter

3). Analysis of the TH-dependent regulation of *mKlf9* gene showed that TRβ associated with the identified T_3REs, as shown by ChIP assay, and this DNA sequence exhibited strong enhancer activity in transient transfection assays. Treatment with TH, both *in vitro* and *in vivo*, caused hyperacetylation of histones at the upstream T_3REs of the mouse *Klf9* promoter (Denver and Williamson 2009) (Chapter 3).

Support for a role for KLF9 in neural development and plasticity comes from studies in the rodent and frog central nervous system (CNS). Thyroid hormone-dependent expression of *Klf9* was shown in primary neonatal rat cortical neurons and astrocytes, but not in oligodendrocytes (Denver, Ouellet et al. 1999). Overexpression of KLF9 in a mouse neuroblastoma cell line (Neuro2a) caused a dose-dependent increase in the number and length of neurites (Denver, Ouellet et al. 1999). The same morphological changes were seen by T_3 treatment of a Neuro2a cell line engineered to stably express TRβ1 (N2a[TRβ1]) (Denver, Ouellet et al. 1999), suggesting that the TH-mediated increase in KLF9 expression promotes neurite outgrowth. The effect of TH on neurite branching in primary rat embryonic neuronal cultures was abolished by knocking down KLF9 with antisense oligonucleotides (Cayrou, Denver et al. 2002). Mice deficient for KLF9 exhibited decreased dendritic arborization in the Purkinje cells of the cerebellum (Morita, Kobayashi et al. 2003), and delayed neuronal maturation and reduced neurogenesis-dependent LTP in the dentate gyrus (Scobie, Hall et al. 2009). In addition, mutant mice showed significantly reduced activity in behavioral tests that define functions of the cerebellum, hippocampus and amygdala, which may be indicative of impaired synapse formation in these regions of the brain (Morita, Kobayashi et al. 2003). Analysis of KLF9 protein in the tadpole brain by immunohistochemistry (IHC) showed

that KLF9 is not expressed in proliferating cells, suggesting that it plays a role in cell differentiation (Hoopfer, Huang et al. 2002). Consistent with these findings, we found that forced expression of KLF9 in tadpole brain led to an increase in the number of Golgi stained cells, that may reflect enhanced neuronal differentiation (Bonett, Hu et al. 2009). Taken together, these findings suggest that KLF9 may be involved in changes in neuronal morphology such as dendritic branching, axonogenesis and synaptogenesis that is induced by TH in the developing brain.

In addition to the TH-mediated expression of *Klf9*, we have shown that GCs can also induce *Klf9* expression in the CNS of *X. laevis*. Expression *Klf9* mRNA was upregulated in the brain of GC-treated tadpoles and juvenile frogs and in XTC-2 cells (a *X. laevis* embryonic fibroblast cell line). The GC-dependent expression of *xKlf9* was found to be a direct transcriptional effect of GR (Bonett, Hu et al. 2009). These findings are intriguing, since the mammalian hippocampus (and frog homolog – the medial pallium (Yao, Hu et al. 2008)) expresses high levels of GR/MR and thus is a target for GCs, which influence memory consolidation and retrieval (Roozendaal 2002). The hippocampus undergoes structural and functional reorganization, also known as neural plasticity, in response to acute and chronic stress (McEwen 2008). Adaptive changes in the hippocampus that occur in response to stress include dendrite remodeling, neurogenesis, and synaptogenesis (McEwen 2007). Structural plasticity of the hippocampus is regarded to be the basis for learning and memory (Leuner and Gould 2010). Given that *Klf9*: (1) is regulated by TH and GCs, (2) is highly expressed in the hippocampus, a brain region targeted by TH and GCs, and (3) functions in neurite outgrowth and dendritic arborization, we hypothesize

that KLF9 functions as an important intermediate that may coordinate TH and stress hormone action on hippocampal plasticity and subsequent memory consolidation.

7. Thesis Summary

In this thesis I describe studies that investigated the molecular mechanisms behind the evolutionarily conserved, synergistic regulation of *Klf9* by TH and GC in the brain. I also describe a study that investigated a role for KLF9 in regulating the expression of TRβ, whose upregulation is necessary for the progression of amphibian metamorphosis and mammalian brain development. My findings have important implications for understanding how TH and GCs cooperate to control animal development and physiology.

The TH-dependent regulation of the *Klf9* gene is well established, and was shown to be conserved between frog and rodent. Based on our previous work in *Xenopus*, I investigated if the molecular mechanism behind GC-dependent regulation of *Klf9* is evolutionarily conserved between frog and rodents. Studies to address this question are described in Chapter 2 where I found GC-dependent expression of *Klf9* in mouse hippocampus that is mediated by the direct transcriptional activity of the GR. I identified two GRE/MREs (GRE/MRE-6.1 and GRE/MRE-5.3) in the mouse and human *Klf9* gene that confer GC-dependent regulation, and I discovered that one of these GRE/MREs (GRE/MRE-5.3) is evolutionarily conserved between frog and mammals, and can also support GC regulation of the frog *Klf9* gene.

In addition to the individual actions of TH and GC on *Klf9* expression, I found that GC and TH synergistically induce *Klf9* expression in both frog and rodent brain. The

conserved GRE/MRE-5.3 is located within an evolutionarily conserved ~180 bp sequence that also contains the putative T_3RE initially identified in frog *Klf9* gene. In Chapter 3, I explored the molecular mechanisms behind the synergistic action of TH and GC on *Klf9* expression. Located within the ~180 bp synergy module is the GRE/MRE-5.3 that I identified in Chapter 2, and a composite response element composed of 3 HRE half sites (T_3RE identified in (Furlow and Kanamori 2002) and another HRE half site) that is critical for the synergistic regulation of the *Klf9* gene by TH and GC. I found that the synergy module was sufficient to support synergistic transactivation of the frog and mouse *Klf9* gene. I then investigated the molecular mechanism behind the transcriptional synergy that occurs between TR and GR in *Klf9* regulation. I tested several hypotheses based on the different mechanisms to explain NR/TF cooperativity in *Klf9* gene transcription.

I found that TR association peaks at the synergy module, which is independent of hormone treatment, consistent with TRs being constitutively bound to DNA in the unliganded state. On the other hand, TH plus GC treatment led to an enhanced recruitment of GR to the synergy module, suggesting that hormone-bound TR may function as a transcriptional switch that derepresses the *Klf9* locus by promoting histone acetylation and chromatin decompaction, leading to a more transcriptionally active chromatin environment. This allows for an enhanced and synergistic recruitment of GR in the presence TH and GC. The presence of ligand-bound TR, and enhanced recruitment of GR at the synergy module was also accompanied by a synergistic association of stalled Pol II at the synergy module, which may indicate that the presence of TH and GC keeps the *Klf9* locus poised for a rapid transcriptional response. The association of Pol II at the

synergy module was also accompanied by transcription at the synergy module and flanking region, and RNA transcripts produced at this region also showed synergistic expression with TH plus GC treatment that was ~10-30 times greater than the *Klf9* mRNA. Work from our collaborators found that the *Xenopus Klf9* synergy module interacts with the *Klf9* promoter region in a TH-dependent manner by chromosomal looping. Thus, synergistic transcription of the *Klf9* gene by TR and GR may be attributed to the synergistic association of GR and stalled Pol II, and chromosomal looping that allows transcriptional information at the synergy module to be relayed to the promoter, resulting in synergistic gene transcription.

In Chapter 4, I investigated whether hormone synergy is a general phenomenon in hippocampal cells by determining if there are other genes synergistically regulated by TH and GC. For this study, I conducted microarray analysis on hormone-treated mouse hippocampal neuronal cells, HT-22. I found 69 genes that are synergistically upregulated, and 80 genes synergistically downregulated by TH plus GC in HT-22 cells. To my knowledge, this is the first study that has looked at coordinate gene regulation by TH and GC in hippocampal cells. Among genes that are synergistically upregulated by TH plus GC, there was an overrepresentation of genes that are involved in remodeling of the cytoskeleton, suggesting that TH and GC may have synergistic effects in shaping neuronal morphology and function.

In Chapter 5, I tested the hypothesis that the coordinate upregulation of *Klf9* and *TRβ* that occurs during tadpole metamorphosis was functionally linked. Specifically, I tested whether *Klf9*, which is induced by TH with faster kinetics than *TRβ*, functions as an accessory TF for TR in promoting *TRβ* autoinduction. The discovery that *Klf9* is a

rapidly responding TH-induced gene, and that the *TRβA* promoter has several potential binding sites for KLF9 (Ranjan, Wong et al. 1994) led to the hypothesis that *TRβA* is a target gene for KLF9. Studies to test this hypothesis are described in Chapter 5 (Bagamasbad, Howdeshell et al. 2008). Analysis of the kinetics of expression of *TRβA* and *Klf9* mRNAs showed that *Klf9* is upregulated earlier than *TRβA* in XTC-2 cells and in the brain of premetamorphic tadpoles treated with TH. Electrophoretic mobility shift assays showed that KLF9 can bind to GC-rich regions of the proximal *TRβA* promoter, and ChIP assays found that KLF9 associates with this region *in vivo* in a TH and developmental stage-dependent manner. Furthermore, forced expression of KLF9 in XTC-2 cells or tadpole brain *in vivo* accelerated and enhanced TRβA autoinduction ((Bagamasbad, Howdeshell et al. 2008), Hu and Denver, unpublished data). These findings support the hypothesis that the immediate early gene KLF9 functions as an accessory transcription factor necessary for *TRβ* autoinduction.

In summary, findings of this thesis describe mechanisms for how two NRs cooperate to synergistically regulate gene expression. My studies also demonstrate how the protein product of the immediate early gene *Klf9* functions in a transcriptional network to enhance the autoinduction of *TRβ*, a NR known to be essential for postembryonic animal development. Results of my thesis demonstrate that through the synergistic actions of liganded GR and TR in inducing the expression of *Klf9*, and together with the role of KLF9 in *TRβ* autoinduction, a positive feed forward loop is formed that, in part, may account for the increased sensitivity to hormone signals, and the amplification of gene expression cascades that control animal development (Fig. 1.7). Together, my findings

demonstrate an important mechanism for how the stress and TH axes interact to influence animal development.

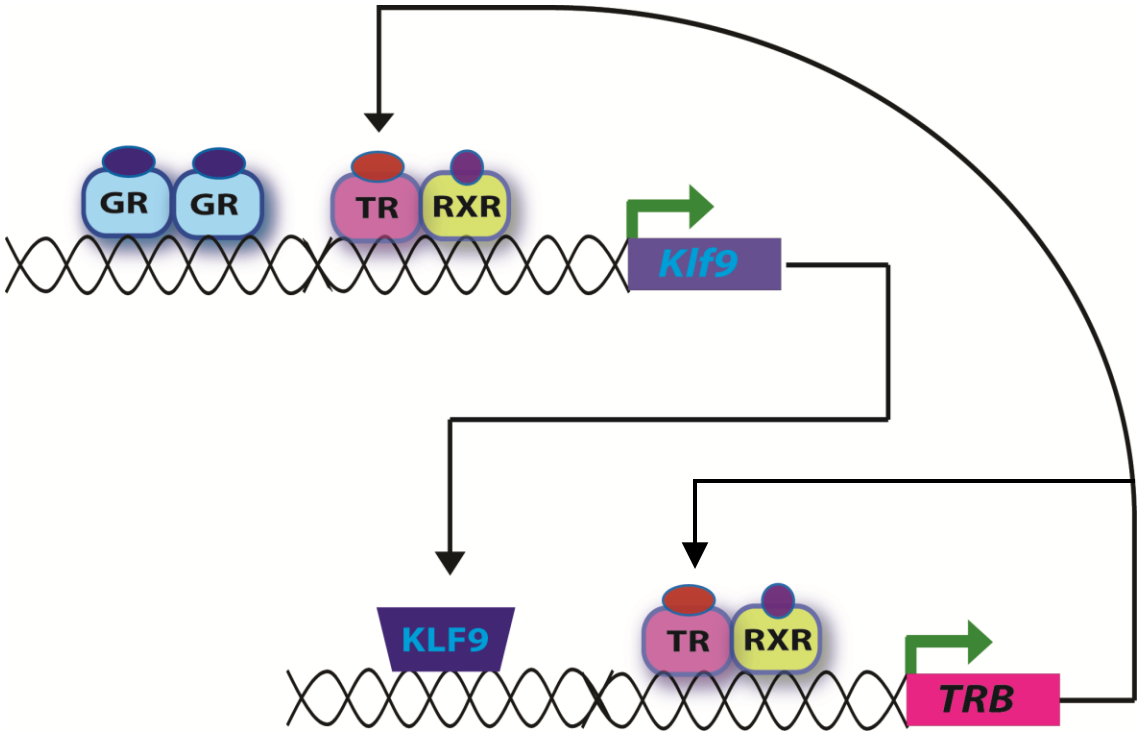

Fig. 1.7. KLF9 functions as an intermediate that enhances sensitivity to thyroid hormone. Ligand-bound GR, TR-retinoid X receptor (RXR) heterodimers bind to and synergistically induce the expression of the *Klf9* gene. KLF9 associates with the promoter region of *TRβ* and enhances TRβ autoinduction. The synergistic action of glucocorticoids and thyroid hormone in upregulating *Klf9* expression creates a positive, feed forward loop that further enhances TRβ autoinduction leading to increased sensitivity to thyroid hormone

References

Amiel-Tison, C., D. Cabrol, et al. (2004). "Fetal adaptation to stress. Part I: acceleration of fetal maturation and earlier birth triggered by placental insufficiency in humans." Early Hum Dev **78**(1): 15-27.

Aranda, A. and A. Pascual (2001). "Nuclear hormone receptors and gene expression." Physiol Rev **81**(3): 1269-1304.

Archer, T. K., P. Lefebvre, et al. (1992). "Transcription factor loading on the MMTV promoter: a bimodal mechanism for promoter activation." Science **255**(5051): 1573-1576.

Bagamasbad, P. and R. J. Denver (2011). "Mechanisms and significance of nuclear receptor auto- and cross-regulation." Gen Comp Endocrinol **170**(1): 3-17.

Bagamasbad, P., K. L. Howdeshell, et al. (2008). "A role for basic transcription element-binding protein 1 (BTEB1) in the autoinduction of thyroid hormone receptor beta." J Biol Chem **283**(4): 2275-2285.

Baker, B. S. and J. R. Tata (1992). "Prolactin prevents the autoinduction of thyroid hormone receptor mRNAs during amphibian metamorphosis." Dev Biol **149**(2): 463-467.

Bedford, M. T. (2007). "Arginine methylation at a glance." J Cell Sci **120**(Pt 24): 4243-4246.

Benkoussa, M., C. Brand, et al. (2002). "Retinoic acid receptors inhibit AP1 activation by regulating extracellular signal-regulated kinase and CBP recruitment to an AP1-responsive promoter." Mol Cell Biol **22**(13): 4522-4534.

Beylin, A. V. and T. J. Shors (2003). "Glucocorticoids are necessary for enhancing the acquisition of associative memories after acute stressful experience." Horm Behav **43**(1): 124-131.

Bonett, R. M., E. D. Hoopfer, et al. (2010). "Molecular mechanisms of corticosteroid synergy with thyroid hormone during tadpole metamorphosis." Gen Comp Endocrinol **168**(2): 209-219.

Bonett, R. M., F. Hu, et al. (2009). "Stressor and glucocorticoid-dependent induction of the immediate early gene kruppel-like factor 9: implications for neural development and plasticity." Endocrinology **150**(4): 1757-1765.

Brown, D. D., Z. Wang, et al. (1996). "The thyroid hormone-induced tail resorption program during Xenopus laevis metamorphosis." Proc Natl Acad Sci U S A **93**(5): 1924-1929.

Brown, D. D., Z. Wang, et al. (1995). "Amphibian metamorphosis: a complex program of gene expression changes controlled by the thyroid hormone." Recent Prog Horm Res **50**: 309-315.

Bruggemeier, U., L. Rogge, et al. (1990). "Nuclear factor I acts as a transcription factor on the MMTV promoter but competes with steroid hormone receptors for DNA binding." EMBO J **9**(7): 2233-2239.

Carey, M. (1998). "The enhanceosome and transcriptional synergy." Cell **92**(1): 5-8.

Cato, A. C., P. Skroch, et al. (1988). "DNA sequences outside the receptor-binding sites differently modulate the responsiveness of the mouse mammary tumour virus promoter to various steroid hormones." EMBO J **7**(5): 1403-1410.

Cato, A. C. and J. Weinmann (1988). "Mineralocorticoid regulation of transcription of transfected mouse mammary tumor virus DNA in cultured kidney cells." J Cell Biol **106**(6): 2119-2125.
Cayrou, C., R. J. Denver, et al. (2002). "Suppression of the basic transcription element-binding protein in brain neuronal cultures inhibits thyroid hormone-induced neurite branching." Endocrinology **143**(6): 2242-2249.
Chakravarti, D., V. J. LaMorte, et al. (1996). "Role of CBP/P300 in nuclear receptor signalling." Nature **383**(6595): 99-103.
Chao, H. M., L. Y. Ma, et al. (1998). "Regulation of glucocorticoid receptor and mineralocorticoid receptor messenger ribonucleic acids by selective agonists in the rat hippocampus." Endocrinology **139**(4): 1810-1814.
Chatterjee, V. K., J. K. Lee, et al. (1989). "Negative regulation of the thyroid-stimulating hormone alpha gene by thyroid hormone: receptor interaction adjacent to the TATA box." Proc Natl Acad Sci U S A **86**(23): 9114-9118.
Chen, H., R. J. Lin, et al. (1997). "Nuclear receptor coactivator ACTR is a novel histone acetyltransferase and forms a multimeric activation complex with P/CAF and CBP/p300." Cell **90**(3): 569-580.
Chen, W. and R. G. Roeder (2007). "The Mediator subunit MED1/TRAP220 is required for optimal glucocorticoid receptor-mediated transcription activation." Nucleic Acids Res **35**(18): 6161-6169.
Cheng, S. Y., J. L. Leonard, et al. (2010). "Molecular aspects of thyroid hormone actions." Endocr Rev **31**(2): 139-170.
Chesnokova, V. and S. Melmed (2002). "Minireview: Neuro-immuno-endocrine modulation of the hypothalamic-pituitary-adrenal (HPA) axis by gp130 signaling molecules." Endocrinology **143**(5): 1571-1574.
Chiba, H., M. Muramatsu, et al. (1994). "Two human homologues of Saccharomyces cerevisiae SWI2/SNF2 and Drosophila brahma are transcriptional coactivators cooperating with the estrogen receptor and the retinoic acid receptor." Nucleic Acids Res **22**(10): 1815-1820.
Crespi, E. J. and R. J. Denver (2005). "Ancient origins of human developmental plasticity." Am J Hum Biol **17**(1): 44-54.
De Bosscher, K., W. Vanden Berghe, et al. (2003). "The interplay between the glucocorticoid receptor and nuclear factor-kappaB or activator protein-1: molecular mechanisms for gene repression." Endocr Rev **24**(4): 488-522.
De Kloet, E. R., E. Vreugdenhil, et al. (1998). "Brain corticosteroid receptor balance in health and disease." Endocr Rev **19**(3): 269-301.
Denver, R. J. (1997). "Environmental stress as a developmental cue: corticotropin-releasing hormone is a proximate mediator of adaptive phenotypic plasticity in amphibian metamorphosis." Horm Behav **31**(2): 169-179.
Denver, R. J. (2009). Endocrinology of complex life cycles: Amphibians Hormones, Brain and Behavior. D. W. Pfaff, A. P. Arnold, A. M. Etgen, R. T. Rubin and S. E. Fahrbach. San Diego, Elsevier
Denver, R. J. (2009). "Stress hormones mediate environment-genotype interactions during amphibian development." Gen Comp Endocrinol **164**(1): 20-31.

Denver, R. J. (2009). "Stress hormones mediate environment-genotype interactions during amphibian development." General & Comparative Endocrinology **164**: 20-31.

Denver, R. J., F. Hu, et al. (2009). "Thyroid hormone receptor subtype specificity for hormone-dependent neurogenesis in *Xenopus laevis*." Developmental Biology **326**: 155-168.

Denver, R. J., L. Ouellet, et al. (1999). "Basic transcription element-binding protein (BTEB) is a thyroid hormone-regulated gene in the developing central nervous system. Evidence for a role in neurite outgrowth." J Biol Chem **274**(33): 23128-23134.

Denver, R. J., S. Pavgi, et al. (1997). "Thyroid hormone-dependent gene expression program for Xenopus neural development." J Biol Chem **272**(13): 8179-8188.

Denver, R. J. and K. E. Williamson (2009). "Identification of a thyroid hormone response element in the mouse Kruppel-like factor 9 gene to explain its postnatal expression in the brain." Endocrinology **150**(8): 3935-3943.

Eberharter, A. and P. B. Becker (2004). "ATP-dependent nucleosome remodelling: factors and functions." J Cell Sci **117**(Pt 17): 3707-3711.

Engblom, D., J. W. Kornfeld, et al. (2007). "Direct glucocorticoid receptor-Stat5 interaction in hepatocytes controls body size and maturation-related gene expression." Genes Dev **21**(10): 1157-1162.

Fondell, J. D., H. Ge, et al. (1996). "Ligand induction of a transcriptionally active thyroid hormone receptor coactivator complex." Proc Natl Acad Sci U S A **93**(16): 8329-8333.

Fondell, J. D., M. Guermah, et al. (1999). "Thyroid hormone receptor-associated proteins and general positive cofactors mediate thyroid hormone receptor function in the absence of the TATA box-binding protein-associated factors of TFIID." Proc Natl Acad Sci U S A **96**(5): 1959-1964.

Fryer, C. J. and T. K. Archer (1998). "Chromatin remodelling by the glucocorticoid receptor requires the BRG1 complex." Nature **393**(6680): 88-91.

Fryer, C. J., S. K. Nordeen, et al. (1998). "Antiprogestins mediate differential effects on glucocorticoid receptor remodeling of chromatin structure." J Biol Chem **273**(2): 1175-1183.

Furlow, J. D. and A. Kanamori (2002). "The transcription factor basic transcription element-binding protein 1 is a direct thyroid hormone response gene in the frog Xenopus laevis." Endocrinology **143**(9): 3295-3305.

Furlow, J. D. and E. S. Neff (2006). "A developmental switch induced by thyroid hormone: Xenopus laevis metamorphosis." Trends in Endocrinology and Metabolism **17**(2): 38-45.

Galton, V. A. (1990). "Mechanisms underlying the acceleration of thyroid hormone-induced tadpole metamorphosis by corticosterone." Endocrinology **127**(6): 2997-3002.

Germain, P., B. Staels, et al. (2006). "Overview of nomenclature of nuclear receptors." Pharmacol Rev **58**(4): 685-704.

Ghosh, B., C. R. Wood, et al. (2000). "Glucocorticoid receptor regulation in the rat embryo: a potential site for developmental toxicity?" Toxicol Appl Pharmacol **164**(2): 221-229.

Gilbert, M. E. and C. Paczkowski (2003). "Propylthiouracil (PTU)-induced hypothyroidism in the developing rat impairs synaptic transmission and plasticity in the dentate gyrus of the adult hippocampus." Brain Res Dev Brain Res **145**(1): 19-29.

Gomez, F., A. Lahmame, et al. (1996). "Hypothalamic-pituitary-adrenal response to chronic stress in five inbred rat strains: Differential responses are mainly located at the adrenocortical level." Neuroendocrinology **63**(4): 327-337.

Gould, E., M. D. Allan, et al. (1990). "Dendritic spine density of adult hippocampal pyramidal cells is sensitive to thyroid hormone." Brain Res **525**(2): 327-329.

Grunstein, M. (1997). "Histone acetylation in chromatin structure and transcription." Nature **389**(6649): 349-352.

Gummow, B. M., J. O. Scheys, et al. (2006). "Reciprocal regulation of a glucocorticoid receptor-steroidogenic factor-1 transcription complex on the Dax-1 promoter by glucocorticoids and adrenocorticotropic hormone in the adrenal cortex." Mol Endocrinol **20**(11): 2711-2723.

Hammes, S. R. and E. R. Levin (2007). "Extranuclear Steroid Receptors: Nature and Actions." Endocr Rev.

Han, F., H. Ozawa, et al. (2007). "Changes in the expression of corticotrophin-releasing hormone, mineralocorticoid receptor and glucocorticoid receptor mRNAs in the hypothalamic paraventricular nucleus induced by fornix transection and adrenalectomy." Journal Of Neuroendocrinology **19**(4): 229-238.

Hebbar, P. B. and T. K. Archer (2007). "Chromatin-dependent cooperativity between site-specific transcription factors in vivo." J Biol Chem **282**(11): 8284-8291.

Heimeier, R. A., V. S. Hsia, et al. (2008). "Participation of Brahma-related gene 1 (BRG1)-associated factor 57 and BRG1-containing chromatin remodeling complexes in thyroid hormone-dependent gene activation during vertebrate development." Mol Endocrinol **22**(5): 1065-1077.

Hittelman, A. B., D. Burakov, et al. (1999). "Differential regulation of glucocorticoid receptor transcriptional activation via AF-1-associated proteins." EMBO J **18**(19): 5380-5388.

Holmes, M. C., J. L. Yau, et al. (1995). "The effect of adrenalectomy on 5-hydroxytryptamine and corticosteroid receptor subtype messenger RNA expression in rat hippocampus." Neuroscience **64**(2): 327-337.

Hong, H., K. Kohli, et al. (1997). "GRIP1, a transcriptional coactivator for the AF-2 transactivation domain of steroid, thyroid, retinoid, and vitamin D receptors." Mol Cell Biol **17**(5): 2735-2744.

Hoopfer, E. D., L. Y. Huang, et al. (2002). "Basic transcription element binding protein is a thyroid hormone-regulated transcription factor expressed during metamorphosis in Xenopus laevis." Development Growth & Differentiation **44**(5): 365-381.

Huang, Z. Q., J. Li, et al. (2003). "A role for cofactor-cofactor and cofactor-histone interactions in targeting p300, SWI/SNF and Mediator for transcription." EMBO J **22**(9): 2146-2155.

Hugin-Flores, M. E., T. Steimer, et al. (2004). "Mineralo- and glucocorticoid receptor mrnas are differently regulated by corticosterone in the rat hippocampus and anterior pituitary." Neuroendocrinology **79**(4): 174-184.

Imataka, H., K. Sogawa, et al. (1992). "Two regulatory proteins that bind to the basic transcription element (BTE), a GC box sequence in the promoter region of the rat P-4501A1 gene." Embo J **11**(10): 3663-3671.
Ito, M. and R. G. Roeder (2001). "The TRAP/SMCC/Mediator complex and thyroid hormone receptor function." Trends Endocrinol Metab **12**(3): 127-134.
Ito, M., C. X. Yuan, et al. (1999). "Identity between TRAP and SMCC complexes indicates novel pathways for the function of nuclear receptors and diverse mammalian activators." Mol Cell **3**(3): 361-370.
Ito, M., C. X. Yuan, et al. (2000). "Involvement of the TRAP220 component of the TRAP/SMCC coactivator complex in embryonic development and thyroid hormone action." Mol Cell **5**(4): 683-693.
Joels, M. (2008). "Functional actions of corticosteroids in the hippocampus." Eur J Pharmacol **583**(2-3): 312-321.
Kabotyanski, E. B., M. Huetter, et al. (2006). "Integration of prolactin and glucocorticoid signaling at the beta-casein promoter and enhancer by ordered recruitment of specific transcription factors and chromatin modifiers." Mol Endocrinol **20**(10): 2355-2368.
Kaczynski, J., T. Cook, et al. (2003). "Sp1- and Kruppel-like transcription factors." Genome Biol **4**(2): 206.
Kagey, M. H., J. J. Newman, et al. (2010). "Mediator and cohesin connect gene expression and chromatin architecture." Nature **467**(7314): 430-435.
Kalman, B. A. and R. L. Spencer (2002). "Rapid corticosteroid-dependent regulation of mineralocorticoid receptor protein expression in rat brain." Endocrinology **143**(11): 4184-4195.
Kanamori, A. and D. D. Brown (1992). "The regulation of thyroid hormone receptor beta genes by thyroid hormone in Xenopus laevis." J Biol Chem **267**(2): 739-745.
Kassel, O. and P. Herrlich (2007). "Crosstalk between the glucocorticoid receptor and other transcription factors: molecular aspects." Mol Cell Endocrinol **275**(1-2): 13-29.
Kikuyama, S., K. Niki, et al. (1983). "Studies on corticoid action on the toad tadpole tail in vitro." Gen Comp Endocrinol **52**(3): 395-399.
Kinyamu, H. K. and T. K. Archer (2004). "Modifying chromatin to permit steroid hormone receptor-dependent transcription." Biochim Biophys Acta **1677**(1-3): 30-45.
Klein-Hitpass, L., M. Kaling, et al. (1988). "Synergism of closely adjacent estrogen-responsive elements increases their regulatory potential." J Mol Biol **201**(3): 537-544.
Kobayashi, A., K. Sogawa, et al. (1995). "Analysis of functional domains of a GC box-binding protein, BTEB." J Biochem (Tokyo) **117**(1): 91-95.
Koh, S. S., D. Chen, et al. (2001). "Synergistic enhancement of nuclear receptor function by p160 coactivators and two coactivators with protein methyltransferase activities." J Biol Chem **276**(2): 1089-1098.
Krain, L. P. and R. J. Denver (2004). "Developmental expression and hormonal regulation of glucocorticoid and thyroid hormone receptors during metamorphosis in Xenopus laevis." J Endocrinol **181**(1): 91-104.

Kurdistani, S. K. and M. Grunstein (2003). "Histone acetylation and deacetylation in yeast." Nat Rev Mol Cell Biol **4**(4): 276-284.
Latchoumanin, O., V. Mynard, et al. (2007). "Reversal of glucocorticoids-dependent proopiomelanocortin gene inhibition by leukemia inhibitory factor." Endocrinology **148**(1): 422-432.
Lechner, J., T. Welte, et al. (1997). "Mechanism of interaction between the glucocorticoid receptor and Stat5: role of DNA-binding." Immunobiology **198**(1-3): 112-123.
Lechner, J., T. Welte, et al. (1997). "Promoter-dependent synergy between glucocorticoid receptor and Stat5 in the activation of beta-casein gene transcription." J Biol Chem **272**(33): 20954-20960.
Lerner, L., M. A. Henriksen, et al. (2003). "STAT3-dependent enhanceosome assembly and disassembly: synergy with GR for full transcriptional increase of the alpha 2-macroglobulin gene." Genes Dev **17**(20): 2564-2577.
Leuner, B. and E. Gould (2010). "Structural plasticity and hippocampal function." Annu Rev Psychol **61**: 111-140, C111-113.
Li, H., P. J. Gomes, et al. (1997). "RAC3, a steroid/nuclear receptor-associated coactivator that is related to SRC-1 and TIF2." Proc Natl Acad Sci U S A **94**(16): 8479-8484.
Liu, H. C. and H. C. Towle (1994). "Functional synergism between multiple thyroid hormone response elements regulates hepatic expression of the rat S14 gene." Mol Endocrinol **8**(8): 1021-1037.
Llopis, J., S. Westin, et al. (2000). "Ligand-dependent interactions of coactivators steroid receptor coactivator-1 and peroxisome proliferator-activated receptor binding protein with nuclear hormone receptors can be imaged in live cells and are required for transcription." Proc Natl Acad Sci U S A **97**(8): 4363-4368.
Lopez, G., F. Schaufele, et al. (1993). "Positive and negative modulation of Jun action by thyroid hormone receptor at a unique AP1 site." Mol Cell Biol **13**(5): 3042-3049.
Losel, R. M., E. Falkenstein, et al. (2003). "Nongenomic steroid action: controversies, questions, and answers." Physiol Rev **83**(3): 965-1016.
Machuca, I., G. Esslemont, et al. (1995). "Analysis of structure and expression of the Xenopus thyroid hormone receptor-beta gene to explain its autoinduction." Mol Endocrinol **9**(1): 96-107.
Machuca, I. and J. R. Tata (1992). "Autoinduction of thyroid hormone receptor during metamorphosis is reproduced in Xenopus XTC-2 cells." Mol Cell Endocrinol **87**(1-3): 105-113.
Madeira, M. D. and M. M. Paula-Barbosa (1993). "Reorganization of mossy fiber synapses in male and female hypothyroid rats: a stereological study." J Comp Neurol **337**(2): 334-352.
Magarinos, A. M., M. Orchinik, et al. (1998). "Morphological changes in the hippocampal CA3 region induced by non-invasive glucocorticoid administration: a paradox." Brain Res **809**(2): 314-318.
Magarinos, A. M., J. M. Verdugo, et al. (1997). "Chronic stress alters synaptic terminal structure in hippocampus." Proc Natl Acad Sci U S A **94**(25): 14002-14008.

Mai, W., M. F. Janier, et al. (2004). "Thyroid hormone receptor alpha is a molecular switch of cardiac function between fetal and postnatal life." Proc Natl Acad Sci U S A **101**(28): 10332-10337.
Malik, S. and R. G. Roeder (2010). "The metazoan Mediator co-activator complex as an integrative hub for transcriptional regulation." Nat Rev Genet **11**(11): 761-772.
Mangelsdorf, D. J., C. Thummel, et al. (1995). "The nuclear receptor superfamily: the second decade." Cell **83**(6): 835-839.
Matsuda, H., B. D. Paul, et al. (2009). "Novel functions of protein arginine methyltransferase 1 in thyroid hormone receptor-mediated transcription and in the regulation of metamorphic rate in Xenopus laevis." Mol Cell Biol **29**(3): 745-757.
McEwen, B. S. (1999). "Stress and hippocampal plasticity." Annu Rev Neurosci **22**: 105-122.
McEwen, B. S. (2007). "Physiology and neurobiology of stress and adaptation: central role of the brain." Physiol Rev **87**(3): 873-904.
McEwen, B. S. (2008). "Central effects of stress hormones in health and disease: Understanding the protective and damaging effects of stress and stress mediators." Eur J Pharmacol **583**(2-3): 174-185.
McKenna, N. J. and B. W. O'Malley (2002). "Combinatorial control of gene expression by nuclear receptors and coregulators." Cell **108**(4): 465-474.
Morita, M., A. Kobayashi, et al. (2003). "Functional analysis of basic transcription element binding protein by gene targeting technology." Mol Cell Biol **23**(7): 2489-2500.
Myers, L. C. and R. D. Kornberg (2000). "Mediator of transcriptional regulation." Annu Rev Biochem **69**: 729-749.
Naar, A. M., J. M. Boutin, et al. (1991). "The orientation and spacing of core DNA-binding motifs dictate selective transcriptional responses to three nuclear receptors." Cell **65**(7): 1267-1279.
Nie, Z., Y. Xue, et al. (2000). "A specificity and targeting subunit of a human SWI/SNF family-related chromatin-remodeling complex." Mol Cell Biol **20**(23): 8879-8888.
O'donnell, D., D. Francis, et al. (1995). "Effects of adrenalectomy and corticosterone replacement on glucocorticoid receptor levels in rat brain tissue: a comparison between Western blotting and receptor binding assays." Brain Research **687**(1-2): 133-142.
Okret, S., Y. Dong, et al. (1991). "Regulation of glucocorticoid receptor expression." Biochimie **73**(1): 51-59.
Ong, C. T. and V. G. Corces (2011). "Enhancer function: new insights into the regulation of tissue-specific gene expression." Nat Rev Genet **12**(4): 283-293.
Park, S. W., G. Li, et al. (2005). "Thyroid hormone-induced juxtaposition of regulatory elements/factors and chromatin remodeling of Crabp1 dependent on MED1/TRAP220." Mol Cell **19**(5): 643-653.
Pfitzner, E., S. Kliem, et al. (2004). "The role of STATs in inflammation and inflammatory diseases." Curr Pharm Des **10**(23): 2839-2850.
Pina, B., U. Bruggemeier, et al. (1990). "Nucleosome positioning modulates accessibility of regulatory proteins to the mouse mammary tumor virus promoter." Cell **60**(5): 719-731.

Porterfield, S. P. and C. E. Hendrich (1993). "The role of thyroid hormones in prenatal and neonatal neurological development--current perspectives." Endocr Rev **14**(1): 94-106.
Pratt, W. B., M. D. Galigniana, et al. (2004). "Role of molecular chaperones in steroid receptor action." Essays Biochem **40**: 41-58.
Rachez, C., B. D. Lemon, et al. (1999). "Ligand-dependent transcription activation by nuclear receptors requires the DRIP complex." Nature **398**(6730): 824-828.
Rami, A., A. J. Patel, et al. (1986). "Thyroid hormone and development of the rat hippocampus: morphological alterations in granule and pyramidal cells." Neuroscience **19**(4): 1217-1226.
Rami, A. and A. Rabie (1990). "Delayed synaptogenesis in the dentate gyrus of the thyroid-deficient developing rat." Dev Neurosci **12**(6): 398-405.
Rami, A., A. Rabie, et al. (1986). "Thyroid hormone and development of the rat hippocampus: cell acquisition in the dentate gyrus." Neuroscience **19**(4): 1207-1216.
Ranjan, M., J. Wong, et al. (1994). "Transcriptional repression of Xenopus TR beta gene is mediated by a thyroid hormone response element located near the start site." J Biol Chem **269**(40): 24699-24705.
Ray, D. W., S. G. Ren, et al. (1996). "Leukemia inhibitory factor (LIF) stimulates proopiomelanocortin (POMC) expression in a corticotroph cell line. Role of STAT pathway." J Clin Invest **97**(8): 1852-1859.
Reichardt, H. M., K. H. Kaestner, et al. (1998). "DNA binding of the glucocorticoid receptor is not essential for survival." Cell **93**(4): 531-541.
Reul, J. M., P. T. Pearce, et al. (1989). "Type I and type II corticosteroid receptor gene expression in the rat: effect of adrenalectomy and dexamethasone administration." Mol Endocrinol **3**(10): 1674-1680.
Ribeiro, R. C., P. J. Kushner, et al. (1995). "The nuclear hormone receptor gene superfamily." Annu Rev Med **46**: 443-453.
Richard-Foy, H. and G. L. Hager (1987). "Sequence-specific positioning of nucleosomes over the steroid-inducible MMTV promoter." EMBO J **6**(8): 2321-2328.
Robyr, D., A. P. Wolffe, et al. (2000). "Nuclear hormone receptor coregulators in action: diversity for shared tasks." Mol Endocrinol **14**(3): 329-347.
Roeder, R. G. (2005). "Transcriptional regulation and the role of diverse coactivators in animal cells." FEBS Lett **579**(4): 909-915.
Roozendaal, B. (2002). "Stress and memory: opposing effects of glucocorticoids on memory consolidation and memory retrieval." Neurobiol Learn Mem **78**(3): 578-595.
Roozendaal, B. and J. L. McGaugh (1996). "Amygdaloid nuclei lesions differentially affect glucocorticoid-induced memory enhancement in an inhibitory avoidance task." Neurobiol Learn Mem **65**(1): 1-8.
Roozendaal, B., G. Portillo-Marquez, et al. (1996). "Basolateral amygdala lesions block glucocorticoid-induced modulation of memory for spatial learning." Behav Neurosci **110**(5): 1074-1083.
Safi, R., A. Begue, et al. (1997). "Thyroid hormone receptor genes of neotenic amphibians." J Mol Evol **44**(6): 595-604.

Safi, R., V. Vlaeminck-Guillem, et al. (2006). "Pedomorphosis revisited: thyroid hormone receptors are functional in Necturus maculosus." Evol Dev **8**(3): 284-292.
Sakai, D. D., S. Helms, et al. (1988). "Hormone-mediated repression: a negative glucocorticoid response element from the bovine prolactin gene." Genes Dev **2**(9): 1144-1154.
Sakurai, A., T. Miyamoto, et al. (1992). "Cloning and Characterization of the Human Thyroid-Hormone Receptor Beta-1 Gene Promoter." Biochemical and Biophysical Research Communications **185**(1): 78-84.
Santos, G. M., L. Fairall, et al. (2011). "Negative regulation by nuclear receptors: a plethora of mechanisms." Trends Endocrinol Metab **22**(3): 87-93.
Sapolsky, R. M., L. C. Krey, et al. (1984). "Stress down-regulates corticosterone receptors in a site-specific manner in the brain." Endocrinology **114**(1): 287-292.
Schule, R., M. Muller, et al. (1988). "Many transcription factors interact synergistically with steroid receptors." Science **242**(4884): 1418-1420.
Schule, R., M. Muller, et al. (1988). "Cooperativity of the glucocorticoid receptor and the CACCC-box binding factor." Nature **332**(6159): 87-90.
Scobie, K. N., B. J. Hall, et al. (2009). "Kruppel-like factor 9 is necessary for late-phase neuronal maturation in the developing dentate gyrus and during adult hippocampal neurogenesis." J Neurosci **29**(31): 9875-9887.
Shi, Y.-B. (2000). Amphibian metamorphosis : from morphology to molecular biology. New York, Wiley-Liss.
Shi, Y. B. (2000). Amphibian Metamorphosis. From Morphology to Molecular Biology. New York, Wiley-Liss.
Shi, Y. B. (2009). "Dual functions of thyroid hormone receptors in vertebrate development: the roles of histone-modifying cofactor complexes." Thyroid **19**(9): 987-999.
Shi, Y. B. and D. D. Brown (1993). "The earliest changes in gene expression in tadpole intestine induced by thyroid hormone." J Biol Chem **268**(27): 20312-20317.
Shors, T. J. (2001). "Acute stress rapidly and persistently enhances memory formation in the male rat." Neurobiol Learn Mem **75**(1): 10-29.
Shors, T. J., C. Chua, et al. (2001). "Sex differences and opposite effects of stress on dendritic spine density in the male versus female hippocampus." J Neurosci **21**(16): 6292-6297.
Spencer, R. L., B. A. Kalman, et al. (2000). "Discrimination between changes in glucocorticoid receptor expression and activation in rat brain using western blot analysis." Brain Research **868**(2): 275-286.
Stoecklin, E., M. Wissler, et al. (1997). "Specific DNA binding of Stat5, but not of glucocorticoid receptor, is required for their functional cooperation in the regulation of gene transcription." Mol Cell Biol **17**(11): 6708-6716.
Strait, K. A., H. L. Schwartz, et al. (1990). "Relationship of c-erbA mRNA content to tissue triiodothyronine nuclear binding capacity and function in developing and adult rats." J Biol Chem **265**(18): 10514-10521.
Suzuki, M. R. and S. Kikuyama (1983). "Corticoids augment nuclear binding capacity for triiodothyronine in bullfrog tadpole tail fins." Gen Comp Endocrinol **52**(2): 272-278.

Suzuki, S., T. Miyamoto, et al. (1994). "2 Thyroid-Hormone Response Elements Are Present in the Promoter of Human Thyroid-Hormone Receptor Beta-1." Molecular Endocrinology **8**(3): 305-314.
Suzuki, S., T. Miyamoto, et al. (1994). "Two thyroid hormone response elements are present in the promoter of human thyroid hormone receptor beta 1." Mol Endocrinol **8**(3): 305-314.
Takeda, T., H. Kurachi, et al. (1998). "Crosstalk between the interleukin-6 (IL-6)-JAK-STAT and the glucocorticoid-nuclear receptor pathway: synergistic activation of IL-6 response element by IL-6 and glucocorticoid." J Endocrinol **159**(2): 323-330.
Takeshita, A., G. R. Cardona, et al. (1997). "TRAM-1, A novel 160-kDa thyroid hormone receptor activator molecule, exhibits distinct properties from steroid receptor coactivator-1." J Biol Chem **272**(44): 27629-27634.
Tan, S. H., A. Dagvadorj, et al. (2008). "Transcription factor Stat5 synergizes with androgen receptor in prostate cancer cells." Cancer Res **68**(1): 236-248.
Tata, J. R. (2000). "Autoinduction of nuclear hormone receptors during metamorphosis and its significance." Insect Biochem Mol Biol **30**(8-9): 645-651.
Tata, J. R., A. Kawahara, et al. (1991). "Prolactin inhibits both thyroid hormone-induced morphogenesis and cell death in cultured amphibian larval tissues." Dev Biol **146**(1): 72-80.
Torchia, J., D. W. Rose, et al. (1997). "The transcriptional co-activator p/CIP binds CBP and mediates nuclear-receptor function." Nature **387**(6634): 677-684.
Tornello, S., E. Orti, et al. (1982). "Regulation of glucocorticoid receptors in brain by corticosterone treatment of adrenalectomized rats." Neuroendocrinology **35**(6): 411-417.
Tronche, F., C. Opherk, et al. (2004). "Glucocorticoid receptor function in hepatocytes is essential to promote postnatal body growth." Genes Dev **18**(5): 492-497.
Trotter, K. W. and T. K. Archer (2004). "Reconstitution of glucocorticoid receptor-dependent transcription in vivo." Mol Cell Biol **24**(8): 3347-3358.
Trotter, K. W. and T. K. Archer (2007). "Nuclear receptors and chromatin remodeling machinery." Mol Cell Endocrinol **265-266**: 162-167.
Ulisse, S., G. Esslemont, et al. (1996). "Dominant-negative mutant thyroid hormone receptors prevent transcription from Xenopus thyroid hormone receptor beta gene promoter in response to thyroid hormone in Xenopus tadpoles in vivo." Proc Natl Acad Sci U S A **93**(3): 1205-1209.
Umesono, K., K. K. Murakami, et al. (1991). "Direct repeats as selective response elements for the thyroid hormone, retinoic acid, and vitamin D3 receptors." Cell **65**(7): 1255-1266.
Vo, N. and R. H. Goodman (2001). "CREB-binding protein and p300 in transcriptional regulation." J Biol Chem **276**(17): 13505-13508.
Voegel, J. J., M. J. Heine, et al. (1996). "TIF2, a 160 kDa transcriptional mediator for the ligand-dependent activation function AF-2 of nuclear receptors." EMBO J **15**(14): 3667-3675.
Voz, M. L., B. Peers, et al. (1991). "Characterization of an unusual thyroid response unit in the promoter of the human placental lactogen gene." J Biol Chem **266**(20): 13397-13404.

Voz, M. L., B. Peers, et al. (1992). "Transcriptional regulation by triiodothyronine requires synergistic action of the thyroid receptor with another trans-acting factor." Mol Cell Biol **12**(9): 3991-3997.
Wang, H., Z. Q. Huang, et al. (2001). "Methylation of histone H4 at arginine 3 facilitating transcriptional activation by nuclear hormone receptor." Science **293**(5531): 853-857.
Wang, Z. and D. D. Brown (1993). "Thyroid hormone-induced gene expression program for amphibian tail resorption." Journal of Biological Chemistry **268**(22): 16270-16278.
Wang, Z. and D. D. Brown (1993). "Thyroid hormone-induced gene expression program for amphibian tail resorption." J Biol Chem **268**(22): 16270-16278.
Watanabe, Y., E. Gould, et al. (1992). "Stress induces atrophy of apical dendrites of hippocampal CA3 pyramidal neurons." Brain Res **588**(2): 341-345.
Wolf, I. M., M. D. Heitzer, et al. (2008). "Coactivators and nuclear receptor transactivation." J Cell Biochem **104**(5): 1580-1586.
Wondisford, F. E., E. A. Farr, et al. (1989). "Thyroid hormone inhibition of human thyrotropin beta-subunit gene expression is mediated by a cis-acting element located in the first exon." J Biol Chem **264**(25): 14601-14604.
Wondisford, F. E., H. J. Steinfelder, et al. (1993). "AP-1 antagonizes thyroid hormone receptor action on the thyrotropin beta-subunit gene." J Biol Chem **268**(4): 2749-2754.
Wu, S. C. and Y. Zhang (2009). "Minireview: role of protein methylation and demethylation in nuclear hormone signaling." Mol Endocrinol **23**(9): 1323-1334.
Wyszomierski, S. L. and J. M. Rosen (2001). "Cooperative effects of STAT5 (signal transducer and activator of transcription 5) and C/EBPbeta (CCAAT/enhancer-binding protein-beta) on beta-casein gene transcription are mediated by the glucocorticoid receptor." Mol Endocrinol **15**(2): 228-240.
Wyszomierski, S. L., J. Yeh, et al. (1999). "Glucocorticoid receptor/signal transducer and activator of transcription 5 (STAT5) interactions enhance STAT5 activation by prolonging STAT5 DNA binding and tyrosine phosphorylation." Mol Endocrinol **13**(2): 330-343.
Xu, W., H. Cho, et al. (2004). "A methylation-mediator complex in hormone signaling." Genes Dev **18**(2): 144-156.
Yao, M., F. Hu, et al. (2008). "Distribution and corticosteroid regulation of glucocorticoid receptor in the brain of Xenopus laevis." J Comp Neurol **508**(6): 967-982.
Yaoita, Y. and D. D. Brown (1990). "A correlation of thyroid hormone receptor gene expression with amphibian metamorphosis." Genes Dev **4**(11): 1917-1924.
Yaoita, Y., Y. Shi, et al. (1990). "Xenopus laevis alpha and beta thyroid hormone receptors." Proc Natl Acad Sci U S A **87**(21): 8684.
York, B. and B. W. O'Malley (2010). "Steroid receptor coactivator (SRC) family: masters of systems biology." J Biol Chem **285**(50): 38743-38750.
Yuan, C. X., M. Ito, et al. (1998). "The TRAP220 component of a thyroid hormone receptor- associated protein (TRAP) coactivator complex interacts directly with nuclear receptors in a ligand-dependent fashion." Proc Natl Acad Sci U S A **95**(14): 7939-7944.

Zhang, X. K., K. N. Wills, et al. (1991). "Novel pathway for thyroid hormone receptor action through interaction with jun and fos oncogene activities." Mol Cell Biol **11**(12): 6016-6025.

Chapter 2

MOLECULAR BASIS FOR GLUCOCORTICOID INDUCTION OF THE KRÜPPEL-LIKE FACTOR 9 GENE IN HIPPOCAMPAL NEURONS

Abstract

Stress has complex effects on hippocampal structure and function, which consequently affects learning and memory. These effects are mediated in part by circulating glucocorticoids (GCs) acting via the intracellular GC receptor (GR) and mineralocorticoid receptor (MR). The molecular mechanisms by which GCs influence hippocampal neurons are poorly understood. Here we investigated GC regulation of Krüppel-like factor 9 (*Klf9*), a transcription factor implicated in neuronal development and plasticity. Injection of corticosterone (CORT) into postnatal day 6 and 30 mice increased *Klf9* mRNA in the hippocampal region. Treatment of the mouse hippocampal cell line HT-22 with CORT caused a time and dose-dependent increase in *Klf9* mRNA. The CORT induction of *Klf9* was resistant to protein synthesis inhibition, suggesting that *Klf9* is a direct CORT response gene. In support of this hypothesis, we identified two GC response elements (GRE/MRE) located -6.1 and -5.3 kb relative to the transcription start site, and we verified their functionality by promoter-reporter, gel shift and chromatin immunoprecipitation assays. The -5.3 kb GRE/MRE is largely conserved across

tetrapods, but conserved orthologs of the -6.1 kb GRE/MRE were only detected in therian mammals. Glucocorticoid treatment caused recruitment of the GR, histone hyperacetylation, and nucleosome removal at *Klf9* upstream regions. Our findings support that GR/MR can directly induce *Klf9* expression acting via two GC response elements located in the 5' flanking region of the mouse *Klf9* gene. Krüppel-like factor 9 may play a key role in GC actions on hippocampal development and plasticity.

Introduction

The hippocampus, a neural structure involved with learning and memory, among other functions, is an important target for the actions of circulating glucocorticoids (GCs) produced basally and in response to stress. Glucocorticoid actions on the hippocampus are complex: they may facilitate or impair hippocampal function by influencing cell survival, dendritic remodeling and synaptic transmission (Joels, Pu et al. 2006; McEwen 2008). The nature of these effects depends on the concentration and duration of elevation in plasma GCs (e.g. severity or duration of the stressor) and the physiological or behavioral context (Joels 2008). In rodents, chronic stress, or repeated exposure to high levels of GCs caused retraction and atrophy of dendrites, neuronal cell death, inhibited long term potentiation (LTP), and impaired hippocampal-dependent cognitive tasks (Watanabe, Gould et al. 1992; Magarinos, Verdugo et al. 1997; McEwen 1999). By contrast, moderate acute stress, mediated in part by GCs, enhanced hippocampal neuronal function and hippocampal-dependent processes (Shors 2001; Shors, Chua et al. 2001; Roozendaal 2002; Beylin and Shors 2003; Karst and Joels 2005; Joels, Pu et al. 2006). Also, basal circulating GCs are required for normal hippocampal function. For example, adrenalectomy in rats caused cell death, reduced cell body area, and decreased dendritic branching in dentate gyrus granule cells, while replacement with CORT prevented these changes (Gould, Woolley et al. 1990). Adrenalectomy also impaired memory in a spatial water-maze task (Roozendaal, Portillo-Marquez et al. 1996; Oitzl, Reichardt et al. 2001).

The actions of GCs are mediated in large part by two nuclear receptors that function as ligand-activated transcription factors - the mineralocorticoid receptor (MR) and the glucocorticoid receptor (GR) (Reul and de Kloet 1985); both are highly expressed in the

mammalian hippocampus (Puymirat 1992; De Kloet, Vreugdenhil et al. 1998). The MR and GR bind to DNA at hormone response elements comprised of two hexanucleotide half sites (Ribeiro, Kushner et al. 1995; Aranda and Pascual 2001) and they recruit coactivator or corepressor complexes that contain histone modifying enzymes. The histone modifications promote an open or closed chromatin environment, thereby influencing the rate of transcription (Aoyagi and Archer 2008).

Stress hormones cause biochemical, physiological and structural changes in neurons, but relatively little is known about the transcriptional mechanisms that underlie these cellular changes (McEwen 2010). Although direct transcriptional targets of the GR have been identified in hippocampal neurons (Datson, van der Perk et al. 2001; Morsink, Steenbergen et al. 2006; Datson, Morsink et al. 2008; Datson, Speksnijder et al. 2010; Datson, Polman et al. 2011) the mechanisms by which GCs influence neuronal structure and function are poorly understood. Earlier we found that the transcription factor Krüppel-like factor 9 (KLF9; or Basic Transcription Element Binding Protein 1; BTEB1) is a direct thyroid hormone (TH) target gene that is strongly upregulated during postnatal brain development (Denver, Ouellet et al. 1999; Denver and Williamson 2009). Krüppel-like factor 9 belongs to the Sp/KLF family of transcription factors that bind to GC and GT rich sequences in the genome (Kaczynski, Cook et al. 2003). Krüppel-like factor 9 plays a key role in TH-dependent actions on neuronal morphology (Denver, Ouellet et al. 1999; Cayrou, Denver et al. 2002). For example, expression of KLF9 in Neuro-2a cells increased neurite extension and branching (Denver, Ouellet et al. 1999), while suppression of KLF9 in primary embryonic rat neuronal cultures inhibited TH-induced neurite branching (Cayrou, Denver et al. 2002). Expression of *Klf9* in the rodent brain

increases in parallel with the postnatal rise in plasma TH (Morita, Kobayashi et al. 2003; Denver and Williamson 2009). Krüppel-like factor 9 deficient mice exhibited reduced dendritic arborization of cerebellar Purkinje cells (Morita, Kobayashi et al. 2003), delayed neuronal maturation and reduced neurogenesis-dependent LTP in the dentate gyrus (Scobie, Hall et al. 2009), and behavioral deficits consistent with abnormal functions of the amygdala, hippocampus and cerebellum (Morita, Kobayashi et al. 2003).

We recently reported that *Klf9* mRNA and protein were strongly induced in *Xenopus* brain by exposure to confinement/shaking stressor (Bonett, Hu et al. 2009). This stressor-induced increase was blocked by treatment with RU486, or mimicked by injection of CORT. Datson et al. (Datson, Polman et al. 2011) recently found *Klf9* to be induced by CORT in primary rat hippocampal neurons, and they provided evidence for two putative GR/MR binding sites in the *Klf9* 5' flanking region. In the current study we investigated the molecular basis for CORT regulation of *Klf9* in mouse hippocampal neurons. We looked at whether CORT could induce *Klf9* expression in mouse hippocampus *in vivo*, and in mouse hippocampal tissue culture cells, and we identified two evolutionarily conserved hormone response elements in the *Klf9* 5' flanking region to which the GR/MR bind to regulate *Klf9* expression.

Materials and Methods

Animal care. We purchased adult wild type C57/BL6J mice from Jackson Laboratories, and Dr. Fujii-Kuriyama kindly provided *Klf9* mutant mice (*Klf9* locus disrupted by insertion of the LacZ gene) (Morita, Kobayashi et al. 2003). Mice were maintained on a 12:12 photoperiod, given food and water *ad libitum*, and bred in the laboratory. We

conducted histochemical staining for β galactosidase using brains from 7 week old heterozygous *Klf9* mutant mice. Wild type mice at postnatal day 6 (PND 6) or 30 (PND 30) were given intraperitonial (i.p.) injections of corticosterone (CORT; Sigma Chemical Co., St. Louis, MO) dissolved in corn oil vehicle at a dose of 14 mg/ kg body weight; control animals received corn oil vehicle or were unhandled. This dose of CORT 1is in the midrange of CORT doses (3-50 mg/kg CORT) reported in the literature to increase plasma CORT within the physiological range (Quadrilatero and Hoffman-Goetz 2005). One hour after injection the animals were killed and brains were collected for analysis. We microdissected the hippocampal region for measurement of *Klf9* mRNA and heteronuclear RNA (hnRNA) by RTqPCR. All experiments were conducted in accordance with the guidelines of the University Committee on the Use and Care of Animals at the University of Michigan.

RNA Extraction, Reverse Transcription and Quantitative PCR. We extracted total RNA from HT-22 cells or the hippocampal region of PND 6 and PND 30 mice using Trizol reagent (Invitrogen) following the manufacturer's protocol. One microgram of total RNA was used for cDNA synthesis using the High Capacity Reverse Transcription kit (Life Technologies Corp., Carlsbad, CA). For quantitative PCR we designed Taqman assays and conducted real time PCR using Absolute qPCR low ROX Mix (ABgene). The primers and Taqman probe used to analyze *Klf9* mRNA expression (Table 1) spanned an exon/intron boundary. Standard curves were constructed using a cDNA pool generated from HT-22 cell RNA to compare relative expression levels. *Klf9* mRNA was

normalized to *GAPDH* mRNA (Applied Biosystems), the expression of which did not change with treatment.

Plasmid Constructs. A chromatin immunoprecipitation (ChIP)-promoter DNA chip (ChIP-chip) assay for MR conducted on a chromatin isolated from HEK293 cells engineered to express myc-tagged human MR (HEK293-hMR+; for methods see (Ziera, Irlbacher et al. 2009) identified two regions of the upstream region of the human *Klf9* gene (T. Ziera and S. Borden, unpublished data). Subsequent bioinformatic analysis revealed that both loci contain putative glucocorticoid/mineralocorticoid response elements (GRE/MRE). These regions were isolated by PCR using human genomic DNA as template; one was 632 bp from -5771 to -5139 bp (fragment 1, centered at ~5.5kb), a second was 336 bp from -4211 to -3875 bp (fragment 2, centered at ~4 kb) relative to the transcription start site (TSS). The DNA fragments were subcloned into the pGL4.23 reporter vector (Promega) at the Xho I and Hind III sites for testing in HEK293-hMR+ cells (Supplemental Materials and Methods). The two orthologous regions of the mouse *Klf9* gene, a 634 bp fragment (fragment 1) located -5776 to -6410 bp upstream of the transcription start site (TSS) and a 336 bp fragment (fragment 2) located -4566 to -4892 bp upstream of the TSS, were isolated by PCR using mouse genomic DNA as template and cloned into pGL4.23. An evolutionarily conserved 179 bp mouse genomic region (from -5333 to -5154 bp upstream of TSS) that contained a GRE/MRE identified by DNAse I footprinting (described below) was also isolated by PCR and cloned into pGL4.23. Plasmid constructs containing genomic DNA fragments with mutated

GRE/MRE half sites were generated using the QuickChange site directed mutagenesis kit (Stratagene) following the manufacturer's protocol (primers in Table 2).

Cell Culture and Transient Transfection Assays. HT-22 is a cell line derived from mouse hippocampus immortalized with the SV40 T antigen (Morimoto and Koshland 1990; Morimoto and Koshland 1990) with properties of differentiated neurons (Morimoto and Koshland 1990; Morimoto and Koshland 1990; Maher and Davis 1996; Sagara, Dargusch et al. 1998). HT-22 expresses functional GR, but has no detectable MR, as ^{3}H-corticosterone binding in HT-22 lysates is completely displaced by RU486 (A. Rozeboom and A. Seasholtz, unpublished data). HT-22/MR16 cells were engineered to express mouse MR by stably transfecting the HT-22 parent cell line with CMV-MR and pPGKpuro plasmids, and selection in 2.5 μg/ml puromycin. The CMV-MR construct contains the full-length mouse MR cDNA (clone pMR-2A; (Rozeboom, Akil et al. 2007) in a CMV expression vector (pCMVneo). The HT-22/MR16 cells exhibit functional MR binding and transcriptional activation of GRE-luciferase constructs with 1-10 nM aldosterone (A. Rozeboom and A. Seasholtz, unpublished data).

We cultured HT-22 and HT-22/MR16 cells in Dulbecco's modified Eagle's medium (DMEM; Invitrogen) supplemented with sodium bicarbonate (2.2 g/L), penicillin G (100 units/mL), streptomycin sulfate (100 μg/mL) and 10% fetal bovine serum (FBS) stripped of thyroid (Samuels, Stanley et al. 1979) and steroid hormones (Yao, Schulkin et al. 2008). Cells were cultured under a humidified atmosphere of 5% CO_2 at 37^{o}C. For gene expression analysis we seeded cells at a density of 2.5 x10^{6} cells per well in 6-well plates; for transient transfection assays we seeded cells at 6.5 x10^{4} cells per well in 24-well

plates. When cells reached 80% confluency, and immediately before hormone treatments, we replaced the growth medium with serum-free DMEM. Corticosterone (CORT; Sigma C2505), dexamethasone (DEX; Sigma D1756), or aldosterone (ALDO; Sigma A9477) were dissolved in 100% ethanol and added to the media to the final concentrations indicated below. Mifepristone (RU486; a GR antagonist; Sigma M8046) was dissolved in ethanol and added to wells to a final concentration of 1 μM 1 h before addition of hormone. 3,5,3'-triiodothyronine (T_3; Sigma T2752) was dissolved in dimethylsulfoxide (DMSO). Control treatments received an equivalent concentration of vehicle (0.001% ethanol and 0.03% DMSO). All hormone treatments were continued for 4 h before cell harvest. Hormone treatment experiments were conducted at least two times with comparable results.

To determine if hormone-dependent induction of *Klf9* mRNA requires ongoing protein synthesis we treated cells with 100 μg/ml of the protein synthesis inhibitor cycloheximide (CHX; Sigma). This dose of CHX reduced protein synthesis by 98% in HT-22 cells (P. Bagamasbad and R. Denver, unpublished data. We treated cells with CHX for 1 h before and for 4 h during treatment with hormone.

For luciferase reporter assays we plated HT-22 cells in DMEM with hormone-stripped FBS, and transfected at 50-60% confluency with 300 ng of the pGL4.23 reporter constructs plus 20 ng of p*Renilla* plasmid (for normalization of transfection efficiency) using the Fugene 6 transfection reagent (Roche, Indianapolis, IN) following the manufacturer's protocol. Immediately before transfection the growth medium was replaced with medium containing hormone-stripped FBS without penicillin/streptomycin, and cells were incubated with the transfection mixture overnight. Twenty four h after

transfection cells were treated in serum free medium with 100 nM CORT or vehicle for 4 h before harvest for luciferase activity using the dual luciferase assay kit (Promega). Each transfection experiment was conducted at least three times with 4-5 wells per treatment.

Electrophoretic mobility shift assay (EMSA). We conducted EMSA as described by Hoopfer et al. (2002) (Hoopfer, Huang et al. 2002) with recombinant human GR generated using the TnT SP6 quick-coupled translation system (Promega) following the manufacturer's protocol. We programmed the reaction with 1 μg of CMV-hGR expression plasmid (OriGene) and confirmed protein expression by [^{35}S]-labeled amino acid incorporation, SDS-PAGE and autoradiography (Hoopfer, Huang et al. 2002). Duplex oligonucleotides corresponding to the predicted GRE/MREs located 6.1 kb and 5.3 kb upstream of the transcription start site (Table 2) were labeled with ^{32}P-dCTP by Klenow fill-in for use as probes in the EMSA. Competitive EMSA using 1.5 μM radioinert wild type or mutant GRE/MRE oligo (Table 2) was done to examine specificity of binding. A ^{32}P-labeled mouse mammary tumor virus (MMTV) probe containing a well characterized GRE was used as a positive control for GR binding (Table 2).

Fluorescent DNAse I footprinting. We conducted DNAse I footprinting as described by Blauwkamp et al. (Blauwkamp, Chang et al. 2008) using the Promega Core Footprinting System protocol. We generated FAM or HEX fluorescent-labeled double stranded DNA probes corresponding to the *mouse Klf9 5' flanking region* (-5333 to -5154 bp; 179 bp). The region corresponding to the DNA binding domain (DBD) of the human GR was PCR-amplified and subcloned it into the TOPO/pET151/D vector (Invitrogen) to make TOPO/pET151/D-hGR-DBD. Bacterially-expressed GR-DBD was purified using the

ProBond system (Invitrogen) following the manufacturer's protocol. We combined 1 μg of GR-DBD with 150 ng HEX(green)-labeled probe in a 50 μl digestion reaction. The FAM(blue)-labeled probe (150 ng) was digested in a 50 μl reaction without added GR-DBD. The two probe digestion reactions were then combined, extracted with phenol/ chloroform, concentrated by ethanol precipitation, and analyzed by Big Dye Terminator Cycle sequencing (Applied Biosystems). Peaks in the chromatograms were assigned to specific nucleotides using FAM-labeled ddATP, ddCTP, ddGTP or ddTTP in a manual sequencing reaction.

Chromatin immunoprecipitation assay. We plated HT-22 cells in 100 mm plates in DMEM with hormone-stripped FBS. Cells were grown to 90% confluency before treatment with 100 nM CORT or EtOH vehicle in serum free medium for 4 h before harvest for chromatin extraction. We also isolated chromatin from the hippocampal region of PND 6 mice 1 h after injection of CORT (14 mg/kg); control animals were left unhandled. Five micrograms of sheared chromatin was used for each reaction, and ChIP assay was conducted as described by Denver and Williamson (Denver and Williamson 2009). Polyclonal rabbit antiserum to mouse GR (5 μg; M-20X; Santacruz Biotechnology) or anti-acetylated histone 3 (AcH3; 5 μl; Millipore) were used for ChIP assay. ChIP samples were analyzed by quantitative real time PCR using Taqman primer/probe sets (Table 1) that were targeted to different regions of the mouse *Klf9* gene.

***Data Analysis and Statistics*.** We analyzed data by one-way ANOVA or Student's *t*-test using the SYSTAT computer program (v.10; SPSS Inc., Chicago, IL). Data from dual luciferase assays (firefly luciferase counts divided by Renilla luciferase counts) and ChIP

assays (the ratio of ChIP signal to input) were $\log_{10}$ transformed before statistical analysis. *P<0.05* was accepted as statistically significant. Gene expression data are reported as the mean±SEM. To predict putative GRE/MRE sites we used the online programs Transcription Element Search System (TESS*;* www.cbil.upenn.edu/tess*)* and Match (www.gene-regulation.com/pub/ programs.html#match) using a library of matrices from TRANSFAC 6.0 (www.gene-regulation.com) with core and matrix similarity of transcription factor binding sites set higher than 0.85. The conservation of the identified GRE/MREs and flanking sequences was assessed using BLAT (http://genome.ucsc.edu/). Extracted sequences were aligned using Clustal W. The percent similarity to mouse was calculated for the GRE/MRE half sites, and nucleotide frequency diagrams were produced with Weblogo (http://weblogo.berkeley.edu/logo.cgi).

Results

Exogenous corticosterone increased *Klf9* mRNA in mouse hippocampus *in vivo*

Immunohistochemical staining for betagalactosidase on coronal brain sections of LacZ-*Klf9* heterozygous mice confirmed that the *Klf9* gene is highly expressed in all regions of the hippocampus (Fig. 1A) (Morita, Kobayashi et al. 2003). Intraperitoneal injection of CORT in PND6 or PND30 mice significantly increased *Klf9* mRNA in the region of the hippocampus 1 h after injection compared with vehicle injected or unhandled controls (Fig. 1B; PND6: $F_{(2, 26)}=17.084$, $p<0.0001$; PND30: $F_{(2, 14)}=6.937$, $p<0.01$; ANOVA). We also observed a significant increase in *Klf9* hnRNA (Fig. 1C; only PND 6 mice were analyzed; $F_{(2, 26)}=10.71$, $p<0.001$; ANOVA).

Corticosterone caused a rapid and dose-dependent increase in *Klf9* mRNA in HT-22 cells

Treatment of HT-22 cells with CORT increased *Klf9* mRNA in a time- and dose-dependent manner (Fig. 2A,B; time: $F_{(5,23)}$=22.06, p<0.0001; dose: $F_{(7,30)}$=37.69, p<0.0001; ANOVA). The level of *Klf9* hnRNA was also greater after CORT treatment (Fig 2C; p<0.05; Student's *t* test). The mean *Klf9* mRNA level was higher at 30 minutes after CORT exposure, and this reached statistical significance at 1 h; a maximal response was reached by 2 h. The EC50 for CORT induction of *Klf9* mRNA (tested at 4 h of hormone exposure) was 5.7 nM, and maximal response was reached at 30 nM. Earlier, we reported that *Klf9* is a TR target gene in rodent and frog brain, and in mouse neuroblastoma cells (Denver, Pavgi et al. 1997; Denver, Ouellet et al. 1999; Hoopfer, Huang et al. 2002; Denver and Williamson 2009). For comparison, we show similar upregulation of *Klf9* mRNA by T_3 in HT-22 cells that was both time and dose-dependent (Supplemental Fig. 1).

Hormone induction of *Klf9* mRNA in HT-22 cells was largely resistant to protein synthesis inhibition. Although CHX tended to reduce basal and hormone-induced (measured after 4 h) *Klf9* mRNA, it did not block the hormone response (Fig. 3A; Control (-CHX): $F_{(2,11)}$= 81.63, p<0.0001; CHX: $F_{(2,11)}$=151.8; p<0.001; ANOVA).

Both GR and MR can regulate the *Klf9* gene, but the GR may predominate

Treatment of HT-22 cells with CORT (100 nM) or the GR-selective agonist DEX (10 nM) caused robust (~3 fold) and similar increases in *Klf9* mRNA measured at 4 h (Fig. 3B; –RU486: $F_{(2,11)}$=42.40, p<0.001; ANOVA). Responses to both CORT and DEX were blocked by co-treatment with the GR receptor antagonist RU486 (Fig. 3B; +RU486:

$F_{(2,11)}$= 3.128; ANOVA). These data clearly show that GC regulation of *Klf9* can be mediated by the GR in HT-22 cells. However, the findings do not rule out a role for the MR in regulating *Klf9* in other cell types because HT-22 cells do not express functional MR protein (A.M. Rozeboom and A.F. Seasholtz, unpublished data). Consistent with a lack of functional MR, HT-22 cells did not respond to ALDO (10 nM; Fig. 3C).

To determine if the MR can mediate corticosteroid actions on *Klf9* gene expression we analyzed hormone responses in HT-22/MR16 cells. Doses of ALDO as low as 1 nM activated a GRE/MRE containing promoter in a transient transfection reporter assay in these cells (A. Rozeboom and A.F Seasholtz unpublished data; the Kd for ALDO binding to the MR is 0.5 - 2.6 nM; (Veldhuis, Van Koppen et al. 1982; Reul and de Kloet 1985; de Kloet, Reul et al. 1990). Treatment of HT-22/MR16 cells with 10 nM ALDO caused a small, but statistically significant increase in *Klf9* mRNA (Fig. 3C; $F_{(8, 27)}$=26.45, $p<0.001$; ANOVA). However, the increase observed with 10 nM ALDO was only 25% of the level induced by 10 nM DEX or 100 nM CORT. In a subsequent experiment we found that ALDO caused a dose-dependent increase in *Klf9* mRNA in HT-22/MR16 cells with an EC50 of 25 nM (Fig. 3D; $F_{(8, 35)}$= 26.45, $p<0.001$; ANOVA). This EC50 is approximately five times greater than the EC50 for CORT in HT-22 cells, and high concentrations of ALDO (>30 nM) can activate GR as well as MR (Arriza, Simerly et al. 1988). Together, these results suggest that MR can mediate induction of *Klf9* transcription in HT-22/MR16 cells, but significantly less than the activation by GR alone (i.e., with DEX) or by GR and MR together (i.e., with CORT).

Identification of functional GRE/MREs in the human and mouse *Klf9* genes

A ChIP-chip assay for MR on chromatin from HEK293-hMR+ cells identified two MR binding sites in the 5' flanking region of the human *Klf9* gene (T. Ziera and S. Borden, unpublished data). One region (fragment 1) was centered at ~-5.5kb, and a second (fragment 2) at ~-4 kb relative to the TSS. Both regions were cloned into the pGL4.23 reporter plasmid to determine whether these MR binding regions support corticosteroid-dependent transcriptional activation. Promoter-reporter assays conducted in HEK293-hMR+ cells showed that only fragment 1 was activated by ALDO, and this response was blocked by the MR specific antagonist RU26752 (Supplemental Fig.2). This genomic region is highly conserved between human and mouse. *In silico* analysis of the human *Klf9* fragment 1 using TESS and Match identified a near perfect palindromic GRE/MRE full site that is completely conserved between mouse (*mKlf9* GRE/MRE 6.1) and human (-5474 bp in human; *hKlf9* GRE/MRE 5.5; Fig. 4A, partial sequence of the 600 bp fragment shown). The GR bound the mouse *Klf9* GRE/MRE-6.1 in EMSA, and this binding was abolished by mutation of the half sites (Fig. 4B).

We cloned the region of the mouse *Klf9* gene (*mKlf9* 634 bp fragment: -6410 to -5776 bp) orthologous to the human fragment 1, and compared the ability of the mouse and human sequences to support CORT-dependent transactivation in transient transfection assays. The *Klf9* promoter-reporter constructs were transfected into HT-22 cells, and the cells treated with 100 nM CORT for 4 h before harvest for dual luciferase assay. Both the human and mouse *Klf9* gene fragments supported CORT-dependent transactivation (Fig. 4C; *hKlf9* GRE/MRE-5.5, 3.3 fold activation, $p<0.0001$; *mKlf9* GRE/MRE-6.1, 2.6 fold activation, $p<0.0001$; Student's *t* test). Mutation of each half site of mouse *Klf9* GRE/MRE-6.1 abolished CORT responsiveness (Fig. 4C).

Earlier we found stressor and CORT-dependent regulation of the *Klf9* gene in *Xenopus* (Bonett, Hu et al. 2009), but we were unable to identify a GRE/MRE in a similar region of the frog gene by comparative sequence analysis using the *Xenopus tropicalis* genome (version 4.1). In a separate study looking for CORT-responsive regions of the frog *Klf9* gene, we used promoter-reporter assays to screen fragments of the frog *Klf9* 5' flanking region, and we discovered that the region -6 to -5 kb relative to the TSS was CORT-responsive (P. Bagamasbad and R.J. Denver, unpublished data). Within this fragment sequence comparison revealed a ~180 bp sequence highly conserved between frog and mammalian *Klf9* genes. This region of the frog *Klf9* gene was previously reported to possess a TH response element (T_3RE) (Furlow and Kanamori 2002). Through DNAse I footprinting with GR-DBD of the orthologous mouse genomic region (179 bp fragment) we identified a GRE/MRE full site that is highly conserved across tetrapods (centered at -5285 bp in mouse, -4634 bp in human, and -5957 bp in frog *Klf9* genes; Fig. 5A, B). We designated this the mouse GRE/MRE-5.3, and confirmed that the GR bound this sequence in EMSA (Fig. 5C). Binding of GR to the GRE/MRE-5.3 probe was competed by unlabeled wildtype, but not by mutated GRE/MRE-5.3 (Fig. 5C). The 179 bp fragment of the mouse *Klf9* gene supported CORT-dependent transactivation in promoter-reporter assay conducted in HT-22 cells (Fig. 5D). Mutation of both half sites of the GRE/MRE-5.3 significantly reduced, but did not eliminate CORT-dependent transactivation (Fig. 5D; $p<0.05$, Student's *t* test).

Chromatin-immunoprecipitation assay conducted with chromatin extracted from the hippocampal region of PND6 mice showed GR association at both the GRE/MRE-6.1 and GRE/MRE-5.3 regions, and this signal was increased by CORT injection (Fig. 6A.

$p<0.05$, Student's *t* test). By comparison, we saw no significant GR ChIP signal at the *Klf9* intronic region (+11 kb from the TSS). In HT-22 cells, acetylation of histone 3 (AcH3) was substantially greater at the two GRE/MRE regions compared to the intron. Treatment of cells with CORT for 4 h increased H3 acetylation at the GRE/MRE-5.3 ($p<0.01$, Student's *t* test) but not at the GRE/MRE- 6.1 or at the intron (Fig. 6B top panel). Treatment with CORT decreased the H3 ChIP signal, but only at the GRE/MRE-5.3 (Fig. 6B bottom panel; $p<0.01$, Student's *t* test).

Evolutionary conservation of the GRE/MREs in vertebrate *Klf9* genes

Bioinformatic analysis of the two GRE/MREs identified in this study (-5.3 and -6.1 kb in mouse) showed that these sequences are highly conserved across species. Both half sites of the mouse GRE/MRE-5.3 are identical across several orders of mammals, a representative lizard and a frog (Fig. 7). There are two nucleotide substitutions in one of the half sites in zebra finch. We located an orthologous region in the galliform genomes (chicken and turkey), but the putative GRE/MRE sequences were highly divergent, and included an insertion mutation in the half site spacer region. We were unable to identify a region orthologous to GRE/MRE-5.3 in ray finned fishes. The GRE/MRE-6.1 is highly conserved across therian mammals, with only a single base substitution in a half site between marsupials and eutherians (Fig. 7). This GRE/MRE occurs within a ~150 base region that is also mostly conserved across therians. We could not identify an orthologous region, nor a GRE/MRE-6.1 in the genomes of a monotreme (platypus), birds (zebra finch, chicken, turkey), a lizard (anole), clawed frogs, or fishes (puffer fish, zebra fish, or stickle back).

Discussion

Glucocorticoids exert profound and complex actions on the central nervous system (CNS), many of which are mediated by the GR and MR. However, the genes regulated by GR and MR, and roles for the protein products of these genes in CNS development and function are poorly understood. Here we describe the identification and functional characterization of two GRE/MREs in the *Klf9* gene, a GC-inducible gene in hippocampal neurons that codes for a transcription factor known to play a role in neuronal structure and function (Denver, Ouellet et al. 1999; Cayrou, Denver et al. 2002; Morita, Kobayashi et al. 2003; Lin, Bloodgood et al. 2008; Bonett, Hu et al. 2009; Scobie, Hall et al. 2009). We found that the mouse *Klf9* gene is induced by GCs, both *in vivo* and in the hippocampal-derived cell line HT-22. The GR is recruited to the *Klf9* gene in a hormone-dependent manner, and this leads to increased histone acetylation and nucleosome eviction at the GRE/MRE-5.3, which is consistent with GCs promoting an open chromatin structure at the *Klf9* locus. These results agree with our prior findings in *Xenopus*, where exposure to handling/shaking stressor or injection of CORT caused rapid and robust increases in *Klf9* mRNA and protein in frog brain (Bonett, Hu et al. 2009).

Injection of CORT increased *Klf9* mRNA in the mouse hippocampal region *in vivo*. Similarly, CORT increased *Klf9* mRNA in HT-22 cells in a time and dose-dependent manner. Increased levels of *Klf9* hnRNA in mouse brain *in vivo* and in HT-22 cells show that CORT increased transcription of the *Klf9* gene. Also, the rapid kinetics of CORT-dependent upregulation of *Klf9* mRNA in HT-22 cells, and the resistance to protein synthesis inhibition support that CORT regulation of *Klf9* transcription is direct. Regulation of *Klf9* by the GR is supported by induction of *Klf9* mRNA in HT-22 cells by

the GR specific agonist DEX, and blockade of DEX and CORT responses by the GR-specific antagonist RU486. These findings parallel our data in *Xenopus* where we found that stressor-induced increases in *Klf9* mRNA in frog brain *in vivo*, or CORT-dependent responses in XTC-2 cells were completely blocked by RU486 (Bonett, Hu et al. 2009).

Our findings in mouse and frog support that *Klf9* is regulated by the GR. We also provide evidence that mammalian *Klf9* genes can be regulated by the MR, although in HT-22 cells the GR may predominate. For example, the GRE/MRE located at -5.5 in human (-6.1 in mouse) was identified by ChIP-chip assay on chromatin from HEK293-hMR+ cells. Promoter-reporter assays conducted in HEK293-hMR+ cells showed that ALDO (10 nM) could induce *Klf9*, which was blocked by the MR-selective antagonist RU26752. ALDO caused a small but significant increase in *Klf9* mRNA in HT-22/MR16 cells; however, this induction was significantly less than the CORT-mediated increase. Taken together, we conclude that while the MR may contribute to the regulation of *Klf9*, this action may be less important than the GR, and may be dependent on the sequence of the GRE/MRE, the cell type, and perhaps the MR:GR ratio.

Krüppel-like factor 9 is directly regulated by GCs in hippocampal neurons via two GRE/MREs located in the 5' flanking region of the gene. ChIP-chip assay identified a GRE/MRE located at -5.5 kb in human *Klf9*, and we confirmed its presence in an orthologous region of the mouse genome (at -6.1 kb), and the functionality of this response element in both species. This sequence, comprising a GRE/MRE of two half sites with a three base spacer (see Fig. 3B) was earlier found by So et al. (So, Cooper et al. 2008) to be bound by GR in mouse C3H10T1/2 mesenchymal stem-like cells. Comparative sequence analysis showed that the GRE/MRE-6.1 is conserved among

several orders of therian mammals, but it is not found in monotremes, or other vertebrates. Datson et al. (Datson, Polman et al. 2011) recently found that the GR binds to this region in rat hippocampal cells. We extend their findings by showing that this sequence supports hormone-dependent transactivation, which is abolished by point mutation of the half sites; that GR binds to this sequence *in vitro;* and that GR associates with this genomic region in a hormone-dependent manner *in vivo*. We also show the therian origin of this response element and conservation over more than 160 million years in mammals (Fig. 7).

We identified a second GRE/MRE located at -5.3 kb in the mouse *Klf9* gene (~800 bp downstream of the GRE/MRE-6.1). This region was not bound by MR in a ChIP-chip assay of chromatin isolated from HEK293-hMR+ cells (T. Ziera and S. Borden, unpublished data); we identified it when doing a promoter-reporter scan of the *Xenopus Klf9* 5' flanking region (P. Bagamasbad and R.J. Denver, unpublished data). The orthologous region of the mouse gene supported GC-dependent transactivation, so we conducted DNAse I footprinting and subsequently identified a GRE/MRE comprised of two half sites with a three base spacer. The GRE/MRE-5.3 half sites are 100% conserved across several mammalian orders, a lizard, and a frog. Datson et al. (Datson, Polman et al. 2011) recently found evidence for a GRE/MRE in this region of the rat *Klf9* gene. We extend their findings by confirming its functionality and high degree of conservation over 370 million years of tetrapod evolution.

The GRE/MRE-5.3 is found within an evolutionarily conserved genomic region of ~180 bp located -5 to -6 kb relative to the TSS in vertebrate *Klf9* genes. Outside of the coding region and the core promoter, there is no evolutionary conservation between frog

and mammal *Klf9* genes, suggesting that this ~180 bp sequence has been subject to strong stabilizing selection owing to the presence of essential *cis* regulatory elements. In *Xenopus* this ~180 bp region was earlier found to contain a functional T_3RE to which TR binds to induce *Klf9* expression during tadpole metamorphosis (Furlow and Kanamori 2002); we confirmed that the mouse has a homologous T_3RE (P. Bagamasbad and R.J. Denver, unpublished data; in addition to a T_3RE located at -3.8 kb relative to the TSS; (Denver and Williamson 2009). The ~180 bp sequence also contains an evolutionarily conserved, predicted GRE/MRE half site adjacent to the T_3RE. However, this region was not protected by the GR-DBD in the DNAse I footprint assay. It is possible that the GR associates with the region of the T_3RE through low affinity DNA binding, or though protein-protein interactions, which could account for the residual CORT response observed when the GRE/MRE-5.3 was mutated.

Chromatin immunoprecipitation assay showed greater GR association at the mouse GRE/MRE-5.3 compared to the GRE/MRE-6.1. This was accompanied by hormone-induced H3 acetylation at the GRE/MRE-5.3 but not at the GRE/MRE-6.1. Histone 3 acetylation is a marker for transcriptionally active chromatin (Aoyagi and Archer 2008), and is necessary to promote nucleosome eviction and chromatin disassembly (Luebben, Sharma et al. 2010). Consistent with this action, we observed hormone-dependent nucleosome eviction (depletion of H3) at the region of the GRE/MRE-5.3 but not at the GRE/MRE-6.1. Although the GR associates with the GRE/MRE-6.1 *in vivo* and *in vitro*, and this sequence can support hormone-dependent transactivation, our findings of GR recruitment and histone modification suggest that the GRE/MRE-5.3 may be a stronger, more important hormone response element *in vivo*. This likely reflects the location of the

GRE/MRE-5.3 within the conserved ~180 bp genomic region, where transcription factors binding to *cis* regulatory elements such as the T_3RE promote an open chromatin structure, thereby allowing for greater GR recruitment and action (P. Bagamasbad and R.J. Denver, unpublished data).

Glucocorticoid actions on the hippocampus require new protein synthesis achieved though transactivation of GC target genes by liganded GR or MR. Recently, some GR/MR genomic targets have been identified in hippocampal neurons (e.g., (Datson, Polman et al. 2011), but little is known about the function of their gene products in hippocampal cell physiology and structure. Earlier we showed that KLF9 is in the pathway induced by TH that promotes differentiation of neuronal cells (Denver, Ouellet et al. 1999; Cayrou, Denver et al. 2002), (Bonett, Hu et al. 2009). Morita et al. (Morita, Kobayashi et al. 2003) found that *Klf9* null mice had reduced dendritic arborization of cerebellar Purkinje cells, and behavioral abnormalities consistent with defects of the hippocampus, cerebellum and amygdala. These mice also displayed impaired late-phase adult hippocampal neurogenesis (Scobie, Hall et al. 2009), a critical component of hippocampal-dependent learning and memory (Toni, Laplagne et al. 2008). Taken together, the findings support a role for KLF9 in mediating corticosteroid and thyroid hormone actions in neuronal development and plasticity.

Table 2.1. Taqman assays used for quantitative real time PCR analysis of gene expression (RT-PCR) and chromatin immunoprecipitation (ChIP) assays.

For RTqPCR

m*Klf9* mRNA
Probe – 5' 6FAM-AAAGTCTATGGAAAATCC 3'
Forward: 5' GCACAAGTGCCCCTACAGT 3'
Reverse: 5' TGTATGCACTCTGTAATGGGCTTT 3'

For ChIP assay

m*Klf9* GRE/MRE-6.1 (-6134 to -6022 relative to the TSS):
Probe – 5' 6FAM- TTCTGACTCACCCAGAGGGCCG 3'
Forward: 5' AAGGACAAACTGTTCCACAACAAC 3'
Reverse: 5' CCCCCCGAGTATGGTTCTG 3'

m*Klf9* GRE/MRE-5.3 (-5232 to -5143 relative to the TSS):
Probe – 5' 6FAM- ACCTGCCTCCTCCGGCTGCTG 3'
Forward: 5' AGAACTGGGACTGTCCTCAAATG 3'
Reverse: 5' TGGCATCGCCCTTTTAAAAA 3'

m*Klf9* intron (+11503 to +11569 relative to the TSS):
Probe – 5' 6FAM-CTTCTGCACTGGTTTTAG 3'
Forward: 5' CGTATAGCTGTTTGAGGTCCATAGTT 3'
Reverse: 5' CCTGGCCTCGTCTCAGAAATT 3'

Table 2.2 Oligonucleotides used for construction of pGL4.23 promoter plasmids, DNAseI footprinting and electrophoretic mobility shift assay (EMSA).

PCR primers to amplify promoter fragments cloned into pGL4.23 vector

mKlf9 GRE/MRE-6.1
Forward: 5' atactcgagGACTAGGGGCTTAAG 3'
Reverse: 5' ataaagcttCGGCCAGGCTGTGCGA 3'

mKlf9 GRE/MRE-5.3
Forward: 5' atactcgagTCCTTGCACGAGTTTGGG 3'
Reverse: 5' ataaagcttATCGCCCTTTTAAAAATCT 3'

PCR primers for site-directed mutagenesis of pGL4.23 promoter plasmids

mKlf9 GRE/MRE 1-6.1 mut: AGGACAaacTGTTCA mutated to GAATTCaacTGTTCA
Forward: 5' GGAGACGGGTGGGAGGGGGGTAAAAGAATTCAACTGTTCCACAACAACCACAG 3'
Reverse: 5' CCTGTGGTTGTTGTGGAACAGTTGAATTCTTTTACCCCCCTCCCACCCGTCTCCA 3'

mKlf9 GRE/MRE 2-6.1 mut: AGGACAaacTGTTCA mutated to AGGACAaacGAAAAA
Forward: 5' GGAGGGGGGTAAAAAGGACAAACGAAAAAACAACAACCACAGGAAACACAGC 3'
Reverse: 5' AGGGCTGTGTTTCCTGTGGTTGTTGTTTTTTCGTTTGTCCTTTTTACCCCCCTCCC 3'

mKlf9 GRE/MRE-5.3 mut: AGGGCAgttTGTTCA mutated to ACCTCAgttGAATCA
Forward:5'GCGGATTCCTCGTCCCCCAATCTACCTCAGTTGAATCAACTGCAGCAAAGAGAG 3'
Reverse: 5'AGCTCTCTTTGCTGCAGTTGATTCAACTGAGGTAGATTGGGGGACGAGGAATCC 3'

PCR primers to amplify fluorescent labeled DNA for DNAseI footprinting

Forward: FAM or HEX 5' TCCTTGCACGAGTTTGGG 3';
Reverse: 5' ATCGCCCTTTTAAAAATCT 3'

EMSA

mKlf9 GRE/MRE-6.1
Sense: 5' gatcAAAAGGACAAACTGTTCCACA 3'
Antisense: 5' gatcTGTGGAACAGTTTGTCCTTTT 3'

mKlf9 GRE/MRE-6.1 mut
Sense: 5' gatcAAAGAATTCAACGAAAAAACA 3'
Antisense: 5' gatcTGTTTTTTCGTTGAATTCTTT 3'

mKlf9 GRE/MRE-5.3
Sense: 5' gatcAATCTAGGGCAGTT TGTTCAACTGCAGCAAA 3'
Antisense: gatcTTTGCTGCAGTTGAACAAACTGCCCTAGATT 3'

mKlf9 GRE/MRE-5.3 mut
Sense: 5' gatcAATCTACCTCAGTTGAATCAACTGCAGCAAA 3'
Antisense: 5' gatcTTTGCTGCAGTTGATTCAACTGAGGTAGATT 3'

MMTV
Sense: 5' gatcGTTGGGTTACAAACTGTTCTAACCA 3'
Antisense: 5' gatcTGGTTAGAACAGTTTGTAACCCAAC 3'

PCR primers for site directed were designed using QuickChange Primer Design tool (Agilent)
Shaded nucleotides represent introduced mutations in the GRE/MRE halfsites.
Lower case letters represent restriction sites for subcloning into the pGL4.23 vector or non-native nucleotides added to the 5' ends for [32P] labeling by Klenow fill-in (for EMSA).

Figures

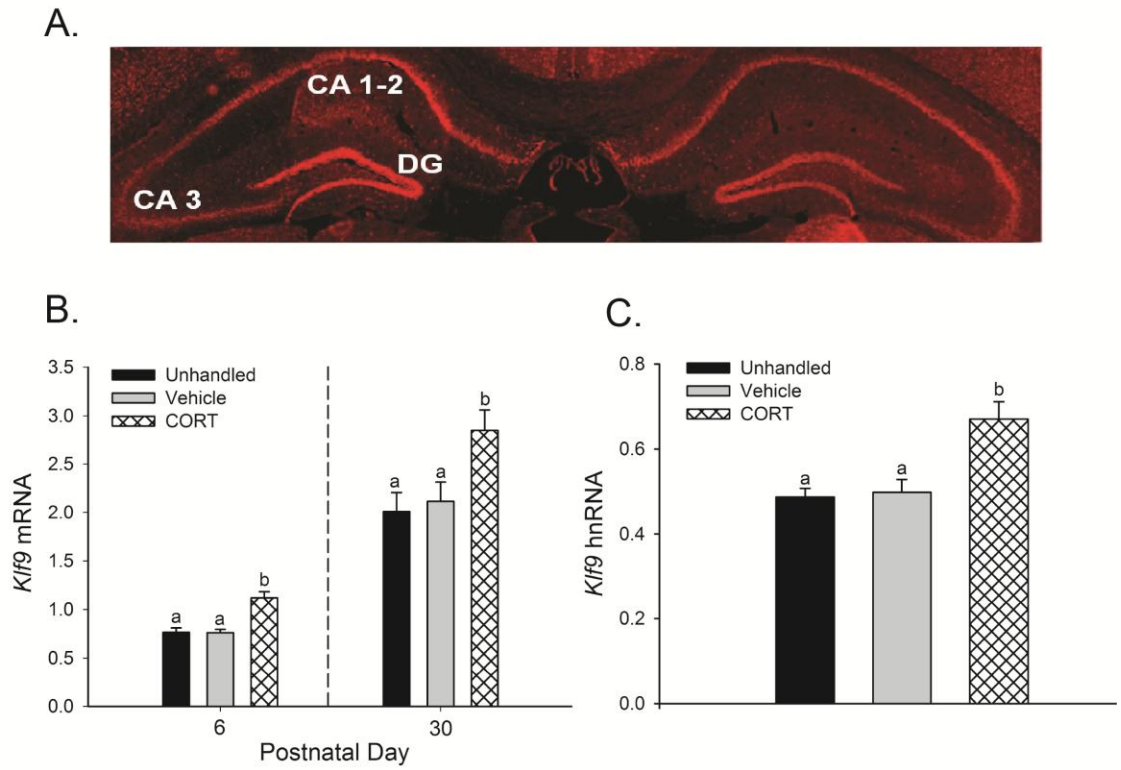

Fig. 2.1. Injection of corticosterone increased *Klf9* mRNA and hnRNA levels in the hippocampal region of the postnatal mouse brain. (A) A representative coronal section of the hippocampal region of a LacZ-*Klf9* heterozygous mouse generated by insertion of LacZ within the coding region of the *Klf9* gene (Morita, Kobayashi et al. 2003). Histochemistry was conducted for beta-galactosidase with immunofluorescent detection using Cy3. **(B)** Postnatal day 6 (PND 6) and day 30 (PND 30) wild type C57/BL6J mice were injected with vehicle (oil), corticosterone (CORT) at a dose of 14 mg/kg bodyweight, or left unhandled. One hour after injection animals were killed, the hippocampal region was dissected and RNA extracted for measurement of *Klf9* mRNA by RTqPCR (n=8 at PND 6, and n=5 at PND 30). **(C)** Postnatal day 6 mice were injected with CORT as described above, and *Klf9* hnRNA was measured by RTqPCR (n= 8). *Klf9* mRNA and hnRNA were normalized to the mRNA level of the housekeeping gene *GAPDH*. Bars represent the mean $\pm$ SEM and letters above the means indicate significant differences among treatments (means with the same letter are not significantly different; Tukey's multiple comparison test; $P<0.05$).

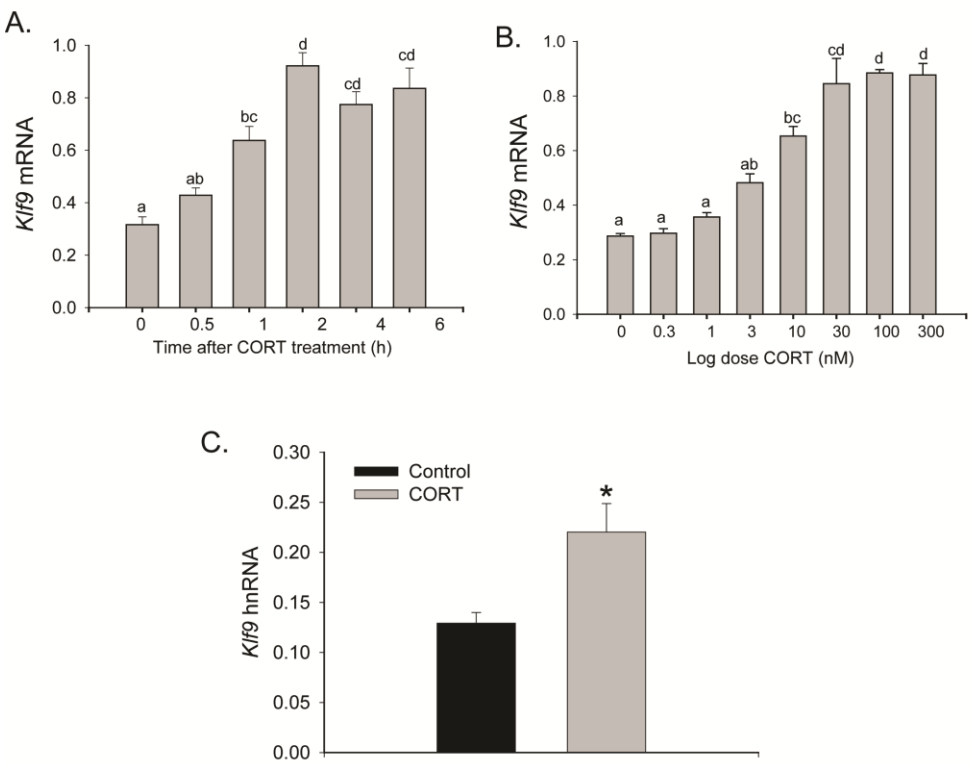

Fig. 2.2. Treatment with corticosterone caused dose and time-dependent increases in *Klf9* mRNA in the mouse hippocampal-derived cell line HT-22. HT-22 cells were treated with 100 nM corticosterone (CORT) for different times **(A)** or with increasing doses of CORT for 4 h **(B)** before harvest and analysis of *Klf9* mRNA. **(C)** HT-22 cells were treated with 100 nM CORT for 4 h before harvest and analysis of *Klf9* hnRNA. In each experiment HT-22 cells were treated with the hormone doses for the times indicated before cell harvest, RNA extraction and analysis by RTqPCR. *Klf9* mRNA and hnRNA were normalized to the mRNA level of the housekeeping gene *GAPDH*. Bars represent the mean $\pm$ SEM (n=4) and letters above the means indicate significant differences among hormone concentrations or time point (means with the same letter are not significantly different; Tukey's multiple comparison test; $P<0.05$).

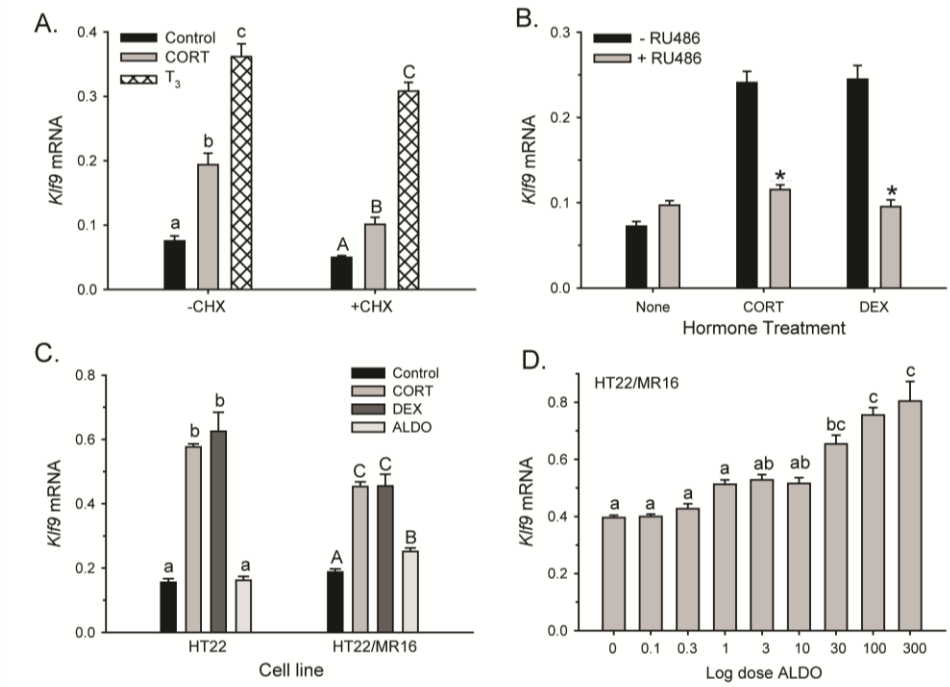

Fig. 2.3. Induction of *Klf9* mRNA by corticosterone in HT-22 cells is resistant to protein synthesis inhibition. *Klf9* can be regulated by the GR or by the MR. (A) HT-22 cells were treated with or without cycloheximide (CHX; 100 μg/ml) for 30 min before addition of corticosterone (CORT; 100 nM) or 3,5,3' triiodothyronine (T_3; 30 nM). Treatment with CHX plus hormones was continued for 4 h before cell harvest for analysis of *Klf9* mRNA. We used T_3 as a positive control since earlier we showed that *Klf9* is a direct TR target gene (Denver and Williamson 2009). **(B)** HT-22 cells were cultured in the presence or absence of the GR-selective antagonist RU486 (1 μM) for 1 h before the addition of vehicle (100% EtOH), 100 nM CORT, or 10 nM of the GR-selective agonist dexamethasone (DEX). Hormone treatment was continued for 4 h before cell harvest and analysis of *Klf9* mRNA. **(C)** HT-22 and HT-22/MR16 cells were treated with vehicle (100% EtOH), 100 nM CORT, 10 nM DEX or 10 nM ALDO for 4 h before cell harvest for analysis of *Klf9* mRNA. **(D)** HT-22/MR16 were treated with increasing concentrations of the MR-selective agonist aldosterone (ALDO) for 4 h before cell harvest for analysis of *Klf9* mRNA. In each experiment cells were treated with the hormone doses for the times indicated before cell harvest, RNA extraction and gene expression analysis by RTqPCR. *Klf9* mRNA was normalized to the mRNA level of the housekeeping gene *GAPDH*. Bars represent the mean ± SEM (n=4) and letters above the means indicate significant differences among hormone concentrations or time point (means with the same letter are not significantly different; Tukey's multiple comparison test; $P<0.05$).

Fig. 2.4. Identification and functional analysis of a GRE/MRE located at -5.5 kb in the human, and -6.1 kb in the mouse *Klf9* genes. **(A)** A ChIP-chip promoter assay conducted on chromatin isolated from HEK293-hMR+ cells identified a fragment of ~600 bp in the human *Klf9* 5' flanking region that contains a functional GRE/MRE (T. Ziera and S. Borden, unpublished data). The sequence alignment is of a portion of this genomic region of human and mouse *Klf9* showing the presence of putative GRE/MRE sites in the two genes (half sites are boxed) predicted by the TESS and Match programs. The numbers to the left of the alignment indicate the positions upstream of the TSS. The GRE/MRE in the human gene is centered at ~-5.5 kb, and the GRE/MRE in the mouse gene is centered at ~-6.1 kb. **(B)** The ability of the GR to bind to the mouse *Klf9* GRE/MRE-6.1 was tested *in vitro* by electrophoretic mobility shift assay (EMSA). Each reaction contained [^{32}P]-labeled GRE/MRE-6.1 oligo as probe (lanes 1-5) and 2 μl of *in vitro* synthesized luciferase protein (control, lane 2) or human GR protein (lanes 3-5). The GR binding to the probe was competed with 1.5 μM radioinert GRE/MRE-6.1 (lane 4) or mutated GRE/MRE-6.1 oligonucleotides (lane 5). We conducted EMSA with a MMTV GRE probe as a positive control for GR binding (right panel). Each reaction contained [^{32}P]-labeled MMTV oligonucleotide as probe (lanes 6-9) and 2 μl of *in vitro* synthesized luciferase protein (control, lane 7) or human GR protein (lanes 8 and 9). The GR binding to the MMTV probe was competed with 1.5 μM radioinert MMTV oligonucleotide (lane 9). The supershifted bands indicated by the arrows are the GR-bound probe. **(C)** Promoter luciferase constructs containing the human GRE/MRE-5.5, mouse GRE/MRE-6.1, and corresponding half site mutants (**X**; A- 5'half site, B- 3'half site) of the mouse GRE/MRE-6.1 were transfected into HT-22 cells. Cells were treated with CORT for 4 h before harvest and analysis by dual luciferase assay. Bars represent the mean $\pm$ SEM (n=5). Asterisks indicate statistically significant differences between vehicle (Control) and CORT treated cells for each promoter-reporter construct ($P<0.0001$; Student's *t* test).

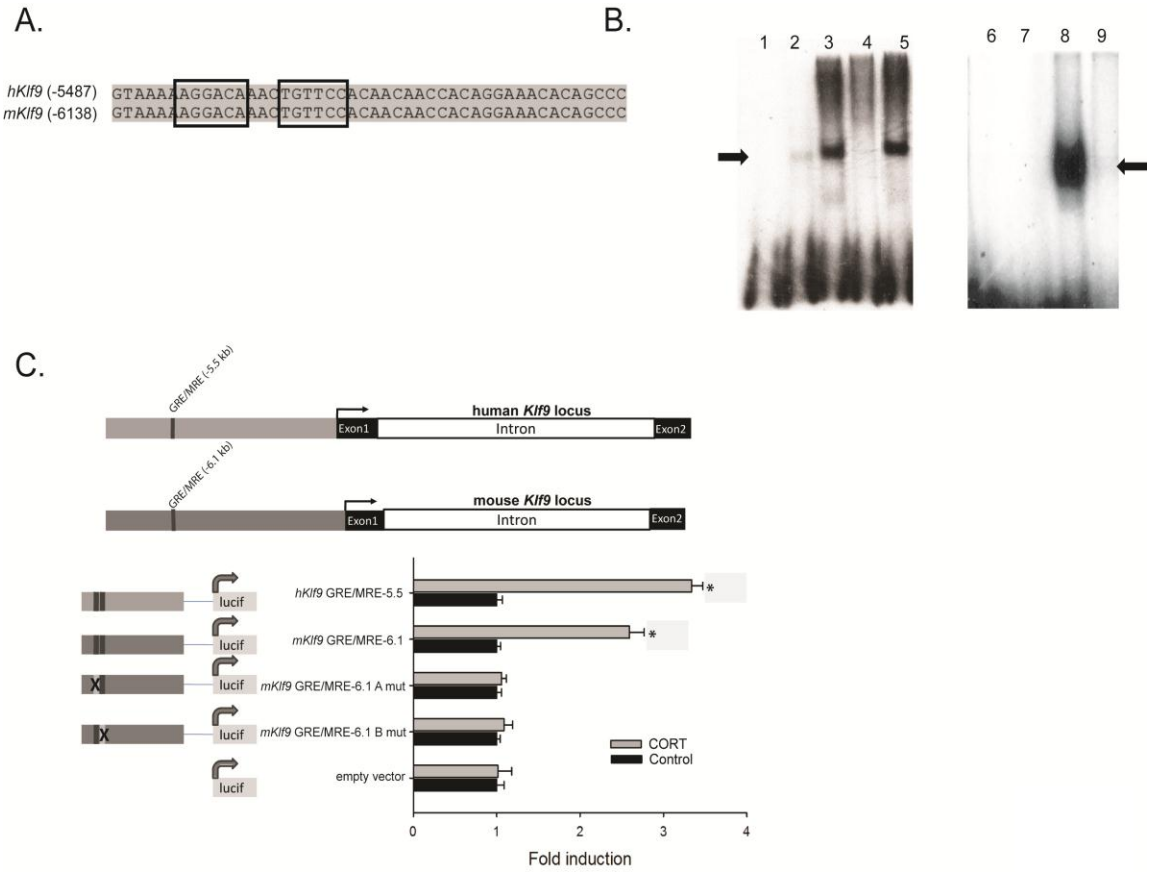
A.
hKlf9 (-5487) GTAAAAAGGACAAACTGTTCCACAACAACCACAGGAAACACAGCCC
mKlf9 (-6138) GTAAAAAGGACAAACTGTTCCACAACAACCACAGGAAACACAGCCC
B.
1 2 3 4 5
6 7 8 9
C.
GRE/MRE (-5.5 kb)
human Klf9 locus
Exon1
Intron
Exon2
GRE/MRE (-6.1 kb)
mouse Klf9 locus
Exon1
Intron
Exon2
lucif
hKlf9 GRE/MRE-5.5
mKlf9 GRE/MRE-6.1
mKlf9 GRE/MRE-6.1 A mut
mKlf9 GRE/MRE-6.1 B mut
empty vector
CORT
Control
0 1 2 3 4
Fold induction

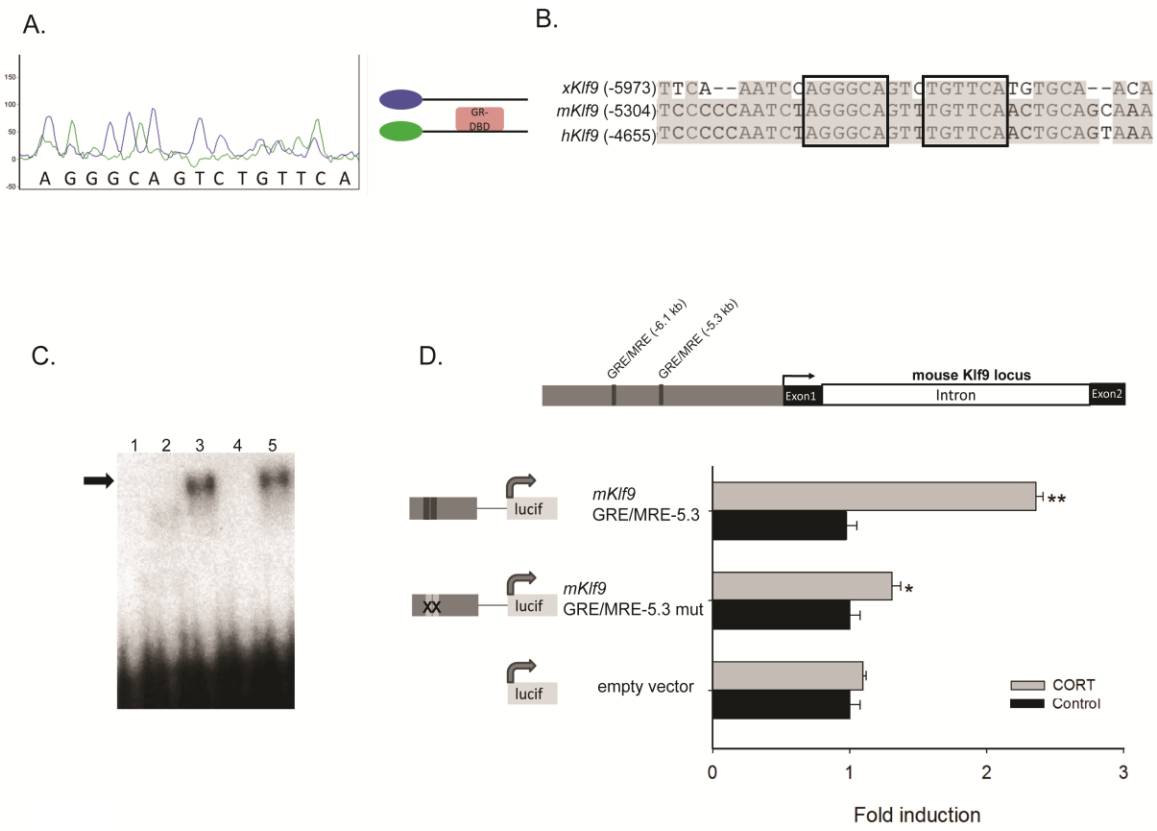

Fig. 2.5. Identification and functional analysis of an evolutionarily conserved GRE/MRE located at -5.3 kb in the mouse (-4.6 kb in the human) *Klf9* gene. (A) DNase I protection assay with the human GR-DBD of the evolutionary conserved 179 bp fragment of the mouse *Klf9* gene identified a GRE/MRE located ~-5.3 kb relative to the TSS (see Materials and Methods). The green traces are from the probe incubated with the GR-DBD, while the blue traces are from the probe incubated without the GR-DBD. Areas where there is a blue peak but no green peak indicate nucleotides protected from DNAse I digestion by the GR-DBD. The nucleotide sequence is shown beneath the traces. **(B)** Sequence alignment showing conservation of the GRE/MREs (mouse GRE/MRE-5.3) in human, mouse and frog *Klf9* genes (GRE/MRE half sites are boxed). The numbers to the left of the alignment indicate the positions upstream of the TSS. The GRE/MRE in the human gene is centered at ~-4.6 kb and in the frog gene at ~-5.9 kb. **(C)** The ability of the GR to bind to the mouse *Klf9* GRE/MRE-5.3 was tested *in vitro* by electrophoretic mobility shift assay. Each reaction contained [^{32}P]-labeled GRE/MRE-5.3 oligo as probe (lanes 1-5) and 2 µl of *in vitro* synthesized luciferase protein (control, lane 2) or human GR protein (lanes 3-5). The GR binding to the probe was competed with 1.5 µM radioinert GRE/MRE-5.3 (lane 4) or mutated GRE/MRE-5.3 oligonucleotides (lane 5). The supershifted bands indicated by the arrow are the GR-bound probe. **(D)** Promoter luciferase constructs containing the mouse GRE/MRE-5.3 and corresponding GRE/MRE-5.3 mutant (**X**) were transfected into HT-22 cells. Cells were treated with CORT for 4 h before harvest and analysis by dual luciferase assay. Bars represent the mean ± SEM (n=5). Asterisks indicate statistically significant differences between vehicle (Control) and CORT treated cells for each promoter-reporter construct (*, P<0.05; **, P<0.0001; Student's *t* test).

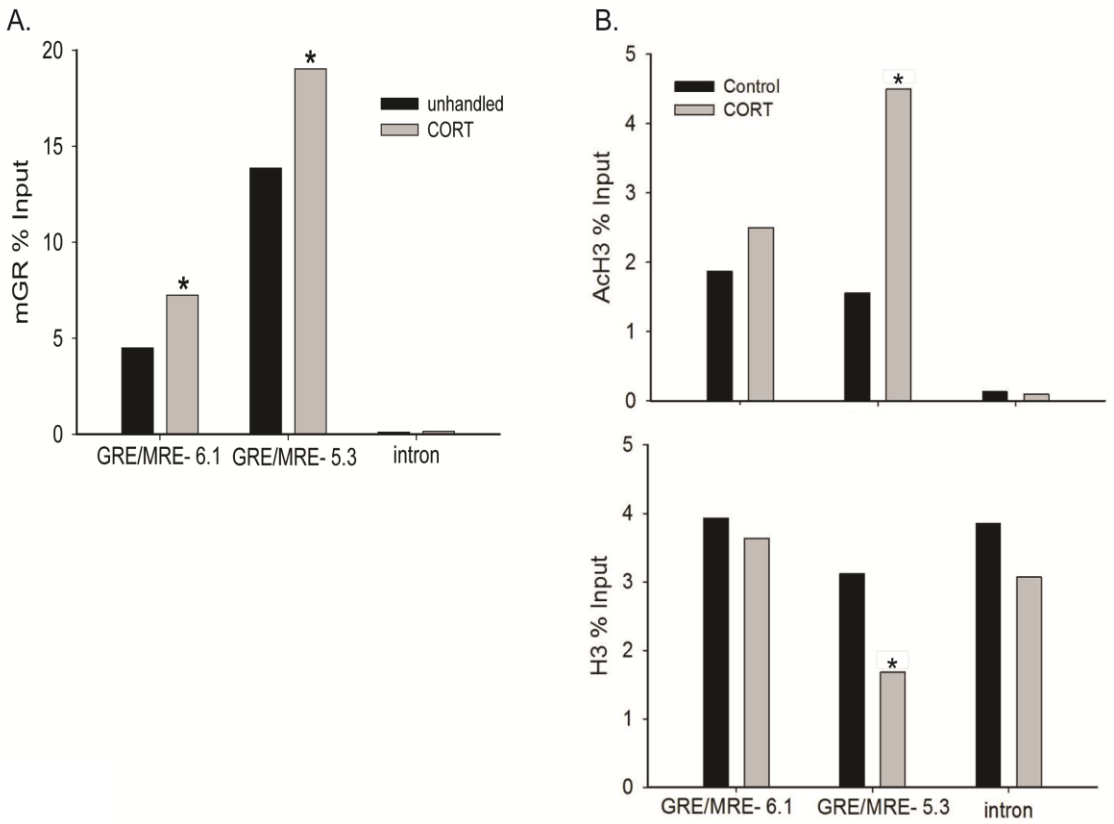

Fig. 2.6. Corticosterone promotes GR association, histone 3 acetylation and nucleosome eviction at the 5' flanking region of the mouse *Klf9* gene. (A) Wild type PND6 mice were injected with corticosterone (CORT) at a dose of 14 mg/kg bodyweight or left unhandled. One hour after injection animals were killed, the hippocampal region was dissected and chromatin extracted for GR ChIP assay. ChIP samples (n=9) were analyzed by RTqPCR using Taqman assays that targeted the GRE/MRE-6.1, GRE/MRE-5.3 or a distal intronic region (negative control) of the mouse *Klf9* gene. Bars represent the mean ChIP signals expressed as a percentage of input. Statistical analysis was conducted on $\log_{10}$ transformed data, and the asterisks indicate statistically significant differences between unhandled and CORT injected animals ($P<0.05$; Student's *t* test). **(B)** HT-22 cells were treated with EtOH vehicle or 100 nM CORT for 4 h before harvest for chromatin extraction and ChIP assay for acetylated histone 3 (AcH3, top panel) and histone 3 (H3, bottom panel). ChIP samples (n=4) were analyzed by RTqPCR using Taqman assays that target the GRE/MRE-6.1, GRE/MRE-5.3 or a distal intronic region (negative control) of the mouse *Klf9* gene. Bars represent the mean ChIP signals expressed as a percentage of input. Statistical analysis was conducted on $\log_{10}$ transformed data, and the asterisks indicate statistically significant differences between vehicle (Control) and CORT treated cells ($P<0.01$; Student's *t* test).

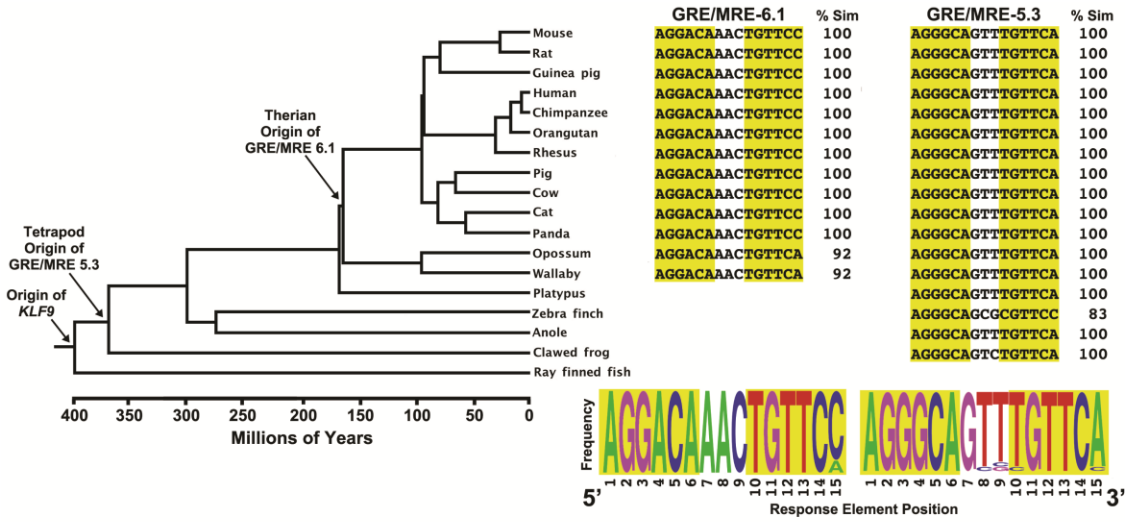

Figure 2.7. **Origin and evolution of two GRE/MREs in vertebrate *Klf9* genes.** Phylogeny of vertebrate relationships with branch lengths scaled to average divergence time estimates (www.timetree.org). Arrows indicate the minimum origin of the *Klf9* gene, and *Klf9* GRE/MREs-5.3 and 6.1 (based on distance from mouse TSS). GRE/MRE sequences for each taxon are shown to the right of the tree (when present). Half sites are highlighted in yellow and their percent similarities to mouse are listed. The frequency of each nucleotide position for the taxa shown is depicted below its respective GRE/MRE alignment.

References

Aoyagi, S. and T. K. Archer (2008). "Dynamics of coactivator recruitment and chromatin modifications during nuclear receptor mediated transcription." Mol Cell Endocrinol **280**(1-2): 1-5.

Aranda, A. and A. Pascual (2001). "Nuclear hormone receptors and gene expression." Physiol Rev **81**(3): 1269-1304.

Arriza, J. L., R. B. Simerly, et al. (1988). "The neuronal mineralocorticoid receptor as a mediator of glucocorticoid response." Neuron **1**(9): 887-900.

Beylin, A. V. and T. J. Shors (2003). "Glucocorticoids are necessary for enhancing the acquisition of associative memories after acute stressful experience." Horm Behav **43**(1): 124-131.

Blauwkamp, T. A., M. V. Chang, et al. (2008). "Novel TCF-binding sites specify transcriptional repression by Wnt signalling." EMBO J **27**(10): 1436-1446.

Bonett, R. M., F. Hu, et al. (2009). "Stressor and glucocorticoid-dependent induction of the immediate early gene kruppel-like factor 9: implications for neural development and plasticity." Endocrinology **150**(4): 1757-1765.

Cayrou, C., R. J. Denver, et al. (2002). "Suppression of the basic transcription element-binding protein in brain neuronal cultures inhibits thyroid hormone-induced neurite branching." Endocrinology **143**(6): 2242-2249.

Datson, N. A., M. C. Morsink, et al. (2008). "Central corticosteroid actions: Search for gene targets." Eur J Pharmacol **583**(2-3): 272-289.

Datson, N. A., J. A. Polman, et al. (2011). "Specific regulatory motifs predict glucocorticoid responsiveness of hippocampal gene expression." Endocrinology **152**(10): 3749-3757.

Datson, N. A., N. Speksnijder, et al. (2010). "The transcriptional response to chronic stress and glucocorticoid receptor blockade in the hippocampal dentate gyrus." Hippocampus.

Datson, N. A., J. van der Perk, et al. (2001). "Identification of corticosteroid-responsive genes in rat hippocampus using serial analysis of gene expression." Eur J Neurosci **14**(4): 675-689.

de Kloet, E. R., J. M. Reul, et al. (1990). "Corticosteroids and the brain." J Steroid Biochem Mol Biol **37**(3): 387-394.

De Kloet, E. R., E. Vreugdenhil, et al. (1998). "Brain corticosteroid receptor balance in health and disease." Endocr Rev **19**(3): 269-301.

Denver, R. J., L. Ouellet, et al. (1999). "Basic transcription element-binding protein (BTEB) is a thyroid hormone-regulated gene in the developing central nervous system. Evidence for a role in neurite outgrowth." J Biol Chem **274**(33): 23128-23134.

Denver, R. J., S. Pavgi, et al. (1997). "Thyroid hormone-dependent gene expression program for Xenopus neural development." J Biol Chem **272**(13): 8179-8188.

Denver, R. J. and K. E. Williamson (2009). "Identification of a thyroid hormone response element in the mouse Kruppel-like factor 9 gene to explain its postnatal expression in the brain." Endocrinology **150**(8): 3935-3943.

Furlow, J. D. and A. Kanamori (2002). "The transcription factor basic transcription element-binding protein 1 is a direct thyroid hormone response gene in the frog Xenopus laevis." Endocrinology **143**(9): 3295-3305.

Gould, E., C. S. Woolley, et al. (1990). "Short-term glucocorticoid manipulations affect neuronal morphology and survival in the adult dentate gyrus." Neuroscience **37**(2): 367-375.

Hoopfer, E. D., L. Huang, et al. (2002). "Basic transcription element binding protein is a thyroid hormone-regulated transcription factor expressed during metamorphosis in Xenopus laevis." Dev Growth Differ **44**(5): 365-381.

Joels, M. (2008). "Functional actions of corticosteroids in the hippocampus." Eur J Pharmacol **583**(2-3): 312-321.

Joels, M., Z. Pu, et al. (2006). "Learning under stress: how does it work?" Trends Cogn Sci **10**(4): 152-158.

Kaczynski, J., T. Cook, et al. (2003). "Sp1- and Kruppel-like transcription factors." Genome Biol **4**(2): 206.

Karst, H. and M. Joels (2005). "Corticosterone slowly enhances miniature excitatory postsynaptic current amplitude in mice CA1 hippocampal cells." J Neurophysiol **94**(5): 3479-3486.

Lin, Y., B. L. Bloodgood, et al. (2008). "Activity-dependent regulation of inhibitory synapse development by Npas4." Nature **455**(7217): 1198-1204.

Luebben, W. R., N. Sharma, et al. (2010). "Nucleosome eviction and activated transcription require p300 acetylation of histone H3 lysine 14." Proc Natl Acad Sci U S A **107**(45): 19254-19259.

Magarinos, A. M., J. M. Verdugo, et al. (1997). "Chronic stress alters synaptic terminal structure in hippocampus." Proc Natl Acad Sci U S A **94**(25): 14002-14008.

Maher, P. and J. B. Davis (1996). "The role of monoamine metabolism in oxidative glutamate toxicity." J Neurosci **16**(20): 6394-6401.

McEwen, B. S. (1999). "Stress and hippocampal plasticity." Annu Rev Neurosci **22**: 105-122.

McEwen, B. S. (2008). "Central effects of stress hormones in health and disease: Understanding the protective and damaging effects of stress and stress mediators." Eur J Pharmacol **583**(2-3): 174-185.

McEwen, B. S. (2010). "Stress, sex, and neural adaptation to a changing environment: mechanisms of neuronal remodeling." Ann N Y Acad Sci **1204 Suppl**: E38-59.

Morimoto, B. H. and D. E. Koshland, Jr. (1990). "Excitatory amino acid uptake and N-methyl-D-aspartate-mediated secretion in a neural cell line." Proc Natl Acad Sci U S A **87**(9): 3518-3521.

Morimoto, B. H. and D. E. Koshland, Jr. (1990). "Induction and expression of long- and short-term neurosecretory potentiation in a neural cell line." Neuron **5**(6): 875-880.

Morita, M., A. Kobayashi, et al. (2003). "Functional analysis of basic transcription element binding protein by gene targeting technology." Mol Cell Biol **23**(7): 2489-2500.

Morsink, M. C., P. J. Steenbergen, et al. (2006). "Acute activation of hippocampal glucocorticoid receptors results in different waves of gene expression throughout time." J Neuroendocrinol **18**(4): 239-252.

Oitzl, M. S., H. M. Reichardt, et al. (2001). "Point mutation in the mouse glucocorticoid receptor preventing DNA binding impairs spatial memory." Proc Natl Acad Sci U S A **98**(22): 12790-12795.
Puymirat, J. (1992). "Thyroid receptors in the rat brain." Prog Neurobiol **39**(3): 281-294.
Quadrilatero, J. and L. Hoffman-Goetz (2005). "In vivo corticosterone administration at levels occurring with intense exercise does not induce intestinal lymphocyte apoptosis in mice." J Neuroimmunol **162**(1-2): 137-148.
Reul, J. M. and E. R. de Kloet (1985). "Two receptor systems for corticosterone in rat brain: microdistribution and differential occupation." Endocrinology **117**(6): 2505-2511.
Ribeiro, R. C., P. J. Kushner, et al. (1995). "The nuclear hormone receptor gene superfamily." Annu Rev Med **46**: 443-453.
Roozendaal, B. (2002). "Stress and memory: opposing effects of glucocorticoids on memory consolidation and memory retrieval." Neurobiol Learn Mem **78**(3): 578-595.
Roozendaal, B., G. Portillo-Marquez, et al. (1996). "Basolateral amygdala lesions block glucocorticoid-induced modulation of memory for spatial learning." Behav Neurosci **110**(5): 1074-1083.
Rozeboom, A. M., H. Akil, et al. (2007). "Mineralocorticoid receptor overexpression in forebrain decreases anxiety-like behavior and alters the stress response in mice." Proc Natl Acad Sci U S A **104**(11): 4688-4693.
Sagara, Y., R. Dargusch, et al. (1998). "Cellular mechanisms of resistance to chronic oxidative stress." Free Radic Biol Med **24**(9): 1375-1389.
Samuels, H. H., F. Stanley, et al. (1979). "Depletion of L-3,5,3'-triiodothyronine and L-thyroxine in euthyroid calf serum for use in cell culture studies of the action of thyroid hormone." Endocrinology **105**(1): 80-85.
Scobie, K. N., B. J. Hall, et al. (2009). "Kruppel-like factor 9 is necessary for late-phase neuronal maturation in the developing dentate gyrus and during adult hippocampal neurogenesis." J Neurosci **29**(31): 9875-9887.
Shors, T. J. (2001). "Acute stress rapidly and persistently enhances memory formation in the male rat." Neurobiol Learn Mem **75**(1): 10-29.
Shors, T. J., C. Chua, et al. (2001). "Sex differences and opposite effects of stress on dendritic spine density in the male versus female hippocampus." J Neurosci **21**(16): 6292-6297.
So, A. Y., S. B. Cooper, et al. (2008). "Conservation analysis predicts in vivo occupancy of glucocorticoid receptor-binding sequences at glucocorticoid-induced genes." Proc Natl Acad Sci U S A **105**(15): 5745-5749.
Toni, N., D. A. Laplagne, et al. (2008). "Neurons born in the adult dentate gyrus form functional synapses with target cells." Nat Neurosci **11**(8): 901-907.
Veldhuis, H. D., C. Van Koppen, et al. (1982). "Specificity of the adrenal steroid receptor system in rat hippocampus." Endocrinology **110**(6): 2044-2051.
Watanabe, Y., E. Gould, et al. (1992). "Stress induces atrophy of apical dendrites of hippocampal CA3 pyramidal neurons." Brain Res **588**(2): 341-345.
Yao, M., J. Schulkin, et al. (2008). "Evolutionarily conserved glucocorticoid regulation of corticotropin-releasing factor expression." Endocrinology **149**(5): 2352-2360.

Ziera, T., H. Irlbacher, et al. (2009). "Cnksr3 is a direct mineralocorticoid receptor target gene and plays a key role in the regulation of the epithelial sodium channel." FASEB J **23**(11): 3936-3946.

Chapter 3

DECIPHERING THE REGULATORY LOGIC OF AN ANCIENT, EVOLUTIONARILY CONSERVED NUCLEAR HORMONE RECEPTOR ENHANCER MODULE

Abstract

Different hormones may cooperate to regulate physiology and development. A striking example is the acceleration of tadpole metamorphosis by the synergistic actions of thyroid hormone (T_3) and glucocorticoid (GC). Krüppel-like factor 9 (KLF9) is a transcription factor that mediates hormone action during development; the *Klf9* gene is directly regulated by T_3 receptor (TR) and GC receptor (GR). We investigated whether the *Klf9* gene is synergistically activated by T_3 plus GC. Gene expression analysis in frog and mouse cell lines, and in tadpole and mouse brain showed that treatment with T_3 plus GC synergistically activated *Klf9*. Kinetic analysis of mRNA and heteronuclear RNA accumulation supported that synergy occurred at the transcriptional level. Transfection assays with reporter constructs containing 1 kb fragments of the 5' flanking region of the frog *Klf9* gene identified a region between -5 and -6 kb that supported synergistic transactivation. Comparative sequence analysis showed an evolutionarily conserved region of ~180 bp within the -5 to -6 kb fragment. The frog and mouse ~180 bp

sequences conferred synergistic transactivation, supporting that this region comprises an enhancer module; we therefore designated this as the *Klf9* synergy module. *In silico* analysis identified three putative hormone response element (HRE) half sites for TR and GR, and a NFκB site that overlaps with the middle and the 3' half sites. Using gel shift, DNAseI footprinting and chromatin immunoprecipitation (ChIP) assays we found that TR and GR associate with specific sequences within the enhancer module. Site-directed mutagenesis of the HRE half sites support that these sequences form a composite TR/GR HRE; mutation of the half sites attenuated or abolished the synergistic response, supporting that direct DNA binding by TR and/or GR are necessary for synergistic transactivation. Using a series of ChIP assays, we found that T_3 plus GC treatment caused synergistic recruitment of GR and stalled RNA polymerase II at the *Klf9* synergy module and surrounding region. Association of RNA pol II also correlated with transcription at the *Klf9* synergy module. These findings support that the synergistic action of GC and T_3 in development may be mediated by the synergistic upregulation of immediate early genes like *Klf9*, and that synergistic gene regulation by T_3 and GC may be a general, and important phenomenon in animal development.

Introduction

The hormones produced by the thyroid (HPT) and adrenocortical (HPA; stress) endocrine axes play critical roles in animal development, physiology and behavior. Recent findings show that thyroid hormone (T_3) and corticosteroids (primarily glucocorticoids – GCs) cooperate during organogenesis, and may act synergistically to regulate tissue formation and remodeling. The broader significance of this interaction is that stress hormones, whose production changes in response to variation in the internal and external environment, may modulate tissue responses to T_3, a potent developmental signaling molecule. This is perhaps best exemplified in amphibians, where GCs have been shown to accelerate T_3-dependent metamorphosis by increasing tissue sensitivity to the T_3 signal (Kikuyama, Niki et al. 1983; Galton 1990; Kikuyama, Kawamura et al. 1993; Denver 2009; Bonett, Hoopfer et al. 2010). In mammals, T_3 and GC act in synergy during fetal lung maturation by promoting alveolar epithelial differentiation, which is essential for air exchange immediately after birth (Smith and Sabry 1983; Metzger, Klein et al. 2008; Pei, Leblanc et al. 2011). Thyroid hormone and GC were found to synergistically regulate the activity of intestinal enzymes required for intestinal maturation at a period that coincides with weaning in rodents. This is hypothesized to be an important adaptative physiological response as the animal switches from liquid to solid food (McDonald and Henning 1992). Synergistic regulation by T_3 and GC is also observed in the expression of the growth hormone (GH) and GH-releasing hormone (GHRH) receptor gene in rat pituitary and somatotropic cell lines (Martial, Seeburg et al. 1977; Shapiro, Samuels et al. 1978; Nogami, Yokose et al. 1995), and may play an important role in controlling body growth in juvenile animals. In humans, stress

hormones and a stressful uterine environment accelerates fetal brain maturation and development, a process which is also developmentally regulated by T_3 (Porterfield and Hendrich 1993; Challis, Sloboda et al. 2001; Welberg and Seckl 2001; Amiel-Tison, Cabrol et al. 2004). The actions of stress hormones and T_3 on organ formation and maturation leads to accelerated fetal development in conditions of intrauterine stress, which is associated with earlier parturition, and may represent an adaptive response that improves postnatal survival (Challis, Sloboda et al. 2001; Amiel-Tison, Cabrol et al. 2004). Thus, through the coordinated action of T_3 and GC in promoting the development of common target tissues, environmental signals may be transduced into developmental responses that enable an organism to modulate its rate of development.

The synergistic actions of T_3 and GC during development are mediated by their cognate nuclear hormone (NR) receptors: thyroid hormone (TR) and the mineralocorticoid (MR) and glucocorticoid (GR) receptors (Reul and de Kloet 1985; Aranda and Pascual 2001). The MR, GR and TR function as ligand-activated transcription factors by binding to DNA at hexanucleotide half sites; NRs typically function as dimers, and therefore bind to two half sites that form a hormone response element (HRE) (Ribeiro, Kushner et al. 1995; Aranda and Pascual 2001). In the unliganded state the TRs are typically bound to DNA where they recruit corepressors that in turn recruit histone deacetylases (HDACs) and other histone modifying enzymes that create a compact, repressive chromatin structure (Cheng, Leonard et al. 2010) Upon hormone binding the corepressors are exchanged for coactivators that acetylate lysine residues on histone tails, among other histone modifications, thereby promoting an open, transcriptionally active chromatin structure (Roeder 2005; Wolf, Heitzer et al. 2008;

Cheng, Leonard et al. 2010) . By contrast, the MR and GR are found in the cytosol in the unliganded state, but translocate to the nucleus and bind to DNA when hormone is present (Aranda and Pascual 2001; Germain, Staels et al. 2006). Depending on the tissue type and target gene, the MR and GR recruit coactivators or corepressors that promote chromatin modifications leading to transactivation or transrepression, respectively (Robyr, Wolffe et al. 2000; Aoyagi and Archer 2008).

The synergistic interaction between transcription factors is a common phenomenon observed during development and allows for a rich array of transcriptional responses to ensure genes are expressed at the appropriate time and place (Courey 2001). The competence of a cell to synergistically respond to T_3 and GC-dependent signaling may depend on GC-dependent enhancement of tissue sensitivity to T_3 and vice versa, resulting from enhanced TR/GR expression by autoinduction or cross-regulation, or the synergistic expression of common TR and GR target genes, most of which are transcription factors. The combined effects of these mechanisms results in an amplification of gene regulation, leading to enhanced responses to T_3 and GC.

Krüppel-like factor 9 (*Klf9*; or Basic Transcription Element Binding Protein 1; *Bteb1*) is a gene that we found to be a direct TR and GR/MR target (Chapter 2; (Denver, Ouellet et al. 1999; Bagamasbad, Howdeshell et al. 2008; Bonett, Hu et al. 2009; Denver and Williamson 2009). Krüppel-like factor 9 belongs to the Sp/KLF family of transcription factors that bind to GC and GT rich sequences in the genome (Kaczynski, Cook et al. 2003). It is strongly upregulated in the brain during postnatal development in frog and rodents (Denver, Ouellet et al. 1999; Denver and Williamson 2009), and its expression is dependent on T_3 (Denver, Pavgi et al. 1997; Denver, Ouellet et al. 1999;

Furlow and Kanamori 2002; Hoopfer, Huang et al. 2002; Denver and Williamson 2009). In both the tadpole and rodent brain, *Klf9* mRNA exhibits a coordinate increase with TRβ mRNA and protein (Porterfield and Hendrich 1993; Denver, Ouellet et al. 1999; Shi 2000; Morita, Kobayashi et al. 2003; Bagamasbad, Howdeshell et al. 2008; Denver and Williamson 2009). We showed that KLF9 function as an intermediary in T_3-dependent neuronal morphologenesis (Denver, Ouellet et al. 1999; Cayrou, Denver et al. 2002). A KLF9-deficient mouse line exhibited decreased dendritic branching of cerebellar Purkinje cells, that was accompanied by reduced activity in behavioral tests that define functions of the cerebellum, hippocampus and amygdala (Morita, Kobayashi et al. 2003). Scobie and colleagues [27] recently showed that these mice have delayed neuronal maturation and reduced neurogenesis-dependent LTP in the dentate gyrus (Scobie, Hall et al. 2009).

In a pilot experiment using frog tissue culture cells we found evidence that *Klf9* mRNA is synergistically upregulated by combined treatment with T_3 and GC. In the present study, we report that synergistic regulation of *Klf9* is observed in frog and mouse brain *in vivo* and in tissue culture cells. This synergy depends on an evolutionarily conserved enhancer module located ~6 kb upstream of the transcription start site which we designate the '*Klf9* synergy module'. We also provide evidence that hormone synergy is mediated by a composite HRE located within the *Klf9* synergy module, that liganded TR creates an open chromatin environment allowing for enhanced recruitment of the GR, that stalled RNA polymerase II (Pol II) is enriched at the synergy module, and that the upstream region interacts with the *Klf9* promoter through chromosomal looping.

Materials and Methods

Animal care. *Xenopus tropicalis* tadpoles at Nieuwkoop-Faber (NF; REF) stage 52-54 were treated with 3,5,3'- triiodothyronine (T_3 Sigma, St. Louis, MO; 1, 5, or 50 nM), CORT (100 nM), T_3 plus CORT or an equivalent volume of ethanol (0.001%) as vehicle control. Tadpoles were maintained in 4L aquaria and hormone was added to their rearing water. Hormone treatment was done for 24 h, with hormones replenished at 12h. At sacrifice, the brain was collected for subsequent RNA isolation and gene expression analysis by RTqPCR (see below).

Adult wild type C57/BL6J mice were purchased from Jackson Laboratories. Mice were maintained on a 12L:12D photoperiod, given food and water *ad libitum*, and bred in the laboratory to generate offspring for analysis. Wild type mice at postnatal day 6 (PND 6) were given intraperitonial (i.p.) injections of (T_3; Sigma) dissolved in 100% DMSO at a dose of 25 ug/kg body weight (Denver and Williamson 2009), corticosterone (CORT; Sigma Chemical Co., St. Louis, MO) dissolved in corn oil vehicle at a dose of 14 mg/ kg body weight (Chapter 2) or T_3 plus CORT; control animals received corn oil plus DMSO as vehicle or were left unhandled. One hour after injection the animals were killed and brains were collected for gene expression analysis. We microdissected the brains to recover the hippocampal region for measurement of *Klf9* mRNA by RTqPCR (described below). All experiments were conducted in accordance with the guidelines of the University Committee on the Care and use of Animals at the University of Michigan.

RNA Extraction, Reverse Transcription and Quantitative PCR. Total RNA was extracted from tadpole and mouse brain, and tissue culture cells using Trizol reagent

(Invitrogen) following the manufacturer's protocol. One microgram of total RNA was used for cDNA synthesis using the High Capacity Reverse Transciption kit with RNAse inhibitors from Applied Biosystems (Life Technologies Corp., Carlsbad, CA). For quantitative PCR we designed Taqman assays and conducted real time PCR using an ABI 7500 fast real time PCR machine with Absolute qPCR low ROX Mix (ABgene). The primers and Taqman probes used to analyze *Klf9* mRNA expression spanned an exon/intron boundary (see Table 1). Standard curves were constructed using cDNA pools to compare relative expression levels. *Klf9* mRNA was normalized to *GAPDH* mRNA (mouse, Applied Biosystems assay # 4331182) and ribosomal protein L8 (frog). Expression of *GAPDH* or *rpL8* mRNAs did not change with any of the treatments (data not shown).

Plasmid Contructs. One kilobase fragments from -7 kb to 0 kb upstream of the *X. tropicalis Klf9* transcription start site (TSS) and the evolutionarily conserved ~180 bp genomic region of the mouse and frog *Klf9* gene (*Klf9* synergy module - described in Results; mouse: from -5333 to -5154 bp; frog: from -6000 to -5836 bp upstream of TSS) were PCR-amplified. The fragments were cloned into the pGL4.23 promoter-luciferase reporter vector at the XhoI and HindIII sites. Plasmid constructs containing the mouse *Klf9* synergy module (a 179 bp fragment) with mutated TRE and GRE/MRE half sites were generated using the QuikChange site directed mutagenesis kit (Stratagene) following the manufacturer's protocol.

Cell Culture and Transient Transfection Assays. *Xenopus laevis* embryonic fibroblast (XTC-2) and renal epithelium (A6)-derived cell lines were cultured in Leibovitz L-15 medium (diluted 1:1.5 for amphibian cells) supplemented with sodium bicarbonate (2.2 g/L), penicillin G (100 units/mL), streptomycin sulfate (100 μg/mL) and 10% fetal bovine serum (FBS) that had been stripped of thyroid (Samuels, Stanley et al. 1979) and steroid hormones (Yao, Schulkin et al. 2008). Amphibian cells were cultured under a humidified atmosphere of 5% CO_2 at 25^{o}C.

HT-22 is a cell line derived from mouse hippocampus immortalized with the SV40 T antigen (Morimoto and Koshland 1990; Morimoto and Koshland 1990). This cell line exhibits properties of differentiated neurons; e.g., they express neuron specific markers such as enolase and the neurofilament triplet, but not the glial cell marker, glial fibrillary acidic protein (Morimoto and Koshland 1990; Morimoto and Koshland 1990; Maher and Davis 1996; Sagara, Dargusch et al. 1998).). HT-22 expresses functional GR, but has no detectable MR, as ^{3}H-corticosterone binding in HT-22 lysates is completely displaced by RU486 (A. Rozeboom and A. Seasholtz, unpublished data; see Chapter 2). We cultured HT-22 cells in Dulbecco's modified Eagle's medium (DMEM; Invitrogen) sodium bicarbonate (2.2 g/L), penicillin G (100 units/mL), streptomycin sulfate (100 μg/mL) and 10% fetal bovine serum (FBS) that had been stripped of thyroid (Samuels, Stanley et al. 1979) and steroid hormones (Yao, Schulkin et al. 2008). Cells were cultured under a humidified atmosphere of 5% CO_2 at 37^{o}C.

For gene expression analysis we seeded cells at a density of 2.5 x10^{6} cells per well in 6-well plates; for transient transfection assays we seeded cells at 6.5 x10^{4} cells per well in 24-well plates. When cells reached 80% confluency, and immediately before hormone

treatments, we replaced the growth medium with serum-free L-15 (XTC-2 and A6) or DMEM (HT-22). Corticosterone (CORT; Sigma C2505) was dissolved in 100% ethanol and added to the medium to the final concentrations indicated below. Triiodothyronine was dissolved in dimethylsulfoxide (DMSO). Control treatments received an equivalent concentration of vehicle (0.001% ethanol and 0.03% DMSO). All hormone treatments were continued for 4 hr before cell harvest.

For luciferase reporter experiments, we plated cells in L-15 (XTC-2 and A6) or DMEM (HT-22) with hormone stripped FBS and transfected at 50-60% confluency with 250 ng of the pGL4.23 reporter constructs plus 20 ng of p*Renilla* plasmid (for normalization of transfection efficiency by dual luciferase assay) using the Fugene 6 transfection reagent (Roche, Indianapolis, IN) following the manufacturer's protocol. Immediately before transfection the growth medium was replaced with medium containing hormone-stripped FBS without penicillin/streptomycin, and cells were incubated with the transfection mixture overnight. Cells were then treated in serum free media with vehicle (0.03 % DMSO, 0.001% ethanol), T3 (30 nM), CORT (100 nM), or T3 plus CORT for 4 h before harvest for luciferase activity using the dual luciferase assay kit (Promega). Luciferase activity was quantified using a luminometer (Femtometer FB 12; Zylux Corp., Maryville, TN). Each transfection experiment was conducted at least three times with 4-5 wells per treatment.

To determine if hormone-dependent induction of *Klf9* mRNA requires ongoing protein synthesis we treated cells with the protein synthesis inhibitor cycloheximide (CHX; Sigma). We first determined the dose of CHX to be used to block protein synthesis in XTC-2 (10 or 20 μg) and HT-22 (100 or 500 μg) cells by labeling cells with

[^{35}S]-ExPress protein labeling mix ([^{35}S]- methionine plus [^{35}S]cysteine; Perkin Elemer) and measuring radioactivity incorporated into trichloroacetic acid (TCA)-precipitable protein. We plated XTC-2 and HT-22 cells in 6-well plates and grew them to 80% confluency in growth medium (L-15 for XTC-2 and DMEM for HT-22 supplemented with pen/strep and 10% FBS). We then replaced the medium with methionine and cysteine-deficient L-15 or DMEM supplemented with penicillin/streptomycin and 10% FBS, and cultured cells for 2 hr before adding 10 μCi/well of [^{35}S]-ExPress protein labeling mix. Simultaneously, we added CHX (10 μg for XTC-2 cells; 100 μg for HT-22 cells) dissolved in ethanol or ethanol vehicle (final concentration 0.001%). After a 6 hr incubation we harvested cells and precipitated proteins with 10% ice-cold TCA. The precipitates were suspended in scintillation cocktail and radioactivity measured by liquid scintillation counting.

Electrophoretic mobility shift assay (EMSA). We conducted EMSA as described by Hoopfer et al. (2002) with recombinant *X. laevis* TRβ and RXRα, and human GR that we synthesized *in vitro* using the TnT SP6 quick-coupled translation system (Promega) following the manufacturer's protocol. We programmed the reactions with 1 μg of the pSP76-xTRβ, pSP76-xRXRα (gifts of Yun Bo Shi) or CMV-hGR (OriGene) plasmids and confirmed protein expression by [^{35}S]-labeled amino acid incorporation, SDS-PAGE and autoradiography (see Hoopfer et al., 2002). Duplex oligonucleotides corresponding to the predicted T_3 response element (T_3RE) and the GRE/MRE located within the *Klf9* synergy module (mouse GRE/MRE-5.3; Chapter 2) both located within the synergy module, and the upstream GRE/MRE (mouse GRE/MRE-6.1; Chapter 2) were labeled

with ^{32}P-dCTP by Klenow fill-in for use as probes in the EMSA. Competitive EMSA for TR/RXR or GR binding to [^{32}P]-labeled probes was conducted with 1.5 μM duplex oligonucleotides corresponding to the wild type and mutant forms of the predicted T_3RE located within the *Klf9* synergy module; wild type and mutant upstream GRE/MRE (mouse GRE/MRE-6.1), or PCR-generated full length mouse *Klf9* synergy module. A [^{32}P]-labeled T_3RE probe from the *X. laevis* TRβ gene (Machuca, Esslemont et al. 1995) and a mouse mammary tumor virus (MMTV) GRE probe (Yao, Schulkin et al. 2008) were used as positive controls for TR/RXR and GR binding, respectively.

Chromatin Immunoprecipitation assay. We isolated chromatin from HT-22 cells treated with vehicle (ethanol and DMSO), T_3 (30 nM), CORT (100 nM) or T_3 plus CORT. We also isolated chromatin from the hippocampal region of PND 6 mice 1 hr after injection of vehicle (oil), or CORT (14 mg/kg); a group of control animals were left unhandled. Five micrograms of sheared chromatin were used for each reaction, and ChIP assay was conducted as described by Denver and Williamson (Denver and Williamson 2009). Polyclonal rabbit antiserum to *X. laevis* TR (PB, 5 μl; gift of Yun Bo Shi), mouse GR (5 μg; M-20X, Santacruz Biotechnology), RNA polymerase II Ser5 (2 μg, abcam 5131-50), RNA polymerase II Ser2 (2 μg, Abcam 5095), histone 3, anti-acetylated histone 3 (AcH3) or histone (AcH4) (5 μl, Millipore) were used for ChIP assay. ChIP samples that were prepared previously by Denver and Williamson (Denver and Williamson 2009) from PND5 T_3-injected mouse brain and T_3-treated N2a[TRβ] cells were also used. ChIP samples were analyzed by quantitative real time PCR using Taqman primer/probe sets that were targeted to different regions of the mouse *Klf9* gene (Table 3.1).

***Data Analysis and Statistics*.** Data were analyzed by one-way ANOVA or Student's *t*-test using the SYSTAT computer program (version 10; SPSS Inc., Chicago, IL). Data for dual luciferase assays (firefly luciferase counts divided by pRenilla luciferase counts) and ChIP assays (expressed as the ratio of ChIP signal to input) were $\log_{10}$ transformed before statistical analysis. *P<0.05* was accepted as statistically significant. Gene expression data are reported as the mean $\pm$ SEM. A synergistic effect of T_3 and CORT on gene expression and ChIP signal is defined as: (1) a greater than additive effect by one standard deviation with combined hormone treatment, or (2) no effect with T_3 or CORT alone but a significant effect with combined hormone treatment (Bonett, Hoopfer et al. 2010).

Results

Treatment with thyroid hormone plus corticosterone produced a synergistic increase in *Klf9* mRNA in tadpole and mouse brain *in vivo*

Treatment with T_3 or CORT alone by addition to the aquarium water caused a significant increase in *Klf9* mRNA in the tadpole brain, while combined treatment with T_3 and CORT led to a synergistic increase in *Klf9* mRNA (1nM T_3: 2.67 fold change; 100 nM CORT: 2 fold change; T_3 plus CORT: 5.75 fold change; $F_{(6, 41)}=47.99$, $p<0.001$; Fig. 3.1A; ANOVA). Similarly in the mouse, intraperitoneal injection of T_3 or CORT alone caused a significant increase in *Klf9* mRNA in the hippocampus 1 hr after injection compared with vehicle injected or unhandled controls. Combined treatment with T_3 plus CORT caused a synergistic increase in *Klf9* mRNA (T_3: 3 fold change; CORT: 1.5 fold change; T_3 plus CORT: 7 fold change; $F_{(4, 25)}=121.4$, $p<0.01$; Fig. 3.1B; ANOVA).

Treatment with thyroid hormone plus corticosterone caused a synergistic increase in *Klf9* mRNA in frog and mouse tissue culture cells

Treatment of frog XTC-2 or A6 cells with T_3 or CORT increased *Klf9* mRNA, while combined treatment of T_3 plus CORT caused a synergistic increase in *Klf9* mRNA (XTC-2; T_3: 1.6 fold change; CORT: 1.6 fold change; T_3 plus CORT: 5 fold change $F_{(3,15)}$= 85.01, $p< 0.01$; A6; T_3: 4 fold change; CORT: 12 fold change; T_3 plus CORT: 53 fold change; $F_{(3,15)}$= 93.59, $p< 0.01$; Fig. 3.1C; ANOVA). In HT-22 cells T_3 and CORT also independently and synergistically increased *Klf9* mRNA. The synergistic effect of T_3 plus CORT on *Klf9* gene expression in HT-22 cells was seen after 1, 2, 4 and 6 h of hormone treatment (T_3: 2.4 fold change; CORT: 2.7 fold change; T_3 plus CORT: 6.5 fold change; 1 h: $F_{(3,15)}$= 216.5, $p< 0.001$; 2 h: $F_{(3,15)}$= 17.6, $p< 0.01$; 4 h: $F_{(3,15)}$= 68.26, $p< 0.001$; 6 h: $F_{(3,15)}$= 42.36, $p< 0.001$; Fig. 3.1D; ANOVA). We also observed a synergistic increase in *Klf9* hnRNA in HT-22 cells, which shows that *Klf9* transcription was synergistically increased by T_3 plus CORT ($F_{(3,11)}$= 13.78, $p< 0.01$, Supplemental Fig. 3.1; ANOVA). We did not measure *Klf9* hnRNA in the frog cell lines.

Synergistic activation of *Klf9* transcription by T_3 plus CORT is resistant to protein synthesis inhibition.

The protein synthesis inhibitor cycloheximide effectively reduced protein synthesis at the two doses tested in XTC-2 and HT-22 cells by 92% and 96% , respectively (XTC-2: $F_{(2,14)}$= 37.46, $p< 0.001$, Fig.2A; HT-22: $F_{(2,17)}$= 102.8, $p< 0.001$, Fig. 3.2B; ANOVA). Hormone-dependent induction of *Klf9* mRNA was resistant to protein synthesis inhibition

in both XTC-2 and HT-22 cells, which supports that the independent and synergistic effects of T_3 and CORT on *Klf9* transcription are mediated by TR and GR/MR directly regulating the *Klf9* gene (XTC-2 (-CHX): $F_{(3,15)} = 85.01$, $p<0.01$; XTC-2(+CHX): $F_{(3,15)} =109.8$, $p<0.01$; Fig. 2C; HT-22 (-CHX): $F_{(3,15)} = 120.7$, $p<0.01$; HT-22 (+CHX): $F_{(2,15)} =359.3$, $p<0.01$; Fig. 3.2D; ANOVA).

Identification of an evolutionarily conserved region of ~180 bp that confers synergistic hormone regulation on vertebrate *Klf9* genes

To identify the genomic region that confers hormone dependent regulation of vertebrate *Klf9* genes we used promoter-reporter assays in XTC-2 cells to screen a series of 1 kb fragments of the frog *Klf9* 5' flanking region covering 0 to 7 kb upstream of the TSS. We found the -6 to -5 kb fragment to be T_3 and CORT-responsive, and this region supported synergistic transactivation by T_3 plus CORT ($F_{(3,15)} = 89.44$, $p<0.001$; Fig 3A; ANOVA). A similar pattern of synergistic transactivation of the -6 to -5 kb frog *Klf9* promoter fragment was seen in HT-22 cells ($F_{(3,19)} = 245.2$, $p<0.001$; Supplemental Fig. 3.2; ANOVA).

Several of the other frog *Klf9* gene fragments showed individual T_3 or CORT-dependent transactivation but not synergy; these effects tended to be small and were cell line-dependent For example, in XTC-2 cells the -7 to -6 kb and -1 to 0 kb fragments showed small responses to CORT and T_3 (-7 to -6 kb TSS: $F_{(3,15)} = 11.64$, $p<0.05$; -1 to 0 kb TSS: $F_{(3,15)} =14.9$, $p<0.05$; Fig. 3.3A; ANOVA) . In HT-22 cells the -3 to -2 kb and -1 to 0 kb fragments showed CORT responsiveness (-3 to -2 kb TSS: $F_{(3,19)} = 48.1$, $p<0.05$; -1 to 0 kb TSS: $F_{(3,19)} = 42.64$, $p<0.05$; Supplemental Fig. 3.2; ANOVA).

Since the -6 to -5 kb frog *Klf9* fragment consistently showed independent and synergistic transactivation by T_3 and CORT in frog and mouse cell lines, we conducted *in silico* comparative genomic analysis to attempt to identify conserved regions that might explain the hormone regulation. Computer analysis revealed a ~180 bp region that is evolutionarily conserved among tetrapod *Klf9* genes (frog: -6000 to -5836 bp relative to the TSS; mouse: -5333 to -5154 bp relative to the TSS; human -4634 to -4505 bp relative to the TSS; Fig. 3.4A, Supplemental Fig. 3.3). We were unable to identify a similar genomic region in fishes (zebrafish and pufferfish). In frogs, this *Klf9* genomic region was previously reported to possess a T_3RE (yellow; comprised of two half sites - HRE h2 and HRE h3; mouse *Klf9* T_3RE at -5.23 relative to the TSS; frog *Klf9* T_3RE at -6.0 relative to the TSS) (Furlow and Kanamori 2002). We also previously identified a functional GRE/MRE (GRE/MRE-5.3, blue) in this region of the mouse *Klf9* gene that is conserved from frog to human (Chapter 2). *In silico* analysis of this conserved ~180 bp fragment using Match and Transcription Element Search System (TESS) identified another highly conserved HRE half site (HRE h1, green, Fig. 3.4A) that was predicted to be a GRE/MRE half site. However, the HRE h1 was not protected by the GR-DBD in a DNAseI footprinting assay (Chapter 2). In addition to TR and GR/MR response elements, TESS also identified estrogen response elements and Sp1 binding sites within the ~180 bp conserved region (Supplementary Fig. 3.3).

To determine if the evolutionarily conserved ~180 bp region supported synergistic transactivation we cloned the mouse *Klf9* fragment (179 bp) and conducted promoter-luciferase assays in HT-22 cells. This showed that this region of the mouse genome supported independent and synergistic transactivation by T_3 and CORT ($F_{(3,15)} = 145.3$,

$p<0.001$; Fig. 3.4B; ANOVA;), and we therefore designated this region the '*Kf9* synergy module'. The frog *Klf9* synergy module also supported independent and synergistic transactivation by T_3 and CORT in XTC-2 cells (*xKlf9* synergy module: $F_{(3,15)} = 515.4$, $p<0.001$; m*Klf9* synergy module: $F_{(3,15)} = 178.3$, $p<0.001$; Supplemental Fig. 3.4B; ANOVA).

Mutation of both half sites of the GRE/MRE-5.3 attenuated but did not eliminate the CORT response, attenuated the T_3 response, but eliminated synergistic transactivation (GRE/MRE-5.3 mut: $F_{(3,15)} = 29.54$, $p<0.001$; Fig. 3.4B; ANOVA). Mutation of both half sites of the predicted T_3RE (HRE h2 and HRE h3) eliminated T_3-dependent transactivation, greatly reduced CORT-dependent transactivation and abolished synergistic transactivation (HRE h2 and HRE h3 mut: $F_{(3,15)} = 3.664$, $p<0.05$; Fig. 3.4B; ANOVA). Mutation of the HRE h1 abolished the CORT response (even with the GRE/MRE-5.3 remaining intact) and reduced, but did not eliminate the T_3 and synergistic responses (HRE h1 mut: $F_{(3,15)} = 42.20$, $p<0.001$; Fig. 3.4B; ANOVA). When the HRE h2 was mutated, all hormone responses were eliminated (HRE h2 mut: $F_{(3,15)} = 2.294$; Fig. 3.4B; ANOVA). However when the HRE h3 was mutated the independent and synergistic transactivation by T_3 and CORT were reduced but not eliminated (HRE h3 mut: $F_{(3,15)} = 77.1$, $p<0.001$; Fig. 3.4B; ANOVA;).

TR and GR bind to the *Klf9* synergy module *in vitro*

The orthologous T_3RE of the frog *Klf9* T_3RE-6.0 in the mouse *Klf9* gene (T3RE-5.23) was bound by TR-RXR heterodimers in EMSA (Fig. 3.5A). Binding could be competed by radioinert wild type but not by mutated oligonucleotide (Fig. 3.5A). The GR can also

bind to GRE/MRE-5.3 within the *mKlf9* synergy module in gel shift assays and that was eliminated by mutation of the GRE/MRE (Chapter 2). Competition binding analysis showed that the binding of GR to the previously identified GRE/MRE-6.1 (Chapter 2) could be competed by the ~180 bp *mKlf9* synergy in gel shift assays (Fig. 3.5B).

TR and GR bind to the *Klf9* synergy module *in vivo*

Chromatin-immunoprecipitation assay conducted with chromatin extracted from the hippocampal region of T_3-injected PND5 mice (chromatin from study by Denver and Williamson, 2009; Fig. 3.5C) showed TR association at the *Klf9* synergy module. The TR ChIP signal was significantly greater than the control (normal rabbit serum ChIP signal) at the *Klf9* synergy module but not at the distal intron (Fig. 3.5C; $p<0.001$, Student's *t* test). Chromatin-immunoprecipitation assay conducted with chromatin extracted from Neuro2a[TRβ] cells treated with T_3 also showed TR association at the *Klf9* synergy module (Supplementary Fig. 3.5 ; *$p<0.01$, **$p<0.001$. Student's *t* test).

Chromatin-immunoprecipitation assay conducted with chromatin extracted from the hippocampal region of CORT injected PND6 mice showed GR association at the GRE/MRE- 6.1 and *Klf9* synergy module, and the GR association was increased 1 hr after CORT injection (Fig. 3.5D. $p<0.05$, Student's *t* test, data as seen in Chapter 2). By comparison, there was no significant GR ChIP signal at the *Klf9* distal intronic region (+11 kb from the TSS).

Hormone-dependent recruitment of TR and GR across the *Klf9* locus

We conducted ChIP assays for TR and GR using chromatin from hormone-treated HT-22 cells to determine if the synergistic effect of T_3 plus CORT on *Klf9* transcription can be attributed to an enhanced recruitment of TR or GR. Looking across the mouse *Klf9* locus TR association peaked at the *Klf9* synergy module, but was unchanged by hormone treatment, consistent with TRs being constitutively bound to DNA (Fig. 3.6A). The ChIP signal for the NRS control was low (maximum 0.06% of input) across the *Klf9* locus and was not affected by hormone treatment (data not shown).

Scanning of GR association across the *mKlf9* locus by ChIP assay revealed an enhanced recruitment of GR at the GRE/MRE-6.1 and *Klf9* synergy module with T_3 plus CORT treatment (Fig. 3.6C). There was a synergistic recruitment of GR at the GRE/MRE-6.1 and *Klf9* synergy module in response to T_3 plus CORT treatment (GRE/MRE-6.1 kb: $F_{(3,21)}= 7.4555$, $p<0.05$; synergy module -5.3 kb: $F_{(3,21)}= 8.631$, $p<0.001$; Fig. 3.6D; ANOVA).

Hormone-dependent histone modifications across the *Klf9* locus

To determine if the synergistic effect of T_3 plus CORT on *Klf9* gene transcription can be observed at the level of chromatin modification, we conducted ChIP assays for histone 3 (H3), acetylated H3 (AcH3) and acetylated H4 (AcH4). All hormone treatments decreased H3 levels at the GRE/MRE-6.1 and at the synergy module (Fig. 3.7A), but this effect was not enhanced by combined treatment with T_3 and CORT (GRE/MRE-6.1 kb: $F_{(3,14)}= 7.168$, $p<0.01$; *Klf9* synergy module -5.3 kb: $F_{(3,15)}= 5.911$, $p<0.05$; Fig. 3.7B; ANOVA;).

Histone 3 (Fig. 3.7C) and H4 (Fig. 3.7E) acetylation was increased by T_3 or CORT alone at the GRE/MRE-6.1 and at the *Klf9* synergy module, but there was no synergistic effect of T_3 plus CORT on AcH3 (AcH3 GRE/MRE- 6.1 kb: $F_{(3,13)}= 16.92$, $p<0.001$; AcH3 *Klf9* synergy module -5.3 kb: $F_{(3,14)}= 25.97$, $p<0.001$; Fig. 3.7D; ANOVA) or AcH4 (AcH4 GRE/MRE- 6.1 kb: $F_{(3,13)}= 4.705$; AcH4 *Klf9* synergy module -5.3 kb: $F_{(3,14)}= 13.99$, $p<0.001$; Fig. 3.7E; ANOVA). Hormone treatment did not alter the H3, AcH3 or AcH4 signal at the -3.8 kb region, nor at the distal intron in HT-22 cells.

Hormone-dependent recruitment of RNA polymerase II across the *Klf9* locus

Using ChIP assay, we looked at the recruitment of two phosphorylated forms of RNA polymerase II (the stalled RNA pol II S5P and the elongating RNA pol II S2P) across the mouse *Klf9* locus in HT-22 cells. The stalled RNA pol II signal peaked at the *Klf9* synergy module and at the TSS (Fig. 3.8A). There was enhanced, synergistic recruitment of stalled RNA pol II S5P at the *Klf9* synergy module by treatment with T_3 plus CORT (*Klf9* synergy module- 5.3 kb: $F_{(3,18)}= 10.6$, $p<0.001$; Fig. 3.8B; ANOVA). There were no hormone-dependent changes in stalled RNA pol II S5P recruitment at any of the other genomic regions analyze. The ChIP signal for elongating RNA pol II S2P was increased by T_3 at both the synergy module and at -3.8 kb, but was not enhanced by T_3 plus CORT (*Klf9* synergy module- 5.3 kb: $F_{(3,21)}= 6.736$, $p<0.01$; -3.7 kb: $F_{(3,20)}= 5.929$, $p<0.05$; Fig. 3.8D; ANOVA).

Detection of transcripts at the *Klf9* synergy module

Since there was a peak in the stalled and elongating RNA pol II at the *Klf9* synergy module, we determined if this genomic region is transcribed by conducting RTqPCR on RNA from hormone-treated HT-22 cells. We detected transcripts at the *Klf9* synergy module (we refer to this RNA as the *Klf9* enhancer RNA – *Klf9* eRNA). In an initial attempt to determine the limits of transcription at this region we conducted RTqPCR assays at regions flanking the *Klf9* synergy module. In addition to the *Klf9* synergy module (~-5.3 kb relative to the TSS), we detected transcript at -3.8 kb, but not at -6.1 kb and -2 kb relative to the TSS (Supplementary Fig. 3.6), suggesting that the transcript is at least 1.5 kb, but smaller than 4 kb in length. The pattern of hormone response of the *Klf9* eRNA was similar to that of the *Klf9* mRNA. However, the magnitude of increase in *Klf9* eRNA by combined hormone treatment was significantly greater than the *Klf9* mRNA (153 fold increase for the *Klf9* eRNA vs. 6 fold increase for the *Klf9* mRNA; *Klf9* eRNA: $F_{(3,11)}$= 15.16, p<0.01; Klf9 mRNA: $F_{(3,11)}$= 276, p<0.001; Fig. 3.9A; ANOVA). Similar to the mRNA, the expression of the *Klf9* eRNA was not affected by cycloheximide treatment (-CHX: $F_{(3,15)}$= 54.31, p<0.001; +CHX: $F_{(3,14)}$= 54.87, p<0.001; Fig. 3.9B; ANOVA).

Discussion

Cooperativity among transcription factors allows a cell to integrate multiple inputs and generate an appropriate transcriptional response (Herschlag and Johnson 1993; Carey 1998; Courey 2001). Synergistic transcriptional responses, in part due to TF cooperativity, provide a means for two or more simultaneous signals to generate a

response greater than additive, or for one signal to increase the sensitivity of the cell to a second, perhaps temporally delayed signal. Here we report synergistic regulation of the *Klf9* gene by T_3 and GC that is explained by an evolutionarily conserved NR enhancer module located in the 5' flanking region of the gene. This module contains a composite TR and GR/MR HRE, in addition to a separate GRE/MRE. We show that the liganded TR functions as a transcriptional 'switch' to create a chromatin environment that allows recruitment of the stress-activated GR (and perhaps MR), thereby increasing transcription. Together the TR and GR/MR generate a synergistic transcriptional response. We also show a synergistic increase in stalled RNA pol II at the *Klf9* synergy module, that correlates with transcription at the synergy module, leading to the generation of an eRNA. Lastly, in collaboration with our colleagues in Paris, France, we report that the upstream region interacts with the *Klf9* promoter through chromosomal looping.

Discovery of hormone synergy on Klf9

Earlier we reported that frog and mouse *Klf9* genes are independently regulated by T_3 and GC ((Denver, Ouellet et al. 1999; Bonett, Hu et al. 2009; Denver and Williamson 2009), Chapter 2). In this study we found that the *Klf9* gene is synergistically induced by T_3 plus CORT in the tadpole and mouse brain, further supporting that hormone regulation of this gene arose very early in tetrapod evolution and has been conserved. The synergistic response was also seen in frog and mouse tissue culture cells, thus allowing us to investigate the molecular mechanisms for hormone synergy. The synergistic increase in *Klf9* mRNA was accompanied by a coordinate increase in heteronuclear RNA, which supported that the synergy occurred at the level of transcription. Moreover, the

synergistic increase in *Klf9* mRNA was resistant to protein synthesis inhibition, supporting that hormone action was due to a direct transcriptional action on the *Klf9* gene.

Identification of an evolutionary conserved genomic region that supports hormone synergy

We conducted a promoter-reporter scan of the 5' flanking region of frog *Klf9* gene to search for a region(s) that supports synergistic transactivation by T_3 and CORT. We found a 1 kb fragment located between 5 and 6 kb upstream of the TSS that supported hormone synergy, and comparative genomic sequence analysis showed that this region possessed a sequence of ~180 bp that was conserved among tetrapods. There is no evolutionary conservation between the frog and mammalian *Klf9* genes outside of the coding region, the core promoter and the *Klf9* synergy module. We cloned this region of the frog and mouse *Klf9* genes and showed that it is sufficient to support synergistic transactivation by T_3 plus CORT.

Located within the *Klf9* synergy module are five hexanucleotide half sites that could support NR action. Earlier we showed that the HRE located at -5.3 kb in the mouse *Klf9* gene was a bonafide GRE/MRE; this GRE/MRE is conserved from frog to human (Chapter 2). Located at ~-5.2 kb are three half sites, two of which were identified previously by Furlow and Kanamori (Furlow and Kanamori 2002) in the frog *Klf9* gene and predicted to form a DR+4 T_3RE. We confirmed that TR associates with the orthologous T_3RE in the *mKlf9* gene (*mKlf9* T_3RE-5.23) by EMSA and ChIP assay. We also identified a third half site, predicted to be a GRE/MRE half site, located 5

(mammals) or 6 (nonmammals) nucleotides downstream of the predicted T_3RE . All three half sites are completely conserved from frog to mammals.

In silico also analysis revealed highly conserved binding sites for Sp1, Nuclear factor 1 (NF-1), NFκB and the estrogen receptor (ER) within the *Klf9* synergy module (Supplemental Fig. 3.3). Apart from these predicted transcription factor binding sites, the *Klf9* synergy module contains stretches of highly conserved sequences which may be important binding sites for other proteins that function in *Klf9* transcriptional regulation. Thus, the *Klf9* synergy module is enriched with evolutionarily conserved regulatory elements suggesting that the *Klf9* synergy module has been subject to strong stabilizing selection due to the presence of important *cis* regulatory elements sufficient to support the conserved hormone- dependent transcriptional regulation of the *Klf9* gene.

Mutagenesis of the predicted HRE half sites identifies a composite TR and GR/MR response element

Since the hormone-dependent transcriptional regulation of the *Klf9* gene is conserved between frog and mouse, and because there are more tools available to analyze the mouse genome, we used the mouse *Klf9* gene as a model to analyze the molecular mechanisms behind the synergistic gene regulation Mutational analysis of the HRE halfsites showed that although the T_3RE-5.23 and GRE/MRE-5.3 are both required for the synergistic activation by T_3 and CORT, the T_3RE-5.23 is necessary for T_3-dependent activation, while the GRE/MRE-5.3 only partly contributes to CORT-dependent response. Mutation of the *Klf9* synergy module T_3RE- 5.23 also increased basal T_3 response compared to the wild type *Klf9* synergy module (Supplemental Fig. 3.2B), consistent with the repressive

role of unliganded TR (Germain, Staels et al. 2006; Shi 2009). Mutation of the HRE half sites suggest that the residual CORT responsiveness of the GRE/MRE-5.3 mutant could be attributed to HRE h1 and HRE h2 acting as composite response element for GR association. More importantly, the absence of any hormone response with the HRE h2 mutant suggests that it is composite HRE half site that plays a central role for synergistic activation by TR and GR. A similar configuration of three hexanucleotide half sites was identified to confer T_3 plus GC synergistic regulation of the rat growth hormone releasing hormone (GHRH) receptor gene in somatotropic cell lines ((Nogami, Hiraoka et al. 2002), Supplemental Fig. 3.7).

Taken together, these data suggest that all of the HRE half sites we tested are important to achieve full synergistic gene by T_3 plus CORT. However, HRE h3 with HRE h2, and HRE h1 and GRE/MRE-5.3, may function to confer independent T_3 and CORT responses, respectively; whereas, HRE h2 functions as part of a composite response element that is critical for synergistic regulation of the *Klf9* gene by T_3 and GC.

It is possible that ligand bound TR and GR association at the HREs within the *Klf9* synergy module is necessary to promote the recruitment of another TF needed to confer synergistic transactivation of the gene; the presence of conserved stretches outside of the identified HREs suggests that multiple TFs can be recruited to this genomic region. A similar example was observed in the synergistic regulation of the *MMTV* promoter by the progesterone receptor (PR) and GR where OTF-1, a TF known to interact with TFIID of the basal transcription machinery, was only recruited to the promoter in the presence ligand bound PR and GR (Bruggemeier, Kalff et al. 1991). This may also be a potential

mechanism for how the composite GRE/MRE (HRE h1 and HRE h2) functions to confer GC-dependent regulation.

The region of the synergy module was not protected by the GR-DBD in a DNAseI footprint assay (Chapter 2) and therefore the GR may associate with the composite response element with low affinity DNA binding, or through protein-protein interactions (or both). In support of this hypothesis, we identified a highly conserved NFκB binding site that encompasses HRE h1 and HRE h2 (see Supplemental. Fig. 3.3). The interaction between GR and NFκB has been a subject of extensive research owing to their antagonistic roles in the immune-inflammatory response. NFκB is comprised of a family of constitutively expressed TFs that are activated by the proinflammatory cytokine tumor necrosis factor alpha (TNF), and bind to NFκB response elements (NFκB RE) of target genes as dimers (p50 and p65 dimers) (Vallabhapurapu and Karin 2009).The most extensively studied mechanism is mutual antagonism of GR and NFκB, most often occuring via a tethering mechanism where the GR is recruited, via protein-protein interactions, by DNA-bound NFκB dimers (De Bosscher, Vanden Berghe et al. 2003). However, recent studies show that GR and p65 are both recruited to genes that are synergistically upregulated by NFκB and GC signaling (Rao, McCalman et al. 2011). Thus, the interaction between TR, GR and NFκB at the *Klf9* gene merits further investigation in the context of hormone synergy to determine if the GR (or the TR) is tethered to the composite response element via interaction with NFkB dimers. There are several examples where the GR dimerization and DNA binding capacity is dispensable for GC-dependent regulation (Reichardt, Kaestner et al. 1998); reviewed in (De Bosscher, Vanden Berghe et al. 2003; Kassel and Herrlich 2007) indicating that tethering by

protein-protein interaction plays a significant role in GR-dependent gene regulation. We also identified a highly conserved NF-1 binding site within the synergy module. Nuclear factor-1 is a constitutively active TF and their binding sites are often found adjacent to clusters of HREs where they have been shown to synergistically enhance thyroid and steroid receptor transcriptional activity (Cato, Skroch et al. 1988; Schule, Muller et al. 1988; Bruggemeier, Rogge et al. 1990; Voz, Peers et al. 1992). Therefore it is likely that the NF-1 binding site within the synergy module also plays a role for synergistic regulation of *Klf9* TH and GC.

Molecular basis for hormone synergy: TR and GR recruitment and marks of active transcription across the Klf9 locus

Results of our ChIP assays for TR and GR confirmed our hypothesis that TR acts as a transcriptional switch that, upon ligand-binding opens up the chromatin to unmask HREs and/or facilitate the access of the GR. In further support of this hypothesis, we have preliminary evidence showing that overexpression of a dominant negative TR that is unable to bind hormone and recruit coactivators, dampens the CORT-dependent expression of *Klf9* (J. Knoedler, unpublished data).

Although a T_3RE located at -3.8 kb from the TSS of the mouse *Klf9* gene was earlier identified in the mouse *Klf9* gene and shown by ChIP assay to recruit TR in hippocampus and neuroblastoma cells (Denver and Williamson 2009), we did not find a significant association of TR at the -3.8 kb TRE in HT-22 cells. The -3.8 kb TRE in the mouse *Klf9* gene is only conserved among mammals, and this suggests that there has been stronger, stabilizing selection for the T_3RE-5.23 of the *Klf9* synergy module. The T_3RE-5.23 is in

close proximity with other highly conserved HREs and TF binding sites indicating that T_3RE-5.23 is within a transcriptionally active chromatin environment and may therefore play a more ubiquitous and significant role in the TH ₋regulation of the *Klf9* gene, while the -3.8 kb T_3RE may function in a cell type-specific manner.

Histone 3 (H3) and histone 4 (H4) acetylation are markers of transcriptionally active chromatin (Aoyagi and Archer 2008), and acetylation is necessary to promote nucleosome eviction and chromatin disassembly (Luebben, Sharma et al. 2010). Consistent with the peak of TR and GR association at the synergy module and at the GRE/MRE-6.1, we also found lower levels of H3 (representative of nucleosome eviction), and higher levels of acetylated H3 and H4 (representing chromatin decompaction) in these regions. However, these changes were not enhanced by combined treatment with T_3 and GC at any of the *Klf9* regions that we analyzed, suggesting that hormone-dependent nucleosome eviction and histone acetylation may be maximal induced by the individual hormones and cannot be enhanced by combined treatment.

Molecular basis for hormone synergy: RNA polymerase II association and hormone-dependent transcription at Klf9 synergy module.

Transcription is a multistep process that involves assembly of the preinitiation complex (PIC), composed of general transcription factors (GTF elongation and RNA polymerase II (Pol II), followed by transcriptional initiation, promoter escape, proximal promoter pausing, elongation and termination (Saunders, Core et al. 2006). Each of these steps can be rate limiting, and the stepwise transitions tightly regulated. The C-terminal

domain (CTD) of the largest subunit of Pol II is composed of heptad repeats (YSPTSPS) that undergoes dynamic phosphorylation at Ser2 and Ser5 during transcription and, the different phosphorylation patterns correlate with Pol II function and cofactor recruitment (Komarnitsky, Cho et al. 2000; Phatnani and Greenleaf 2006). The CTD of Pol II is hypophosphorylated upon assembly of the PIC and it undergoes hyperphosphorylation as it transitions into transcriptional elongation. Phosphorylation at Ser5 predominantly peaks at the 5' end of a gene and decreases or remains constant towards the 3' end of the gene while Ser2 phosphorylation is found mostly at the center and at the 3' end of the gene (Komarnitsky, Cho et al. 2000; Morris, Michelotti et al. 2005). The phosphorylation of the CTD at Ser5 is a characteristic marker of Pol II stalling predominantly at proximal promoters and released upon phosphorylation of the CTD at Ser2, enabling the transition to productive elongation (Komarnitsky, Cho et al. 2000; Morris, Michelotti et al. 2005; Saunders, Core et al. 2006).

Although we did not see an enhancement of transcriptionally active chromatin marks by combined hormone treatment, we found that the peak of TR and GR association was accompanied by a peak, and synergistic association of stalled Pol II at the synergy module with T_3 plus GC treatment. There was a smaller peak of stalled Pol II at the promoter. Pol II stalling is hypothesized to be an important regulatory step in transcription. In *Drosophila*, stalled Pol II is highly enriched among genes implicated in development and response to stimuli suggesting that Pol II stalling keeps the gene poised and ready to afford a rapid transcriptional response to developmental and environmental signals (Muse, Gilchrist et al. 2007; Zeitlinger, Stark et al. 2007; Margaritis and Holstege 2008). Although Pol II stalling is hypothesized to keep Pol II in a poised state for active

transcription, Pol II stalling is also observed in genes that are actively transcribed, which indicates that modulating the residence time of Pol II at transcribed genes provides an additional regulatory step in transcription (O'Brien and Lis 1991; Nechaev and Adelman 2008).

These findings suggest that the synergistic association of stalled Pol II at the synergy module with T_3 plus CORT may keep the locus poised to initiate a faster and synergistic response to hormone treatment. There are several possibilities to account for the synergistic association of stalled Pol II at the synergy module that need to be tested. Enhanced association of stalled Pol II may be due to synergistic recruitment of hypophosphorylated Pol II, enhanced phosphorylation of Ser5 or increased stability and time of association of stalled Pol II at the synergy module. Kinetic analysis by ChIP assays for hypophosphorylated, stalled and elongating pol II, and kinases that function in Pol II phosphorylation may be done to address these possibilities.

Results of our Pol II ChIP assays are consistent with recent findings that the PIC is not only recruited to core promoters but also to enhancers, and that Pol II-bound enhancers may function in promoter targeting and regulation (Szutorisz, Dillon et al. 2005). For example, in the *prostate specific antigen (PSA)* gene, androgen induces recruitment of the androgen receptor (AR) and Pol II at an enhancer element located ~5 kb upstream of the TSS of the *PSA* gene (Louie, Yang et al. 2003). There was also greater Pol II recruitment at the enhancer than at the *PSA* promoter (Louie, Yang et al. 2003), which may be an additional step of transcriptional regulation that keeps the gene in a potentiated state without the risk of premature gene transcription (Szutorisz, Dillon et al. 2005). Recruitment of the PIC and other chromatin modifying proteins were also

observed at enhancer elements of the mouse *λ5-VpreBI* (Szutorisz, Canzonetta et al. 2005) and α and *β-globin* (Vieira, Levings et al. 2004) loci in embryonic stem cells, and in the locus control region of the growth hormone gene in pituitary and liver cells (Ho, Elefant et al. 2006).

The peak in Pol II association at the *Klf9* synergy module was accompanied by transcription at the synergy module and surrounding region. We detected eRNA transcripts by RTqPCR of hormone-treated HT-22 cells and XTC-2 (Supplemental Fig. 3.8), where the pattern of eRNA expression was similar and correlated with the hormone-dependent regulation of *Klf9* mRNA. Furthermore, eRNA levels were induced by combined hormone treatment to a significantly higher level compared to the mRNA (~150x greater in HT-22 and ~10x greater in XTC-2). Our preliminary analysis by RTqPCR suggests that the eRNA is probably transcribed towards the direction of the *Klf9* promoter.

Our discovery of eRNA transcripts at the synergy module is consistent with studies that found noncoding RNA transcripts at the Pol II-associated enhancer elements of the α and *β-globin* and *growth hormone* gene (Vieira, Levings et al. 2004; Ho, Elefant et al. 2006). Genome wide ChIP-seq analysis also recently found GTF (CBP) and Pol II to be recruited at ~3,000 activity-regulated enhancers in mouse cortical neurons, and ~2,000 of these Pol II-bound activity-regulated enhancers are transcribed into short noncoding transcripts of <2 kb (Kim, Hemberg et al. 2010). Enhancer RNA synthesis was dependent on the presence of the promoter of the associated gene and correlated with induction of nearby genes (Kim, Hemberg et al. 2010). Coincidentally, others have shown *Klf9* is also an activity regulated gene (Lin, Bloodgood et al. 2008; Scobie, Hall et al. 2009). More

recent studies suggest that noncoding RNA transcripts detected at the enhancer elements also have important functions in transcription. For example, the *β globin* and the human *growth hormone* noncoding enhancer transcripts are hypothesized to play important roles in enhancer-promoter dynamics. Insertion of transcription termination sequences in the region between the enhancer and promoter to block synthesis of noncoding RNA transcripts significantly reduced the transcription of the *β globin* and the human *growth hormone* gene (Ling, Ainol et al. 2004; Ho, Elefant et al. 2006). In addition, siRNA-mediated depletion of long noncoding RNAs, identified through the GENCODE annotation of the human genome, decreased the expression of the neighboring protein coding gene (Orom, Derrien et al. 2010) indicating that transcripts produced at enhancer elements play a functional role in the target gene transcription.

Chromosomal looping brings the Klf9 synergy module in contact with the core promoter.

Using a genome wide analysis by chromatin interaction analysis with paired end tag sequencing (ChIA-PET) (Li, Fullwood et al. 2010) to look at T_3 dependent genomic interactions, Laurent Sachs and colleagues have shown that there is a T_3-dependent interaction between the *Klf9* synergy module and the core promoter (and several other genomic regions; Fig. 3.10) which supports the role of the synergy module as a bona fide enhancer that functionally communicates with the *Klf9* promoter to mediate synergistic transcription. Whether the *Klf9* eRNA is a byproduct of Pol II association and chromosomal looping, or plays a function in *Klf9* mRNA transcription needs to be determined.

The assembly of activators and the PIC at enhancers needs to be relayed or transferred to gene promoters for gene transcription to occur. For example, association of PIC at the enhancer elements of the α and *β globin* was found to be required for the PIC to bind to the promoters (Vieira, Levings et al. 2004; Vernimmen, De Gobbi et al. 2007). Through chromosome conformation capture (3C) assay, a technique used to detect physical long range chromosomal interaction (Hagege, Klous et al. 2007), physical interactions were found between the enhancer elements and promoter of the *α globin* indicating that PIC transfer from the enhancer to the promoter may occur by chromosome looping. The PIC at enhancers could also be transferred to the promoter by tracking from the enhancer towards the target gene promoters or through a combination of tracking that leads to chromosomal looping (Zhu, Ling et al. 2007). The interaction of enhancer and promoter by chromosomal looping can also be facilitated by cohesin complexes (Ong and Corces 2011) and the multisubunit Mediator complex (Kagey, Newman et al. 2010).

The Mediator complex directly recruits and interacts with Pol II at gene promoters (Myers and Kornberg 2000). Among the many proteins that make up the Mediator complex, a 220 kDa subunit called TR associated protein 220 (TRAP220)/Vitamin D receptor interacting protein (DRIP205)/ MED1 was found to associate with TR (Ito and Roeder 2001) and GR (Hittelman, Burakov et al. 1999; Chen and Roeder 2007) in a ligand-dependent manner. Recent evidence showed that TRAP220/MED1 plays a role in linking enhancers to gene promoters by chromosomal looping (Park, Li et al. 2005; Kagey, Newman et al. 2010). Since both TR and GR are known to recruit TRAP220 (DRIP205/ MED1), it would be interesting to determine if TRAP220 is recruited to the

Klf9 synergy module and if it facilitates the interaction of the synergy module with the promoter in regulating *Klf9* transcription.

In this study we identified an evolutionarily conserved enhancer (synergy module) in the *Klf9* gene that contains functional HREs and we elucidated the molecular mechanisms that lead to the synergistic transcription of *Klf9* gene. We propose a model (Fig. 3.11) whereby TR is bound to the synergy module in the unliganded state and associates with corepressors to repress *Klf9* transcription. Upon T_3 binding, TR releases exchanges corepressors for coactivators that promote histone acetylation and chromatin decompaction, which leads to a more transcriptionally active chromatin environment. This allows for an enhanced and synergistic recruitment of GR in the presence T_3 and CORT. The presence of ligand-bound TR, and enhanced recruitment of GR at the synergy module leads to a synergistic association of stalled Pol II at the synergy module maintaining the *Klf9* locus poised for a rapid transcriptional response. Association of hormone bound TR, GR and Pol II at the synergy module leads to transcription at that region, and to chromosomal looping that allows the regulatory information at the synergy module to be relayed to the promoter, ultimately resulting in synergistic gene transcription.

The coordinate and synergistic actions of GC and T_3 in common target tissues is observed during critical periods of vertebrate development, and is regarded to allow for important adaptive responses to changing environments (Smith and Sabry 1983; McDonald and Henning 1992; Bonett, Hu et al. 2009; Denver 2009; Bonett, Hoopfer et al. 2010; Pei, Leblanc et al. 2011). However, the molecular basis behind the synergistic actions of T_3 and GC in regulating these developmental transitions is poorly understood.

In this study, we report the synergistic action of TR and GR/MR in upregulating the expression of a transcription factor KLF9, which is plays an important role in amphibian and mammalian development. We hypothesize that through the synergistic regulation of common T_3 and GC target genes, physiological and developmental processes are promoted as a consequence of the amplification of gene regulatory networks that underlie organogenesis.

Table 3.1. Taqman assays used for quantitative real time PCR analysis of gene expression (RT-PCR) and chromatin immunoprecipitation (ChIP) assays.

For RTqPCR

m*Klf9* mRNA
Probe – 5' 6FAM-AAAGTCTATGGAAAATCC 3'
Forward: 5' GCACAAGTGCCCCTACAGT 3'
Reverse: 5' TGTATGCACTCTGTAATGGGCTTT 3'

m*Klf9* eRNA
Probe – 5' 6FAM- TTCTGACTCACCCAGAGGGCCG 3'
Forward: 5' AAGGACAAACTGTTCCACAACAAC 3'
Reverse: 5' CCCCCCGAGTATGGTTCTG 3'

m*Klf9* hnRNA
Probe – 5' 6FAM-CTTCTGCACTGGTTTTAG 3'
Forward: 5' CGTATAGCTGTTTGAGGTCCATAGTT 3'
Reverse: 5' CCTGGCCTCGTCTCAGAAATT 3'

For ChIP assay

m*Klf9* GRE/MRE-6.1 (-6134 to -6022 relative to the TSS):
Probe – 5' 6FAM- TTCTGACTCACCCAGAGGGCCG 3'
Forward: 5' AAGGACAAACTGTTCCACAACAAC 3'
Reverse: 5' CCCCCCGAGTATGGTTCTG 3'

m*Klf9* synergy module-5.3 (-5232 to -5143 relative to the TSS):
Probe – 5' 6FAM- ACCTGCCTCCTCCGGCTGCTG 3'
Forward: 5' AGAACTGGGACTGTCCTCAAATG 3'
Reverse: 5' TGGCATCGCCCTTTTAAAAA 3'

m*Klf9* -3.8(-3861 to -3777 relative to the TSS):
Probe – 6FAM-ACCTCACTTCACCTCTCC 3'
Forward primer – 5' TCCAGTCCGCAGATAAGAAAATGG 3'
Reverse primer – 5' GGCCTCTTCTGCCTTAAATGAGAT 3'

m*Klf9* -2.0 (-2097 to -2025 relative to the TSS)
Probe – 6FAM- TGT CTC AAA AAA CCC CCC AAA AAG GC 3'
Forward primer – 5' CAG CCA AGG ATA CAC AGA GAA ACC 3'
Reverse primer – 5' GGGAAGCCATCTTGGAAATCT3'

m*Klf9* promoter (-973 to -903 relative to the TSS)
Probe – 6FAM- CCA GCC CTC AAA CAG T 3'
Forward primer – 5' AGC GTT TGC AGG AAG TCA CTT A 3'
Reverse primer – 5' CTA GGG ACG AAA CAG AAC TTC AAC T3'

m*Klf9* TSS (+164 to +230 relative to the TSS)
Probe – 6FAM- CTT TCT CTG GGA CTC CGA CAC GTT TGC3’
Forward primer – 5’ CGC CTG GCT CGC AGT T 3’
Reverse primer – 5’ GCG GTC GCA AGT TTA TTC GA 3’

m*Klf9* + 2kb (+1934 to +2018 relative to the TSS)
Probe – 6FAM- CAG CGG GCC TTA CCT TGT CCT GAG A 3’
Forward primer – 5’ GGG TCG TTT GTA ACT GTT GTT ATG A 3’
Reverse primer – 5’ CAC GAT GCC AAC AAC TCT GAA3’

m*Klf9* intron (+11503 to +11569 relative to the TSS):
Probe – 5’ 6FAM-CTTCTGCACTGGTTTTAG 3’
Forward: 5’ CGTATAGCTGTTTGAGGTCCATAGTT 3’
Reverse: 5’ CCTGGCCTCGTCTCAGAAATT 3’

Table 3.2 Oligonucleotides used for construction of pGL4.23 promoter plasmids and electrophoretic mobility shift assay (EMSA).

PCR primers to amplify promoter fragments cloned into pGL4.23 vector

xtKlf9 -7 to -6 kb
Forward: 5' ata ctcgag ATG GTG TAC CTT TGG CAC TGA CA 3'
Reverse: 5' ata aagctt GAC GAA ACT GTG GAG CTC ACG ATC 3'

xtKlf9 -6 to -5 kb
Forward: 5' ata ctcgag AGC TCC ACA GTT TCG TCC CTG 3'
Reverse: 5' ata aagctt CTG CCA TGC TGG TTA CGT TAT TTA AT 3'

xtKlf9 -5 to -4 kb
Forward: 5' ata ctcgag TAA ATA ACG TAA CCA GCA TGG CAG AA 3'
Reverse: 5' ata agatct CTG TGG TTG GTG ATG TCA TTT ATG T 3'

xtKlf9 -4 to -3 kb
Forward: 5' ata ctcgag CCA ACC ACA GGA TAT AAC TTA TGA T 3'
Reverse: 5' ata aagctt TCT TAT CCA AGA ATC AAT GCT TGA 3'

xtKlf9 -3 to -2 kb
Forward: 5' ata ctcgag TCA AGC ATT GAT TCT TGG ATA AGA 3'
Reverse: 5' ata aagctt CAC TTT GAC TCA TTA GTG TGA GTG T 3'

xtKlf9 -2 to -1 kb
Forward: 5' ata ctcgag TGA GTC AAA GTG AAC AAT AGC ACA T 3'
Reverse: 5' ata aagctt GAT CCA TAG AGT AAC CAA TGG TGT C 3'

xtKlf9 -1 to 0 kb
Forward: 5' ata ctcgag GAC ACC ATT GGT TAC TCT ATG GAT C 3'
Reverse: 5' ata agatct GAC AAA GCT GCA TAT GAG ACA CTC 3'

xKlf9 synergy moldule -6.0
Forward: 5' ata ctcgag CCC TGT ACC ATTTAGGGC c 3'
Reverse: 5' ataaagctt AGC GCC GCT TTAAGAAAT 3'

mKlf9 synergy moldule -5.3
Forward: 5' atactcgagTCCTTGCACGAGTTTGGG 3'
Reverse: 5' ataaagcttATCGCCCTTTTAAAAATCT 3'

PCR primers for site-directed mutagenesis of pGL4.23 mKlf9 synergy module

mKlf9 GRE/MRE- 5.3 mut: AGGGCAgttTGTTCA mutated to ACCTCAgttGAATCA
Forward:5'GCGGATTCCTCGTCCCCCAATCTACCTCAGTTGAATCAACTGCAGCAAAGAGAG 3'
Reverse: 5'AGCTCTCTTTGCTGCAGTTGATTCAACTGAGGTAGATTGGGGGACGAGGAATCC 3'

mKlf9 T_3RE- 5.23 mut: TGTCCT caaa TGA ACC mutated to TAACCT caaa ATAACC
Forward: 5' ATTTCTGAGAACTGGGACTAACCTCAAAATAACCTGCCTCCTCCGGCTG 3'
Reverse: 5' CAGCCGGAGGAGGCAGGTTATTTTGAGGTTAGTCCCAGTTCTCAGAAAT 3'

mKlf9 HRE h2 mut: TGTCCT caaa TGA ACC mutated to TAACCT caaa TGA ACC
Forward: 5'GGGATTTCTGAGAACTGGGACTAACCTCAAATGAACCTGC3'
Reverse: 5' GCAGGTTCATTTGAGGTTAGTCCCAGTTCTCAGAAATCCCT 3'

mKlf9 HRE h3 mut: TGTCCT caaa TGA ACC mutated to TGTCCT caaa ATAACC
Forward: 5' CTGGGACTGTCCTCAAAATAACCTGCCTCCTCCG 3'
Reverse: 5' CGGAGGAGGCAGGTTATTTTGAGGACAGTCCCAG 3'

mKlf9 HRE h1 mut: AGAACT mutate to ACCAAA
Forward: 5'GATGTTCCAGCAGGGAAGGGATTTCTGACCAAAGGGACTGTCCTCAAA 3'
Reverse: 5' TTTGAGGACAGTCCCTTTGGTCAGAAATCCCTTCCCTGCTGGAACATCA 3'

EMSA
mKlf9 T_3RE- 5.23
Sense: 5' gatc TCTG AGAACT GGGAC TGTCCT CAAA TGAACCTGC 3'
Antisense: 5' gatc GCA GGT TCA TTT GAG GAC AGT CCC AGT TCT CAGA 3'

mKlf9 T_3RE- 5.23 mut
Sense: 5'gatc TCTG AGAACT GGGAC TAACCT CAAA ATAACCTGC 3'
Antisense: 5' gatc GCAGGTCATTTTGAGGTTAGTCCCAGTTCTCAGA 3'

xTRβ T_3RE
Sense: 5' gatc CGTCCTCCCTAGGCAGGTCATTTCAGGACAGCCCAGCGCCC 3'
Antisense: 5' gatc ACCAGGGCGCTGGGCTGTCCTGAAATGACCTGCCTAGGGAG 3'

PCR primers for site directed were designed using QuickChange Primer Design tool (Agilent)
Shaded nucleotides represent introduced mutations in the GRE/MRE halfsites.
Lower case letters represent restriction sites for subcloning into the pGL4.23 vector or non-native nucleotides added to the 5' ends for [32P] labeling by Klenow fill-in (for EMSA).

Figures

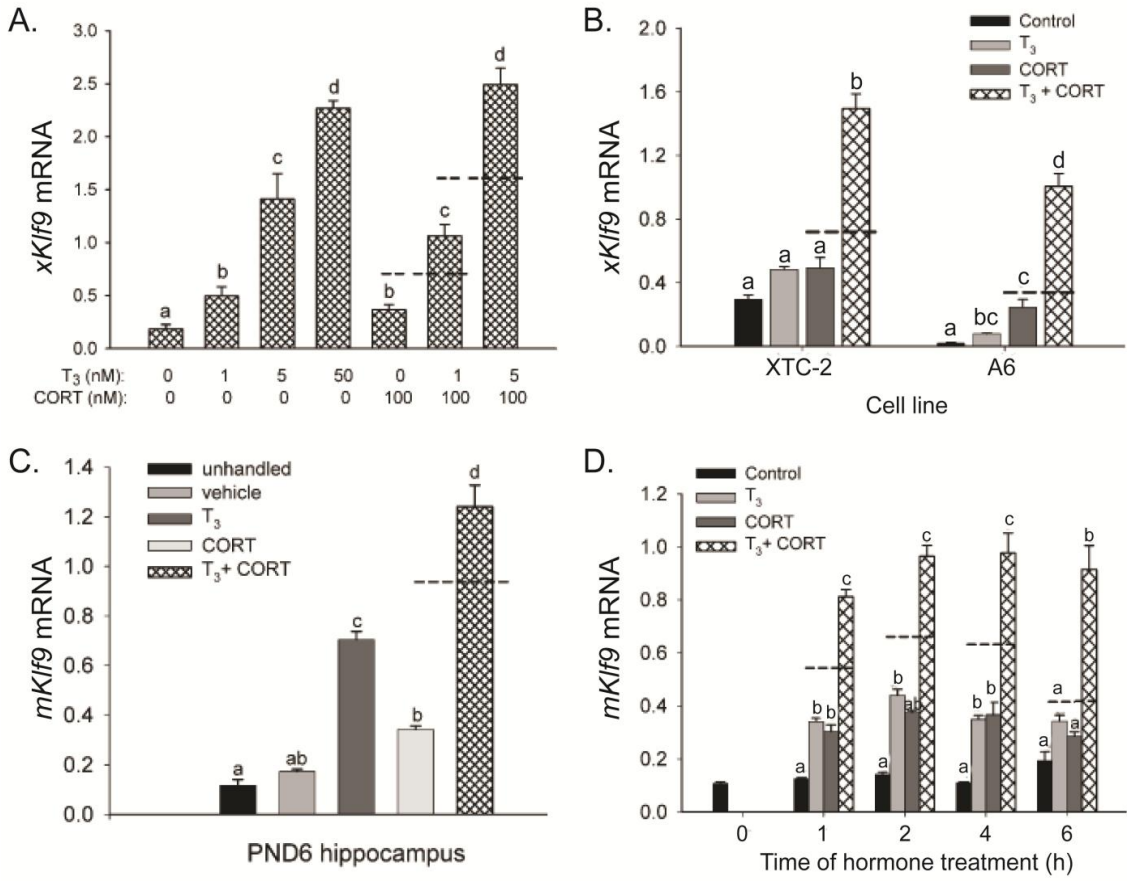

Fig. 3.1. Corticosterone (CORT) synergizes with 3,5,3'-triiodothyronine (T_3) to induce *Klf9* mRNA in frog and mouse brain. (A) Nieuwkoop- Faber stage 52-54 *X. tropicalis* tadpoles were treated with T_3 and CORT at the doses indicated and brain was collected for RNA isolation 24h post hormone treatment. **(B)** The *X.laevis* embryonic fibroblast (XTC-2) and renal epithelium(A6) derived cell line were treated with 5 nM T_3, 100 nM CORT or T_3 plus CORT for 4h before harvest and RNA isolation. **(C)** Postnatal day 6 (PND 6) wild type C57/BL6J mice were injected with vehicle (oil and DMSO), T_3 (25 ug/kg bodyweight) , CORT (14 mg/ kg bodyweight), T_3 plus CORT or left unhandled. One hour after injection animals were killed, the hippocampal region was dissected and RNA extracted (n=5-6/ treatment group). **(D)** HT-22 cells were treated with 30 nM T_3, 100 nM CORT or T_3 plus CORT for different times before harvest and RNA extraction. All RNA samples were used to measure *Klf9* mRNA by RTqPCR using Taqman assay. Frog and mouse *Klf9* mRNA were normalized to the mRNA level of the housekeeping gene *rpL8* and *GAPDH*, respectively. Bars represent the mean $\pm$ SEM and letters above the means indicate significant differences among treatments (means with the same letter are not significantly different; Tukey's multiple comparison test; $P<0.05$). Dashed lines represent the additive effects of T_3 plus CORT on *Klf9* mRNA levels.

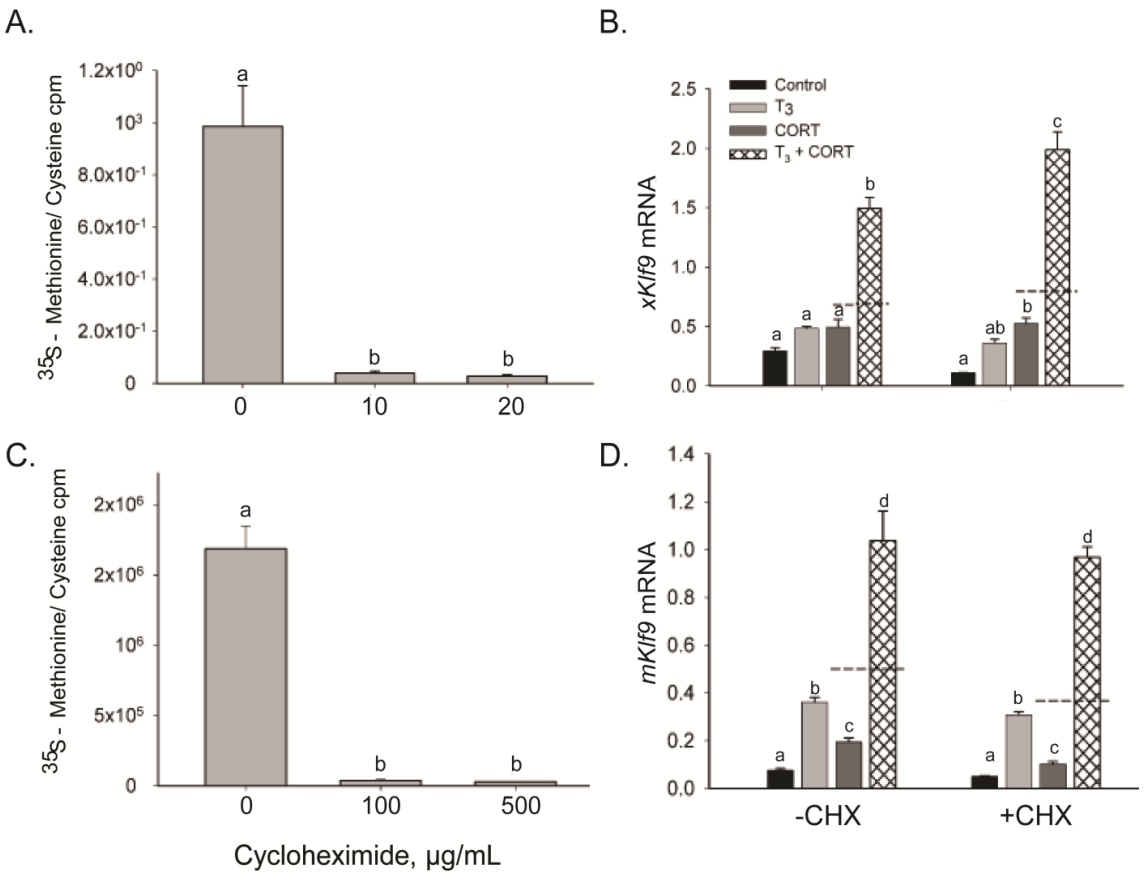

Fig. 3.2. Induction of *Klf9* mRNA by corticosterone (CORT) and 3,5,3'-triiodothyronine (T_3) in XTC-2 and HT-22 cells is resistant to protein synthesis inhibition. XTC-2 **(A)** and HT-22 **(C)** cells were grown to 80% confluency in growth medium (L-15 for XTC-2 and DMEM for HT-22 supplemented with pen/strep and 10% FBS), after which it was replaced with methionine and cysteine-deficient L-15 or DMEM supplemented with penicillin/streptomycin and 10% FBS, Cells were cultured for 2 hr before addition 10 µCi/well of [^{35}S]-ExPress protein labeling mix. Different doses of cycloheximide (CHX) or ethanol as vehicle (final concentration 0.001%) were added simultaneously to the protein labeling mix. Cells were harvested after a 6h incubation and proteins were precipitated with 10% ice-cold TCA. Radioactivity of the precipitated proteins was measured by liquid scintillation counting**.** XTC-2 **(B)** and **(D)** HT-22 cells were treated with or without CHX (10 µg/ml in XTC-2; 100 µg/ml in HT-22) for 30 min before addition of 3,5,3' triiodothyronine (T_3; 5 nM in XTC-2; 30 nM in HT-22), corticosterone (CORT; 100 nM) or T_3 plus CORT. Treatment with CHX plus hormones was continued for 4 h before cell harvest for analysis of *Klf9* mRNA by RTqPCR. Frog and mouse *Klf9* mRNA were normalized to the mRNA level of the housekeeping gene *rpL8* and *GAPDH*, respectively. Bars represent the mean ± SEM (n=4) and letters above the means indicate significant differences among treatments (means with the same letter are not significantly different; Tukey's multiple comparison test; $P<0.05$). Dashed lines represent the additive effects of T_3 plus CORT on *Klf9* mRNA levels.

.

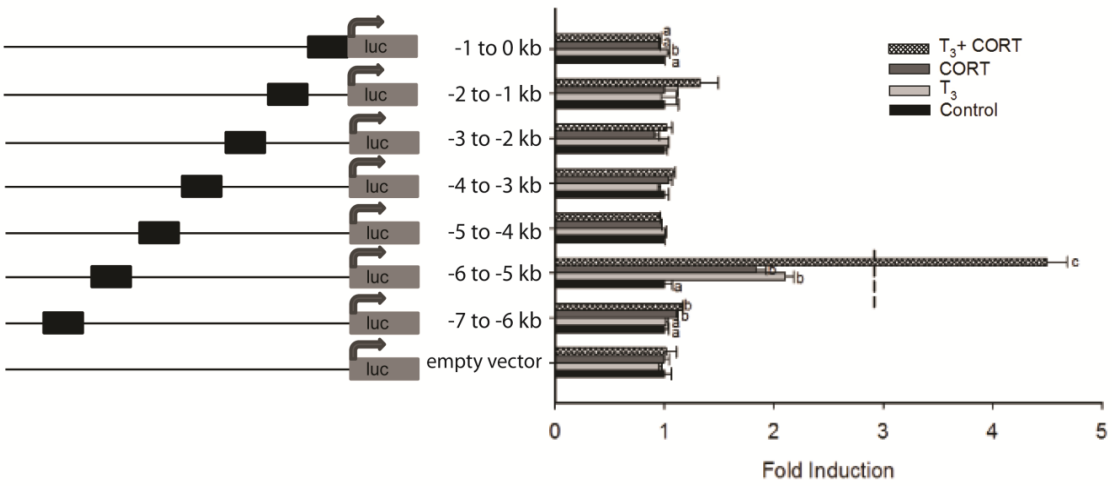

Fig. 3.3. Identification of the *Klf9* genomic region that supports corticosterone (CORT) and 3,5,3'-triiodothyronine (T_3) synergistic transactivation. A series of 1 kilobase fragments covering from -7 kb to 0 kb upstream of the *X. tropicalis Klf9* transcription start site were cloned into a luciferase vector and transfected into XTC-2 cells. Cells were treated with T_3, CORT or T_3 plus CORT for 4 h before harvest and analysis by dual luciferase assay. Bars represent the mean $\pm$ SEM (n=4-5) fold induction and letters above the means indicate significant differences among hormone concentrations or time point (means with the same letter are not significantly different; Tukey's multiple comparison test; $P<0.05$). Dashed lines represent the additive effects of T_3 plus CORT on luciferase activity.

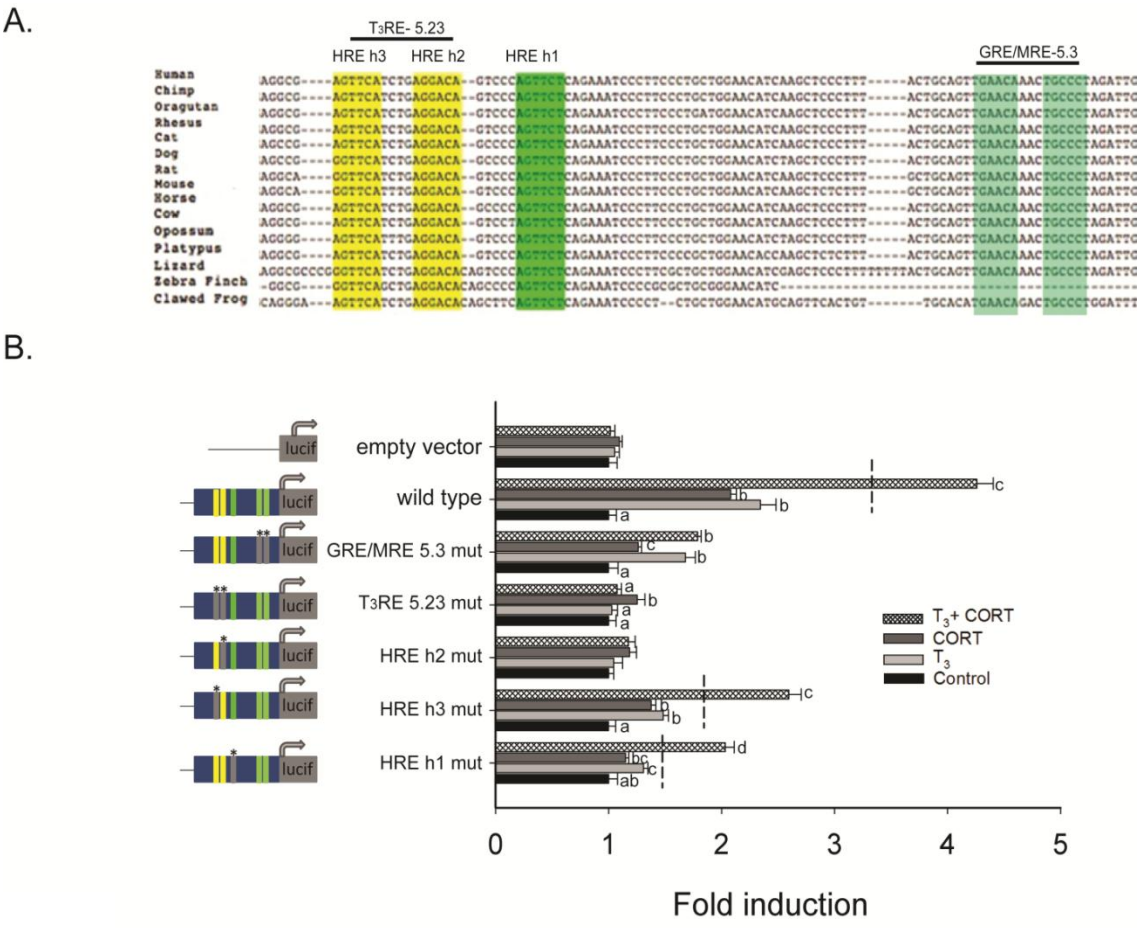

Fig.3.4. Identification and functional analysis of an evolutionarily conserved ~180 bp synergy module located -6 kb of the mouse *Klf9* gene. (A). Comparative sequence analysis of the -6 to -5 kb *X.tropicalis Klf9* genomic region that supported 3,5,3'-triiodothyronine (T_3) plus corticosterone (CORT) synergistic activation revealed a ~180 bp fragment (partial sequence shown), containing five hormone response element (HRE) half sites that are evolutionarily conserved across vertebrates. Sequence alignment showing conservation of the T_3RE (yellow; HRE h2 and HRE h3), GRE/MRE (blue; mouse GRE/MRE-5.3) and a hormone response element half site (HRE h1; green) across several vertebrate species. The conserved 180 bp fragment, we call the *Klf9* synergy module is centered at ~-4.6 kb in human, ~-5.3 kb in mouse and ~-5.9 kb in the frog *Klf9* gene. **(B)** Promoter luciferase constructs containing the mouse *Klf9* 179 bp synergy module, and corresponding site mutants (*****) were transfected into HT-22 cells. Cells were treated with T_3, CORT or T_3 plus CORT for 4 h before harvest and analysis by dual luciferase assay. Bars represent the mean $\pm$ SEM (n=4) and letters above the means indicate significant differences among treatments (means with the same letter are not significantly different; Tukey's multiple comparison test; $P<0.05$). Dashed lines represent the additive effects of T_3 plus CORT on luciferase activity.

Fig. 3.5. The thyroid hormone receptor (TR) and glucocorticoid receptor GR associate with the synergy module *in vitro* and in mouse hipppocampus *in vivo*. (A) The ability of the TR to bind to the mouse *Klf9* synergy module TRE was tested *in vitro* by electrophoretic mobility shift assay. Each reaction contained [^{32}P]-labeled synergy module T_3RE oligo as probe (lanes 1-5) and 2 μl of *in vitro* synthesized luciferase protein (control, lane 2) or frog TRβ plus frog RXRα protein (lanes 3-5). The TRβ/RXRα binding to the probe was competed with 1.5 μM radioinert synergy module T_3RE (lane 4) or mutated synergy module T_3RE oligonucleotides (lane 5). We conducted EMSA with a probe containing the previously identified T_3RE in the frog *TRβ* promoter as a positive control for TRβ/RXRα binding. Each reaction contained [^{32}P]-labeled xTRβ T_3RE oligonucleotide as probe (lanes 6-9) and 2 μl of *in vitro* synthesized luciferase protein (control, lane 7) or TRβ/RXRα (lanes 8 and 9). The TRβ/RXRα binding to the xTRβ TRE probe was competed with 1.5 μM radioinert xTRβ TRE oligonucleotide (lane 9). The supershifted bands indicated by the arrows are the TRβ/RXRα -bound probe. **(B)** The ability of the GR to bind to the mouse *Klf9* GRE/MRE-5.3 within the synergy module was tested *in vitro* by electrophoretic mobility shift assay. Each reaction contained [^{32}P]-labeled GRE/MRE-5.3 oligo as probe (lanes 1-5) and 2 μl of *in vitro* synthesized luciferase protein (control, lane 2) or human GR protein (lanes 3-5). The GR binding to the probe was competed with 1.5 μM radioinert GRE/MRE-5.3 (lane 4) or mutated GRE/MRE-5.3 oligonucleotides (lane 5). The supershifted bands indicated by the arrow are the GR-bound probe. **(C)** Wild type PND5 mice were injected with T_3 at a dose of 25 μg/kg bodyweight. Four hours after injection animals were killed, the hippocampal region was dissected and chromatin extracted for TR ChIP assay. ChIP samples (n=4-5) were analyzed by RTqPCR using Taqman assays that targeted the synergy module or a distal intronic region (negative control) of the mouse *Klf9* gene. Bars represent the mean ChIP signals expressed as a percentage of the input for TR serum (anti-TR) or normal rabbit serum (NRS) as negative control. Statistics were conducted on the normalized TR (the mean ChIP signals expressed as a percentage of the input minus the NSB where NSB was assessed by ChIP using NRS). Statistical analysis was conducted on $\log_{10}$ transformed data, and the asterisks indicate statistically significant differences between anti-TR and NRS ChIP signal ($P<0.01$; Student's *t* test). **(D)** Wild type PND6 mice were injected with corticosterone (CORT) at a dose of 14 mg/kg bodyweight or left unhandled. One hour after injection animals were killed, the hippocampal region was dissected and chromatin extracted for GR ChIP assay. ChIP samples (n=9) were analyzed by RTqPCR using Taqman assays that targeted the GRE/MRE-6.1,synergy module or a distal intronic region (negative control) of the mouse *Klf9* gene. Bars represent the mean ChIP signals expressed as a percentage of input. Statistical analysis was conducted on $\log_{10}$ transformed data, and the asterisks indicate statistically significant differences between unhandled and CORT-injected animals ($P<0.05$; Student's *t* test). Dashed lines represent the additive effects of T_3 plus CORT on ChIP signal.

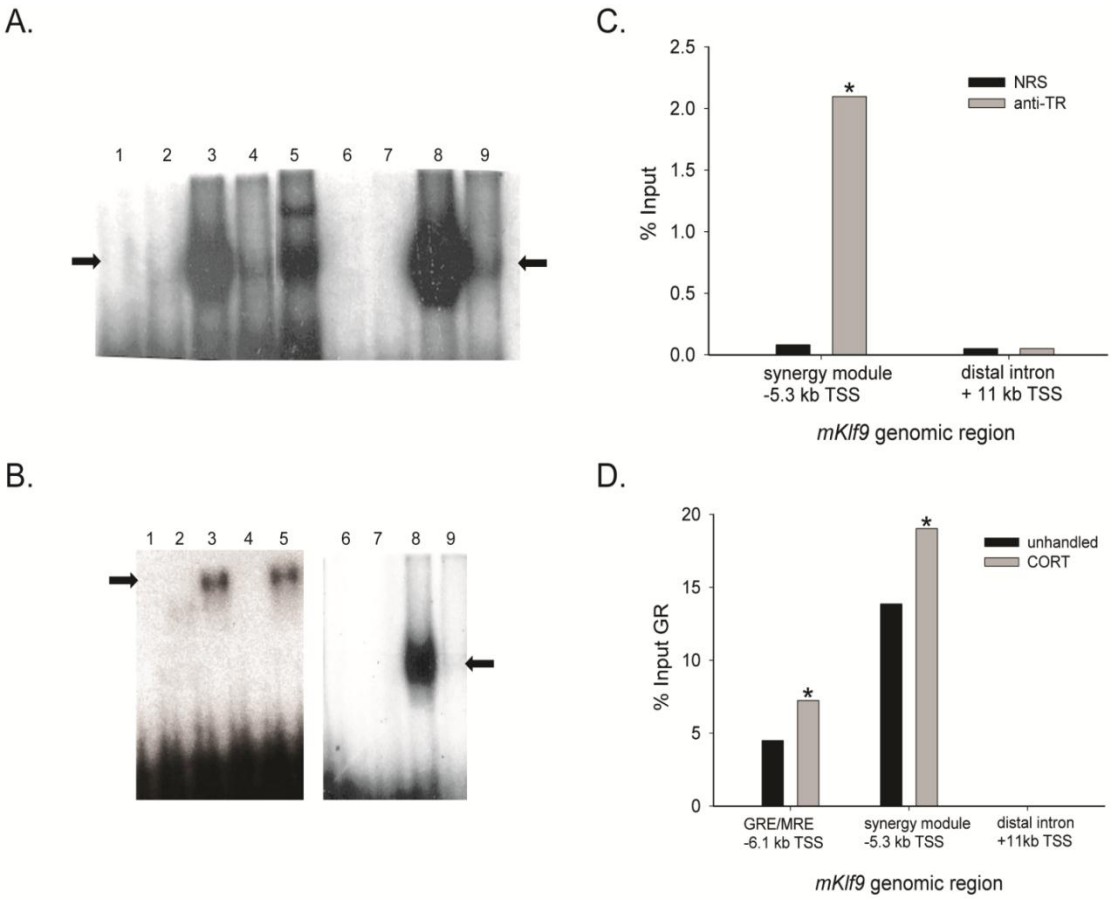
A.
1 2 3 4 5 6 7 8 9
B.
1 2 3 4 5 6 7 8 9
C.
2.5
2.0
1.5
1.0
0.5
0.0
% Input
*
NRS
anti-TR
synergy module
-5.3 kb TSS
distal intron
+ 11 kb TSS
mKlf9 genomic region
D.
20
15
10
5
0
% Input GR
*
*
unhandled
CORT
GRE/MRE
-6.1 kb TSS
synergy module
-5.3 kb TSS
distal intron
+11kb TSS
mKlf9 genomic region

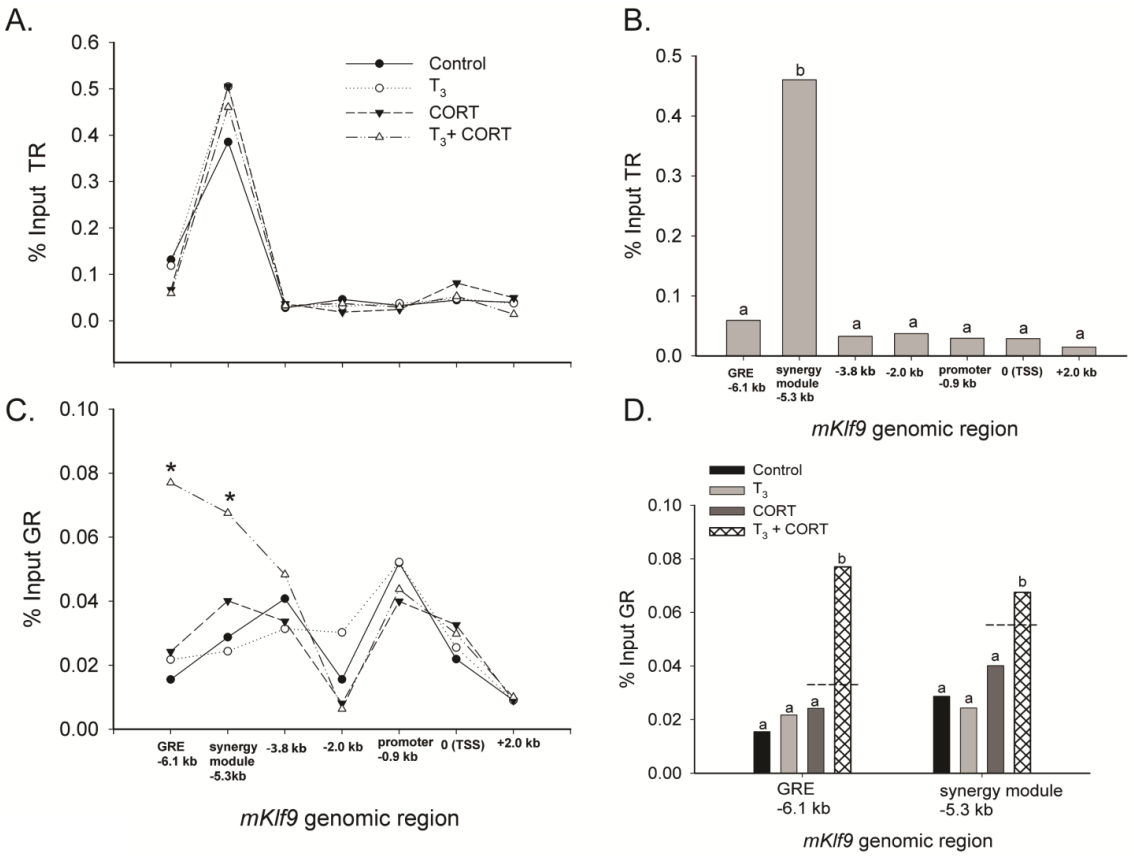

Fig. 3.6. Hormone- dependent recruitment of TR and GR across the *Klf9* locus. HT-22 cells were treated with T_3 (30 nM), CORT (100 nM) or T_3 plus CORT for 4 h before harvest for chromatin extraction and ChIP assay for TR **(A, B)** and GR **(C,D)**. ChIP samples (n=6) were analyzed by RTqPCR using Taqman assays that target different genomic regions of mouse *Klf9* gene indicated by their distance from the *Klf9* transcription start site (TSS). Line plots represent the hormone dependent association of TR **(A)** or GR **(C)** across the *Klf9* genomic locus expressed as percentage of input. Asterisks indicate a statistically significant synergistic effect of T_3 plus CORT on TR or GR association. Representative bar graphs of ChIP signals expressed as a percentage of input of a subset of data points for TR with T_3 plus CORT treatment **(B)** and GR **(D)** are also shown. Statistical analysis was conducted on $\log_{10}$ transformed data, and the letters above the means indicate significant differences among treatments (means with the same letter are not significantly different; Tukey's multiple comparison test; $P<0.05$).

Fig. 3.7. Corticosterone (CORT) or 3,5,3'-triiodothyronine (T_3) promotes nucleosome eviction, histone 3 and histone 4 acetylation at the synergy module of the mouse *Klf9* gene. HT-22 cells were treated with T_3 (30 nM), CORT (100 nM) or T_3 plus CORT for 4 h before harvest for chromatin extraction and ChIP assay for histone 3(H3) **(A, B)**, acetylated histone 3 (AcH3) **(C,D)** or acetylated histone 4 (AcH4) **(E,F)**. ChIP samples (n=4) were analyzed by RTqPCR using Taqman assays that target different genomic regions of mouse *Klf9* gene indicated by their distance from the *Klf9* transcription start site (TSS). Line plots represent the hormone dependent ChIP signals for H3 **(A),** AcH3 **(C)** or AcH4 **(E)** across the *Klf9* genomic locus expressed as percentage of input. Asterisks indicate a statistically significant effect of T_3 or CORT. Representative bar graphs of ChIP signals expressed as a percentage of input of a subset of data points for H3 **(B),** AcH3 **(D)** or AcH4 **(F)** are also shown**.** Statistical analysis was conducted on $\log_{10}$ transformed data, and the letters above the means indicate significant differences among treatments (means with the same letter are not significantly different; Tukey's multiple comparison test; $P<0.05$).

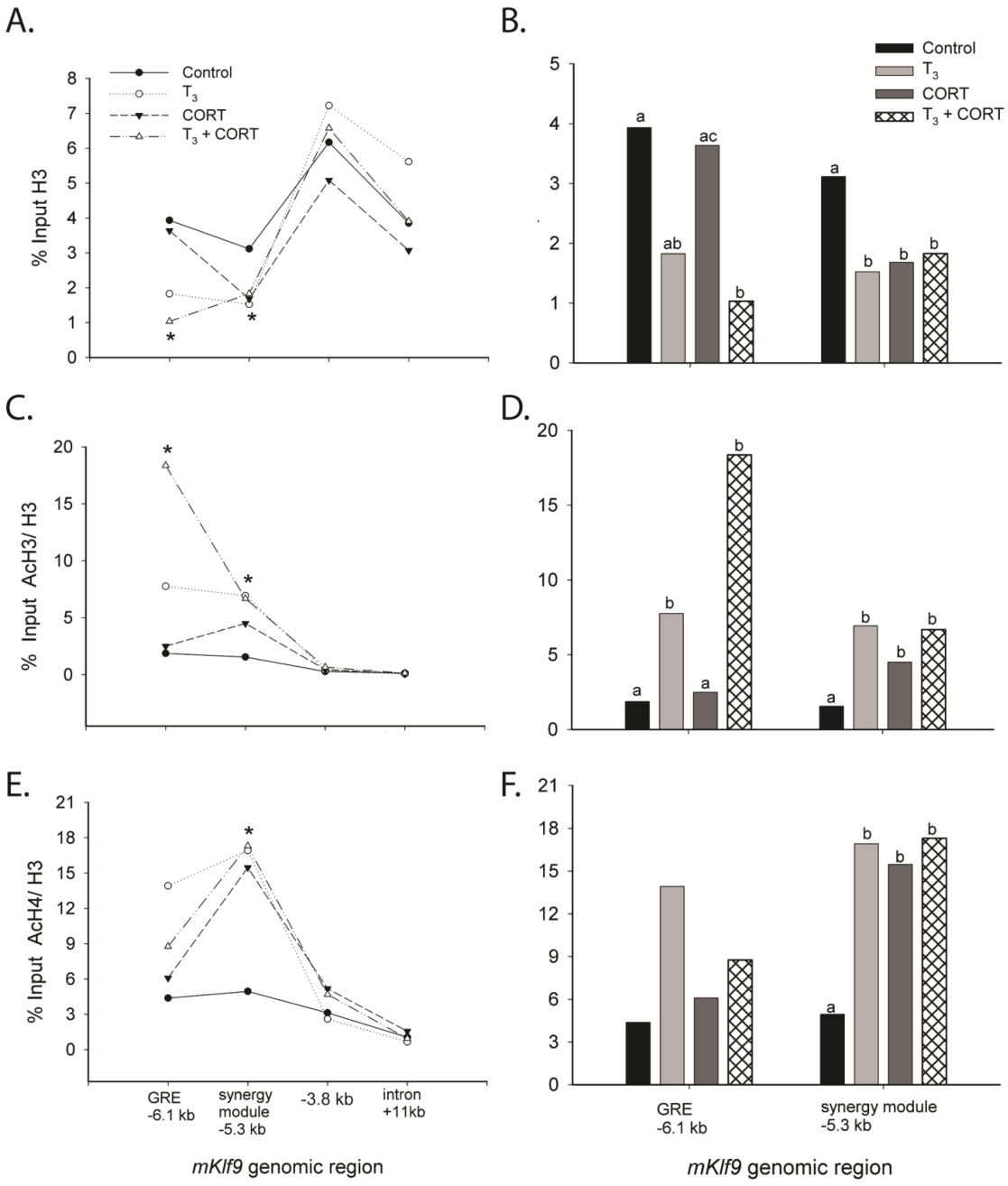
A.
B.
C.
D.
E.
F.
Control
T3
CORT
T3 + CORT
% Input H3
% Input AcH3/ H3
% Input AcH4/ H3
GRE -6.1 kb
synergy module -5.3 kb
-3.8 kb
intron +11kb
mKlf9 genomic region

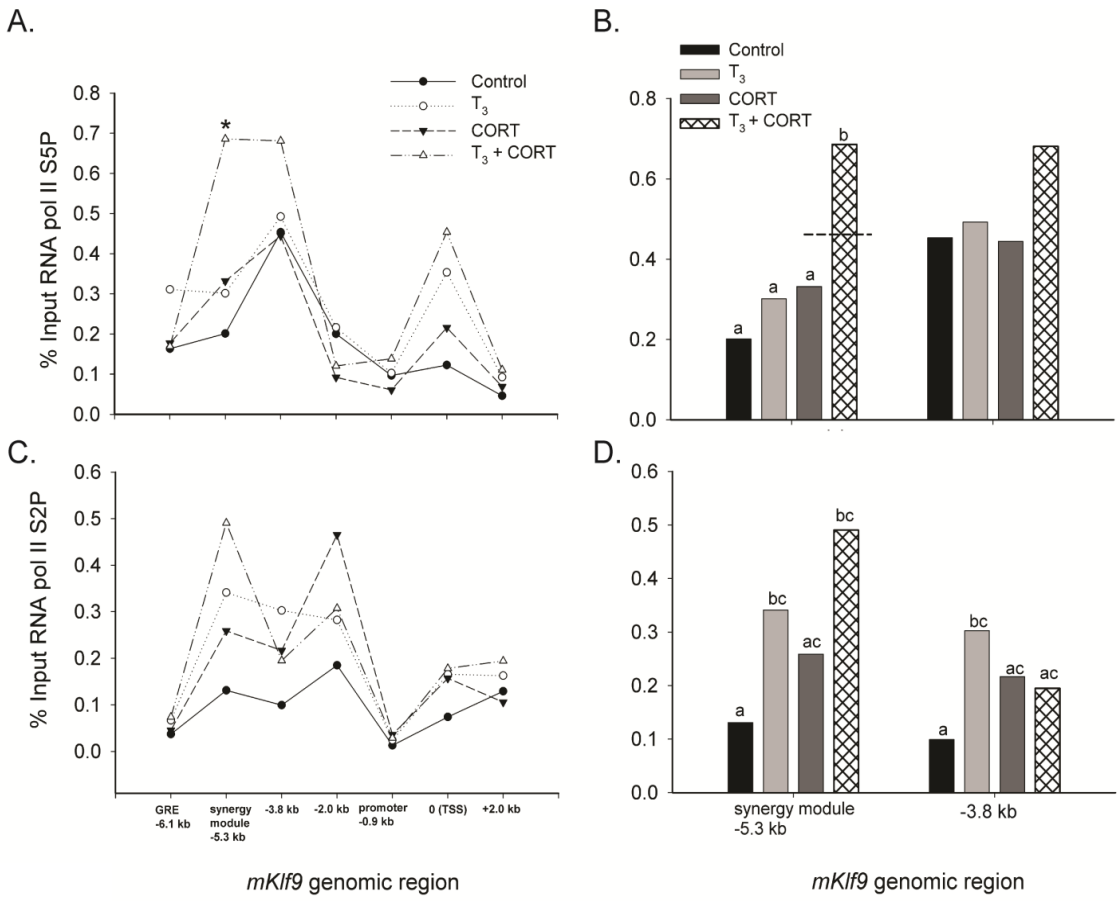

Fig. 3.8. Hormone-dependent recruitment of stalled RNA polymerase II (S5P) and elongating RNA polymerase II (S2P) across the *Klf9* locus. HT-22 cells were treated with T_3 (30 nM), CORT (100 nM) or T_3 plus CORT for 4 h before harvest for chromatin extraction and ChIP assay for stalled RNA pol II S5P **(A, B)** and elongating RNA pol II S2P **(C,D)**. ChIP samples (n=6) were analyzed by RTqPCR using Taqman assays that target different genomic regions of mouse *Klf9* gene indicated by their distance from the *Klf9* transcription start site (TSS). Line plots represent the hormone dependent association of stalled (S5P) **(A)** or elongating (S2P) **(C)** RNA polymerase II across the *Klf9* genomic locus expressed as percentage of input. Asterisks indicate a statistically significant synergistic effect of T_3 plus CORT on stalled RNA polymerase II association. Representative bar graphs of ChIP signals expressed as a percentage of input of a subset of data points for stalled (S5P) **(B)** or elongating (S2P) **(D)** RNA polymerase II are also shown. Statistical analysis was conducted on $\log_{10}$ transformed data, and the letters above the means indicate significant differences among treatments (means with the same letter are not significantly different; Tukey's multiple comparison test; $P<0.05$). Dashed lines represent the additive effects of T_3 plus CORT on ChIP signal.

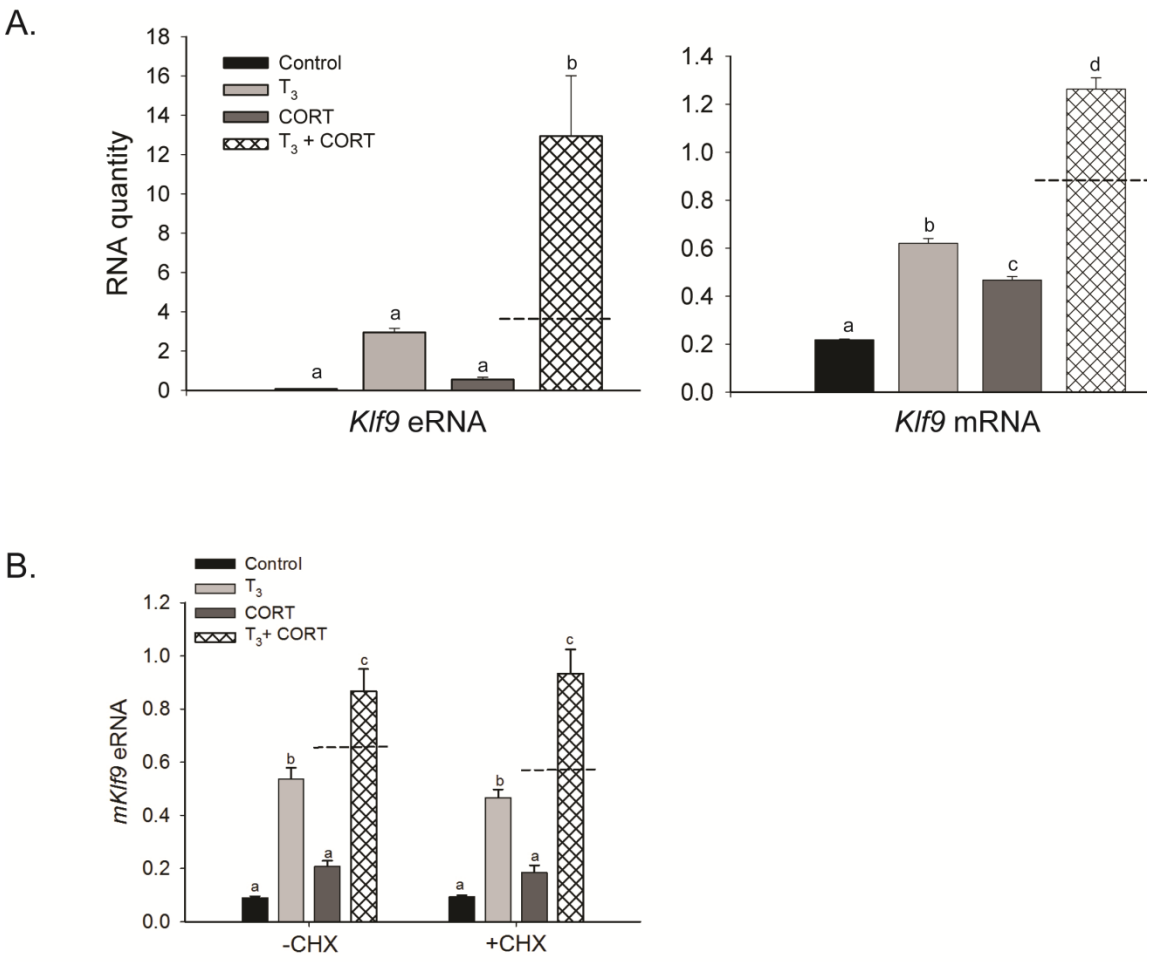

Fig. 3.9. Corticosterone (CORT) synergizes with 3,5,3'-triiodothyronine (T_3) to induce transcription at the *Klf9* synergy module. (A) HT-22 cells were treated with30 nM T_3, 100 nM CORT or T_3 plus CORT and (B) with or without cycloheximide (CHX) for 30 min before addition of 30 nM T_3, 100 nM CORT or T_3 plus CORT for 4h before harvest and RNA extraction. RNA samples were treated with DNAseI and were measured by RTqPCR using Taqman assay targeted to the synergy module (eRNA) and an exon-exon boundary of the *Klf9* gene (mRNA). RTqPCR without reverse transcriptase was used as a negative control and did not yield any amplicons. RNA transcripts at were normalized to the mRNA level of the housekeeping gene *GAPDH*. Bars represent the mean $\pm$ SEM and letters above the means indicate significant differences among treatments (means with the same letter are not significantly different; Tukey's multiple comparison test; $P<0.05$). Dashed lines represent the additive effects of T_3 plus CORT on RNA levels.

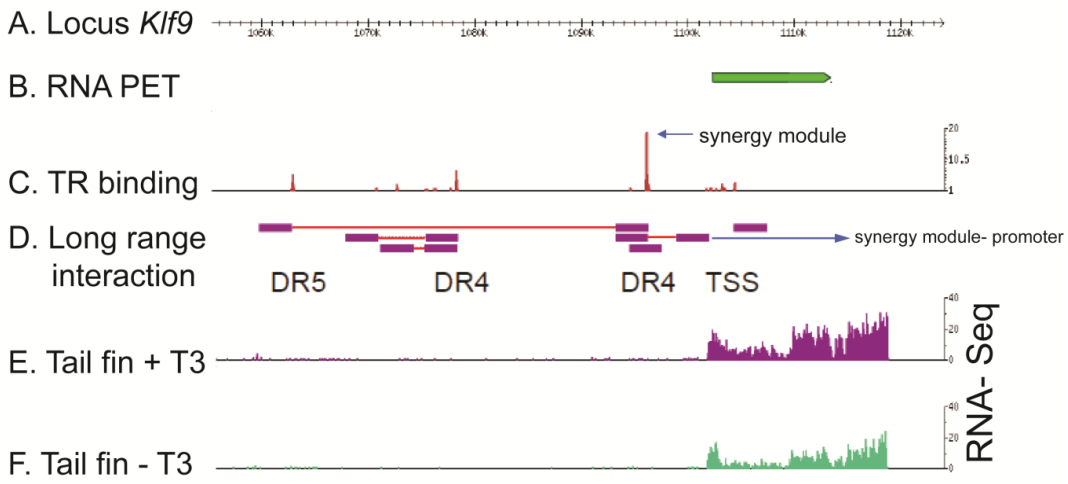

Fig. 3.10. The synergy module interacts with the *Klf9* promoter as shown by Chromosomal interaction analysis by paired end tag sequencing (ChIA-PET). (A) The frog *Klf9* locus shown as reference to locate genomic regions identified by RNA-paired end tag sequencing (RNA- PET) **(B),** or RNA-Seq to identify and measure *Klf9* mRNA transcript levels across the locus produced with **(E)** or without **(F)** T_3 treatment of tadpole tail fin tissue. **(C)** Thyroid hormone receptor (TR) binding sites and the corresponding levels of TR bound across the *Klf9* locus, indicated as red peaks, were identified by TR ChIP- Seq using chromatin from T_3-treated tadpole tail fin tissue.. Within the genomic region shown, highest levels of TR binding were found in a region corresponding to the synergy module (blue arrow) **(D)** Thyroid hormone-dependent long-range chromosomal interactions across the *Klf9* locus were identified by (ChIA-PET). Long range interaction between genomic regions are shown as two purple bars connected by a red line. Data from Laurent Sachs.

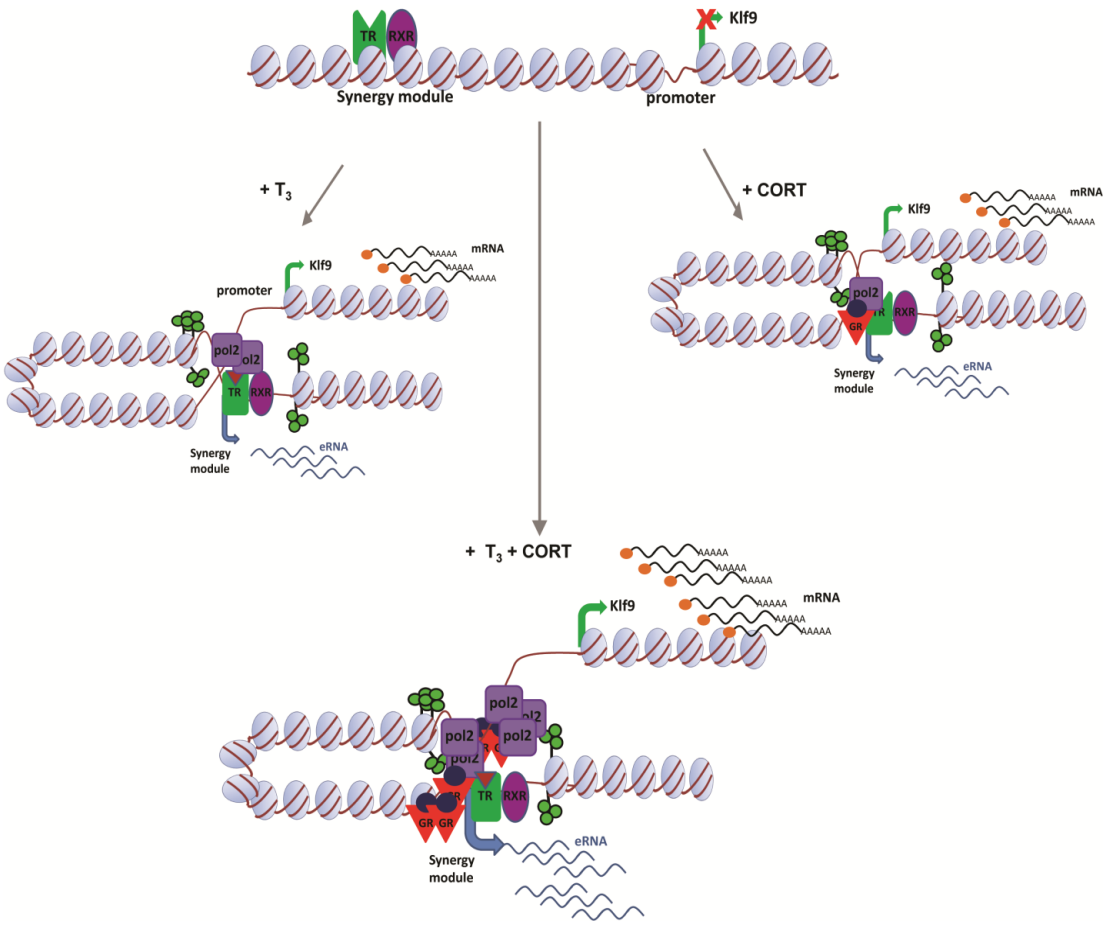

Fig. 3.11. *Klf9* is synergistically regulated by corticosterone (CORT) and 3,5,3'-triiodothyronine (T_3) at the transcriptional level. In the absence of T_3, thyroid hormone receptor (TR) is bound to the *Klf9* synergy module and is associated with corepressors to maintain a compact chromatin environment that is not permissive for *Klf9* transcription. Upon T_3 binding, TR releases the corepressors in exchange for coactivators that promote histone acetylation, chromatin decompaction, looping and RNA polymerase II mediated transcription of the synergy module (eRNA) and *Klf9* gene (mRNA). On the other hand, CORT treatment activates the glucocorticoid receptor (GR) located in the cytoplasm followed by translocation to the nucleus where it associates with the synergy module and other GRE/MRE and recruits coactivators leading to possible chromatin looping and RNA pol II mediated transcription or *Klf9* eRNA and mRNA. Combined treatment with T_3 plus CORT leads to T_3 dependent depression of the *Klf9* locus that allows an enhanced and synergistic recruitment of GR. The presence of ligand bound TR and enhanced recruitment of GR at the synergy module leads to a synergistic association of stalled RNA polymerase II (pol2) at the synergy module maintaining the *Klf9* locus poised for a rapid transcriptional response. Association of hormone bound TR, GR and pol2 at the synergy module leads to transcription at that region and to chromosomal looping that allows the regulatory information at the synergy module to be relayed to the promoter ultimately resulting in synergistic gene transcription.

References

Amiel-Tison, C., D. Cabrol, et al. (2004). "Fetal adaptation to stress. Part I: acceleration of fetal maturation and earlier birth triggered by placental insufficiency in humans." Early Hum Dev **78**(1): 15-27.

Aoyagi, S. and T. K. Archer (2008). "Dynamics of coactivator recruitment and chromatin modifications during nuclear receptor mediated transcription." Mol Cell Endocrinol **280**(1-2): 1-5.

Aranda, A. and A. Pascual (2001). "Nuclear hormone receptors and gene expression." Physiol Rev **81**(3): 1269-1304.

Bagamasbad, P., K. L. Howdeshell, et al. (2008). "A role for basic transcription element-binding protein 1 (BTEB1) in the autoinduction of thyroid hormone receptor beta." J Biol Chem **283**(4): 2275-2285.

Bonett, R. M., E. D. Hoopfer, et al. (2010). "Molecular mechanisms of corticosteroid synergy with thyroid hormone during tadpole metamorphosis." Gen Comp Endocrinol **168**(2): 209-219.

Bonett, R. M., F. Hu, et al. (2009). "Stressor and glucocorticoid-dependent induction of the immediate early gene kruppel-like factor 9: implications for neural development and plasticity." Endocrinology **150**(4): 1757-1765.

Bruggemeier, U., M. Kalff, et al. (1991). "Ubiquitous transcription factor OTF-1 mediates induction of the MMTV promoter through synergistic interaction with hormone receptors." Cell **64**(3): 565-572.

Bruggemeier, U., L. Rogge, et al. (1990). "Nuclear factor I acts as a transcription factor on the MMTV promoter but competes with steroid hormone receptors for DNA binding." EMBO J **9**(7): 2233-2239.

Carey, M. (1998). "The enhanceosome and transcriptional synergy." Cell **92**(1): 5-8.

Cato, A. C., P. Skroch, et al. (1988). "DNA sequences outside the receptor-binding sites differently modulate the responsiveness of the mouse mammary tumour virus promoter to various steroid hormones." EMBO J **7**(5): 1403-1410.

Cayrou, C., R. J. Denver, et al. (2002). "Suppression of the basic transcription element-binding protein in brain neuronal cultures inhibits thyroid hormone-induced neurite branching." Endocrinology **143**(6): 2242-2249.

Challis, J. R., D. Sloboda, et al. (2001). "The fetal placental hypothalamic-pituitary-adrenal (HPA) axis, parturition and post natal health." Mol Cell Endocrinol **185**(1-2): 135-144.

Chen, W. and R. G. Roeder (2007). "The Mediator subunit MED1/TRAP220 is required for optimal glucocorticoid receptor-mediated transcription activation." Nucleic Acids Res **35**(18): 6161-6169.

Cheng, S. Y., J. L. Leonard, et al. (2010). "Molecular aspects of thyroid hormone actions." Endocr Rev **31**(2): 139-170.

Courey, A. J. (2001). "Cooperativity in transcriptional control." Curr Biol **11**(7): R250-252.

De Bosscher, K., W. Vanden Berghe, et al. (2003). "The interplay between the glucocorticoid receptor and nuclear factor-kappaB or activator protein-1: molecular mechanisms for gene repression." Endocr Rev **24**(4): 488-522.

Denver, R. J. (2009). "Stress hormones mediate environment-genotype interactions during amphibian development." Gen Comp Endocrinol **164**(1): 20-31.
Denver, R. J., L. Ouellet, et al. (1999). "Basic transcription element-binding protein (BTEB) is a thyroid hormone-regulated gene in the developing central nervous system. Evidence for a role in neurite outgrowth." J Biol Chem **274**(33): 23128-23134.
Denver, R. J., S. Pavgi, et al. (1997). "Thyroid hormone-dependent gene expression program for Xenopus neural development." J Biol Chem **272**(13): 8179-8188.
Denver, R. J. and K. E. Williamson (2009). "Identification of a thyroid hormone response element in the mouse Kruppel-like factor 9 gene to explain its postnatal expression in the brain." Endocrinology **150**(8): 3935-3943.
Furlow, J. D. and A. Kanamori (2002). "The transcription factor basic transcription element-binding protein 1 is a direct thyroid hormone response gene in the frog Xenopus laevis." Endocrinology **143**(9): 3295-3305.
Galton, V. A. (1990). "Mechanisms underlying the acceleration of thyroid hormone-induced tadpole metamorphosis by corticosterone." Endocrinology **127**(6): 2997-3002.
Germain, P., B. Staels, et al. (2006). "Overview of nomenclature of nuclear receptors." Pharmacol Rev **58**(4): 685-704.
Hagege, H., P. Klous, et al. (2007). "Quantitative analysis of chromosome conformation capture assays (3C-qPCR)." Nat Protoc **2**(7): 1722-1733.
Herschlag, D. and F. B. Johnson (1993). "Synergism in transcriptional activation: a kinetic view." Genes Dev **7**(2): 173-179.
Hittelman, A. B., D. Burakov, et al. (1999). "Differential regulation of glucocorticoid receptor transcriptional activation via AF-1-associated proteins." EMBO J **18**(19): 5380-5388.
Ho, Y., F. Elefant, et al. (2006). "Locus control region transcription plays an active role in long-range gene activation." Mol Cell **23**(3): 365-375.
Hoopfer, E. D., L. Huang, et al. (2002). "Basic transcription element binding protein is a thyroid hormone-regulated transcription factor expressed during metamorphosis in Xenopus laevis." Dev Growth Differ **44**(5): 365-381.
Ito, M. and R. G. Roeder (2001). "The TRAP/SMCC/Mediator complex and thyroid hormone receptor function." Trends Endocrinol Metab **12**(3): 127-134.
Kaczynski, J., T. Cook, et al. (2003). "Sp1- and Kruppel-like transcription factors." Genome Biol **4**(2): 206.
Kagey, M. H., J. J. Newman, et al. (2010). "Mediator and cohesin connect gene expression and chromatin architecture." Nature **467**(7314): 430-435.
Kassel, O. and P. Herrlich (2007). "Crosstalk between the glucocorticoid receptor and other transcription factors: molecular aspects." Mol Cell Endocrinol **275**(1-2): 13-29.
Kikuyama, S., K. Kawamura, et al. (1993). "Aspects of amphibian metamorphosis: hormonal control." Int Rev Cytol **145**: 105-148.
Kikuyama, S., K. Niki, et al. (1983). "Studies on corticoid action on the toad tadpole tail in vitro." Gen Comp Endocrinol **52**(3): 395-399.
Kim, T. K., M. Hemberg, et al. (2010). "Widespread transcription at neuronal activity-regulated enhancers." Nature **465**(7295): 182-187.

Komarnitsky, P., E. J. Cho, et al. (2000). "Different phosphorylated forms of RNA polymerase II and associated mRNA processing factors during transcription." Genes Dev **14**(19): 2452-2460.
Li, G., M. J. Fullwood, et al. (2010). "ChIA-PET tool for comprehensive chromatin interaction analysis with paired-end tag sequencing." Genome Biol **11**(2): R22.
Lin, Y., B. L. Bloodgood, et al. (2008). "Activity-dependent regulation of inhibitory synapse development by Npas4." Nature **455**(7217): 1198-1204.
Ling, J., L. Ainol, et al. (2004). "HS2 enhancer function is blocked by a transcriptional terminator inserted between the enhancer and the promoter." J Biol Chem **279**(49): 51704-51713.
Louie, M. C., H. Q. Yang, et al. (2003). "Androgen-induced recruitment of RNA polymerase II to a nuclear receptor-p160 coactivator complex." Proc Natl Acad Sci U S A **100**(5): 2226-2230.
Luebben, W. R., N. Sharma, et al. (2010). "Nucleosome eviction and activated transcription require p300 acetylation of histone H3 lysine 14." Proc Natl Acad Sci U S A **107**(45): 19254-19259.
Machuca, I., G. Esslemont, et al. (1995). "Analysis of structure and expression of the Xenopus thyroid hormone receptor-beta gene to explain its autoinduction." Mol Endocrinol **9**(1): 96-107.
Maher, P. and J. B. Davis (1996). "The role of monoamine metabolism in oxidative glutamate toxicity." J Neurosci **16**(20): 6394-6401.
Margaritis, T. and F. C. Holstege (2008). "Poised RNA polymerase II gives pause for thought." Cell **133**(4): 581-584.
Martial, J. A., P. H. Seeburg, et al. (1977). "Regulation of growth hormone gene expression: synergistic effects of thyroid and glucocorticoid hormones." Proc Natl Acad Sci U S A **74**(10): 4293-4295.
McDonald, M. C. and S. J. Henning (1992). "Synergistic effects of thyroxine and dexamethasone on enzyme ontogeny in rat small intestine." Pediatr Res **32**(3): 306-311.
Metzger, R. J., O. D. Klein, et al. (2008). "The branching programme of mouse lung development." Nature **453**(7196): 745-750.
Morimoto, B. H. and D. E. Koshland, Jr. (1990). "Excitatory amino acid uptake and N-methyl-D-aspartate-mediated secretion in a neural cell line." Proc Natl Acad Sci U S A **87**(9): 3518-3521.
Morimoto, B. H. and D. E. Koshland, Jr. (1990). "Induction and expression of long- and short-term neurosecretory potentiation in a neural cell line." Neuron **5**(6): 875-880.
Morita, M., A. Kobayashi, et al. (2003). "Functional analysis of basic transcription element binding protein by gene targeting technology." Mol Cell Biol **23**(7): 2489-2500.
Morris, D. P., G. A. Michelotti, et al. (2005). "Evidence that phosphorylation of the RNA polymerase II carboxyl-terminal repeats is similar in yeast and humans." J Biol Chem **280**(36): 31368-31377.
Muse, G. W., D. A. Gilchrist, et al. (2007). "RNA polymerase is poised for activation across the genome." Nat Genet **39**(12): 1507-1511.

Myers, L. C. and R. D. Kornberg (2000). "Mediator of transcriptional regulation." Annu Rev Biochem **69**: 729-749.
Nechaev, S. and K. Adelman (2008). "Promoter-proximal Pol II: when stalling speeds things up." Cell Cycle **7**(11): 1539-1544.
Nogami, H., Y. Hiraoka, et al. (2002). "A composite hormone response element regulates transcription of the rat GHRH receptor gene." Endocrinology **143**(4): 1318-1326.
Nogami, H., T. Yokose, et al. (1995). "Regulation of growth hormone expression in fetal rat pituitary gland by thyroid or glucocorticoid hormone." Am J Physiol **268**(2 Pt 1): E262-267.
O'Brien, T. and J. T. Lis (1991). "RNA polymerase II pauses at the 5' end of the transcriptionally induced Drosophila hsp70 gene." Mol Cell Biol **11**(10): 5285-5290.
Ong, C. T. and V. G. Corces (2011). "Enhancer function: new insights into the regulation of tissue-specific gene expression." Nat Rev Genet **12**(4): 283-293.
Orom, U. A., T. Derrien, et al. (2010). "Long noncoding RNAs with enhancer-like function in human cells." Cell **143**(1): 46-58.
Park, S. W., G. Li, et al. (2005). "Thyroid hormone-induced juxtaposition of regulatory elements/factors and chromatin remodeling of Crabp1 dependent on MED1/TRAP220." Mol Cell **19**(5): 643-653.
Pei, L., M. Leblanc, et al. (2011). "Thyroid hormone receptor repression is linked to type I pneumocyte-associated respiratory distress syndrome." Nat Med **17**(11): 1466-1472.
Phatnani, H. P. and A. L. Greenleaf (2006). "Phosphorylation and functions of the RNA polymerase II CTD." Genes Dev **20**(21): 2922-2936.
Porterfield, S. P. and C. E. Hendrich (1993). "The role of thyroid hormones in prenatal and neonatal neurological development--current perspectives." Endocr Rev **14**(1): 94-106.
Rao, N. A., M. T. McCalman, et al. (2011). "Coactivation of GR and NFKB alters the repertoire of their binding sites and target genes." Genome Res **21**(9): 1404-1416.
Reichardt, H. M., K. H. Kaestner, et al. (1998). "DNA binding of the glucocorticoid receptor is not essential for survival." Cell **93**(4): 531-541.
Reul, J. M. and E. R. de Kloet (1985). "Two receptor systems for corticosterone in rat brain: microdistribution and differential occupation." Endocrinology **117**(6): 2505-2511.
Ribeiro, R. C., P. J. Kushner, et al. (1995). "The nuclear hormone receptor gene superfamily." Annu Rev Med **46**: 443-453.
Robyr, D., A. P. Wolffe, et al. (2000). "Nuclear hormone receptor coregulators in action: diversity for shared tasks." Mol Endocrinol **14**(3): 329-347.
Roeder, R. G. (2005). "Transcriptional regulation and the role of diverse coactivators in animal cells." FEBS Lett **579**(4): 909-915.
Sagara, Y., R. Dargusch, et al. (1998). "Cellular mechanisms of resistance to chronic oxidative stress." Free Radic Biol Med **24**(9): 1375-1389.
Samuels, H. H., F. Stanley, et al. (1979). "Depletion of L-3,5,3'-triiodothyronine and L-thyroxine in euthyroid calf serum for use in cell culture studies of the action of thyroid hormone." Endocrinology **105**(1): 80-85.

Saunders, A., L. J. Core, et al. (2006). "Breaking barriers to transcription elongation." Nat Rev Mol Cell Biol **7**(8): 557-567.
Schule, R., M. Muller, et al. (1988). "Many transcription factors interact synergistically with steroid receptors." Science **242**(4884): 1418-1420.
Scobie, K. N., B. J. Hall, et al. (2009). "Kruppel-like factor 9 is necessary for late-phase neuronal maturation in the developing dentate gyrus and during adult hippocampal neurogenesis." J Neurosci **29**(31): 9875-9887.
Shapiro, L. E., H. H. Samuels, et al. (1978). "Thyroid and glucocorticoid hormones synergistically control growth hormone mRNA in cultured GH1 cells." Proc Natl Acad Sci U S A **75**(1): 45-49.
Shi, Y.-B. (2000). Amphibian metamorphosis : from morphology to molecular biology. New York, Wiley-Liss.
Shi, Y. B. (2009). "Dual functions of thyroid hormone receptors in vertebrate development: the roles of histone-modifying cofactor complexes." Thyroid **19**(9): 987-999.
Smith, B. T. and K. Sabry (1983). "Glucocorticoid-thyroid synergism in lung maturation: a mechanism involving epithelial-mesenchymal interaction." Proc Natl Acad Sci U S A **80**(7): 1951-1954.
Szutorisz, H., C. Canzonetta, et al. (2005). "Formation of an active tissue-specific chromatin domain initiated by epigenetic marking at the embryonic stem cell stage." Mol Cell Biol **25**(5): 1804-1820.
Szutorisz, H., N. Dillon, et al. (2005). "The role of enhancers as centres for general transcription factor recruitment." Trends Biochem Sci **30**(11): 593-599.
Vallabhapurapu, S. and M. Karin (2009). "Regulation and function of NF-kappaB transcription factors in the immune system." Annu Rev Immunol **27**: 693-733.
Vernimmen, D., M. De Gobbi, et al. (2007). "Long-range chromosomal interactions regulate the timing of the transition between poised and active gene expression." EMBO J **26**(8): 2041-2051.
Vieira, K. F., P. P. Levings, et al. (2004). "Recruitment of transcription complexes to the beta-globin gene locus in vivo and in vitro." J Biol Chem **279**(48): 50350-50357.
Voz, M. L., B. Peers, et al. (1992). "Transcriptional regulation by triiodothyronine requires synergistic action of the thyroid receptor with another trans-acting factor." Mol Cell Biol **12**(9): 3991-3997.
Welberg, L. A. and J. R. Seckl (2001). "Prenatal stress, glucocorticoids and the programming of the brain." J Neuroendocrinol **13**(2): 113-128.
Wolf, I. M., M. D. Heitzer, et al. (2008). "Coactivators and nuclear receptor transactivation." J Cell Biochem **104**(5): 1580-1586.
Yao, M., J. Schulkin, et al. (2008). "Evolutionarily conserved glucocorticoid regulation of corticotropin-releasing factor expression." Endocrinology **149**(5): 2352-2360.
Zeitlinger, J., A. Stark, et al. (2007). "RNA polymerase stalling at developmental control genes in the Drosophila melanogaster embryo." Nat Genet **39**(12): 1512-1516.
Zhu, X., J. Ling, et al. (2007). "A facilitated tracking and transcription mechanism of long-range enhancer function." Nucleic Acids Res **35**(16): 5532-5544.

Chapter 4

IDENTIFICATION OF GENES SYNERGISTICALLY REGULATED BY THYROID HORMONE AND GLUCOCORTICOIDS IN HIPPOCAMPAL NEURONS BY MICROARRAY ANALYSIS

Abstract

The hippocampus is a well-known target of thyroid hormone (T_3) and glucocorticoid action. Deficiency in T_3 during neonatal development results in morphological and functional changes in the hippocampus such as reduced dendritic arborization, delayed synaptogenesis and impaired synaptic transmission. Glucocorticoids (e.g., corticosterone - CORT) both facilitate and inhibit hippocampal development and function depending on their level and duration of elevation. Despite evidence that these two hormones play critical roles in neural development and function, few studies have looked at whether these hormones interact to regulate similar or different sets of target genes, or if they may cooperate to regulate gene expression. In this study we investigated gene regulation by T_3 or CORT alone, or the two hormones together in the mouse hippocamapal-derived cell line HT-22. We treated cells with T_3 (30 nM) or CORT (100 nM), or T3 plus CORT for 4 hr before cell harvest and RNA isolation for microarray analysis. We identified 425 genes that were regulated by CORT, 293 induced and 132 repressed. There were 203 genes regulated by T3, 116 induced and 87 repressed. We found 69 genes synergistically up-

regulated, and 80 genes synergistically down-regulated by T_3 plus CORT treatment. Among the synergistically up-regulated genes, gene ontology analysis identified a group of genes involved with cytoskeletal remodeling, supporting that a major synergistic action of T_3 and CORT in hippocampal cells is to shape neuronal morphology.

Introduction

The hippocampus, a neural structure important for learning and memory, is strongly influenced by the actions of thyroid hormone (T_3) and glucocorticoids (GCs; stress hormones; e.g., corticosterone - CORT) A deficienty of T_3 during neonatal and postnatal life results in morphological and functional changes in the hippocampus that include delayed neuronal migration, reduction in cell body size and dendritic arborization of granular and pyramidal neurons, delayed synaptogenesis in the dentate gyrus, reduction of synapses between mossy fibers and CA3 pyramidal neurons, impaired synaptic transmission in the CA1 region and impaired performance in behavioral tasks related to hippocampal function (Rami, Patel et al. 1986; Rami, Rabie et al. 1986; Gould, Allan et al. 1990; Rami and Rabie 1990; Akaike, Kato et al. 1991; Madeira and Paula-Barbosa 1993; Gilbert and Paczkowski 2003; Darbra, Balada et al. 2004; Gilbert 2004; Dong, Yin et al. 2005; Gilbert and Sui 2006; Gilbert and Sui 2008). Glucocorticoids also play important roles in hippocampal development and function, but they may have facilitatory or inhibitory effects depending on the physiological and behavioral context and, severity and duration of the stressor (Joels 2008). For example, in rodents, chronic stress, or prolonged treatment with GC causes retraction and atrophy of dendrites in the CA3 region of the hippocampus (Watanabe, Gould et al. 1992; Magarinos, Verdugo et al. 1997; McEwen 1999), neuronal loss, inhibits long term potentiation (LTP) and impairs hippocampal-dependent cognitive tasks (McEwen 1999). In contrast, moderate acute stress, mediated in part by GCs, has been shown to enhance hippocampal neuronal function and hippocampal-dependent processes (Shors 2001; Shors, Chua et al. 2001; Roozendaal 2002; Beylin and Shors 2003; Karst and Joels 2005; Joels, Pu et al. 2006).

Although several studies have established that T_3 and GCs influence structure and function of hippocampal neurons (Porterfield and Hendrich 1993; McEwen 1999; Porterfield 2000), few have investigated the interaction between, and combined effects of T_3 and GC (Gould, Woolley et al. 1991). Several gene expression analyses have been conducted to identify GC-induced genes in hippocampal neurons (Datson, van der Perk et al. 2001; Morsink, Steenbergen et al. 2006; Datson, Morsink et al. 2008; Royland, Parker et al. 2008; Datson, Speksnijder et al. 2010; Datson, Polman et al. 2011). However, to my knowledge, no gene expression analysis has been done on hippocampus to identify genes that are coordinately regulated by T_3 and GC. A gene that we found to be independently and synergistically regulated by T_3 and GC in hippocampal neurons is Krüppel-like factor 9 (*Klf9*) (Denver, Pavgi et al. 1997; Denver, Ouellet et al. 1999; Furlow and Kanamori 2002; Bagamasbad, Howdeshell et al. 2008; Bonett, Hu et al. 2009; Denver and Williamson 2009), Chapter 2,3). This transcription factor is known to influence neuronal structure and function(Denver, Ouellet et al. 1999; Cayrou, Denver et al. 2002; Morita, Kobayashi et al. 2003; Lin, Bloodgood et al. 2008; Scobie, Hall et al. 2009). The synergistic regulation of *Klf9* by T_3 and GC is marked (see Chapter 3), but this is the only gene identified to be regulated in this manner in the hippocampus. We therefore sought to determine if the synergistic regulation of *Klf9* was an isolated phenomenon, or if there are other genes that are similarly regulated. If other genes show similar synergistic induction by hormones, this might point to similar transcriptional mechanisms, and perhaps related functions in hormone action on hippocampal cells. We identified 69 synergistically up-regulated and 80 genes synergistically down-regulated by T_3 and GC. Gene ontology analysis of the synergistically up-regulated genes showed that there is an enrichment of

genes involved in organization of the actin cytoskeleton, and in cell growth and proliferation, suggesting that T_3 and GCs may coordinately regulate genes involved in neuroprogenitor proliferation, and neuronal morphology.

Materials and methods

Cell Culture and Transient Transfection Assays. HT-22 is a cell line derived from mouse hippocampus immortalized with the SV40 T antigen (Morimoto and Koshland 1990; Morimoto and Koshland 1990). This cell line exhibits properties of differentiated neurons; e.g., they express neuron specific markers such as enolase and the neurofilament triplet, but not the glial cell marker, glial fibrillary acidic protein (Morimoto and Koshland 1990; Morimoto and Koshland 1990; Maher and Davis 1996; Sagara, Dargusch et al. 1998). HT-22 cells were cultured in Dulbecco's modified Eagle's medium (DMEM; Invitrogen) supplemented with sodium bicarbonate (2.2 g/L), penicillin G (100 units/mL), streptomycin sulfate (100 μg/mL) and 10% fetal bovine serum (FBS) that had been stripped of thyroid (Samuels, Stanley et al. 1979) and steroid hormones (Yao, Schulkin et al. 2008). Cells were cultured under a humidified atmosphere of 5% CO_2 at 37^{o}C. For gene expression analysis we seeded cells at a density of 1 x10^7 cells per well in 100 cm^2 plates. When cells reached ~90-95% confluency, and immediately before hormone treatments, we replaced the growth medium with serum-free DMEM. Corticosterone (CORT; Sigma C2505) was dissolved in 100% ethanol and added to the media to a final concentration of 100 nM. 3,5,3'-triiodothyronine (T_3; Sigma T2752) was dissolved in dimethylsulfoxide (DMSO) and added to a final concentration of 30 nM. Control treatments received an equivalent concentration of vehicle (0.001% ethanol and

0.03% DMSO). All hormone treatments were continued for 4 h before cell harvest. Each hormone treatment was performed in triplicate for RNA extraction and microarray analysis.

RNA Extraction, Reverse Transcription and Quantitative PCR. We extracted total RNA from HT-22 cells using the Trizol reagent (Invitrogen) following the manufacturer's protocol. The extracted RNA was further purified using the RNAeasy Kit (Qiagen) to obtain a UV absorbance ratio at $A_{260/280}$ to be between 1.8 to 2.0. We conducted RTqPCR for *Klf9* expression (as described in Chapter 2) to verify that the hormone treatments worked before microarray analysis.

Microarray analysis. Total RNA (175 ng per sample) was amplified using the Illumina Totalprep RNA Amplification Kit (Ambion, Inc.) to generate biotinylated amplified RNA. The biotinylated RNA (2 µg) was hybridized at 55° C for 22 hr to Illumina Bead Chips (Illumina Mouse WG-6 v2.0). Microarrays were washed and scanned for data collection as directed by the manufacturer. Microarray data was normalized (Rank Invariant), and analysed with Illumina Genome Studio software. The mean array values of three replicates per treatment were used to compute fold change over control.

***Data Analysis and Statistics*.** We filtered the microarray data set using the Statisical Analysis Program SAS (version 9.5, SAS Institute, Inc). Gene expression fold change was computed as the ratio between the average of the hormone treatment hybridization signal intensity (n=3/ hormone treatment) and average of the control treatment

hybridization intensity. Hormone-dependent regulation was identified based on a cut-off P value <0.05, and a 1.2 fold change for T_3 treated samples; and P<0.02, and a 1.5 fold change for CORT, and T_3 plus CORT-treated samples. The P value cutoff was set higher and fold change cutoff was set lower for the T_3 data set than the CORT and T_3 plus CORT data set since we only found 10 genes to be regulated by T_3 at a P <0.02, 1.5 fold change. The HT-22 cells are differentiated neurons and may have a weak T_3 response. Genes considered to be synergistically regulated by T_3 plus CORT are , those that were not regulated by T_3 or CORT alone but were regulated with T3 plus CORT based on a P<0.02 and a 1.5 fold change, or genes that were regulated by T_3 and/or CORT alone that showed a greater than additive effect of positive or negative regulation with T_3 plus CORT treatment. Whether the combined effect of T_3 and CORT on gene expression was greater than the additive effect of either hormone alone was determined by unpaired Student's t-test. This compared the combined hormone treatment array signal to the sum of the T_3 alone and the CORT alone array signals. Gene ontology analysis was conducted using the Ingenuity Pathway Analysis (IPA) Software (Illumina).

Results

Identification of genes differentially regulated by T_3, CORT and T_3 plus CORT.

Genome wide expression analysis of hormone treated HT-22 cells identified 116 genes to be up-regulated (Table 4.1; Supplemental Table 4.3) and 87 genes to be down-regulated (Table 4.2; Supplemental Table 4.4) by T_3. Treatment with CORT up-regulated the expression of 293 genes regulated (Table 4.4; Supplemental Table 4.5) and down-regulated the expression of 132genes (Table 4.4; Supplemental Table 4.6). Treatment

with T_3 plus CORT treatment up-regulated the expression of 252 genes (Table 4.5; Supplemental Table 4.7) and down-regulated the expression of 148 genes (Table 4.6; Supplemental Table 4.8). A summary of the number of genes differentially regulated by each of the hormone treatments is shown in Table 4.7. The number of genes commonly regulated by the individual or combined hormone treatments is depicted in Fig. 4.1 as a Venn diagram.

Genes regulated by T_3 plus CORT treatment, but not by treatment with T_3 or CORT alone were considered to be synergistically regulated. In addition to this group of genes, we conducted statistical analysis to determine which genes that were regulated by one or both hormones alone showed a greater than additive effect of combined hormone treatment (either positive or negative); i.e., genes found at the intersections of sectors in the Venn diagram in Fig 4.1.) By these criteria we found 69 genes to be synergistically up-regulated (Table 4.8), and 80 genes to be synergistically down-regulated (Table 4.9) by T_3 plus CORT treatment.

Gene ontology (GO) analysis of genes differentially regulated by T3, CORT and T3 plus CORT in HT-22 cells. We used the Ingenuity Pathway Analysis Program to identify pathways and biological functions that are enriched in our microarray dataset. The top associated networks and biological functions, subdivided into disease and disorders, molecular and cellular functions and physiological system development and function, identified by GO analysis are presented in Table 4.10 to 4.14 (T_3-regulated GO analysis, Table 4.10; CORT-regulated GO analysis, Table 4.11; T_3 plus CORT-regulated GO

analysis, Table 4.12; synergistically up-regulated GO analysis, Table 4.13; synergistically down-regulated GO analysis, Table 4.14).

Discussion

The hippocampus is a well-known target for T_3 and GC action, where both hormones influence basic developmental processes such as neurogenesis, dendritic arborization, synaptogenesis and synaptic plasticity. Here we report results of a microarray analysis for genes that are regulated by T_3 or CORT, and with combined treatment of the two hormones. We placed emphasis on finding genes that were synergistically up- or down-regulated by T_3 plus CORT. Using the Ingenuity Knowledgebase Pathway Interaction Analysis, which identifies direct and indirect transcriptional targets, and other molecules known to interact with hormone-dependent pathways, we found ten of the T_3-regulated genes to be in the T_3 and T_3 receptor interaction pathways (Supplemental Table 4.7). Eighteen CORT-regulated genes were in the GC and GC receptor interaction pathways (Supplemental Table 4.8).

Gene ontology analysis of genes regulated by T_3 revealed an enrichment of genes involved in gene expression (transcription factors), cell death, and cell growth and proliferation. Among the CORT-regulated genes, there is an enrichment of genes involved in apoptosis, cell movement (migration and invasion), and differentiation of various cell types (blood cells, hematopoietic progenitor cells, connective tissue cells and endothelial cells). There was also an enrichment of genes involved in nervous system development and function, particularly those related to the development of neurological diseases such as encephalopathy, Huntington's disease and neuromuscular disease.

Among the genes regulated by T_3 plus CORT, we found an enrichment of genes involved in cellular development and differentiation of cells (blood cells, hematopoietic progenitor cells, connective tissue cells, muscle cells), cell movement and cell homing, and apoptosis.

Among the genes synergistically up-regulated by T_3 plus CORT, 12 of the 69 genes were found to be related to cellular assembly and reorganization. There was also an enrichment of genes involved in DNA replication and repair, and post-translational modification. It is noteworthy that the gene synergistically induced by T_3 plus CORT with the highest fold change (~10 fold) is cytochrome b-561 (Cyb561), a transmembrane electron transport protein that is found in catecholamine and neuropeptide secretory vesicles in the adrenal medulla, pituitary gland and other neuroendocrine tissues (McBride, Yi et al. 1994). This may indicate that one of the physiological processes affected by hormone synergy is the formation of secretory vescicles, or the process of neurotransmitter secretion. In the brain, this could impact synaptic strength and signaling, and may represent an important component of hormone action on synaptic function/plasticity. Cytochrome b-561 was also identified as a senescence-associated gene in human keratinocytes (Kang, Kameta et al. 2003). Genes that were synergistically down-regulated by T_3 plus CORT were enriched for genes involved in proliferation of embryonic, mesenchymal and neuronal cells, and in differentiation of muscle cells.

Since we found *Klf9* to be synergistically up-regulated in the mouse hippocampus *in vivo* and in HT-22 cells, and KLF9 has been shown to influence neuronal morphology, we were interested to discover that among the genes synergistically up-regulated by T_3 plus CORT, there was an overrepresentation of genes (12 of the 69 genes) related to

cellular assembly and reorganization, with 5 of the 12 genes (ARFIP2, CALR, PI3K signaling complex, Rac, SLC3A2) involved in remodeling of the cytoskeleton. This suggests that similar to *Klf9*, other genes involved in shaping neuronal structure are synergistically regulated by T_3 and CORT. I hypothesize that through the synergistic gene regulation by T_3 and CORT, cell biological processes such as dendritic elaboration, axonogenesis and synaptogenesis may be accelerated or enhanced. To my knowledge, our microarray dataset represents the first of its kind to identify genes that are coordinately regulated by T_3 and CORT in any cell type. These results need to be further validated by RTqPCR, and compared with other published microarray datasets of genes regulated by CORT in the hippocampus.

Table 4.1. Top 25 genes upregulated by 4h of T_3 treatment in HT-22 cells.

PROBE ID	SYMBOL	DEFINITION	P value	Fold change
ILMN_1254031	**Klf9**	Mus musculus Kruppel-like factor 9 (Klf9), mRNA.	0	3.09
ILMN_1220280	**Tas1r1**	Mus musculus taste receptor, type 1, member 1 (Tas1r1), mRNA.	0	2.68
ILMN_1232601	**Cyb561**	Mus musculus cytochrome b-561 (Cyb561), mRNA.	0	2.61
ILMN_2430906	**2310051E17 Rik**	PREDICTED: Mus musculus RIKEN cDNA 2310051E17 gene (2310051E17Rik), mRNA.	0.00009	2.23
ILMN_1229547	**Spon2**	Mus musculus spondin 2, extracellular matrix protein (Spon2), mRNA.	0	1.93
ILMN_2616226	**Dbp**	Mus musculus D site albumin promoter binding protein (Dbp), mRNA.	0	1.79
ILMN_2484932	**C030002B11 Rik**		0	1.74
ILMN_3127391	**Npr3**	Mus musculus natriuretic peptide receptor 3 (Npr3), transcript variant 1, mRNA.	0	1.59
ILMN_1217117	**Cdon**		0	1.51
ILMN_2420341	**9629514_325**		0.02144	1.5
ILMN_2457585	**Trp53inp2**	Mus musculus transformation related protein 53 inducible nuclear protein 2 (Trp53inp2), mRNA.	0	1.49
ILMN_1243564	**Plekha1**	Mus musculus pleckstrin homology domain containing, family A (phosphoinositide binding specific) member 1 (Plekha1), mRNA.	0	1.48
ILMN_1253191	**E230024B12 Rik**		0	1.48
ILMN_2708877	**Plekha1**	Mus musculus pleckstrin homology domain containing, family A (phosphoinositide binding specific) member 1 (Plekha1), mRNA.	0	1.47
ILMN_2812215	**Plekhg5**	Mus musculus pleckstrin homology domain containing, family G (with RhoGef domain) member 5 (Plekhg5), mRNA.	0.00009	1.46
ILMN_2918002	**Gbp3**	Mus musculus guanylate nucleotide binding protein 3 (Gbp3), mRNA.	0.00276	1.46
ILMN_1246733	**Gm22**	PREDICTED: Mus musculus gene model 22, (NCBI) (Gm22), mRNA.	0	1.43
ILMN_2517631	**SV40_small_t_Ag_specific**		0.01358	1.42
ILMN_1255967	**B430216N15 Rik**		0.01463	1.41
ILMN_2772155	**LOC100045780**	PREDICTED: Mus musculus similar to metalloprotease-disintegrin meltrin beta (LOC100045780), mRNA.	0.005	1.41
ILMN_2966104	**Htra1**	Mus musculus HtrA serine peptidase 1 (Htra1), mRNA.	0	1.38
ILMN_2746738	**Htra1**	Mus musculus HtrA serine peptidase 1 (Htra1), mRNA.	0	1.37
ILMN_2433213	**Klf7**		0	1.37
ILMN_2482756	**Usf2**	Mus musculus upstream transcription factor 2 (Usf2), mRNA.	0.00049	1.36
ILMN_2702193	**Mxra7**	Mus musculus matrix-remodelling associated 7 (Mxra7), mRNA.	0	1.36

Table 4.2. Top 25 genes downregulated by 4h of T_3 treatment in HT-22 cells.

PROBE ID	SYMBOL	DEFINITION	P value	Fold change
ILMN_2606667	**Ddx6**	Mus musculus DEAD (Asp-Glu-Ala-Asp) box polypeptide 6 (Ddx6), mRNA.	0.0318	-1.72
ILMN_2654822	**Chd4**	Mus musculus chromodomain helicase DNA binding protein 4 (Chd4), mRNA.	0.0072	-1.49
ILMN_1230786	**5730588I11Rik**		0.01204	-1.47
ILMN_1253178	**Aldh3a1**	Mus musculus aldehyde dehydrogenase family 3, subfamily A1 (Aldh3a1), mRNA.	0	-1.47
ILMN_2543842	**2810417K24Rik**		0.03291	-1.46
ILMN_1230788	**Tle1**	Mus musculus transducin-like enhancer of split 1, homolog of Drosophila E(spl) (Tle1), mRNA. XM_984202 XM_984240 XM_984277 XM_984316 XM_984359 XM_984397 XM_984426 XM_984456 XM_984492 XM_984530	0	-1.44
ILMN_1237565	**EG626367**	PREDICTED: Mus musculus predicted gene, EG626367 (EG626367), misc RNA.	0	-1.44
ILMN_1256844	**EG668850**	PREDICTED: Mus musculus predicted gene, EG668850 (EG668850), misc RNA.	0	-1.42
ILMN_1235652	**Usp37**	Mus musculus ubiquitin specific peptidase 37 (Usp37), mRNA.	0.00158	-1.41
ILMN_1241320	**Clspn**	Mus musculus claspin homolog (Xenopus laevis) (Clspn), mRNA.	0.00029	-1.41
ILMN_1243988	**LOC269251**		0.00022	-1.41
ILMN_3031781	**Arid5b**	Mus musculus AT rich interactive domain 5B (MRF1-like) (Arid5b), mRNA.	0.01249	-1.39
ILMN_1248733	**Pa2g4**	Mus musculus proliferation-associated 2G4 (Pa2g4), mRNA.	0.03204	-1.36
ILMN_1254307	**1810011O10Rik**	Mus musculus RIKEN cDNA 1810011O10 gene (1810011O10Rik), mRNA.	0.00027	-1.35
ILMN_1219839	**mtDNA_ND6**		0	-1.35
ILMN_2682279	**Gkap1**	Mus musculus G kinase anchoring protein 1 (Gkap1), mRNA.	0.02019	-1.35
ILMN_3038404	**Tcf25**	Mus musculus transcription factor 25 (basic helix-loop-helix) (Tcf25), transcript variant 3, mRNA.	0.0094	-1.34
ILMN_2710678	**Nfic**		0.04947	-1.34
ILMN_1255731	**Dnm3os**	Mus musculus dynamin 3, opposite strand (Dnm3os), non-coding RNA.	0.01697	-1.33
ILMN_2741677	**Bach1**	Mus musculus BTB and CNC homology 1 (Bach1), mRNA.	0.03548	-1.32
ILMN_2874853	**Eef1b2**	Mus musculus eukaryotic translation elongation factor 1 beta 2 (Eef1b2), mRNA.	0.04617	-1.31
ILMN_1259322	**Pdk4**	Mus musculus pyruvate dehydrogenase kinase, isoenzyme 4 (Pdk4), mRNA.	0	-1.31
ILMN_1230726	**5430406J06Rik**		0.01611	-1.31
ILMN_2529519	**LOC230592**		0.02703	-1.3
ILMN_2568488	**A530089A20Rik**		0.0165	-1.3

Table 4.3. Top 25 genes upregulated by 4h of CORT treatment in HT-22 cells.

PROBE ID	SYMBOL	DEFINITION	P value	Fold change
ILMN_2701664	**Tsc22d3**	Mus musculus TSC22 domain family, member 3 (Tsc22d3), transcript variant 2, mRNA.	0	8.82
ILMN_3150811	**Tsc22d3**	Mus musculus TSC22 domain family, member 3 (Tsc22d3), transcript variant 1, mRNA.	0	5.41
ILMN_1259322	**Pdk4**	Mus musculus pyruvate dehydrogenase kinase, isoenzyme 4 (Pdk4), mRNA.	0	5.02
ILMN_2813484	**Per1**	Mus musculus period homolog 1 (Drosophila) (Per1), mRNA.	0	4.64
ILMN_2588249	**S3-12**	Mus musculus plasma membrane associated protein, S3-12 (S3-12), mRNA.	0	4.48
ILMN_2987862	**Per2**	Mus musculus period homolog 2 (Drosophila) (Per2), mRNA.	0	4.21
ILMN_2770894	**Map3k6**		0	3.82
ILMN_2768972	**Fam107a**	Mus musculus family with sequence similarity 107, member A (Fam107a), mRNA.	0	3.8
ILMN_1232601	**Cyb561**	Mus musculus cytochrome b-561 (Cyb561), mRNA.	0	3.78
ILMN_2712075	**Lcn2**	Mus musculus lipocalin 2 (Lcn2), mRNA.	0	3.74
ILMN_2638923	**Rn18s**	Mus musculus 18S RNA (Rn18s), non-coding RNA.	0	3.69
ILMN_1226935	**Orm1**	Mus musculus orosomucoid 1 (Orm1), mRNA.	0	3.44
ILMN_1219154	**Mt2**	Mus musculus metallothionein 2 (Mt2), mRNA.	0	3.4
ILMN_2654074	**Sesn1**	Mus musculus sestrin 1 (Sesn1), mRNA.	0	3.35
ILMN_1232884	**Sphk1**	Mus musculus sphingosine kinase 1 (Sphk1), transcript variant 1, mRNA.	0	3.24
ILMN_2813487	**Per1**	Mus musculus period homolog 1 (Drosophila) (Per1), mRNA.	0	3.06
ILMN_2987863	**Per2**	Mus musculus period homolog 2 (Drosophila) (Per2), mRNA.	0	3.03
ILMN_2822000	**Slc10a6**	Mus musculus solute carrier family 10 (sodium/bile acid cotransporter family), member 6 (Slc10a6), mRNA.	0	3.03
ILMN_3136744	**Sesn1**	Mus musculus sestrin 1 (Sesn1), mRNA.	0	3.02
ILMN_2622983	**Dusp1**	Mus musculus dual specificity phosphatase 1 (Dusp1), mRNA.	0	3.02
ILMN_2517483	**D15Bwg0759e**		0	2.98
ILMN_1226712	**Ccdc134**	Mus musculus coiled-coil domain containing 134 (Ccdc134), mRNA.	0	2.92
ILMN_2637714	**Rasa3**	Mus musculus RAS p21 protein activator 3 (Rasa3), mRNA.	0	2.87
ILMN_1255287	**Mela**		0	2.71
ILMN_2718266	**Fkbp5**	Mus musculus FK506 binding protein 5 (Fkbp5), mRNA.	0	2.67

Table 4.4. Top 25 genes downregulated by 4h of CORT treatment in HT-22 cells.

PROBE ID	SYMBOL	DEFINITION	Pvalue	Fold change
ILMN_2710253	**Cyr61**	Mus musculus cysteine rich protein 61 (Cyr61), mRNA.	0	-3.17
ILMN_2754985	**Phlda1**	Mus musculus pleckstrin homology-like domain, family A, member 1 (Phlda1), mRNA.	0	-3.09
ILMN_2662926	**Egr1**	Mus musculus early growth response 1 (Egr1), mRNA.	0	-2.91
ILMN_2794645	**Cyr61**	Mus musculus cysteine rich protein 61 (Cyr61), mRNA.	0	-2.88
ILMN_2483786	**1110004P21Rik**		0	-2.43
ILMN_1251193	**A630084D02Rik**		0	-2.42
ILMN_2937596	**Ngfb**	Mus musculus nerve growth factor, beta (Ngfb), mRNA.	0	-2.36
ILMN_2660233	**Ngfb**	Mus musculus nerve growth factor, beta (Ngfb), mRNA.	0	-2.34
ILMN_1229745	**Sertad4**	Mus musculus SERTA domain containing 4 (Sertad4), mRNA.	0	-2.34
ILMN_2959272	**Rnu6**	Mus musculus U6 small nuclear RNA (Rnu6), non-coding RNA.	0	-2.33
ILMN_2752569	**Paip1**	Mus musculus polyadenylate binding protein-interacting protein 1 (Paip1), transcript variant 1, mRNA.	0	-2.17
ILMN_1235571	**Cyr61**	Mus musculus cysteine rich protein 61 (Cyr61), mRNA.	0	-2.16
ILMN_1253178	**Aldh3a1**	Mus musculus aldehyde dehydrogenase family 3, subfamily A1 (Aldh3a1), mRNA.	0	-2.01
ILMN_2551741	**0610010I05Rik**		0	-1.98
ILMN_2868220	**Inhba**	Mus musculus inhibin beta-A (Inhba), mRNA.	0	-1.92
ILMN_2833706	**Fgf7**	Mus musculus fibroblast growth factor 7 (Fgf7), mRNA.	0	-1.91
ILMN_2937735	**Irak2**	Mus musculus interleukin-1 receptor-associated kinase 2 (Irak2), mRNA.	0	-1.87
ILMN_2451115	**1500001E21Rik**		0	-1.83
ILMN_2684563	**Cldnd1**	Mus musculus claudin domain containing 1 (Cldnd1), mRNA.	0	-1.8
ILMN_2507810	**mtDNA_ND5**		0	-1.79
ILMN_2988299	**Srf**	Mus musculus serum response factor (Srf), mRNA.	0	-1.79
ILMN_2683593	**Fubp1**		0	-1.79
ILMN_2778655	**Vcam1**	Mus musculus vascular cell adhesion molecule 1 (Vcam1), mRNA.	0	-1.77
ILMN_2550570	**Fibp**		0.00095	-1.76
ILMN_2937738	**Irak2**	Mus musculus interleukin-1 receptor-associated kinase 2 (Irak2), mRNA.	0	-1.75

Table 4.5. Top 25 genes upregulated by 4h of T_3 plus CORT treatment in HT-22 cells.

PROBE ID	SYMBOL	DEFINITION	P value	Fold change
ILMN_1232601	**Cyb561**	Mus musculus cytochrome b-561 (Cyb561), mRNA.	0	10.52
ILMN_2701664	**Tsc22d3**	Mus musculus TSC22 domain family, member 3 (Tsc22d3), transcript variant 2, mRNA.	0	7.25
ILMN_1254031	**Klf9**	Mus musculus Kruppel-like factor 9 (Klf9), mRNA.	0	5.518
ILMN_2430906	**2310051E17 Rik**	PREDICTED: Mus musculus RIKEN cDNA 2310051E17 gene (2310051E17Rik), mRNA.	0	5.245
ILMN_1259322	**Pdk4**	Mus musculus pyruvate dehydrogenase kinase, isoenzyme 4 (Pdk4), mRNA.	0	4.71
ILMN_3150811	**Tsc22d3**	Mus musculus TSC22 domain family, member 3 (Tsc22d3), transcript variant 1, mRNA.	0	4.506
ILMN_2813484	**Per1**	Mus musculus period homolog 1 (Drosophila) (Per1), mRNA.	0	4.291
ILMN_2987862	**Per2**	Mus musculus period homolog 2 (Drosophila) (Per2), mRNA.	0	3.917
ILMN_2524986	**Ear3**	Mus musculus eosinophil-associated, ribonuclease A family, member 3 (Ear3), mRNA.	0	3.793
ILMN_2638923	**Rn18s**	Mus musculus 18S RNA (Rn18s), non-coding RNA.	0	3.65
ILMN_1220280	**Tas1r1**	Mus musculus taste receptor, type 1, member 1 (Tas1r1), mRNA.	0	3.196
ILMN_2770894	**Map3k6**		0	3.102
ILMN_2822000	**Slc10a6**	Mus musculus solute carrier family 10 (sodium/bile acid cotransporter family), member 6 (Slc10a6), mRNA.	0	3.064
ILMN_2813487	**Per1**	Mus musculus period homolog 1 (Drosophila) (Per1), mRNA.	0	3.008
ILMN_2622983	**Dusp1**	Mus musculus dual specificity phosphatase 1 (Dusp1), mRNA.	0	2.93
ILMN_2738345	**Lims2**	Mus musculus LIM and senescent cell antigen like domains 2 (Lims2), mRNA.	0	2.913
ILMN_2712075	**Lcn2**	Mus musculus lipocalin 2 (Lcn2), mRNA.	0	2.821
ILMN_2588249	**S3-12**	Mus musculus plasma membrane associated protein, S3-12 (S3-12), mRNA.	0	2.805
ILMN_2768972	**Fam107a**	Mus musculus family with sequence similarity 107, member A (Fam107a), mRNA.	0	2.783
ILMN_2654074	**Sesn1**	Mus musculus sestrin 1 (Sesn1), mRNA.	0	2.765
ILMN_2637714	**Rasa3**	Mus musculus RAS p21 protein activator 3 (Rasa3), mRNA.	0	2.758
ILMN_2987863	**Per2**	Mus musculus period homolog 2 (Drosophila) (Per2), mRNA.	0	2.683
ILMN_1219154	**Mt2**	Mus musculus metallothionein 2 (Mt2), mRNA.	0	2.571
ILMN_2517483	**D15Bwg0759 e**		0	2.552
ILMN_1226935	**Orm1**	Mus musculus orosomucoid 1 (Orm1), mRNA.	0	2.541

Table 4.6. Top 25 genes downregulated by 4h of T_3 plus CORT treatment in HT-22 cells.

PROBE ID	SYMBOL	DEFINITION	P value	Fold change
ILMN_2754985	**Phlda1**	Mus musculus pleckstrin homology-like domain, family A, member 1 (Phlda1), mRNA.	0	-2.883
ILMN_2835117	**Ccl7**	Mus musculus chemokine (C-C motif) ligand 7 (Ccl7), mRNA.	0	-2.716
ILMN_2771176	**Ccl7**		0	-2.687
ILMN_1229745	**Sertad4**	Mus musculus SERTA domain containing 4 (Sertad4), mRNA.	0	-2.673
ILMN_2660233	**Ngfb**	Mus musculus nerve growth factor, beta (Ngfb), mRNA.	0	-2.653
ILMN_2937596	**Ngfb**	Mus musculus nerve growth factor, beta (Ngfb), mRNA.	0	-2.427
ILMN_1251193	**A630084D02Rik**		0	-2.259
ILMN_1253178	**Aldh3a1**	Mus musculus aldehyde dehydrogenase family 3, subfamily A1 (Aldh3a1), mRNA.	0	-2.244
ILMN_2662926	**Egr1**	Mus musculus early growth response 1 (Egr1), mRNA.	0	-2.137
ILMN_2833706	**Fgf7**	Mus musculus fibroblast growth factor 7 (Fgf7), mRNA.	0	-2.124
ILMN_2778655	**Vcam1**	Mus musculus vascular cell adhesion molecule 1 (Vcam1), mRNA.	0	-2.122
ILMN_2759365	**Angptl4**	Mus musculus angiopoietin-like 4 (Angptl4), mRNA.	0	-2.099
ILMN_2752569	**Paip1**	Mus musculus polyadenylate binding protein-interacting protein 1 (Paip1), transcript variant 1, mRNA.	0	-2.068
ILMN_2794645	**Cyr61**	Mus musculus cysteine rich protein 61 (Cyr61), mRNA.	0.00002	-2.044
ILMN_2479290	**Fas**	Mus musculus Fas (TNF receptor superfamily member 6) (Fas), mRNA.	0	-2.014
ILMN_2959272	**Rnu6**	Mus musculus U6 small nuclear RNA (Rnu6), non-coding RNA.	0	-2.011
ILMN_1245710	**Ccl2**	Mus musculus chemokine (C-C motif) ligand 2 (Ccl2), mRNA.	0	-2.003
ILMN_2606210	**Dpt**	Mus musculus dermatopontin (Dpt), mRNA.	0	-2.002
ILMN_2483786	**1110004P21Rik**		0.00001	-1.993
ILMN_2695412	**AI451617**	Mus musculus expressed sequence AI451617 (AI451617), mRNA.	0	-1.974
ILMN_2710253	**Cyr61**	Mus musculus cysteine rich protein 61 (Cyr61), mRNA.	0	-1.94
ILMN_2776603	**Ccl9**	Mus musculus chemokine (C-C motif) ligand 9 (Ccl9), mRNA.	0	-1.898
ILMN_2902979	**Fas**	Mus musculus Fas (TNF receptor superfamily member 6) (Fas), mRNA.	0	-1.89
ILMN_2996648	**Prl2c4**	Mus musculus prolactin family 2, subfamily c, member 4 (Prl2c4), mRNA.	0	-1.823
ILMN_2623793	**Zfhx3**	Mus musculus zinc finger homeobox 3 (Zfhx3), mRNA.	0	-1.821

Table 4.7 Summary of the representative number of genes independently and synergistically regulated by T_3 and CORT treatment in HT-22 cells.

	UP	DOWN	TOTAL
T_3	116	87	203
CORT	293	132	425
T_3 plus CORT	252	148	400
Synergistic upregulation	69		69
Synergistic downregulation		80	80

Table 4.8. Genes synergistically upregulated by 4h of T_3 plus CORT treatment in HT-22 cells. The probe IDs highlighted in grey are genes that were found to be regulated by T_3 and/ or CORT alone and synergistically upregulated by T_3 plus CORT.

PROBE ID	SYMBOL	DEFINITION	T_3 Fold Change	CORT Fold Change	T_3 plus CORT Fold Change
ILMN_1232601	**Cyb561**	Mus musculus cytochrome b-561 (Cyb561), mRNA.	2.61	3.78	10.52
ILMN_1254031	**Klf9**	Mus musculus Kruppel-like factor 9 (Klf9), mRNA.	3.09	2.17	5.52
ILMN_2430906	**2310051E17 Rik**	PREDICTED: Mus musculus RIKEN cDNA 2310051E17 gene (2310051E17Rik), mRNA.	2.23	2.19	5.25
ILMN_1253191	**E230024B1 2Rik**		1.48	1.2	2.28
ILMN_2868480	**Ear4**	Mus musculus eosinophil-associated, ribonuclease A family, member 4 (Ear4), mRNA.	1.08	1.75	2.21
ILMN_2714031	**Errfi1**	Mus musculus ERBB receptor feedback inhibitor 1 (Errfi1), mRNA.	1.21	1.46	2.1
ILMN_2509988	**Lbr**		1.13	1.46	1.85
ILMN_1256943	**Ear3**	Mus musculus eosinophil-associated, ribonuclease A family, member 3 (Ear3), mRNA.	-1.05	1.37	1.76
ILMN_1221494	**Ubtd2**	Mus musculus ubiquitin domain containing 2 (Ubtd2), mRNA.	1.15	1.43	1.74
ILMN_2602597	**Sh3rf1**	Mus musculus SH3 domain containing ring finger 1 (Sh3rf1), mRNA.	1.02	1.48	1.73
ILMN_2595359	**Slc3a2**	Mus musculus solute carrier family 3 (activators of dibasic and neutral amino acid transport), member 2 (Slc3a2), mRNA.	1.2	1.48	1.73
ILMN_2752010	**Mcm4**	Mus musculus minichromosome maintenance deficient 4 homolog (S. cerevisiae) (Mcm4), mRNA.	1.09	1.49	1.65
ILMN_1215803	**Slc38a4**	Mus musculus solute carrier family 38, member 4 (Slc38a4), mRNA.	1.11	1.46	1.65
ILMN_1229416	**1110034A24 Rik**		1.03	1.29	1.64
ILMN_2682945	**Psmd2**	Mus musculus proteasome (prosome, macropain) 26S subunit, non-ATPase, 2 (Psmd2), mRNA.	-1.03	1.42	1.63
ILMN_1233813	**Ss18**	Mus musculus synovial sarcoma translocation, Chromosome 18 (Ss18), mRNA.	1.06	1.4	1.63
ILMN_2633777	**Rab34**	Mus musculus RAB34, member of RAS oncogene family (Rab34), mRNA.	1.02	1.42	1.62
ILMN_1232055	**9330175B01 Rik**		1.08	1.45	1.6
ILMN_1230422	**BC018507**	PREDICTED: Mus musculus cDNA sequence BC018507, transcript variant 5 (BC018507), mRNA.	1.05	1.46	1.6
ILMN_1257772	**BC026590**	Mus musculus cDNA sequence BC026590 (BC026590), mRNA.	-1.05	1.47	1.6

ILMN_1224250	**B230342M21Rik**	Mus musculus RIKEN cDNA B230342M21 gene (B230342M21Rik), mRNA.	1.02	1.47	1.59
ILMN_1228557	**Id2**	Mus musculus inhibitor of DNA binding 2 (Id2), mRNA.	-1.12	1.27	1.59
ILMN_2648937	**Pdzrn3**	Mus musculus PDZ domain containing RING finger 3 (Pdzrn3), mRNA.	1.14	1.32	1.59
ILMN_3160881	**Vrk3**	Mus musculus vaccinia related kinase 3 (Vrk3), mRNA.	1.08	1.48	1.59
ILMN_2944646	**Cope**	Mus musculus coatomer protein complex, subunit epsilon (Cope), mRNA.	1.01	1.44	1.58
ILMN_1228245	**Prickle1**	Mus musculus prickle like 1 (Drosophila) (Prickle1), mRNA.	-1.05	1.43	1.58
ILMN_2682947	**Psmd2**	Mus musculus proteasome (prosome, macropain) 26S subunit, non-ATPase, 2 (Psmd2), mRNA.	1.01	1.34	1.58
ILMN_1243908	**Sh3gl1**	Mus musculus SH3-domain GRB2-like 1 (Sh3gl1), mRNA.	1.17	1.45	1.58
ILMN_2461582	**4732460K03Rik**	PREDICTED: Mus musculus RIKEN cDNA 4732460K03 gene, transcript variant 1 (4732460K03Rik), mRNA.	1.08	1.4	1.57
ILMN_2955806	**Arfip2**	Mus musculus ADP-ribosylation factor interacting protein 2 (Arfip2), mRNA.	1	1.43	1.57
ILMN_2636832	**Cyb5r3**	Mus musculus cytochrome b5 reductase 3 (Cyb5r3), mRNA.	1.03	1.49	1.57
ILMN_2490548	**Tspan4**	Mus musculus tetraspanin 4 (Tspan4), mRNA.	1.18	1.32	1.57
ILMN_1226366	**Uck1**	Mus musculus uridine-cytidine kinase 1 (Uck1), mRNA.	1.06	1.42	1.57
ILMN_1257501	**Pet112l**	Mus musculus PET112-like (yeast) (Pet112l), mRNA.	-1.05	1.43	1.56
ILMN_2644920	**Plekhf1**	Mus musculus pleckstrin homology domain containing, family F (with FYVE domain) member 1 (Plekhf1), mRNA.	1.08	1.49	1.56
ILMN_2776585	**Slc1a5**	Mus musculus solute carrier family 1 (neutral amino acid transporter), member 5 (Slc1a5), mRNA.	1.05	1.44	1.56
ILMN_2764205	**Tor1a**	Mus musculus torsin family 1, member A (torsin A) (Tor1a), mRNA.	1.01	1.36	1.56
ILMN_2511971	**Whsc1l1**	Mus musculus Wolf-Hirschhorn syndrome candidate 1-like 1 (human) (Whsc1l1), transcript variant 1, mRNA.	1.01	1.45	1.56
ILMN_2845839	**1700065O13Rik**	Mus musculus RIKEN cDNA 1700065O13 gene (1700065O13Rik), mRNA.	1.06	1.43	1.55
ILMN_2489314	**2500002G23Rik**		1.03	1.32	1.55
ILMN_2819530	**D15Ertd682e**	Mus musculus DNA segment, Chr 15, ERATO Doi 682, expressed (D15Ertd682e), mRNA.	-1.06	1.39	1.55
ILMN_1250036	**Tmem201**	Mus musculus transmembrane protein 201 (Tmem201), transcript variant 1, mRNA.	1.06	1.39	1.55

ILMN_2547078	**Zc3h13**	Mus musculus zinc finger CCCH type containing 13 (Zc3h13), mRNA.	1.02	1.33	1.55
ILMN_2861176	**Calr**	Mus musculus calreticulin (Calr), mRNA.	-1.05	1.4	1.54
ILMN_2709681	**Hdlbp**	Mus musculus high density lipoprotein (HDL) binding protein (Hdlbp), mRNA.	-1.03	1.45	1.54
ILMN_2455637	**Top1mt**	Mus musculus DNA topoisomerase 1, mitochondrial (Top1mt), nuclear gene encoding mitochondrial protein, mRNA.	1.06	1.48	1.54
ILMN_2631192	**Vps26b**	Mus musculus vacuolar protein sorting 26 homolog B (yeast) (Vps26b), mRNA.	1.03	1.45	1.54
ILMN_2971721	**2410025L10 Rik**	Mus musculus RIKEN cDNA 2410025L10 gene (2410025L10Rik), mRNA.	1.16	1.32	1.53
ILMN_3051252	**BC026590**	Mus musculus cDNA sequence BC026590 (BC026590), mRNA.	1.05	1.33	1.53
ILMN_2933399	**Ppp1r10**	Mus musculus protein phosphatase 1, regulatory subunit 10 (Ppp1r10), mRNA.	1.02	1.49	1.53
ILMN_1216116	**Smarcd2**	Mus musculus SWI/SNF related, matrix associated, actin dependent regulator of chromatin, subfamily d, member 2 (Smarcd2), mRNA.	1.09	1.47	1.53
ILMN_1217144	**Tbc1d5**	Mus musculus TBC1 domain family, member 5 (Tbc1d5), mRNA.	1.07	1.36	1.53
ILMN_1228501	**Tob2**	Mus musculus transducer of ERBB2, 2 (Tob2), mRNA.	1.03	1.42	1.53
ILMN_2497581	**Uhrf1**	Mus musculus ubiquitin-like, containing PHD and RING finger domains, 1 (Uhrf1), mRNA.	-1.11	1.42	1.53
ILMN_1214918	**LOC546015**	PREDICTED: Mus musculus similar to ribosomal protein S9 (LOC546015), misc RNA.	-1	1.44	1.52
ILMN_1234112	**Tomm70a**	Mus musculus translocase of outer mitochondrial membrane 70 homolog A (yeast) (Tomm70a), mRNA.	1.16	1.35	1.52
ILMN_2443831	**Uba1**	Mus musculus ubiquitin-like modifier activating enzyme 1 (Uba1), mRNA.	1.02	1.36	1.52
ILMN_2746328	**BC003993**	Mus musculus cDNA sequence BC003993 (BC003993), mRNA.	1.18	1.41	1.51
ILMN_2773862	**C730025P1 3Rik**	Mus musculus RIKEN cDNA C730025P13 gene (C730025P13Rik), mRNA.	-1.01	1.45	1.51
ILMN_1243679	**Cep55**	Mus musculus centrosomal protein 55 (Cep55), mRNA.	1.06	1.45	1.51
ILMN_2985111	**Chfr**	Mus musculus checkpoint with forkhead and ring finger domains (Chfr), mRNA.	-1.01	1.32	1.51
ILMN_1225363	**E430025E2 1Rik**	Mus musculus RIKEN cDNA E430025E21 gene (E430025E21Rik), mRNA.	1.03	1.38	1.51
ILMN_2794686	**Fam152b**	Mus musculus family with sequence similarity 152, member B	1.1	1.3	1.51

		(Fam152b), mRNA.			
ILMN_2727309	**LOC100044204**	PREDICTED: Mus musculus hypothetical protein LOC100044204 (LOC100044204), mRNA.	-1.12	1.36	1.51
ILMN_2820379	**Rnf135**	Mus musculus ring finger protein 135 (Rnf135), mRNA.	1.04	1.26	1.51
ILMN_2515982	**Ugt1a6b**	Mus musculus UDP glucuronosyltransferase 1 family, polypeptide A6B (Ugt1a6b), mRNA.	1.06	1.43	1.51
ILMN_1223015	**Dedd2**	Mus musculus death effector domain-containing DNA binding protein 2 (Dedd2), mRNA.	-1.01	1.27	1.5
ILMN_2695150	**Smc5l1**		-1.05	1.25	1.5
ILMN_2480463	**Trim25**	Mus musculus tripartite motif-containing 25 (Trim25), mRNA.	1.06	1.44	1.5

Table 4.9. Genes synergistically downregulated by 4h of T_3 plus CORT treatment in HT-22 cells. The probe IDs highlighted in grey are genes that were found to be regulated by T_3 and/ or CORT alone and synergistically downregulated by T_3 plus CORT.

PROBE ID	SYMBOL	DEFINITION	T_3 Fold Change	CORT Fold Change	T_3 plus CORT Fold Change
ILMN_2759365	**Angptl4**	Mus musculus angiopoietin-like 4 (Angptl4), mRNA.	1.15	-1.39	-2.1
ILMN_2996648	**Prl2c4**	Mus musculus prolactin family 2, subfamily c, member 4 (Prl2c4), mRNA.	-1.01	-1.2	-1.82
ILMN_2623793	**Zfhx3**	Mus musculus zinc finger homeobox 3 (Zfhx3), mRNA.	1.07	-1.27	-1.82
ILMN_2741096	**Timp3**	Mus musculus tissue inhibitor of metalloproteinase 3 (Timp3), mRNA.	1.06	-1.34	-1.79
ILMN_2506727	**9430052C07 Rik**		-1.26	-1.22	-1.78
ILMN_2875585	**Prl2c3**	Mus musculus prolactin family 2, subfamily c, member 3 (Prl2c3), mRNA.	-1.03	-1.3	-1.76
ILMN_2937136	**Tceal1**	Mus musculus transcription elongation factor A (SII)-like 1 (Tceal1), mRNA.	-1.21	-1.32	-1.72
ILMN_1217489	**LOC671878**	PREDICTED: Mus musculus similar to spermine synthase (LOC671878), mRNA.	-1.04	-1.43	-1.68
ILMN_1259982	**LOC100046616**	PREDICTED: Mus musculus similar to aquaporin 5 (LOC100046616), mRNA.	-1.04	-1.05	-1.68
ILMN_3115472	**Aqp5**	Mus musculus aquaporin 5 (Aqp5), mRNA.	-1.09	1	-1.66
ILMN_2816180	**Lbh**	Mus musculus limb-bud and heart (Lbh), mRNA.	-1	-1.2	-1.65
ILMN_2806159	**Tmsb4x**	Mus musculus thymosin, beta 4, X chromosome (Tmsb4x), mRNA.	-1.01	-1.45	-1.64
ILMN_2474666	**4933411D12 Rik**		1.01	-1.38	-1.64
ILMN_3007428	**Sox9**	Mus musculus SRY-box containing gene 9 (Sox9), mRNA.	-1.05	-1.12	-1.64
ILMN_2775937	**Plat**		1.13	-1.34	-1.62
ILMN_2617996	**Prl2c2**	Mus musculus prolactin family 2, subfamily c, member 2 (Prl2c2), mRNA.	1	-1.1	-1.62
ILMN_1236123	**Tomm6**	Mus musculus translocase of outer mitochondrial membrane 6 homolog (yeast) (Tomm6), nuclear gene encoding mitochondrial protein, mRNA.	-1.04	-1.49	-1.62
ILMN_2643241	**Accn2**	Mus musculus amiloride-sensitive cation channel 2, neuronal (Accn2), mRNA.	1.1	-1.35	-1.62
ILMN_2696592	**C77080**		-1.07	-1.26	-1.62
ILMN_1230152	**Adamts4**		-1.08	-1.38	-1.62
ILMN_1250075	**Dpysl3**	Mus musculus dihydropyrimidinase-like 3 (Dpysl3), mRNA.	-1.06	-1.35	-1.62
ILMN_2653207	**Tead2**	Mus musculus TEA domain family	-1.07	-1.48	-1.6

		member 2 (Tead2), mRNA.			
ILMN_1222565	**A930002H24 Rik**	PREDICTED: Mus musculus RIKEN cDNA A930002H24 gene (A930002H24Rik), mRNA.	1.02	-1.07	-1.6
ILMN_2760979	**Tgfbr2**	Mus musculus transforming growth factor, beta receptor II (Tgfbr2), transcript variant 1, mRNA.	1.05	-1.17	-1.6
ILMN_1216381	**Nfic**	Mus musculus nuclear factor I/C (Nfic), transcript variant 2, mRNA.	1.02	-1.32	-1.6
ILMN_2841720	**Ttc3**	Mus musculus tetratricopeptide repeat domain 3 (Ttc3), mRNA.	-1.02	-1.3	-1.59
ILMN_2623776	**Eps8**	Mus musculus epidermal growth factor receptor pathway substrate 8 (Eps8), mRNA.	1.08	-1.4	-1.59
ILMN_1228031	**Dusp8**	Mus musculus dual specificity phosphatase 8 (Dusp8), mRNA.	1.1	-1.28	-1.59
ILMN_1213376	**Cfl1**	Mus musculus cofilin 1, non-muscle (Cfl1), mRNA.	1.16	-1.42	-1.59
ILMN_1244343	**B230369L08 Rik**		-1.04	-1.5	-1.57
ILMN_2495703	**Clip2**	Mus musculus CAP-GLY domain containing linker protein 2 (Clip2), transcript variant 2, mRNA.	1.07	-1.43	-1.57
ILMN_1238838	**LOC100045005**	PREDICTED: Mus musculus similar to Deltex3 (LOC100045005), misc RNA.	-1.07	-1.44	-1.57
ILMN_2828916	**Frmd6**	Mus musculus FERM domain containing 6 (Frmd6), mRNA.	1.11	-1.48	-1.56
ILMN_1246841	**Relb**	Mus musculus avian reticuloendotheliosis viral (v-rel) oncogene related B (Relb), mRNA.	1.11	-1.37	-1.56
ILMN_2617265	**Ipo13**	Mus musculus importin 13 (Ipo13), mRNA.	-1.03	-1.42	-1.56
ILMN_2757870	**Psmb10**	Mus musculus proteasome (prosome, macropain) subunit, beta type 10 (Psmb10), mRNA.	-1.02	-1.43	-1.55
ILMN_2642913	**Emp1**	Mus musculus epithelial membrane protein 1 (Emp1), mRNA.	1.09	-1.37	-1.55
ILMN_1219807	**Hoxd4**	Mus musculus homeo box D4 (Hoxd4), mRNA.	1.03	-1.36	-1.55
ILMN_1223697	**Cd44**	Mus musculus CD44 antigen (Cd44), transcript variant 2, mRNA.	-1.11	-1.31	-1.55
ILMN_1227131	**Ehbp1l1**	Mus musculus EH domain binding protein 1-like 1 (Ehbp1l1), mRNA.	1.17	-1.49	-1.55
ILMN_2747381	**Ddx24**	Mus musculus DEAD (Asp-Glu-Ala-Asp) box polypeptide 24 (Ddx24), mRNA.	-1.06	-1.38	-1.54
ILMN_1235173	**LOC386218**		-1.02	-1.47	-1.54
ILMN_1213200	**Med16**	Mus musculus mediator complex subunit 16 (Med16), mRNA.	1.03	-1.36	-1.54
ILMN_1225835	**Mfap5**	Mus musculus microfibrillar associated protein 5 (Mfap5), mRNA.	-1.18	-1.08	-1.54
ILMN_2449019	**Tnk2**	Mus musculus tyrosine kinase, non-receptor, 2 (Tnk2), mRNA.	1.17	-1.44	-1.53
ILMN_3160416	**2900024O10 Rik**	Mus musculus RIKEN cDNA 2900024O10 gene (2900024O10Rik), mRNA.	-1.15	-1.38	-1.53

ILMN_2625351	**Sh3bgrl3**	Mus musculus SH3 domain binding glutamic acid-rich protein-like 3 (Sh3bgrl3), mRNA.	-1.04	-1.27	-1.53
ILMN_2440530	**Vat1**	Mus musculus vesicle amine transport protein 1 homolog (T californica) (Vat1), mRNA.	1.01	-1.21	-1.53
ILMN_2760254	**Mrgprf**	Mus musculus MAS-related GPR, member F (Mrgprf), mRNA.	1.1	-1.14	-1.53
ILMN_1249547	**Zfp292**	PREDICTED: Mus musculus zinc finger protein 292, transcript variant 4 (Zfp292), mRNA.	-1.13	-1.47	-1.53
ILMN_3161105	**Ahnak2**	Mus musculus AHNAK nucleoprotein 2 (Ahnak2), mRNA.	1.06	-1.08	-1.52
ILMN_2656422	**BC028528**	Mus musculus cDNA sequence BC028528 (BC028528), mRNA.	-1.18	-1.35	-1.52
ILMN_1238535	**4832420L08 Rik**		-1.14	-1.29	-1.52
ILMN_2974720	**Igf2bp2**	Mus musculus insulin-like growth factor 2 mRNA binding protein 2 (Igf2bp2), mRNA.	-1.02	-1.38	-1.52
ILMN_2629601	**Slc4a7**		1.03	-1.42	-1.52
ILMN_2441921	**Trim56**	Mus musculus tripartite motif-containing 56 (Trim56), mRNA.	-1.05	-1.33	-1.52
ILMN_1259610	**Cd276**	Mus musculus CD276 antigen (Cd276), mRNA.	1.08	-1.36	-1.52
ILMN_1252222	**Hectd2**	Mus musculus HECT domain containing 2 (Hectd2), mRNA.	1.02	-1.47	-1.52
ILMN_1235732	**Cdsn**	Mus musculus corneodesmosin (Cdsn), mRNA.	1.09	-1.14	-1.51
ILMN_2658815	**Tmem98**	Mus musculus transmembrane protein 98 (Tmem98), mRNA.	-1.13	-1.35	-1.51
ILMN_1228441	**C230043G09 Rik**		-1.12	-1.44	-1.51
ILMN_1225373	**C1qbp**	Mus musculus complement component 1, q subcomponent binding protein (C1qbp), nuclear gene encoding mitochondrial protein, mRNA.	1.06	-1.4	-1.51
ILMN_2689307	**Spnb2**	Mus musculus spectrin beta 2 (Spnb2), transcript variant 2, mRNA.	-1.13	-1.26	-1.5
ILMN_2731057	**Psme2**	Mus musculus proteasome (prosome, macropain) 28 subunit, beta (Psme2), transcript variant 1, mRNA.	-1.1	-1.41	-1.5
ILMN_1259967	**Prl2c2**	Mus musculus prolactin family 2, subfamily c, member 2 (Prl2c2), mRNA.	-1.04	-1.01	-1.5
ILMN_2759365	**Angptl4**	Mus musculus angiopoietin-like 4 (Angptl4), mRNA.	1.15	-1.39	-2.1
ILMN_2776603	**Ccl9**	Mus musculus chemokine (C-C motif) ligand 9 (Ccl9), mRNA.	1.1	-1.52	-1.9
ILMN_2996648	**Prl2c4**	Mus musculus prolactin family 2, subfamily c, member 4 (Prl2c4), mRNA.	-1.01	-1.2	-1.82
ILMN_2741096	**Timp3**	Mus musculus tissue inhibitor of metalloproteinase 3 (Timp3), mRNA.	1.06	-1.34	-1.79
ILMN_3115472	**Aqp5**	Mus musculus aquaporin 5 (Aqp5),	-1.09	1	-1.66

		mRNA.			
ILMN_1222565	**A930002H24 Rik**	PREDICTED: Mus musculus RIKEN cDNA A930002H24 gene (A930002H24Rik), mRNA.	1.02	-1.07	-1.6
ILMN_2828916	**Frmd6**	Mus musculus FERM domain containing 6 (Frmd6), mRNA.	1.11	-1.48	-1.56
ILMN_2449019	**Tnk2**	Mus musculus tyrosine kinase, non-receptor, 2 (Tnk2), mRNA.	1.17	-1.44	-1.53
ILMN_2760254	**Mrgprf**	Mus musculus MAS-related GPR, member F (Mrgprf), mRNA.	1.1	-1.14	-1.53
ILMN_3161105	**Ahnak2**	Mus musculus AHNAK nucleoprotein 2 (Ahnak2), mRNA.	1.06	-1.08	-1.52
ILMN_2520249	**Hspg2**		1.28	-1.31	-1.52
ILMN_1235732	**Cdsn**	Mus musculus corneodesmosin (Cdsn), mRNA.	1.09	-1.14	-1.51
ILMN_1229547	**Spon2**	Mus musculus spondin 2, extracellular matrix protein (Spon2), mRNA.	1.93	-1.23	-1.51
ILMN_2778151	**Sox9**		1.04	1.02	-1.51
ILMN_1259967	**Prl2c2**	Mus musculus prolactin family 2, subfamily c, member 2 (Prl2c2), mRNA.	-1.04	-1.01	-1.5

Table 4.10. Gene ontology analysis of genes differentially regulated by T_3. The top biological functions that are over represented in T_3 regulated genes are listed based on P value of statistical significance of enrichment and the total number of molecules involved in a biological pathway out of the total 203 T_3 regulated genes.

Top networks
Drug Metabolism, Endocrine System Development and Function, Lipid Metabolism
Gene Expression, Cell Cycle, Cellular Growth and Proliferation
Cell Death, Cellular Growth and Proliferation, Cell-To-Cell Signaling and Interaction

Top Biological Functions		
Diseases and Disorders	**P value**	**No. of molecules**
Cancer	2.43E-05 - 1.63E-02	48
Gastrointestinal Disease	4.42E-04 - 1.34E-02	26
Genetic Disorder	4.42E-04 - 1.34E-02	14
Neurological Disease	4.42E-04 - 1.34E-02	11
Molecular and Cellular Functions		
Gene Expression	3.22E-07 - 4.48E-04	36
Cell Death	1.90E-05 - 1.57E-02	34
Cellular Growth and Proliferation	1.03E-04 - 1.72E-02	46
Cellular Development	1.96E-04 - 1.72E-02	38
Cell Cycle	2.65E-04 - 1.62E-02	20
Physiological System Development and Function		
Hematological System Development and Function	4.48E-05 - 1.70E-02	20
Organismal Development	4.48E-05 - 1.51E-02	20
Tissue Development	4.48E-05 - 1.72E-02	39
Organismal Survival	5.37E-05 - 4.63E-03	22
Skeletal and Muscular System Development and Function	1.59E-04 - 1.34E-02	18

Table 4.11. Gene ontology analysis of genes differentially regulated by CORT. The top biological functions that are over represented in CORT regulated genes are listed based on P value of statistical significance of enrichment and the total number of molecules involved in a biological pathway out of the total 425 CORT regulated genes.

Top networks
Gene Expression, Free Radical Scavenging, Cell Death
Cell Death, Cellular Function and Maintenance, Hematological System Development and Function
Cell-To-Cell Signaling and Interaction, Nervous System Development and Function, Cellular Disassembly and Organization

Top Biological Functions		
Diseases and Disorders	**P value**	**No. of molecules**
Neurologic Disease	2.08E-08 – 2.74E-03	58
Inflammatory Response	5.27E-08 – 3.66E-03	57
Cancer	1.13E-07 – 3.86E-03	107
Reproductive System Disease	4.04E-07 – 1.20E-03	57
Molecular and Cellular Functions		
Cell Death	6.11E-14 – 3.90E-03	109
Cellular Movement	4.08E-13 – 2.77E-03	76
Cellular Development	2.80E-11 – 3.57E-03	89
Cellular Growth and Proliferation	6.56E-11 – 3.25E-03	107
Cellular Function and Maintenance	1.70E-07 – 3.81E-03	69
Physiological System Development and Function		
Tissue Development	3.09E-08 – 3.14E-03	91
Cardiovascular System Development and Function	3.35E-08 – 3.25E-03	51
Organismal Survival	4.36E-08 – 1.26E-04	53
Organismal Development	5.54E-08 – 3.73E-03	62
Hematological System Development and Function	1.10E-07 – 3.18E-03	71

Table 4.12. Gene ontology analysis of genes differentially regulated by T_3 plus CORT. The top biological functions that are over represented in T3 plus CORT regulated genes are listed based on P value of statistical significance of enrichment and the total number of molecules involved in a biological pathway out of the total 400 T3 plus CORT regulated genes.

Top networks
Lipid Metabolism, Small Molecule Biochemistry, Cell Death
Cell Morphology, Organismal Function, Cellular Movement
Cellular Development, Cell Cycle, Cancer

Top Biological Functions		
Diseases and Disorders	**P value**	**No. of molecules**
Cancer	1.96E-07 – 7.37E-03	105
Inflammatory Response	1.73E-06 – 6.83E-03	55
Reproductive System Disease	4.74E-06 – 7.37E-03	71
Genetic Disorder	2.86E-05 – 4.79E-03	73
Molecular and Cellular Functions		
Cellular Development	1.26E-09 – 7.46E-03	84
Cellular Movement	1.46E-09 – 7.26E-03	66
Cell Death	2.57E-08 – 7.51E-03	94
Cellular Growth and Proliferation	1.18E-07 – 7.40E-03	105
Gene Expression	3.15E-06 – 7.51E-03	68
Physiological System Development and Function		
Tissue Development	1.30E-07 –7.46E-03	85
Cardiovascular System Development and Function	5.66E-07 – 7.46E-03	40
Organismal Development	5.66E-07 – 7.46E-03	65
Embryonic Development	1.09E-05 – 7.46E-03	57
Organ Development	1.09E-05 – 7.46E-03	53

Table 4.13. Gene ontology analysis of genes synergistically upregulated regulated by T_3 plus CORT. The top biological functions that are over represented in T_3 plus CORT regulated genes are listed based on P value of statistical significance of enrichment and the total number of molecules involved in a biological pathway out of the total 69 genes synergistically upregulated by T_3 plus CORT treatment.

Top Networks
Cellular Development, Cellular Assembly and Organization, Skeletal and Muscular System Development and Function
Drug Metabolism, Cellular Development, Hematological System Development and Function
Infectious Disease, Post-Translational Modification, Hematological Disease

Top Biological Functions		
Disease and Disorders	**P value**	**No. of Molecules**
Cancer	2.96E-03 - 4.21E-02	19
Connective Tissue Disorders	2.96E-03 - 2.34E-02	3
Developmental Disorder	2.96E-03 - 2.96E-03	3
Molecular and Cellular Functions		
Cellular Assembly and Organization	8.56E-06 - 4.91E-02	12
DNA Replication, Recombination, and Repair	1.27E-04 - 4.26E-02	5
Post-Translational Modification	5.70E-04 - 4.11E-02	9

Table 4.14. Gene ontology analysis of genes synergistically downregulated regulated by T_3 plus CORT. The top biological functions that are over represented in T_3 plus CORT regulated genes are listed based on P value of statistical significance of enrichment and the total number of molecules involved in a biological pathway out of the total 80 genes synergistically downregulated by T_3 plus CORT treatment.

Top networks
Cellular Movement, Cellular Assembly and Organization, Cellular Function and Maintenance
DNA Replication, Recombination and, Repair, Molecular Transport, Cell Death
Cell to Cell Signaling and Interaction, Cellular Growth and Proliferation, Connective Tissue Development and Function

Top Biological Functions		
Diseases and Disorders	**P value**	**No. of molecules**
Cancer	3.97E-04 – 4.86E-02	22
Gastrointestinal Disease	7.88E-04 – 2.17E-02	10
Infectious Disease	8.58E-04 – 4.81E-02	9
Cardiovascular Disease	1.49E-03 – 4.81E-02	4
Molecular and Cellular Functions		
Cellular Growth and Proliferation	1.19E-04 – 4.81E-02	17
Cellular Development	1.28E-04 – 4.81E-02	16
Cell to Cell Signaling and Interaction	2.11E-04 – 4.81E-02	14
Cellular Movement	3.25E-04 – 4.81E-02	14
Molecular Transport	5.61E-04 – 4.81E-02	8
Physiological System Development and Function		
Digestive System Development and Function	2.19E-05 –4.55E-02	6
Embryonic Development	1.19E-04 – 4.03E-02	17
Skeletal and Muscular System Development and Function	2.88E-04 – 4.29E-02	10
Tissue Development	5.89E-04 – 4.81E-02	19
Hematological System Development and Function	8.58E-04 – 4.81E-02	12

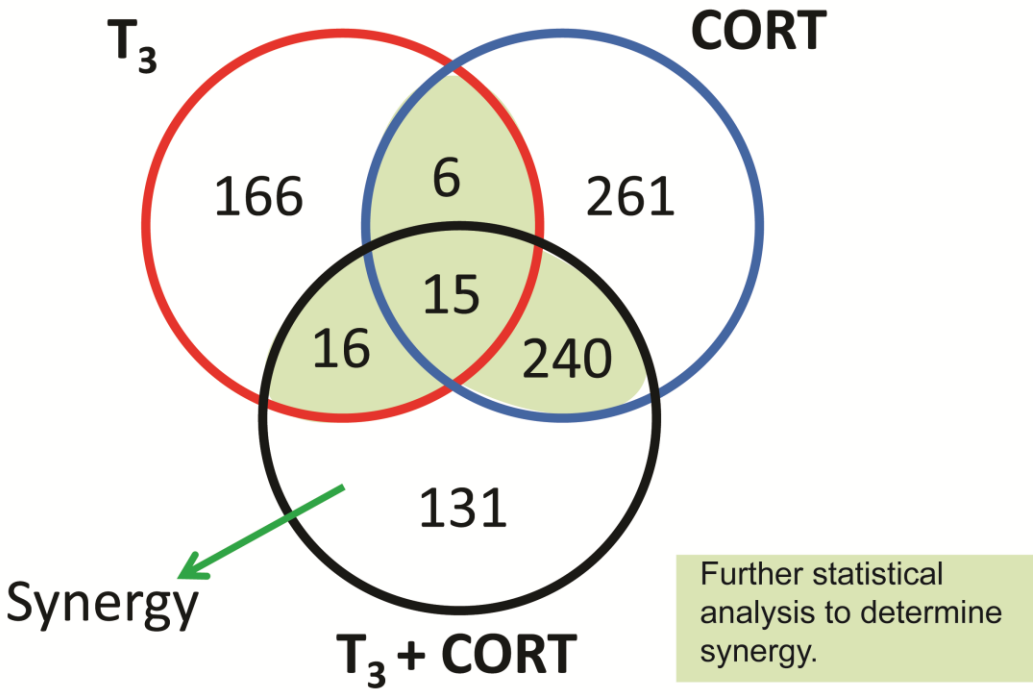

Fig. 4.1. Representative number of genes regulated by T_3, CORT, T_3 plus CORT in cultured mouse hippocampal cells by microarray analysis. Genes that are differentially based on a p value of <0.01 (n=3/ hormone treatment) and 1.2 fold change for T_3; 1.5 fold change for CORT and T_3 plus CORT. Fold change is calculated as the ratio of hormone array signal over control array signal.

References

Akaike, M., N. Kato, et al. (1991). "Hyperactivity and spatial maze learning impairment of adult rats with temporary neonatal hypothyroidism." Neurotoxicol Teratol **13**(3): 317-322.

Bagamasbad, P., K. L. Howdeshell, et al. (2008). "A role for basic transcription element-binding protein 1 (BTEB1) in the autoinduction of thyroid hormone receptor beta." J Biol Chem **283**(4): 2275-2285.

Beylin, A. V. and T. J. Shors (2003). "Glucocorticoids are necessary for enhancing the acquisition of associative memories after acute stressful experience." Horm Behav **43**(1): 124-131.

Bonett, R. M., F. Hu, et al. (2009). "Stressor and glucocorticoid-dependent induction of the immediate early gene kruppel-like factor 9: implications for neural development and plasticity." Endocrinology **150**(4): 1757-1765.

Cayrou, C., R. J. Denver, et al. (2002). "Suppression of the basic transcription element-binding protein in brain neuronal cultures inhibits thyroid hormone-induced neurite branching." Endocrinology **143**(6): 2242-2249.

Darbra, S., F. Balada, et al. (2004). "Perinatal hypothyroidism effects on step-through passive avoidance task in rats." Physiol Behav **82**(2-3): 497-501.

Datson, N. A., M. C. Morsink, et al. (2008). "Central corticosteroid actions: Search for gene targets." Eur J Pharmacol **583**(2-3): 272-289.

Datson, N. A., J. A. Polman, et al. (2011). "Specific regulatory motifs predict glucocorticoid responsiveness of hippocampal gene expression." Endocrinology **152**(10): 3749-3757.

Datson, N. A., N. Speksnijder, et al. (2010). "The transcriptional response to chronic stress and glucocorticoid receptor blockade in the hippocampal dentate gyrus." Hippocampus.

Datson, N. A., J. van der Perk, et al. (2001). "Identification of corticosteroid-responsive genes in rat hippocampus using serial analysis of gene expression." Eur J Neurosci **14**(4): 675-689.

Denver, R. J., L. Ouellet, et al. (1999). "Basic transcription element-binding protein (BTEB) is a thyroid hormone-regulated gene in the developing central nervous system. Evidence for a role in neurite outgrowth." J Biol Chem **274**(33): 23128-23134.

Denver, R. J., S. Pavgi, et al. (1997). "Thyroid hormone-dependent gene expression program for Xenopus neural development." J Biol Chem **272**(13): 8179-8188.

Denver, R. J. and K. E. Williamson (2009). "Identification of a thyroid hormone response element in the mouse Kruppel-like factor 9 gene to explain its postnatal expression in the brain." Endocrinology **150**(8): 3935-3943.

Dong, J., H. Yin, et al. (2005). "Congenital iodine deficiency and hypothyroidism impair LTP and decrease C-fos and C-jun expression in rat hippocampus." Neurotoxicology **26**(3): 417-426.

Furlow, J. D. and A. Kanamori (2002). "The transcription factor basic transcription element-binding protein 1 is a direct thyroid hormone response gene in the frog Xenopus laevis." Endocrinology **143**(9): 3295-3305.

Gilbert, M. E. (2004). "Alterations in synaptic transmission and plasticity in area CA1 of adult hippocampus following developmental hypothyroidism." Brain Res Dev Brain Res **148**(1): 11-18.
Gilbert, M. E. and C. Paczkowski (2003). "Propylthiouracil (PTU)-induced hypothyroidism in the developing rat impairs synaptic transmission and plasticity in the dentate gyrus of the adult hippocampus." Brain Res Dev Brain Res **145**(1): 19-29.
Gilbert, M. E. and L. Sui (2006). "Dose-dependent reductions in spatial learning and synaptic function in the dentate gyrus of adult rats following developmental thyroid hormone insufficiency." Brain Res **1069**(1): 10-22.
Gilbert, M. E. and L. Sui (2008). "Developmental exposure to perchlorate alters synaptic transmission in hippocampus of the adult rat." Environ Health Perspect **116**(6): 752-760.
Gould, E., M. D. Allan, et al. (1990). "Dendritic spine density of adult hippocampal pyramidal cells is sensitive to thyroid hormone." Brain Res **525**(2): 327-329.
Gould, E., C. S. Woolley, et al. (1991). "The hippocampal formation: morphological changes induced by thyroid, gonadal and adrenal hormones." Psychoneuroendocrinology **16**(1-3): 67-84.
Joels, M. (2008). "Functional actions of corticosteroids in the hippocampus." Eur J Pharmacol **583**(2-3): 312-321.
Joels, M., Z. Pu, et al. (2006). "Learning under stress: how does it work?" Trends Cogn Sci **10**(4): 152-158.
Kang, M. K., A. Kameta, et al. (2003). "Senescence-associated genes in normal human oral keratinocytes." Exp Cell Res **287**(2): 272-281.
Karst, H. and M. Joels (2005). "Corticosterone slowly enhances miniature excitatory postsynaptic current amplitude in mice CA1 hippocampal cells." J Neurophysiol **94**(5): 3479-3486.
Lin, Y., B. L. Bloodgood, et al. (2008). "Activity-dependent regulation of inhibitory synapse development by Npas4." Nature **455**(7217): 1198-1204.
Madeira, M. D. and M. M. Paula-Barbosa (1993). "Reorganization of mossy fiber synapses in male and female hypothyroid rats: a stereological study." J Comp Neurol **337**(2): 334-352.
Magarinos, A. M., J. M. Verdugo, et al. (1997). "Chronic stress alters synaptic terminal structure in hippocampus." Proc Natl Acad Sci U S A **94**(25): 14002-14008.
Maher, P. and J. B. Davis (1996). "The role of monoamine metabolism in oxidative glutamate toxicity." J Neurosci **16**(20): 6394-6401.
McBride, O. W., H. F. Yi, et al. (1994). "The human cytochrome b561 gene (CYB561) is located at 17q11-qter." Genomics **21**(3): 662-663.
McEwen, B. S. (1999). "Stress and hippocampal plasticity." Annu Rev Neurosci **22**: 105-122.
Morimoto, B. H. and D. E. Koshland, Jr. (1990). "Excitatory amino acid uptake and N-methyl-D-aspartate-mediated secretion in a neural cell line." Proc Natl Acad Sci U S A **87**(9): 3518-3521.
Morimoto, B. H. and D. E. Koshland, Jr. (1990). "Induction and expression of long- and short-term neurosecretory potentiation in a neural cell line." Neuron **5**(6): 875-880.

Morita, M., A. Kobayashi, et al. (2003). "Functional analysis of basic transcription element binding protein by gene targeting technology." Mol Cell Biol **23**(7): 2489-2500.

Morsink, M. C., P. J. Steenbergen, et al. (2006). "Acute activation of hippocampal glucocorticoid receptors results in different waves of gene expression throughout time." J Neuroendocrinol **18**(4): 239-252.

Porterfield, S. P. (2000). "Thyroidal dysfunction and environmental chemicals--potential impact on brain development." Environ Health Perspect **108 Suppl 3**: 433-438.

Porterfield, S. P. and C. E. Hendrich (1993). "The role of thyroid hormones in prenatal and neonatal neurological development--current perspectives." Endocr Rev **14**(1): 94-106.

Rami, A., A. J. Patel, et al. (1986). "Thyroid hormone and development of the rat hippocampus: morphological alterations in granule and pyramidal cells." Neuroscience **19**(4): 1217-1226.

Rami, A. and A. Rabie (1990). "Delayed synaptogenesis in the dentate gyrus of the thyroid-deficient developing rat." Dev Neurosci **12**(6): 398-405.

Rami, A., A. Rabie, et al. (1986). "Thyroid hormone and development of the rat hippocampus: cell acquisition in the dentate gyrus." Neuroscience **19**(4): 1207-1216.

Roozendaal, B. (2002). "Stress and memory: opposing effects of glucocorticoids on memory consolidation and memory retrieval." Neurobiol Learn Mem **78**(3): 578-595.

Royland, J. E., J. S. Parker, et al. (2008). "A genomic analysis of subclinical hypothyroidism in hippocampus and neocortex of the developing rat brain." J Neuroendocrinol **20**(12): 1319-1338.

Sagara, Y., R. Dargusch, et al. (1998). "Cellular mechanisms of resistance to chronic oxidative stress." Free Radic Biol Med **24**(9): 1375-1389.

Samuels, H. H., F. Stanley, et al. (1979). "Depletion of L-3,5,3'-triiodothyronine and L-thyroxine in euthyroid calf serum for use in cell culture studies of the action of thyroid hormone." Endocrinology **105**(1): 80-85.

Scobie, K. N., B. J. Hall, et al. (2009). "Kruppel-like factor 9 is necessary for late-phase neuronal maturation in the developing dentate gyrus and during adult hippocampal neurogenesis." J Neurosci **29**(31): 9875-9887.

Shors, T. J. (2001). "Acute stress rapidly and persistently enhances memory formation in the male rat." Neurobiol Learn Mem **75**(1): 10-29.

Shors, T. J., C. Chua, et al. (2001). "Sex differences and opposite effects of stress on dendritic spine density in the male versus female hippocampus." J Neurosci **21**(16): 6292-6297.

Watanabe, Y., E. Gould, et al. (1992). "Stress induces atrophy of apical dendrites of hippocampal CA3 pyramidal neurons." Brain Res **588**(2): 341-345.

Yao, M., J. Schulkin, et al. (2008). "Evolutionarily conserved glucocorticoid regulation of corticotropin-releasing factor expression." Endocrinology **149**(5): 2352-2360.

Chapter 5

A ROLE FOR KRÜPPEL-LIKE FACTOR 9 (KLF9) IN THE AUTOINDUCTION OF THYROID HORMONE RECEPTOR BETA

Abstract

Thyroid hormone (T_3) induces gene regulation programs necessary for tadpole metamorphosis. Among the earliest responses to T_3 are the up-regulation of T_3 receptor beta (TRβ; autoinduction) and the Krüppel-like factor 9 (Klf9/ also known as Basic transcription element binding protein 1 (BTEB1)). KLF9 is a member of the Krüppel family of transcription factors that bind to GC-rich regions in gene promoters. The proximal promoter of the *Xenopus laevis TrβA* gene has seven GC-rich sequences, which led us to hypothesize that KLF9 binds to and regulates *TrβA*. In tadpoles and the frog fibroblast-derived cell line XTC-2, T_3 upregulated *Klf9* mRNA with faster kinetics than *TrβA*, and *Klf9* mRNA correlated with increased KLF9 protein expression. KLF9 bound to GC-rich sequences in the proximal *TrβA* promoter *in vitro*. Using chromatin immunoprecipitation assay we show that KLF9 associates with the *TrβA* promoter *in vivo* in a T_3 and developmental stage-dependent manner. Induced expression of KLF9 in XTC-2 cells caused accelerated and enhanced autoinduction of the *TrβA* gene. This enhancement was lost in N-terminal truncated mutants of KLF9. However, point mutations in the zinc fingers of KLF9 that destroyed DNA binding did not alter the

protein's activity on *TrβA* autoinduction, suggesting that KLF9 can function in this regard through protein-protein interactions. Our findings support the hypothesis that KLF9 associates with the *TrβA* promoter *in vivo* and enhances autoinduction, but this action does not depend on its DNA binding activity. Cooperation among the protein products of immediate early genes may be a common mechanism for driving developmental signaling pathways.

Introduction

Autoinduction of nuclear hormone receptors is a common, although poorly understood phenomenon in animal development (Tata 2000). The autoinduction of thyroid hormone (T_3) receptor genes (*Tr*) during amphibian metamorphosis is a dramatic example of this form of gene regulation (Tata 2000). All vertebrates possess two *Tr* genes designated *Trα* and *Trβ* (also known as NR1A1 and NR1A2, respectively; *Xenopus laevis* has two *Trα* and two *Trβ* genes each designated A or B owing to its pseudotetraploidy (Yaoita, Shi et al. 1990). Thyroid hormone is the primary morphogen controlling tadpole metamorphosis and TRs are ligand-dependent transcription factors. One of the earliest gene regulation events during amphibian metamorphosis is the upregulation of *TrβA* by T_3 (Yaoita and Brown 1990). This regulation depends on TRs binding to thyroid hormone response elements (TREs) present in the *TrβA* promoter (receptor autoinduction; (Yaoita, Shi et al. 1990; Machuca, Esslemont et al. 1995). It is hypothesized that autoinduction of *Trβ* genes is essential for metamorphosis (Tata 2000). The gene regulation programs induced by the T_3-TR complex that lead to tissue morphogenesis have been characterized in several tadpole tissues (Wang and Brown 1991; Buckbinder and Brown 1992; Shi and Brown 1993; Brown, Wang et al. 1996; Denver, Pavgi et al. 1997; Veldhoen, Crump et al. 2002; Helbing, Werry et al. 2003; Das, Cai et al. 2006).

Krüppel-like factor 9 (*Klf9*) is an immediate early gene induced by T_3 in most tadpole tissues during metamorphosis (there are two *Klf9* genes in *X. laevis* designated ‘a’ and ‘b’; (Brown, Wang et al. 1996; Furlow and Kanamori 2002; Hoopfer, Huang et al. 2002). The direct regulation of the *X. laevis Klf9* genes by T_3 is explained by one or more TREs

located upstream of the transcription initiation sites (Brown, Wang et al. 1996; Furlow and Kanamori 2002). KLF9 is a member of the Krüppel family of transcription factors (KLF; also known as Basic transcription element binding protein 1 (BTEB1) (Kaczynski, Cook et al. 2003)) first isolated in a screen for proteins that bind to a GC-rich (GC box) sequence in the promoter of the rat cytochrome P-450IA1 gene (designated the basic transcription element or BTE; (Yanagida, Sogawa et al. 1990; Imataka, Sogawa et al. 1992). KLF9 possesses a DNA binding domain (DBD) consisting of three Cys2-His2 zinc finger domains (Philipsen and Suske 1999; Dang 2000). Krüppel-like proteins are distantly related to the specificity protein (Sp) family members, including Sp1 (Philipsen and Suske 1999; Dang 2000). The KLF9 DBD shares 72% sequence similarity with rat Sp1 (Imataka, Sogawa et al. 1992) and the two proteins bind with similar affinity to the BTE sequence (Sogawa, Kikuchi et al. 1993). While Sp1 and KLF9 have very similar DNA binding domains, and they bind to similar or identical consensus DNA sequences, the two proteins are completely different outside of the DBD. In addition to other KLF family members, three proteins designated KLF2, 3 and 4 have been identified in mammals, although the KLF2 appears to be more distantly related to KLF9 than the other two proteins (Sogawa, Imataka et al. 1993; Dang 2000; Martin, Cooper et al. 2000; Kaczynski, Conley et al. 2002). As with KLF9 and Sp1, the KLF proteins share almost identical DNA binding domains, but are divergent in their N-terminal regions that harbor domains necessary for their transactivation, and in some cases transrepression functions (Kaczynski, Cook et al. 2003).

Krüppel-like factor 9 mRNA and protein are strongly upregulated by T_3 in tadpole tissues ((Hoopfer, Huang et al. 2002)), but the genes that KLF9 regulates, and thus its

functions in tadpole development are unknown. It is noteworthy that KLF9 is the only KLF/Sp 1-like family member known to be upregulated by T_3 in tadpole tissues (Wang and Brown 1991; Buckbinder and Brown 1992; Shi and Brown 1993; Brown, Wang et al. 1996; Denver, Pavgi et al. 1997; Veldhoen, Crump et al. 2002; Helbing, Werry et al. 2003; Das, Cai et al. 2006). Earlier, we and others showed that KLF9 is also regulated by T_3 in developing rodent brain where it promotes neurite outgrowth (Denver, Ouellet et al. 1999; Cayrou, Denver et al. 2002; Morita, Kobayashi et al. 2003). KLF9 is expressed in uterine endometrial cells where it transactivates the uteroferrin gene, and may influence cell proliferation by regulating cell cycle and growth-associated genes (Simmen, Chung et al. 1999; Simmen, Zhang et al. 2000; Simmen, Zhang et al. 2002). The actions of KLF9 in endometrial cells appear to involve direct protein-protein interactions with the progesterone receptor (Zhang, Zhang et al. 2002). We found that *X. laevis* KLF9 is capable of activating synthetic promoter constructs containing multiple or single GC boxes (Hoopfer, Huang et al. 2002). Mammalian KLF9 also has transactivation function on several synthetic and native promoters (Imataka, Sogawa et al. 1992; Imataka, Mizuno et al. 1993; Sjottem, Anderssen et al. 1996; Foti, Stroup et al. 1998; Simmen, Chung et al. 1999; Chen and Davis 2000). KLF proteins have been reported to activate or repress transcription depending on the number of GC boxes present in the promoter construct tested, the target gene analyzed and the cell type (Imataka, Mizuno et al. 1993; Sjottem, Anderssen et al. 1996; Foti, Stroup et al. 1998; Imhof, Schuierer et al. 1999; Simmen, Chung et al. 1999; Chen and Davis 2000; Furlow and Kanamori 2002; Hoopfer, Huang et al. 2002; Hsiang and Straus 2002; Zhang, Zhang et al. 2002; Kaczynski, Cook et al. 2003). Whether these proteins function as transcriptional activators or repressors may

depend on the architecture of the specific promoter and the chromatin environment (Kaczynski, Cook et al. 2003).

Based on the early response kinetics of the *Klf9* and *TrβA* genes, the observation that the protein products of these genes are expressed in the same cells (Hoopfer, Huang et al. 2002) and the identification of seven GC rich regions in the proximal *X. laevis TrβA* promoter, we hypothesized that *TrβA* may be a target gene for KLF9. We further hypothesized that the upregulation of KLF9 plays a role in the autoinduction of *TrβA*, perhaps functioning as an accessory transcriptional activator. Here we show that the kinetics of *Klf9* mRNA upregulation in response to T_3 are faster than *TrβA*, and that KLF9 binds to regions of the proximal *TrβA* promoter that contain GC boxes. Using chromatin immunoprecipitation (ChIP) assay we show that KLF9 associates with the *TrβA* promoter *in vivo* in a T_3– and developmental stage-dependent manner. Forced expression of BTEB1 in the *X. laevis* fibroblast cell line XTC-2 (Pudney, Varma et al. 1972) accelerates the activation of the *TrβA* promoter and expression of endogenous *TrβA* mRNA in response to T_3. This action depends on the first 30 amino acids of KLF9, but not on its DNA binding capacity, since point mutations in the zinc fingers did not alter the activity. Taken together, our findings support the hypothesis that the upregulation of KLF9 by T_3 plays a role in the transcriptional regulation of the *TrβA* gene during tadpole development.

Materials and Methods

Animals and hormone treatments. Tadpoles of *X.laevis* were reared in dechlorinated tap water (water temperature, 20-22 °C) and fed pulverized frog brittle (Nasco, Fort Atkinson, WI). Developmental stages were assigned according to Nieuwkoop and Faber (NF; (Nieuwkoop and Faber 1956). Tadpoles were treated with 3,5,3'-L-triiodothyronine (T_3; sodium salt; Sigma, St. Louis, MO) by adding it to the aquarium water to a final concentration of 10 nM for various times; water was changed and hormone replenished daily over the treatment period. Tadpoles were then euthanized by immersion in 0.01% benzocaine (Sigma), and whole brains and tails were collected for RNA or ChIP analyses (see below). Animal care was in accordance with institutional guidelines.

RNA extraction and reverse transcriptase-PCR (RT-PCR) analysis. Total RNA was isolated from tadpole brains or XTC-2 cells using the Trizol reagent (Invitrogen, Carlsbad, CA) following the manufacturer's instructions. The RNA was treated with DNase I (Roche, Indianapolis, IN) prior to reverse transcription to remove genomic DNA contamination following the methods of Manzon and Denver (Manzon and Denver 2004). The DNase-treated RNA was reverse transcribed using SuperScript II (0.5 μl, 200 U/μl; Invitrogen) and 0.2 to 2 microliters of the resulting cDNA was used for PCR. *Semi-quantitative RT-PCR*: Standard PCR reactions were initiated in 25 μl containing 10X PCR buffer, 1.5 mM $MgCl_2$, dNTP mix (1.25 mM each), forward and reverse primers for each gene of interest (10 uM), and Taq DNA polymerase (1.25 U; Promega, Madison, WI). Each thermal cycle consisted of 94 °C for 1 min, 55 °C for 1 min and 72 °C for 2 min. The number of cycles for each gene was determined empirically by

constructing linear amplification curves. We used 32 cycles for *Bteb1*, 36 for *TrβA* and 28 for ribosomal protein L8 (*rpL8*; a housekeeping gene used to normalize for RNA loading and cDNA synthesis). Oligonucleotide primer sequences for *Klf9* are given in Table 5.1. Primer sequences used for *rpL8* and *TrβA* were as described by Manzon and Denver (Manzon and Denver 2004). PCR products were electrophoresed on 1% agarose gels, stained with ethidium bromide, and densitometry conducted using Scion Image Software (version 3.0, Scion Corporation). The band densities of *Klf9* and *TrβA* amplicons for each sample were normalized to the densities of the *rpL8* bands.

Quantitative, real time PCR (qPCR): For quantitative RT-PCR (RTqPCR) we developed TaqMan assays and analyzed samples on an ABI 7500 fast real time PCR machine using TaqMan Universal PCR Master Mix (Applied Biosystems, Inc., Foster City, CA). The primer/probe sets used are given in Table 5.1 and were designed to span exon/intron boundaries. Standard curves were generated using cDNAs from the time point that exhibited the highest expression level for each gene to provide for a relative quantitation. *TrβA* and *Klf9* mRNAs were normalized to the level of *rpL8* mRNA.

Plasmid Constructs. The pCMV-xKLF9 expression plasmid was described by Hoopfer et al. (Hoopfer, Huang et al. 2002). The *X. laevis TrβA* promoter-luciferase plasmid (Ranjan, Wong et al. 1994) was a generous gift of Dr. Yun-Bo Shi. Full-length and N-terminal truncated mutants of KLF9 were generated by PCR (primers in Table 5.2) and cDNA fragments were directionally cloned into the pCS2 vector. The choice of deletions was based on the location of two putative transactivation domains (A and B) located in rat KLF9 (Kobayashi, Sogawa et al. 1995) that are highly conserved in *Xenopus* KLF9

(Hoopfer, Huang et al. 2002). The plasmid pCS2-xKLF9Δ30 has a deletion of the first 30 amino acids that includes transactivation domain A; pCS2-xKLF9Δ99 has both transactivation domains A and B removed; and pCS2-xKLF9Δ120 represents only the DNA binding domain.

The plasmid construct pCS2-xKLF9 C_2AH harbors histidine to alanine substitutions (H211A, H241A, H296A) in the first histidine residues of each of the three zinc fingers of KLF9. This construct was generated using the QuikChange Multi Site-Directed Mutagenesis Kit (Stratagene) with pCS2-xKLF9 as template and three primers shown in Table 5.2.

Electrophoretic mobility shift assay. We conducted electrophoretic mobility shift assay (EMSA) as described by Hoopfer et al. (Hoopfer, Huang et al. 2002) with minor modifications. The BTE and mutated BTE (mBTE) probes used were as described by Yanagida et al. (Yanagida, Sogawa et al. 1990). Bacterial cell lysate containing the fusion protein GST-xKLF9[DBD] was prepared as described by Hoopfer et al. (Hoopfer, Huang et al. 2002). Recombinant wild type KLF9 or KLF9 C_2AH mutant were produced *in vitro* using the TnT SP6 Quick Coupled Translation System (Promega). For EMSA, one microliter of a 1:512 dilution of GST-xKLF9[DBD] lysates or varying volumes of the *in vitro* translated proteins were incubated in a volume of 35 μl with 20,000 cpm [^{32}P]-BTE and 1.4 μg double-stranded poly(deoxyinosinic-deoxycytidylic)acid [poly (dI-dC)] in buffer containing 20 mM HEPES (pH 7.8), 1 mM dithiothreitol (DTT), 0.1% Nonidet P-40, 50 mM KCl and 20% glycerol. For antibody supershifts, proteins were pre-incubated for 20 min prior to the addition of ^{32}P-BTE with 1 μg normal rabbit serum IgG or affinity

purified anti-xKLF9 IgG that recognizes only the N-terminal region of the protein (see below). The reaction continued at room temperature for 40 min before fractionation by non-denaturing 6% polyacrylamide gel electrophoresis in 0.25X Tris-borate-EDTA (TBE). Gels were fixed in 30% methanol/10% acetic acid, dried and processed for autoradiography.

The ability of regions of the proximal *X. laevis TrβA* promoter (Genbank Accession #U04675) to displace GST-xKLF9[DBD] binding to the [^{32}P]-BTE was tested by competitive EMSA (1.89 μM for each competitor DNA). The *X. laevis trβA* promoter fragments were generated by PCR and gel-purified using QIAEX II (Qiagen, Valencia, CA). The regions of the promoter that we analyzed are shown in Fig. 2 and Supplemental Table 5.1, and the oligonucleotides used to amplify the sequences by PCR are given in Table 5.3.

We then synthesized short oligonucleotide probes for EMSA containing predicted GC boxes in the *TrβA* promoter fragments that demonstrated competitive binding to GST-xKLF9[DBD] (see above). Oligonucleotides (24 bp) were synthesized, each of which encompassed one or two GC boxes within each *TrβA* promoter region (see Fig. 2 and Table 5.4). Each GC-box containing oligonucleotide was labeled with [^{32}P]-dCTP and used as a probe in EMSA.

Cell culture and transfection assays. We plated XTC-2 cells at a density of 2 x 10^5 cells per well in 6 well plates for gene expression and transfection assays. For ChIP assays, we plated cells at a density of 1 x 10^6 cells per 100 mm plate. Before transfections or hormone treatments cells were cultured overnight in a humidified atmosphere of 5% CO2

at 25°C. Cells were cultured in Leibovitz-15 medium (L-15; diluted 1:1.5 for amphibian cells; Invitrogen Life Technologies, Carlsbad, CA) supplemented with sodium bicarbonate (2.47 g/L), penicillin G sodium (100 U/ml), streptomycin sulfate (100 μg/mL) and 10% fetal bovine serum that had been stripped of thyroid hormone following the method of Samuels et al. (Samuels, Stanley et al. 1979). For gene expression, transfection and ChIP assays, cells were treated for different times with or without 5 nM T_3 before harvest.

For the luciferase reporter assay experiments, we transfected cells using the polyethylenimine (pEi; Sigma) method (Meunier-Durmort, Grimal et al. 1997). The total amount of DNA per well was normalized by adding empty vector (pCMVneo). All cells were cotransfected with the pRenilla-luciferase plasmid for normalization of cell transfection by dual reporter luciferase assay following the manufacturer's instructions (Promega, Madison, WI). Just prior to transfection the cells were washed twice with serum-free L-15, and the pEi/DNA solution was added directly to the wells. After 1 hr the transfection medium was replaced with growth medium and the cells were incubated overnight. Cells were then treated with or without T_3 for different times before harvest and analysis of luciferase activity. Luciferase activity was quantified (measured as relative light units) using a luminometer (Femtomater FB 12; Zylux Corp., Maryville, TN). Each transfection experiment was conducted three times with 4-5 wells per treatment.

For analysis of the effects of forced expression of wild type or mutant KLF9 on endogenous *TrβA* mRNA we used the pCS2-based expression vectors described above, and transfected XTC-2 cells using Fugene 6 Transfection Reagent (Roche). Each well of

a 6 well plate received 1 μg of plasmid DNA and the total amount of DNA per well was normalized by adding empty vector (pCS2). Forty eight hours after transfection cells treated with or without T_3 for different times before harvest and RNA extraction. Each transfection experiment was done two to three times with 6 replicates per treatment.

Western blotting and Immunocytochemistry. We prepared Western blots following the methods of Ranjan et al. (Ranjan, Wong et al. 1994) with protein extracts of XTC-2 cells transfected with pCS2-xKLF9, or pCS2 and extracts of XTC-2 cells treated +/- T_3. Forty micrograms of total protein for each sample were separated by electrophoresis on 10% denaturing SDS-polyacrylamide gels. Proteins were transferred to nitrocellulose membranes and probed with an affinity-purified antiserum to *X. laevis* KLF9 (Hoopfer, Huang et al. 2002). The antiserum was generated in a rabbit against the full-length *X. laevis* KLF9 protein, and affinity-purified such that the IgGs recognize only the N-terminal region of the frog KLF9 protein (Hoopfer, Huang et al. 2002); 0.2 μg purified IgG/ml). These antibodies do not recognize the DNA binding domain (DBD) of xKLF9 (Hoopfer, Huang et al. 2002), which is critical to the specificity of the reagent given the high degree of conservation of the DBDs among Krüppel and Sp 1-like family members. This purified antiserum was also used for ChIP assays (described below).

We conducted immunocytochemistry for KLF9 protein following the methods that we described previously (Hoopfer, Huang et al. 2002). Briefly, NF stage 52 tadpoles were treated with or without T_3 (10 nM) for 24 hr before sacrifice. Brains were fixed for 24 hr at 4^{o}C in 4% paraformaldehyde and then saturated in 30% sucrose for 24 hr. Tissues were embedded in M-1 embedding matrix (Shandon Lipshaw Inc., Pittsburgh, PA), frozen and

cryosectioned saggitally at 20 μm. We used five brains per treatment in the analyses. Cryosections were blocked, incubated with anti-*X. laevis* KLF9 IgG and immune complexes detected with either a goat anti-rabbit horseradish peroxidase secondary antibody (Vectastain elite ABC and Vector VIP kits; Vector Laboratories Inc., Burlingame, CA) or with a goat anti-rabbit Cy3-conjugated fluorescence secondary antibody (Jackson Immunoresearch Laboratories, West Grove, PA). To test for the specificity of the immunohistochemical reaction we preabsorbed the antibody with *E. coli* expressed GST-xKLF9 (10 μg/ml; (Hoopfer, Huang et al. 2002). Tissue sections were analyzed using an Olympus IX81 inverted fluorescence microscope.

Chromatin immunoprecipitation assay. We conducted ChIP assays as described previously for tadpole tissues (Sachs and Shi 2000). We used the Upstate Biochemicals, Inc. ChIP assay kit (Lake Placid, NY) following the manufacturer's instructions. The negative controls included: no primary antibody, replacement of the primary antibody with normal rabbit serum, and the analysis of regions outside of the proximal *TrβA* promoter (*Ef1α* promoter, *TrβA* exon 3/4, *TrβA* exon 5, intestinal fatty acid binding protein [*Ifabp*] promoter). For ChIP we used affinity-purified IgGs against *X. laevis* KLF9; 4 μg purified IgG/reaction). The PCR reactions for ChIP on tadpole brain or tail included [^{32}P]-dCTP (1 μCi/reaction) and the PCR products were analyzed on 6% polyacrylamide gels followed by autoradiography, or using an Agilent Technologies 2100 Bioanalyzer (Agilent Technologies, Inc., Santa Clara, CA). ChIP assays on XTC-2 cells were analyzed using quantitative, real-time PCR using the iCycler iQ real time PCR detection system from Bio-Rad (Hercules, CA). We used iQ Syber Green Supermix (Bio-

Rad) following the manufacturer's protocol with annealing temperatures adjusted for each primer set. Oligonucleotide PCR primers used for ChIP analyses are in Table 5.3.

Results

Klf9 mRNA is upregulated by T_3 in premetamorphic tadpole brain with faster kinetics than *TrβA* mRNA

Exposure of premetamorphic (NF Stage 52) tadpoles to T_3 (10 nM in the aquarium water) resulted in significant time-dependent increases in brain *Klf9b* ($F=222.35$, $P<0.0001$; ANOVA) and *TrβA* ($F=74.03$, $P<0.001$) mRNA levels (Fig. 1). The earliest time point at which a significant increase in *Klf9b* mRNA was detected was 8h ($P<0.0001$; Scheffe's test) and the mRNA level continued to increase up to 16 h. By contrast, a significant increase in *TrβA* mRNA expression was not detected until 16 h.

Thyroid hormone upregulates KLF9 protein in premetamorphic tadpole brain

Similar to results that we reported earlier (Hoopfer, Huang et al. 2002) we observed a strong increase of KLF9 protein expression in premetamorphic tadpole brain (NF stage 52) following treatment with T_3 (10 nM for 24 h; representative brain sections shown in Fig. 1B, panels 1 & 2). The strong nuclear staining for KLF9 was completely abolished by preabsorption with GST-xKLF9 (Fig. 1B, panels 3 & 4).

Western blot analysis with affinity purified anti-xKLF9 IgG on protein extracts of transfected XTC-2 cells showed that the antiserum detected the overexpressed KLF9 protein but did not crossreact with endogenous cellular proteins (Fig. 1C upper panel). Native KLF9 protein was increased in untransfected XTC-2 cells by 24 h treatment with

T_3 (Fig. 1C lower panel). We routinely detected two bands by Western blot that corresponded to the KLF9 protein. The basis for KLF9 protein heterogeneity is currently unknown, but likely reflects posttranslational modifications (*X. laevis* KLF9 is predicted to have up to four phosphorylation and two N-linked glycosylation sites; (Hoopfer, Huang et al. 2002)).

KLF9 binds to the proximal *TrβA* promoter *in vitro*

Computer analysis of the proximal *X. laevis TrβA* promoter sequence showed the presence of seven GC-rich regions commonly characterized as Sp1 binding sites (based on (Ranjan, Wong et al. 1994). The approximate locations of these GC-rich regions are shown in schematic in Fig. 2, and the precise locations are given in Supplemental Table 5.1. We used EMSA to determine if KLF9 can bind to the *TrβA* promoter *in vitro*. We generated ~200-300 bp fragments of the *TrβA* promoter by PCR (Fig. 2, Supplemental Table 5.1, Table 5.3) and used them as competitors in EMSA for binding of bacterially expressed GST-xKLF9[DBD] (Hoopfer, Huang et al. 2002) to a [^{32}P]-labeled probe consisting of the BTE sequence of the rat CYP1A1 gene (Imataka, Sogawa et al. 1992). Each of the *TrβA* gene promoter fragments with GC-rich sequences competed for binding in the EMSA, and the degree of competition correlated with the number of GC boxes contained within the fragment. By contrast, promoter fragments that did not possess GC boxes exhibited no competition in the EMSA (Fig. 3A).

We next synthesized short oligonucleotide probes (24 bp) encompassing one or two GC boxes within the proximal *TrβA* promoter region (to include all seven predicted GC boxes; Fig. 2 and Table 5.4) and tested for KLF9 binding to these DNA elements by

EMSA. Radioinert oligonucleotides were used as competitors to verify the specificity of binding. This experiment showed that KLF9 bound to all but one of these GC box sequences, and that the binding could be competed with unlabeled probe (Fig. 3B). We observed no binding with probe #5 which contains one GC box of identical sequence to the GC box elements found in other regions. As a positive control for the quality of the oligonucleotide probes we conducted EMSAs with nuclear extracts from *X. laevis* tadpole brain, which has abundant GC box binding activity (Hoopfer, Huang et al. 2002). This showed that nuclear proteins formed complexes to an equal extent with each of the radiolabeled DNAs (including probe #5; data not shown.)

KLF9 associates with the proximal *TrβA* promoter *in vivo* in a T_3 and developmental stage-dependent manner

To determine if KLF9 associates with the proximal *TrβA* promoter *in vivo* we conducted ChIP assays on brain and tail of premetamorphic *X. laevis* tadpoles that had been treated with or without T_3 for 48 hr before sacrifice. We found KLF9 associated with the proximal *TrβA* promoter *in vivo* and the signal was increased in a T_3-dependent manner in both brain and tail on most regions (not region G in brain or tail, nor region B in tail; Fig. 4). As controls for the ChIP assays we included the elimination of the primary antibody or the replacement of the primary antibody with normal rabbit serum. In each case the ChIP signal was below or at the limit of detection in the assay (data not shown). Another important control was the analysis of regions outside of the proximal *TrβA* promoter (*Ef1α* promoter, *TrβA* exon 3/4, *TrβA* exon 5, *Ifabp* promoter) which showed little or no association of KLF9. It should be noted that although we analyzed the

promoter by targeting relatively small regions for PCR (~200-300 bp), the nature of the ChIP assay, in which genomic fragments ranging from 500-1000 bp are produced by sonication, does not allow us to determine with precision where within the promoter KLF9 is associating. Nevertheless, our data show that KLF9 associates with the proximal *TrβA* promoter *in vivo* and that the signal is increased following T_3 treatment.

We found no KLF9 associated with control DNA sequences that included an intronic region of the *TrβA* gene that is at least 30 kb downstream from the start site (*TrβA* exon 3/exon 4), the *Ef1α* or the *Ifabp* promoters (an indirect T_3 response gene that is downregulated by T_3; (Shi and Hayes 1994).

Earlier we showed that *Klf9* mRNA and protein exhibit dramatic increases in tadpole brain during spontaneous or T_3–induced metamorphosis (Hoopfer, Huang et al. 2002). We therefore tested whether the increased KLF9 protein expression in brain during spontaneous metamorphosis resulted in increased association of KLF9 with the proximal *TrβA* promoter. As predicted, we found that the amount of KLF9 associated with the *TrβA* promoter (regions A/B were analyzed) was increased in animals at metamorphic climax (NF stage 62) when T_3 production and KLF9 protein is highest (Hoopfer, Huang et al. 2002) compared with premetamorphic tadpoles (NF stage 54) when T_3 and KLF9 are low (Fig. 4B).

Klf9 and *TrβA* mRNAs are coordinately upregulated and KLF9 associates with the proximal *TrβA* promoter in XTC-2 cells

We found statistically significant, time-dependent effects of T_3 on *Klf9* ($F=11.255$, $P<0.0001$; ANOVA) and *TrβA* ($F=36.936$, $P<0.0001$) mRNA expression in XTC-2 cells

(Fig. 5A). Significant upregulation of *Klf9* mRNA occurred by 3 hr (P=0.009; Scheffe's test), which was the maximum level of induction observed, and was maintained through 48 hr of treatment. By contrast, *TrβA* mRNA was not significantly increased until 6 hr (P=0.001), then reached a maximum by 12 hr that was maintained through 48 hr.

Using ChIP assay on XTC-cells that had been treated with T_3 for 24h, we observed association of KLF9 with two regions of the proximal *TrβA* promoter. Real-time PCR analysis of the ChIP assay showed significantly greater association of KLF9 with the upstream region of the *TrβA* promoter (region A/B; see Fig. 2 and 3), compared with the region located in the 5' UTR (region G; Fig. 5B; F=12.957, P<0.0001; ANOVA). The KLF9 signal at exon 5 of the *TrβA* gene (which is far downstream from the transcription start site) was not significantly different from background (i.e., ChIP with NRS, data not shown; Fig. 5B). We observed a small but statistically significant (P=0.043; t-test) T_3-dependent increase in KLF9 association with the upstream region of the *TrβA* promoter (region A/B) in XTC-2 cells (Fig. 5C). Note that the level of KLF9 induction by T_3 was lower in XTC-2 cells (~2.5 fold) compared with the brain *in vivo* (~10.5 fold).

Induced expression of KLF9 in XTC-2 cells accelerates autoinduction of the *TrβA* gene.

We used XTC-2 cell transfection and promoter-reporter assays to test the hypothesis that KLF9 enhances autoinduction of the *TrβA* gene. Treatment with T_3 caused significant time-dependent increases in luciferase activity in cells transfected with empty vector (ANOVA: F=55.564, P<0.0001) and pCMV-xKLF9 (F=601.043, P<0.0001; luciferase activity was significantly elevated by 2 hr in both treatments; P<0.05;

Scheffe's test; Fig. 6A). Forced expression of KLF9 had no effect on basal promoter activity, but resulted in a significant acceleration of *TrβA* promoter autoinduction. Luciferase activity in pCMV-xKLF9 transfected cells was significantly greater than empty vector controls at 2 hr and 6 hr of T_3 treatment ($P<0.0001$ for both; unpaired t-test; Fig. 6A).

We also used XTC-2 cells to determine if forced expression of KLF9 could alter the autoinduction of the endogenous *TrβA* gene. Treatment with T_3 caused a time-dependent increase in endogenous *TrβA* mRNA in cells transfected with empty vector (pCS2; ANOVA: $F=86.02$, $P<0.0001$) and pCS2-xKLF9 (ANOVA: $F=215.2$, $P<0.0001$; Fig. 6B). At all time points measured, *TrβA* mRNA was significantly greater in pCS2-xKLF9 transfected cells compared with empty vector controls ($P<0.05$ for 0h; $P<0.01$ for 2, 4, and 6h; unpaired t-test). Furthermore, the increase in *TrβA* mRNA caused by forced KLF9 expression occurred in a dose dependent manner, with 0.3 μg and 1 μg of pCS2-xKLF9 plasmid increasing *TrβA* mRNA 1.2 and 1.4 fold, respectively, over empty vector controls (data not shown).

KLF9 transactivation domain is required for *TrβA* autoinduction.

Two N-terminal transactivation domains in rodent KLF9 that were identified by mutagenesis are highly conserved with the frog proteins (Kobayashi, Sogawa et al. 1995; Hoopfer, Huang et al. 2002). We constructed truncated xKLF9 mutants in which one or both of these transactivation domains were removed to determine if they are necessary for the action of KLF9 on *TrβA* autoinduction in XTC-2 cells. Removal of transactivation domain A (pCS2-xKLF9Δ30) or both domains A and B (pCS2-

xKLF9Δ99 or pCS2-xBTEB1Δ120) abolished the activity of KLF9 on *TrβA* autoinduction (compare to cells transfected with pCS2-xKLF9; Fig. 7A; P<0.001). Deletion of only transactivation domain A (pCS2-xKLF9Δ30) resulted in apparent dominant negative activity, for it also reduced the T_3-induced *TrβA* mRNA as compared with the empty vector control (P<0.001; Fig 7A).

DNA binding capacity of KLF9 is not required for *TrβA* autoinduction.

We introduced point mutations into the zinc fingers of KLF9 to disrupt its DNA binding capacity. Histidine to alanine substitutions of the first histidine residue in each of the three Cys_2His_2 zinc fingers were generated by site-directed mutagenesis. The histidine to alanine substitution was previously shown to eliminate the DNA binding capacity of KLF1 (Pandya and Townes 2002) and another zinc finger protein JAZ (Yang, May et al. 1999). The mutant KLF9 (pCS2-xKLF9 C_2AH) retained full activity on *TrβA* autoinduction compared with wildtype KLF9 (Fig 7B). The loss of DNA binding capacity in the KLF9 C_2AH mutant was confirmed by EMSA (Fig. 7C). Similar amounts of wildtype KLF9 and KLF9 C_2AH mutant were used in the EMSA as verified by Western blotting (data not shown).

Discussion

Thyroid hormone initiates programs of gene expression in diverse tadpole tissues that underlie the dramatic transformation that occurs during amphibian metamorphosis (Shi 2000). Several of the early T_3 response genes that were identified through gene expression screens code for transcription factors (Buckbinder and Brown 1992; Kanamori

and Brown 1993; Shi and Brown 1993; Brown, Wang et al. 1996; Denver, Pavgi et al. 1997; Das, Cai et al. 2006). These proteins are hypothesized to regulate a secondary response program of genes necessary for adult phenotypic expression (Brown, Wang et al. 1995). The transcription factor KLF9, whose hormone-dependent expression depends on one or more TREs located upstream of the transcription start site, is the earliest responding gene thus far identified in the tadpole (Wang and Brown 1993; Denver, Pavgi et al. 1997; Furlow and Kanamori 2002; Hoopfer, Huang et al. 2002). The *TrβA* gene is strongly upregulated by T_3, which requires direct binding of the T_3-TR complex to the *TrβA* promoter (a phenomenon referred to as autoinduction; (Machuca, Esslemont et al. 1995). Here we show that KLF9 associates with the promoter region of the *TrβA* gene and can enhance T_3–dependent transcription. Our findings support the hypothesis that the early upregulation of KLF9 during tadpole metamorphosis plays a role in the autoinduction of *Trβ* genes, which is hypothesized to be essential for metamorphosis (Brown, Wang et al. 1995). Therefore, the protein products of two primary response genes regulate each other's promoter. Crossregulation among primary response transcription factors is likely to be an important means for developmental gene regulation causing robust gene expression responses necessary for driving tissue morphogenesis.

The autoinduction of *Trβ* genes was originally thought to be the earliest molecular response to T_3 in tadpole tissues (Yaoita and Brown 1990; Tata 2000). Previous studies that relied on Northern blotting suggested that the upregulation of *TrβA* and *Klf9* mRNAs by T_3 was, by and large, coordinate (Furlow and Brown 1999; Furlow and Kanamori 2002). However, several lines of evidence support the view that the *Klf9* genes are the most rapidly responding genes yet identified in tadpole tissues (Wang and Brown 1993;

Furlow and Kanamori 2002). Using RT-PCR we clearly show that KLF9 is induced by T_3 with faster kinetics than TRβ, both in the tadpole *in vivo* and in the *X. laevis* fibroblast-derived cell line XTC-2. We found detectable accumulation, and maximal induction of KLF9 transcripts several hours earlier than TRβ (the precise timing depends on whether tissues or cultured cells are analyzed; see also (Hoopfer, Huang et al. 2002; Krain and Denver 2004). Also, KLF9 protein is upregulated during spontaneous metamorphosis or by exogenous T_3 in tadpoles (see Fig. 1B; (Hoopfer, Huang et al. 2002), and KLF9 and TRβ are expressed in the same cells (Hoopfer, Huang et al. 2002). These findings are consistent with the hypothesis that KLF9 is present within the cell, either commensurate with or prior to the upregulation of TRβ, and could thus influence transcription of the *TrβA* gene.

The presence of GC-rich sequences in the proximal *TrβA* promoter (commonly referred to as Sp1 sites; (Ranjan, Wong et al. 1994)), and the early and robust T_3 response kinetics of KLF9 led us to hypothesize that this protein binds to and regulates the *TrβA* gene. We used EMSA to test whether regions of the proximal *TrβA* promoter possess binding sites for KLF9. We found that KLF9 could directly bind to the GC boxes located in the *TrβA* promoter. However, while the binding of protein to DNA in an EMSA is suggestive of the presence of a transcription factor binding site, it does not determine whether the DNA binding protein actually associates with the gene of interest *in vivo*. To test this for KLF9 and *TrβA,* we used ChIP assay, that depended on a specific, affinity purified antiserum directed against the unique N-terminal region of the frog KLF9 protein. Our ChIP experiments clearly show that KLF9 associates with the proximal *TrβA* promoter *in vivo* in a hormone and developmental stage-dependent manner. Earlier,

we showed that KLF9 protein is strongly induced by T_3 in tadpole brain *in vivo* and is highly expressed during metamorphic climax (compared with premetamorphosis; (Hoopfer, Huang et al. 2002). The enhanced association of KLF9 with the *TrβA* promoter with T_3 treatment and at metamorphic climax could be due to the increased expression of KLF9 and/or an active T_3-dependent recruitment of KLF9 to the promoter.

Similar to our findings in the tadpole *in vivo* we found that *Klf9* and *TrβA* mRNAs are upregulated in XTC-2 cells, and that *Klf9* exhibits faster kinetics than *TrβA*. We also found that KLF9 associates with the proximal *TrβA* promoter in XTC-2 cells by ChIP assay, and that the degree of association was higher at an upstream region (region A/B with multiple GC boxes) vs. a region in the 5' UTR (region G with one GC box; and vs. the *TrβA* exon 5 where there are no identifiable GC boxes; see Fig. 5B). Furthermore, association of KLF9 with region A/B in XTC-2 cells was T_3-dependent.

Given that KLF9 and TRs are expressed in the same cells (Hoopfer, Huang et al. 2002) and KLF9 associates with the proximal *TrβA* promoter *in vitro* and *in vivo*, and frog KLF9 possesses transactivation function (Hoopfer, Huang et al. 2002), we hypothesized that KLF9 positively regulates the *TrβA* gene. In support of this hypothesis we found that induced expression of KLF9 in XTC-2 cells resulted in faster kinetics and greater absolute magnitude of induction by T_3 of the *TrβA* gene, as determined by promoter-reporter transfection assay and by analysis of the endogenous mRNA expression.

By contrast to the full-length KLF9, forced expression of N-terminal truncated mutants of KLF9 in which one or both transactivation domains were removed eliminated activity on *TrβA* autoinduction. Kobayashi et al. (Kobayashi, Sogawa et al. 1995)

identified two transactivation domains in rat KLF9 by mutagenesis. Earlier we showed that frog KLF9 has transactivation activity, and the identified transactivation domains are very similar among the frog and rodent proteins, suggesting conserved functions ((Hoopfer, Huang et al. 2002). Our present findings point to an essential role for these regions of KLF9 for activity on *TrβA* autoinduction.

Up to this point our results were consistent with KLF9 binding to GC rich regions of the frog *TrβA* gene leading to enhanced autoinduction. We were therefore surprised to discover that this DNA binding capacity was dispensable for KLF9 action. Subsitution of alanines for each of the zinc-chelating histidine residues in the three zinc fingers of KLF9 destroyed DNA binding but did not alter activity of the protein on *TrβA.* Thus, while KLF9 associates with chromatin at the *TrβA* promoter *in vivo*, binding to DNA is not required for it to enhance *TrβA* autoinduction, suggesting that KLF9 functions in this regard through protein-protein interaction. The GC boxes present in the *TrβA* promoter could facilitate the targeting of the protein to this genomic region.

Members of the KLF and Sp factor families have been found to synergize with nuclear hormone receptors through protein-protein interactions. For example, Sp1 interacts with the estrogen receptor to regulate several promoters (Porter, Saville et al. 1997; Duan, Porter et al. 1998; Sun, Porter et al. 1998). KLF9 was shown to interact with progesterone receptor (PR) in the regulation of PR target genes in endometrial epithelial cells (Zhang, Zhang et al. 2002). However, in a preliminary study we found no direct interaction between KLF9 and TRs using co-immunoprecipitation assays (K.L. Howdeshell and R.J. Denver, unpublished data.) To our knowledge, other than the PR, KLF9 interactions with nuclear proteins have not been studied. KLF9 is a member of a

family of proteins (KLF/Sp 1-like) that bind to GC or GT rich regions in gene promoters (Kaczynski, Cook et al. 2003). It is possible that other KLFs or Sp-like factors regulate the *TrβA* promoter, and this deserves further study. However, it is noteworthy that KLF9 is the only KLF identified in several gene expression screens of tadpole tissues that is strongly upregulated by T_3 during metamorphosis (Wang and Brown 1991; Buckbinder and Brown 1992; Kanamori and Brown 1993; Shi and Brown 1993; Brown, Wang et al. 1996; Denver, Pavgi et al. 1997; Veldhoen, Crump et al. 2002; Helbing, Werry et al. 2003; Das, Cai et al. 2006). Also, to our knowledge, KLF9 is the only KLF/Sp 1-like family member found to be regulated by T_3 in mammalian cells (Denver, Ouellet et al. 1999). Thus, if other KLFs participate in *Trβ* gene regulation they would likely do so as basal, or constitutive factors. We propose here that the strong upregulation of KLF9 by T_3 is critical to the role that KLF9 plays in regulating the *TrβA* promoter *in vivo*.

In conclusion, our results support the hypothesis that the protein product of the immediate early gene *Klf9* associates with the *TrβA* genomic region *in vivo*, and can enhance autoinduction; i.e., it forms a positive regulatory loop. The surge in plasma T_3 that occurs during metamorphic climax in the tadpole is accompanied by a dramatic autoinduction of *Trβ* genes (Shi, Yaoita et al. 1992). The autoinduction of *Trβ* genes is thought to be essential for metamorphosis, especially for later developmental events such as cell differentiation and programmed cell death (e.g., tail resorption; (Tata 2000). Thus, to achieve maximal TR expression to initiate tissue transformation may require that TRs bind to and activate the *Trβ* promoters (Machuca, Esslemont et al. 1995), and induce the expression of KLF9 which cooperates with TRs in the autoinduction of their genes. Such

cooperativity among the protein products of immediate early genes may be a common phenomenon in animal development.

Table 5.1. Oligonucleotides used for semi-quantitative and quantitative real time RT-PCR.

Semi-quantitative RT-PCR:

Klf9:

Forward	5'-CGTGGCAAAGTTTATGGG-3'
Reverse	5'-GGATGGAAGTCGGTATGG-3'

TaqMan assays:

Trβ A:

Forward	5’-GGAAGCCACTGGAAACAGAAAA-3’
Reverse	5’-CATTAACTATGGGAGCTTGTCCAA-3’
Probe	FAM-AAAATTTTTGCCAGAGGAC-MGBNFQ

Klf9b:

Forward	5’-CCAGTCAGGTCAACCAATGAAA-3’
Reverse	5’-AAACTTTGCCACACCCAGTGT-3’
Probe	FAM-AGG CAC AGG TGT CC-MGBNFQ

rpL8:

Forward	5’-TTTGCTGAAAGAAATGGCTACATC-3’
Reverse	5’-CAC GGC CTG GAT CAT GGA-3’
Probe	VIC-AGG GTA TTG TGA AAG ACA-MGBNFQ

Oligonucleotide primers for semi-quantitative RT-PCR and TaqMan assays were designed to span exon/intron boundaries. The primers for semi-quantitative RT-PCR amplified mRNAs derived from both *Klf9A* and *Klf9B* genes.

Table 5.2. Oligonucleotide primers used to generate truncated mutants and point mutations in the three zinc fingers of *X. laevis* KLF9.

Primers used to generate N-terminal truncated xKLF9 mutants:

Δ30 xKLF9 For	5'-ATAGGATCCGCCGCCATGGAAGTGGAGCAGCCC-3'
Δ99 xKLF9 For	5'-ATAGGATCCGCCGCCATGGAGTTAAACAAGTACC-3'
Δ120 xKLF9 For	5'-ATAGGATCCGCCGCCATGGACAGCGATGTCACCA-3'
xKLF9 Rev	5'-ATACTCGAGTCAGGTGAATGATGAATTGGAC-3'

Primers used to generate point mutations in the three zinc finger domains of xKLF9:

xKLF9 H211A	5'-GTCTTCCCATCTCAAAGCCGCTTACAGAGTCCATACAGGT-3'
xKLF9 H241A	5'-CCGATGAGTTAACTCGCGCCTACAGAACCCACACAG-3'
xKLF9 H269A	5'-TGAGAAGCGATCACTTGACCAAAGCTGCACGTCGCCA-3'

The Δ indicates deletion of the first 30-120 amino acids. Primers used for point mutations generated a histidine → alanine substitution in each of the three zinc fingers.

Table 5.3. Oligonucleotide primers used for the analysis of the *X. laevis* *Trβ*A promoter.

*Trβ*A promoter region	
-1138/-823 (A)	5'-CAG TGG AGT AAC TAC CAG-3'
	5'-GTA CAC ATG CCT GCA CTA-3'
-841/-604 (B)	5'-TAG TGC AGG CAT GTG TAC-3'
	5'-GAG CAG GTG CAG CAT CTA-3'
-622/-414 (C)	5'-TAG ATG CTG CAC CTG CTC-3'
	5'-ACT ATG GCA TGT TAC AGC-3'
-432/-266 (D)	5'-GCT GTA ACA TGC CAT AGT-3'
	5'-GCC TGA GTG AAG ACC CAT-3'
-283/-92 (E)	5'-ATG GGT CTT CAC TCA GGC-3'
	5'-GTC ATG AAA CTC CTC GGT-3'
-109/+182 (F)	5'-ACC GAG GAG TTT CAT GAC-3'
	5'-TAT AGA CAC AGG CAG CTT A-3'
+164/+366 (G)	5'-TAA GCT GCC TGT GTC TAT A-3'
	5'-TGA CAG TCA GAG GAA CTG A-3'
exon 3/exon 4	5'-CAG AAA CCT GAA CCC ACA CAA-3'
	5'-CAC TTT TCC ACC CTC GGG CGC ATT-3'
qPCR -885/-752	5'-TTG TGC CTG CTT GCT TGC TA-3'
	5'-ACT ATA ATA GGC GGG CCA AGC TGA-3'
qPCR +165/+322	5'-AGC TGC CTG TGT CTA TAC TGA TGG-3'
	5'-ACA GGG AGA TCT ACA GCT GAT CGT-3'
qPCR exon 5	5'-CCC CGA AAG TGA AAC TCT AAC GT-3'
	5'-AAA CCA CTC CAA GTC CTC CAT TTT-3'
Ef1α promoter	5'-TGC ACA GTT GGC GCA GTG-3'
	5'-TGA GGA AGA GAG CGA ACC-3'
Ifabp promoter	5'-ATA GCA GCA GGT GGT TGC G-3'
	5'-GGC CAC AAG ATC TAC TCG-3'

For each pair of oligonucleotides the top sequence is the forward primer, the bottom sequence is the reverse primer. Capital letters in parentheses correspond to promoter regions given in Figure 2 and Supplemental Table 1.
qPCR – indicates primer sets that were used for quantitative real-time PCR using SYBR green. All other primer sets were used for standard PCR with radiolabeled precursor.

Table 5.4. Short oligonucleotides corresponding to GC-rich regions (bold, underlined) of the *X. laevis Trβ*A promoter used as probes and competitors in EMSA.

GC box number*	Region of *Trβ*A promoter	Oligonucleotide sequence
1,2	-1032/-1013	5'gatcGGG**GGCGGG**GGG**CCCGCC**CT3' 3'-CCCCGCCCCCCGGGCGGGActag-5'
3	-978/-957	5'-gatcAGATA**GGCGGG**GGGGTGGTG-3 3'-TCTATCCGCCCCCCCACCACctag-5'
4	-770/-751	5'-gatcTGG**CCCGCC**TATTATAGTTT-3' 3'-ACCGGGCGGATAATATCAAActag-5'
5	-723/-704	5'-gatcTCT**GGCGGG**GCCCTGTTATC-3' 3'-AGACCGCCCCGGGACAATAGctag-5'
6	-545/-526	5'-gatcGGATGCG**GGCGGG**CGCGGGC-3' 3'-CCTACGCCCGCCCGCGCCCGctag-5'
7	+228/+247	5'-gatcCTC**CCCGCC**CCCCCTATCCT-3' 3'-GAGGGGCGGGGGGGATAGGActag-5'

* Numbering based on position within the *Trβ*A gene as depicted in Figure 2.
For each pair of oligonucleotides the top sequence is the forward primer, the bottom sequence is the reverse primer.

Figures

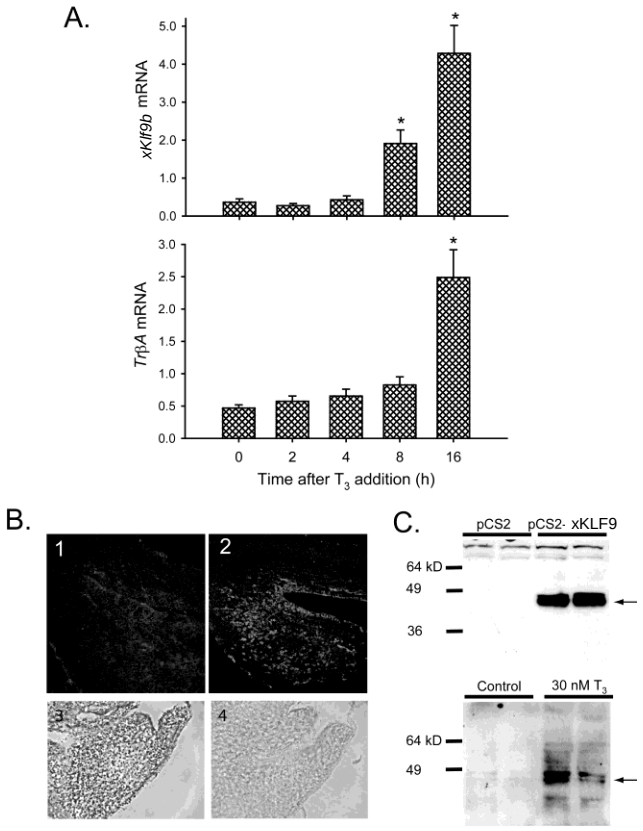

Fig 5.1. Thyroid hormone upregulates *Klf9* mRNA in tadpole brain with faster kinetics than *TrβA* mRNA. Increased *Klf9* mRNA correlates with elevated KLF9 protein. **(A)** Upregulation of *Klf9* (top) and *TrβA* (bottom) mRNAs in premetamorphic *X. laevis* tadpole brain (NF Stage 52) following exposure to T_3 (10 nM) added to the aquarium water (n=4/time point). Gene expression was analyzed by RTqPCR. Asterisks designate significant differences from the zero time point ($P<0.0001$; Scheffe's test). **(B)** Treatment with T_3 increases KLF9 protein expression in *X. laevis* tadpole brain. Panel 1: KLF9 protein is expressed at a very low level in NF stage 52 tadpole brain (optic tectum shown) but is increased dramatically by T_3 treatment (panel 2; 10 nM in aquarium water for 24 h). Panel 3: Representative saggital brain section (hypothalamic region) from a NF stage 52 tadpole treated with T_3 in the aquarium water (10 nM; 24 h). Strong KLF9 staining was restricted to cell nuclei. Panel 4: Immunostaining for KLF9 was eliminated by preabsorption with GST-xKLF9. KLF9 immunoreactivity was detected by Cy3 immunofluorescence (panels 1, 2) or by horseradish peroxidase staining (panels 3, 4). **(C)** Western blot analysis of xKLF9 in protein extracts from pCS2 or pCS2-xKLF9 transfected XTC-2 cells (upper panel); endogenous KLF9 in protein extracts of XTC-2 cells treated with or without T_3 (30 nM) for 24h (lower panel). This dose of T_3 causes a maximal response in *TrβA* and *Klf9* mRNA (data not shown). Immunoblotting was conducted using affinity purified IgG that recognizes the N-terminal region of xKLF9 (see Materials and Methods). Arrows point to the two KLF9 bands.

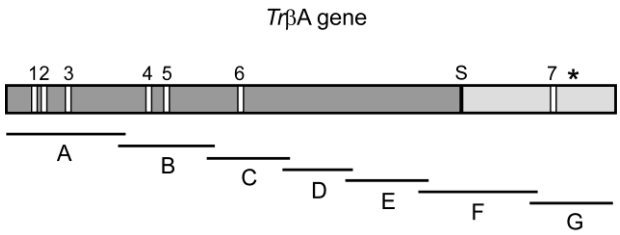

Fig 5.2. Schematic representation of the *X. laevis TrβA* gene with locations of GC boxes and regions analyzed by EMSA and ChIP assay. The bars with letters underneath indicate the general regions of the *TrβA* gene targeted for analysis by EMSA and in the ChIP assay, and correspond to the specific sequences given in Supplemental Table 1. The numbering of the seven GC boxes corresponds to that given in Table 4. The dark grey filled box represents the upstream region, the 'S' indicates the transcription start site, the light grey filled box represents the 5' UTR, and the asterisk indicates a TRE that has been characterized and proposed to mediate T_3-dependent transactivation (Ranjan, Wong et al. 1994; Wong, Liang et al. 1998).

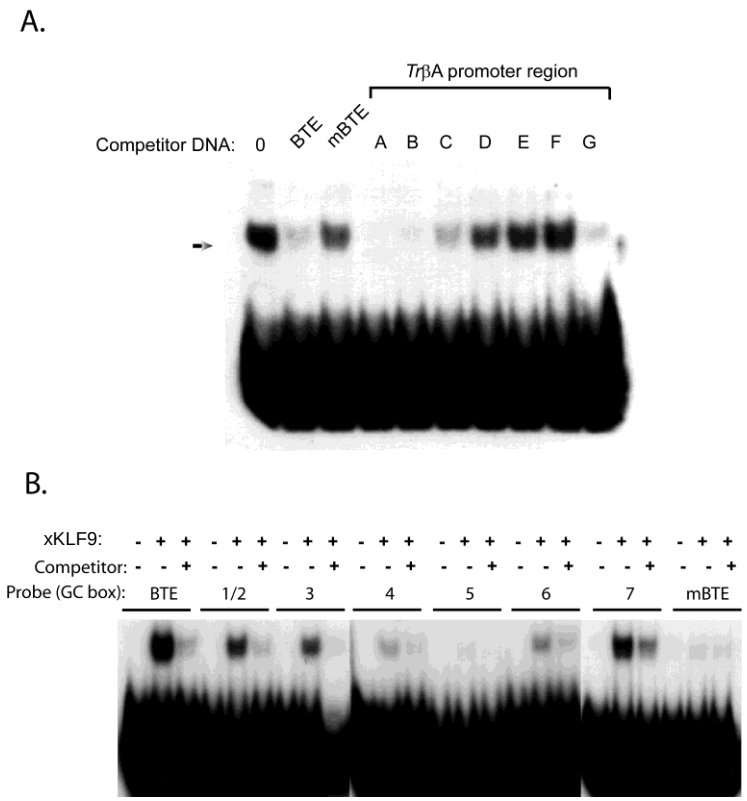

Fig 5.3. (A) Binding of GST-xKLF9[DBD] to regions of the proximal *X. laevis TrβA* promoter *in vitro*. We used electrophoretic mobility shift assay (EMSA) to test the ability of radioinert DNA fragments (1.89 μM/reaction) corresponding to different regions of the proximal *TrβA* promoter (generated by PCR; see Fig. 2 and Supplemental Table 1) to displace GST-xKLF9[DBD] binding to the [^{32}P]-BTE probe. BTE – basic transcription element; mBTE – mutated BTE. **(B)** Binding of GST-xKLF9[DBD] to GC-rich regions of the proximal *TrβA* promoter. We used EMSA to test whether GST-xKLF9[DBD] could bind to short, [^{32}P]-labeled oligonucleotides encompassing one or two GC boxes in the *TrβA* promoter. The numbering of the GC boxes included in each oligonucleotide probe is based on that given in Fig. 2 and Table 4. In each case homologous, radioinert competitors (1.89 μM) were used to displace binding. BTE – basic transcription element; mBTE – mutated BTE.

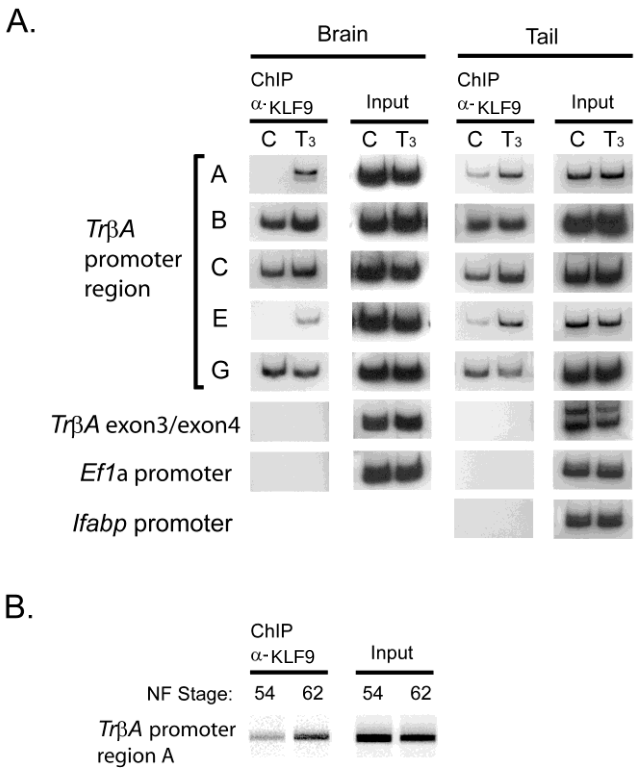

Fig 5.4. KLF9associates with the proximal *TrβA* promoter *in vivo* in a T_3 and developmental stage-dependent manner. ChIP assay was conducted using an affinity purified IgG directed against the N-terminal region of *X. laevis* KLF9. **(A)** T_3-dependent association of KLF9 with the proximal *TrβA* promoter in tadpole brain and tail. Premetamorphic (NF stage 52) *X. laevis* tadpoles were treated with 10 nM T_3 added to the aquarium water for 48 hours prior to tissue collection for ChIP assay (see Materials and Methods). The lettered *TrβA* promoter regions analyzed correspond to those given in Fig. 2 and Supplemental Table 1. The *TrβA* exon 1/exon 2, and the *Efα1* and *Ifabp* promoters were used as negative controls. **(B)** Developmental stage-dependent association of KLF9 with the proximal *TrβA* promoter in early prometamorphic (NF stage 54) and climax stage (NF stage 62) *X. laevis* tadpole brain. Only region A of *TrβA* promoter, which showed robust T_3-dependent association of KLF9 was targeted for ChIP analysis in this experiment. Each of the ChIP experiments was repeated three times with similar results.

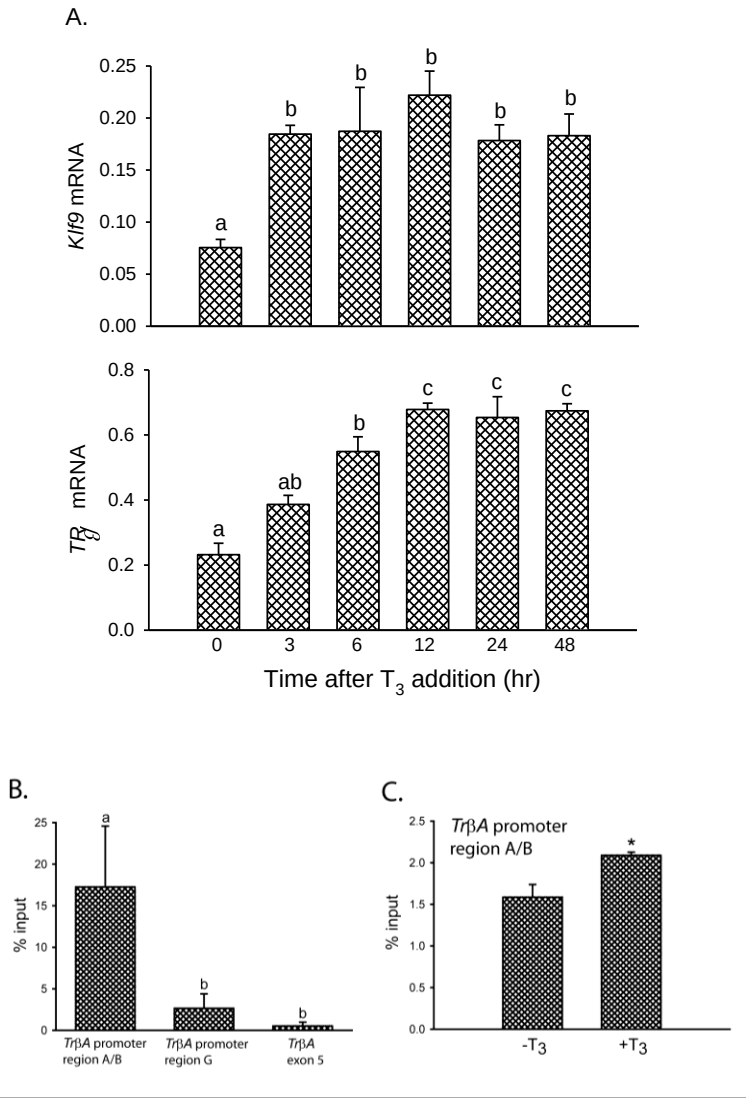

Fig 5.5. *Klf9* and *TrβA* mRNAs are upregulated by T_3, and KLF9 associates with the proximal *TrβA* promoter in XTC-2 cells. (A) T_3 upregulates *Klf9* mRNA in XTC-2 cells with faster kinetics than TRβ. XTC-2 cells were treated with T_3 (5 nM) for various times before harvest for RNA isolation and semi-quantitative RT-PCR analysis of *Klf9* and *TrβA* mRNA expression. Gene expression was normalized to the level of *rpL8* expression (a housekeeping gene). *Klf9* mRNA was maximally induced at 3 hr (P=0.009; Scheffe's test) and maintained through 48 hr of treatment. *TrβA* mRNA was significantly induced at 6 hr (P=0.001), reached a maximum by 12 hr and was maintained through 48 hr. Bars represent the mean + SEM (n=6 wells/time point) and letters above the means indicate significant differences among time points (i.e., means with the same letter are not significantly different; P<0.05; Scheffe's test). **(B)** KLF9 associates with the proximal *TrβA* promoter in XTC-2 cells. XTC-2 cells were treated with T_3 (5 nM) for 24h, and we used ChIP assay coupled with quantitative real time PCR to detect BTEB1 association with the *TrβA* gene. We found significantly greater association of KLF9 at an upstream region of the promoter (overlapping with regions A and B shown in Fig. 2; -885 to -752) which contains multiple GC boxes compared with a region in the 5' UTR (region G; +166 to +322) that has only one GC box, or the exon 5 of the *TrβA* gene which has no GC boxes. Letters indicate significant differences among gene regions (i.e., means with the same letter are not significantly different; P<0.05; Scheffe's test). **(C)** Treatment of XTC-2 cells with T_3 (5 nM, 24 h) increases KLF9 association with the upstream TRβA promoter (region A/B) as analyzed by ChIP assay (* P=0.043; t-test).

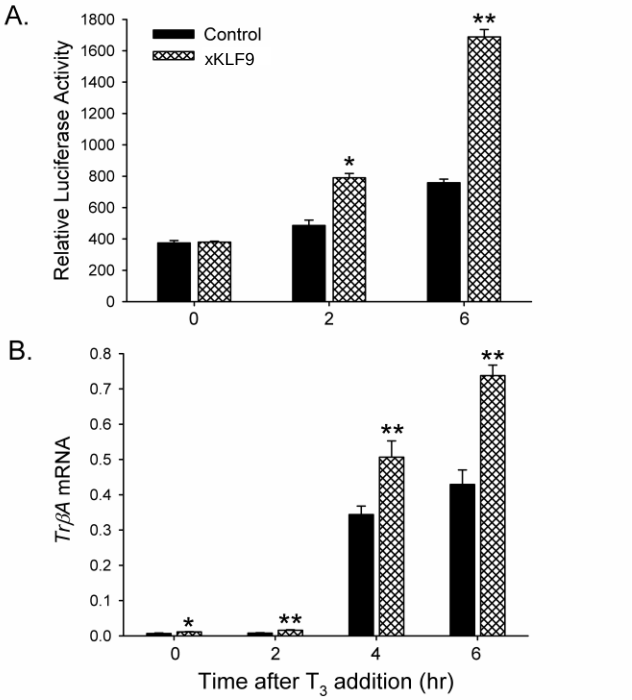

Fig 5.6. Expression of KLF9 enhances *TrβA* autoinduction in XTC-2 cells. (A) Forced expression of KLF9 accelerates and enhances autoinduction of the *TrβA* promoter. XTC-2 cells were cotransfected with the *X. laevis TrβA* promoter-luciferase plasmid, pCMV-xKLF9 and pRenilla (to normalize for transfection efficiency using a dual reporter luciferase assay; see Experimental Procedures). Cells were treated with 5 nM T_3 for 0, 2 or 6 h before harvest. Bars represent the mean + SEM. The data shown are the means + SEM from one transfection experiment (n=4/treatment group) and the experiment was repeated three times with similar results. The T_3-dependent activation of the *TrβA* promoter was not altered by transfection with empty vector (pCMVneo; data not shown.) Asterisks denote significant differences from empty vector controls (* $P<0.01$; ** $P<0.001$; Student's unpaired t-test). **(B)** Forced expression of KLF9 increases the expression of endogenous *TrβA* mRNA. XTC-2 cells were cotransfected with 1 μg pCS2-xKLF9 or pCS2 empty vector plus pRenilla. Forty eight hr after transfection the cells were treated with 5 nM T_3 for 0, 2, 4, or 6h before harvest. Gene expression analysis was done by RTqPCR. Data shown are the means + SEM from one transfection experiment (n=6/treatment) and the experiment was repeated four times with similar results. Asterisks denote significant differences from empty vector controls (*$P<0.05$; **$P<0.001$; unpaired t-test).

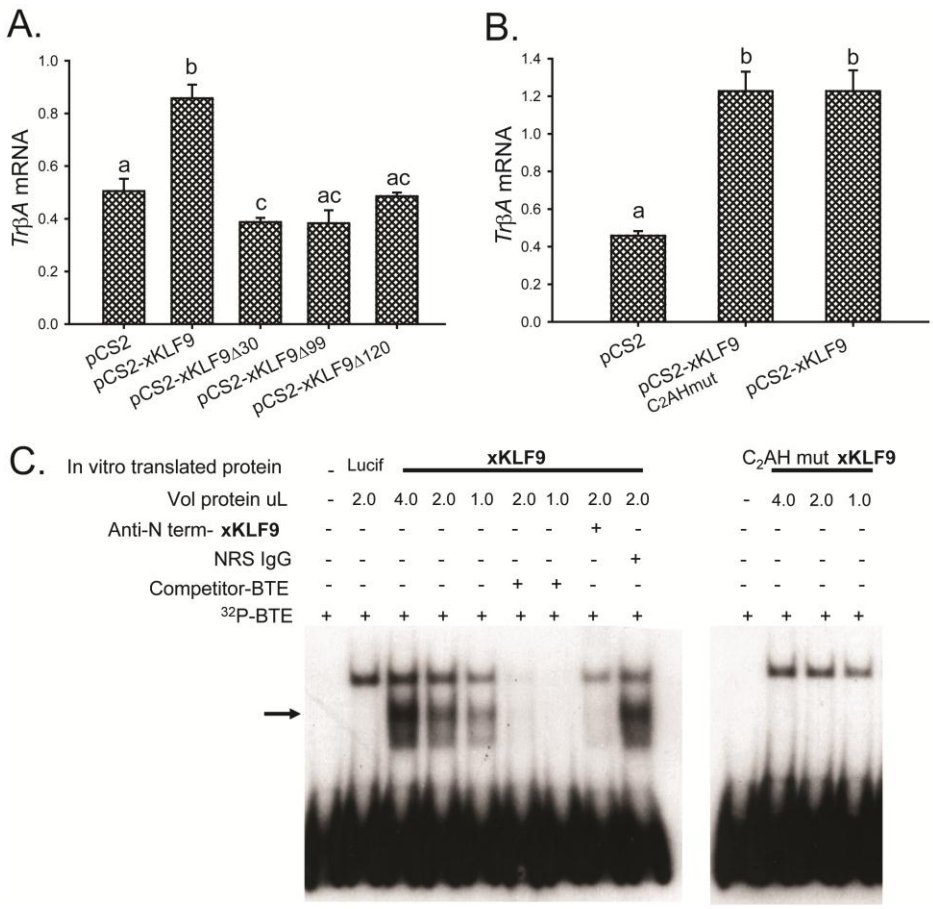

Fig. 5.7. The N-terminal transactivation domains, but not the DNA binding capacity of the zinc fingers of KLF9 are required for *TrβA* autoinduction. (A) N-terminal truncated forms of xKLF9 fail to enhance *TrβA* autoinduction in XTC-2 cells. XTC-2 cells were transfected with the indicated expression vectors and 48 hr later cells were treated with 5 nM T_3 for 6h. Gene expression analysis was done by RTqPCR. Data shown are the means + SEM for the T_3 –treated cells only; n=6/treatment. Letters indicate significant differences among treatments (i.e., means with the same letter are not significantly different; $P<0.05$; Bonferroni's multiple comparison test). **(B)** Mutations in the three zinc fingers of KLF9 do not affect activity on *TrβA* autoinduction. The first histidine residue in each of the Cys_2His_2 zinc finger DNA binding domain of KLF9 was mutated to alanine to generate pCS2-xKLF9 C_2AH. XTC-2 cells were transfected with the indicated expression vectors and 48h later cells were treated with 5 nM T_3 for 6h. Data shown are the means + SEM from one transfection experiment (n=6/treatment) and the experiment was repeated twice with similar results. Letters indicate significant differences among treatments (i.e., means with the same letter are not significantly different; $P<0.05$; Bonferroni's multiple comparison test). **(C)** Electrophoretic mobility shift assay showed that the KLF9 C_2AH mutant does not bind to DNA. Recombinant wildtype KLF9 and KLF9 C_2AH mutant proteins were generated by coupled in vitro transcription/translation and varying amounts were tested for their ability to bind to the [^{32}P]-BTE probe *in vitro*. Radioinert BTE oligonucleotide was added to some reactions as a competitor, and antibody supershift was used to verify the presence of KLF9 protein in the protein-DNA complexes formed. Western blot analysis confirmed that equal amounts of wildtype and mutant KLF9 proteins were used in the EMSA (data not shown).

References

Brown, D. D., Z. Wang, et al. (1996). "The thyroid hormone-induced tail resorption program during Xenopus laevis metamorphosis." Proceedings of the National Academy of Sciences of the United States of America **93**(5): 1924-1929.

Brown, D. D., Z. Wang, et al. (1995). "Amphibian metamorphosis: a complex program of gene expression changes controlled by the thyroid hormone." Recent Progress in Hormone Research **50**: 309-315.

Buckbinder, L. and D. D. Brown (1992). "Thyroid hormone-induced gene expression changes in the developing frog limb." J. Biol. Chem. **262**: 11221-11227.

Cayrou, C., R. J. Denver, et al. (2002). "Suppression of the basic transcription element-binding protein in brain neuronal cultures inhibits thyroid hormone-induced neurite branching." Endocrinology **143**(6): 2242-2249.

Chen, A. and B. H. Davis (2000). "The DNA binding protein BTEB mediates acetaldehyde-induced, Jun N-terminal kinase-depedent αI(I) collagen gene expression in rat hepatic stellate cells." Molecular and Cellular Biology **20**(8): 2818-2826.

Dang, D. T., Pevsner, J. and Yang, V.W. (2000). "The biology of the mammalian Kruppel-like family of transcription factors." International Journal of Biochemistry and Cell Biology **32**: 1103-1121.

Das, B., L. Q. Cai, et al. (2006). "Gene expression changes at metamorphosis induced by thyroid hormone in Xenopus laevis tadpoles." Developmental Biology **291**(2): 342-355.

Denver, R. J., L. Ouellet, et al. (1999). "Basic transcription element-binding protein (BTEB) is a thyroid hormone-regulated gene in the developing central nervous system - Evidence for a role in neurite outgrowth." Journal of Biological Chemistry **274**(33): 23128-23134.

Denver, R. J., S. Pavgi, et al. (1997). "Thyroid hormone-dependent gene expression program for Xenopus neural development." Journal of Biological Chemistry **272**: 8179-8188.

Duan, R., W. Porter, et al. (1998). "Estrogen-induced c-fos protooncogene expression in MCF-7 human breast cancer cells: Role of estrogen receptor Sp1 complex formation." Endocrinology **139**(4): 1981-1990.

Foti, D., D. Stroup, et al. (1998). "Basic transcription element binding protein (BTEB) transactivates the cholesterol 7α-hydroxylase gene (CYP7A)." Biochemical and biophysical research communications **253**: 109-113.

Furlow, J. D. and D. D. Brown (1999). "In vitro and in vivo analysis of the regulation of a transcription factor gene by thyroid hormone during Xenopus laevis metamorphosis." Molecular Endocrinology **13**(12): 2076-2089.

Furlow, J. D. and A. Kanamori (2002). "The transcription factor basic transcription element-binding protein 1 is a direct thyroid hormone response gene in the frog Xenopus laevis." Endocrinology **143**(9): 3295-3305.

Helbing, C. C., K. Werry, et al. (2003). "Expression profiles of novel thyroid hormone-responsive genes and proteins in the tail of Xenopus laevis tadpoles undergoing precocious metamorphosis." Molecular Endocrinology **17**(7): 1395-1409.

Hoopfer, E. D., L. Y. Huang, et al. (2002). "Basic transcription element binding protein is a thyroid hormone-regulated transcription factor expressed during metamorphosis in Xenopus laevis." Development Growth & Differentiation **44**(5): 365-381.

Hsiang, C. H. and D. S. Straus (2002). "Cyclopentenone causes cell cycle arrest and represses cyclin D1 promoter activity in MCF-7 breast cancer cells." Oncogene **21**(14): 2212-2226.

Imataka, H., A. Mizuno, et al. (1993). "Activation of the human immunodeficiency virus type 1 long terminal repeat by BTEB, a GC box-binding transcription factor." AIDS Research in Human Retroviruses **9**(9): 825-831.

Imataka, H., K. Sogawa, et al. (1992). "Two regulatory proteins that bind to the basic transcription element (BTE), a GC box sequence in the promoter of the rat P-4501A1 gene." EMBO Journal **11**(10): 3663-3671.

Imhof, A., M. Schuierer, et al. (1999). "Transcriptional regulation of the AP-2 alpha promoter by BTEB-1 and AP-2rep, a novel wt-1/egr-related zinc finger repressor." Molecular And Cellular Biology **19**(1): 194-204.

Kaczynski, J., A. Conley, et al. (2002). "Functional analysis of basic transcription element (BTE)-binding protein (BTEB) 3 and BTEB4, a novel Sp1-like protein, reveals a subfamily of transcriptional repressors for the BTE site of the cytochrome P4501A1 gene promoter." Biochem. J. **366**: 873-882.

Kaczynski, J., T. Cook, et al. (2003). "Sp1-and Kruppel-like transcription factors." Genome Biology **4**(2): 209.

Kanamori, A. and D. D. Brown (1993). "Cultured cells as a model for amphibian metamorphosis." Proceedings of the National Academy of Sciences of the United States of America **90**(13): 6013-6017.

Kobayashi, A., K. Sogawa, et al. (1995). "Analysis of functional domains of a GC box binding protein, BTEB." Journal of Biochemistry **117**(1): 91-95.

Krain, L. P. and R. J. Denver (2004). "Developmental expression and hormonal regulation of glucocorticoid and thyroid hormone receptors during metamorphosis in Xenopus laevis." Journal of Endocrinology **181**(1): 91-104.

Machuca, I., G. Esslemont, et al. (1995). "Analysis of structure and expression of *Xenopus* thyroid hormone receptor-β gene to explain its autoinduction." Mol Endo **9**(1): 96-107.

Manzon, R. G. and R. J. Denver (2004). "Regulation of pituitary thyrotropin gene expression during Xenopus metamorphosis: negative feedback is functional throughout metamorphosis." Journal of Endocrinology **182**(2): 273-285.

Martin, K. M., W. N. Cooper, et al. (2000). "Mouse BTEB3, a new member of the basic transcription element binding protein (BTEB) family, activates expression from GC- rich minimal promoter regions." Biochemical Journal **345**: 529-533.

Meunier-Durmort, C., H. Grimal, et al. (1997). "Adenovirus enhancement of polyethylenimine-mediated transfer of regulated genes in differentiated cells." Gene Therapy **4**(8): 808-814.

Morita, M., A. Kobayashi, et al. (2003). "Functional analysis of basic transcription element binding protein by gene targeting technology." Molecular and Cellular Biology **23**(7): 2489-2500.

Nieuwkoop, P. D. and J. Faber (1956). Normal Table of *Xenopus laevis* Daudin. Amsterdam, North Holland Publishers.

Pandya, K. and T. M. Townes (2002). "Basic residues within the Kruppel zinc finger DNA binding domains are the critical nuclear localization determinants of EKLF/KLF-1." Journal Of Biological Chemistry **277**(18): 16304-16312.

Philipsen, S. and G. Suske (1999). "A tale of three fingers: the family of mammalian Sp/XKLF transcription factors." Nucleic Acids Research **27**(15): 2991-3000.

Porter, W., B. Saville, et al. (1997). "Functional synergy between the transcription factor Sp1 and the estrogen receptor." Molecular Endocrinology **11**(11): 1569-1580.

Pudney, M., M. G. R. Varma, et al. (1972). "Establishment of a cell line (XTC-2) from the South African Clawed Toad, *Xenopus laevis*." Experientia **29**(4): 466-467.

Ranjan, M., J. Wong, et al. (1994). "Transcriptional repression of *Xenopus* TRβ gene is mediated by a thyroid hormone response element located near the start site." J Biol. Chem. **269**(40): 24699-24705.

Sachs, L. M. and Y. B. Shi (2000). "Targeted chromatin binding and histone acetylation in vivo by thyroid hormone receptor during amphibian development." Proceedings of the National Academy of Sciences of the United States of America **97**(24): 13138-13143.

Samuels, H. H., F. Stanley, et al. (1979). "Depletion of L-3,5,3'-triiodothyrothyronine and L-thyroxine in euthyroid calf serum for use in cell-culture studies of thyroid hormone." Endocrinology **105**(1): 80-85.

Shi, Y. B. (2000). Amphibian Metamorphosis. From Morphology to Molecular Biology. New York, Wiley-Liss.

Shi, Y. B. and D. D. Brown (1993). "The earliest changes in gene expression in tadpole intestine induced by thyroid hormone." Journal of Biological Chemistry **268**(27): 20312-20317.

Shi, Y. B. and W. P. Hayes (1994). "Thyroid hormone-dependent regulation of the intestinal fatty acid-binding protein gene during amphibian metamorphosis." Developmental Biology (Orlando) **161**(1): 48-58.

Shi, Y. B., Y. Yaoita, et al. (1992). "Genomic Organization and Alternative Promoter Usage of the 2 Thyroid-Hormone Receptor Beta Genes in Xenopus-Laevis." Journal of Biological Chemistry **267**(2): 733-738.

Simmen, R. C. M., T. E. Chung, et al. (1999). "Trans-activation functions of the Sp-related nuclear factor, basic transcription element-binding protein, and progesterone receptor in endometrial epithelial cells." Endocrinology **140**(6): 2517-2525.

Simmen, R. C. M., X. L. Zhang, et al. (2002). "Molecular markers of endometrial epithelial cell mitogenesis mediated by the Sp/Kruppel-like factor BTEB1." DNA and Cell Biology **21**(2): 115-128.

Simmen, R. C. M., X. L. Zhang, et al. (2000). "Expression and regulatory function of the transcription factor Sp1 in the uterine endometrium at early pregnancy: implications for epithelial phenotype." Molecular and Cellular Endocrinology **159**(1-2): 159-170.

Sjottem, E., S. Anderssen, et al. (1996). "The promoter activity of long terminal repeats of the HERV-H family of human retrovirus-like elements is critically dependent on Sp1 family proteins interacting with a GC/GT box located immediately 3' to the TATA box." J. Virology **70**(1): 188-198.

Sogawa, K., H. Imataka, et al. (1993). "cDNA cloning and transcriptional properties of a novel GC box-binding protein, Bteb2." Nucleic Acids Research **21**(7): 1527-1532.

Sogawa, K., Y. Kikuchi, et al. (1993). "Comparison of DNA-binding properties between BTEB and Sp1." Journal of Biochemistry **114**(4): 605-609.

Sun, G. L., W. Porter, et al. (1998). "Estrogen-induced retinoic acid receptor alpha 1 gene expression: Role of estrogen receptor Sp1 complex." Molecular Endocrinology **12**(6): 882-890.

Tata, J. R. (2000). "Autoinduction of nuclear hormone receptors during metamorphosis and its significance." Insect Biochemistry and Molecular Biology **30**(8-9): 645-651.

Veldhoen, N., D. Crump, et al. (2002). "Distinctive gene profiles occur at key points during natural metamorphosis in the Xenopus laevis tadpole tail." Developmental Dynamics **225**(4): 457-468.

Wang, Z. and D. D. Brown (1991). "A gene expression screen." Proceedings of the National Academy of Sciences of the United States of America **88**(24): 11505-11509.

Wang, Z. and D. D. Brown (1993). "Thyroid Hormone-Induced Gene-Expression Program for Amphibian Tail Resorption." Journal of Biological Chemistry **268**(22): 16270-16278.

Wong, J., V. C. Liang, et al. (1998). "Transcription from the thyroid hormone-dependent promoter of the Xenopus laevis thyroid hormone receptor betaA gene requires a novel upstream element and the initiator, but not a TATA Box." Journal of Biological Chemistry **273**(23): 14186-14193.

Yanagida, A., K. Sogawa, et al. (1990). "A novel cis-acting DNA element required for a high level of inducible expression of the rat P-450c gene." Molecular and Cellular Biology **10**: 1470-1475.

Yang, M. L., W. S. May, et al. (1999). "JAZ requires the double-stranded RNA-binding zinc finger motifs for nuclear localization." Journal Of Biological Chemistry **274**(39): 27399-27406.

Yaoita, Y. and D. D. Brown (1990). "A correlation of thyroid hormone receptor gene expression with amphibian metamorphosis." Genes Dev. **4**: 1917-1924.

Yaoita, Y., Y. B. Shi, et al. (1990). "Xenopus laevis alpha and beta thyroid hormone receptors." Proceedings of the National Academy of Sciences of the United States of America **87**(18): 7090-7094.

Zhang, D. Y., X. L. Zhang, et al. (2002). "Direct interaction of the Kruppel-like family (KLF) member, BTEB1, and PR mediates progesterone-responsive gene expression in endometrial epithelial cells." Endocrinology **143**(1): 62-73.

Chapter 6

CONCLUSIONS AND FUTURE DIRECTIONS

Synergistic gene regulation by nuclear hormone receptors is an important mechanism for amplifying gene regulatory cascades that are initiated by hormones. We have identified the transcription factor (TF), Krüppel like factor 9 (*Klf9)* as an important intermediate for the synergistic effect of GC on TH action during vertebrate development. In this thesis, I describe the molecular mechanisms of GC (GR/MR) and TH (TR) receptor transcriptional synergy in regulating the expression of an immediate early TF, *Krüppel like factor 9* (*Klf9*) in the brain. I further demonstrate a functionally significant role for KLF9 in TRβ autoinduction, which has important implications for understanding the function of immediate early transcriptional responses in morphogenesis.

Conserved hormone-dependent regulation of the *Klf9* gene

Hormone-dependent regulation of *Klf9* was first discovered in *X. laevis* where it was found to be the most rapidly and strongly induced gene in TH-treated tadpole tissue (Denver, Pavgi et al. 1997). Frog *Klf9* expression also parallels the increase in plasma TH that occurs during tadpole metamorphosis (Shi and Brown 1993; Wang and Brown 1993; Brown, Wang et al. 1995; Brown, Wang et al. 1996; Denver, Pavgi et al. 1997; Shi 2000;

Furlow and Kanamori 2002; Hoopfer, Huang et al. 2002). Similar to *X .laevis*, the expression of rat and mouse *Klf9* in the brain is upregulated by TH, and also coincides with the postnatal rise in brain thyroid hormone receptor (TRβ) expression and plasma T_3 concentration (Porterfield and Hendrich 1993; Denver, Ouellet et al. 1999; Morita, Kobayashi et al. 2003; Denver and Williamson 2009). Thyroid hormone-dependent regulation of *Klf9* has been attributed to a near perfect DR+4 T_3RE located ~6.0 kb and ~3.8 kb upstream of the transcription start site of the frog and mouse *Klf9* gene, respectively (Furlow and Kanamori 2002; Denver and Williamson 2009). Comparative sequence analysis showed that the T_3RE-3.8 in the mouse *Klf9* gene is not conserved between frogs and rodents. As part of the studies conducted in Chapter 3, I found the T_3RE previously identified in frog *Klf9* (T_3RE-6.0) to be evolutionarily and functionally conserved across tetrapods (T_3RE-5.23 in mouse *Klf9*, T_3RE-4.6 in human *Klf9*), and that TR associates with the conserved T_3RE- 5.23. Comparative functional analysis of the mouse *Klf9* T_3RE-5.23 and T_3RE-3.8 by ChIP scan showed a higher association of TR and transcriptionally active histone marks at the mouse *Klf9* T_3RE-5.23 than at the T_3RE- 3.8.

In addition to the conserved TH-dependent regulation of the *Klf9* gene, we also found that GCs, acting mainly through the GR, upregulate *Klf9* expression in tadpole and juvenile frog brain (Bonett, Hu et al. 2009). In Chapter 2, I showed that GC-dependent regulation is evolutionarily conserved between frog and mouse. More importantly, I identified two functional GC response elements (GRE/MRE- 6.1 and GRE/MRE-5.3) in the mouse *Klf9* gene. Between these two GRE/MREs, comparative sequence analysis revealed that only the GRE/MRE-5.3 is evolutionarily conserved

across tetrapods, and also showed a greater association of GR and transcriptionally active histone marks at the conserved GRE/MRE-5.3. Thus, studies in Chapter 2 led to the discovery of an evolutionarily conserved functional GRE/MRE that supports the conserved GC-dependent regulation of the frog and mouse *Klf9* genes.

In addition to the independent effects of TH and GC in regulating *Klf9* expression, work from my thesis also found that TH and GC directly and synergistically upregulated transcription of the *Klf9* gene in the hippocampus, and this synergistic regulation is conserved between frogs and rodents. Promoter reporter scans together with comparative genomic analysis identified an evolutionarily conserved ~180 bp sequence located -5.3 kb upstream of the TSS of the mouse *Klf9* gene (centered at-5.9 kb upstream of the TSS in *Xenopus Klf9*) that supports synergistic transactivation by TH and GC, and I therefore called this the *Klf9* synergy module. Interestingly, the evolutionarily conserved T_3RE (mouse *Klf9* T_3RE-5.23) and GRE/MRE (mouse *Klf9* GRE/MRE-5.3) I identified is also located within this ~180 bp synergy module. There is also a highly conserved hormone response element HRE half site (HRE h1) that was predicted to be GRE/MRE half site by *in silico* analysis located 5 bp downstream of the predicted T_3RE (composed of HRE h2 and HRE h3). Mutational analysis show that HRE h1, h2 and h3 function as a composite response element that supports TH and GC-dependent regulation, and that HRE h2 is the most important half site needed for synergistic activation (Chapter 3). The enrichment of HRE half sites and other conserved *cis* regulatory elements (Sp-1, NF-1 and NF-κB) within the *Klf9* synergy module suggest that it is an important and more transcriptionally active regulatory

region. This may account for our findings that there is greater association of TR, GR and chromatin marks of active transcription at the at the *Klf9* synergy module HREs than at the other identified HREs (T_3RE- 3.8 and GRE/MRE- 6.1).

The activity of the T_3RE- 3.8 and GRE/MRE- 6.1 was mostly tested in neuronal cell types and it is possible that they may play more significant roles in hormone-dependent regulation of the *Klf9* gene in a cell type- specific manner. The additional T_3RE-3.8 and GRE/MRE-6.1 in the mouse *Klf9* gene arose later in evolution and perhaps due to the more complex organization and function of the mammalian brain, the evolution of additional HREs may confer an another level of hormone regulation that is separate and independent from the synergistic regulation that occurs at the *Klf9* synergy module. Given the importance of hormone-dependent regulation of the *Klf9* gene that occurs at the synergy module, additional HREs may have evolved in some lineages to refine and/ or reinforce hormone-dependent gene activation.

To better understand the contribution of the composite response element and other conserved TF binding sites within the synergy in the hormone- dependent regulation of *Klf9*, additional mutational analysis of the HREs within the synergy module and in combination with the other HRE outside of the synergy module need to be performed. Since the HRE h1 and HRE h2 was not protected by the GR DNA binding domain in DNAseI footprinting assay, we need to test if GC-dependent activation at the HRE h1/HRE h2 occurs independent of GR binding to DNA (i.e protein-protein interaction). In support of this hypothesis, I found a predicted NFκB site that encompasses HRE h1 and HRE h2. Proinflammatory cytokine- activated NFκB TF dimers have been mostly shown to antagonize GR-dependent regulation of common

target genes through several mechanisms that include protein-protein interactions or tethering(Vallabhapurapu and Karin 2009). However, recent evidence suggests that GR and NFκB TF are co-recruited to common target genes to synergistically upregulate their expression (Rao, McCalman et al. 2011). Therefore, it would be interesting to determine the interaction between the NFκB and TH and/or GC-dependent signaling in regulation of the *Klf9* gene. This can be tested by an NFκB siRNA knockdown or NFκB overexpression systems and determining their effect on hormone-dependent gene expression of *Klf9*. By EMSA, we can also test if GR binds to the composite response element in the presence of the NFκB TF, or if TR association is affected by NFκB . In the same manner, we can perform mutational analysis, knockdown or overexpression to determine contributions or interactions of Sp1 and NF-1 with the hormone-dependent regulation of the *Klf9* gene.

Combined mutational analysis of the HREs within and outside the mouse *Klf9* synergy module using a larger promoter fragment of the mouse *Klf9* gene can help us better understand the contributions of the additional HREs and their interaction with the synergy module. We may be able to identify and separate the HREs that are important for the independent versus the synergistic response with TH and GC within a particular cell type. These studies may provide some of the evolutionary significance of why mammalian species gained additional HREs.

Molecular mechanisms of synergistic transcriptional regulation of the *Klf9* gene by TR and GR

Transcriptional synergy between TFs is an important mechanism for integrating multiple pathways and is regarded to be an important means to ensure genes are expressed at the appropriate time and place (Courey 2001). There are several mechanisms for how two TFs can enhance each other's function leading to transcriptional synergy that were described in Chapter 1 (Fig. 1.6). In the studies described in Chapter 3, I confirmed that two out of the four mechanisms described may, in part, explain the transcriptional synergy that occurs at the *Klf9* gene. Scanning the mouse *Klf9* locus by ChIP assays, I found TR association peaks at the synergy module, and that there is TH-dependent enhancement of GR association at the synergy module and at the GRE/MRE-6.1 which is consistent with the role of TR as a transcriptional switch (Mai, Janier et al. 2004; Shi 2009). Synergistic transcriptional regulation of *Klf9* was also seen at the level of synergistic association of stalled RNA polymerase II (pol II) where TH plus GC treatment led to a peak in Pol II association at *Klf9* the synergy module. There was a lower peak of stalled Pol II at the promoter but its association did not change with any of the hormone treatments suggesting that the *Klf9* synergy module is a more important site for transcriptional regulation. Stalled RNA pol II is highly enriched among genes implicated in development and response to stimuli suggesting that Pol II stalling keeps the gene poised and ready to afford a rapid transcriptional response to developmental and environmental signals (Muse, Gilchrist et al. 2007; Zeitlinger, Stark et al. 2007; Margaritis and Holstege 2008). Thus, the hormone- dependent and peak of Pol II

association at the synergy module may be a key mechanism behind the rapid and synergistic response of *Klf9* to TH and GC.

There are still several outstanding questions that need to be addressed to fully understand the role of Pol II in the transcriptional events mediated by TR and GR at the *Klf9* synergy module. For example, there are several possibilities to account for the synergistic association of stalled Pol II at the synergy module that remains to be tested. Is the enhanced association of stalled Pol II at the synergy module due to synergistic recruitment of unphosphorylated Pol II, enhanced phosphorylation of Ser5 or an increase in the stability and time of association of stalled Pol II at the synergy module? ChIP assays with unphosphorylated pol II, proteins that regulate Pol II phosphorylation, and the kinetics of their association need to be done to address these possibilities.

In chapter 3, I also found that the peak in association of stalled Pol II at the synergy module was accompanied by hormone-dependent transcription at the enhancer region. My findings are consistent with a recent study that identified ~2,000 activity regulated enhancers bound by pol II are transcribed into noncoding RNA or enhancer RNA (eRNA) that were less than 2 kb in length. Enhancer RNA synthesis was dependent on the presence of a promoter of the associated gene and correlated with induction of nearby genes (Kim, Hemberg et al. 2010). My preliminary data suggest that the noncoding transcripts are short and transcribed towards the direction of the promoter. Using genome wide analysis using Chromatin interaction analysis with paired end tag sequencing (ChIA-PET) (Li, Fullwood et al. 2010) to look at TH-dependent long range genomic interactions, Laurent Sachs and colleagues have

shown that there is a TH-dependent interaction between the synergy module and *Klf9* promoter which supports the role of the synergy module as a bona fide enhancer where the assembly of TR, GR, Pol II and other yet unidentified TFs is physically relayed to the *Klf9* promoter to mediate synergistic transcription.

The role of noncoding eRNAs in gene regulation is a fairly recent concept that remains to be further investigated. The eRNA I discovered at the synergy module showed a similar pattern but more robust hormone-dependent regulation as the *Klf9* mRNA consistent with the peak in Pol II association at the that region. It remains to be determined whether the eRNA plays a functional role in target gene regulation similar to what was found with the eRNAs of the *β globin* gene, the human *growth hormone* and other long noncoding RNAs identified through the GENCODE annotation of the human genome (Ling, Ainol et al. 2004; Ho, Elefant et al. 2006; Vernimmen, De Gobbi et al. 2007; Orom, Derrien et al. 2010). Since we also know that the synergy module communicates with *Klf9* promoter by chromosomal looping, it would be interesting to determine if the eRNA influences the physical interaction between the synergy module and promoter. This could be tested by knocking down eRNA by siRNA or blocking eRNA transcription by insertion of a transcription termination signal close to the *Klf9* synergy module. Once eRNA synthesis or expression is blocked, we can determine how this affects expression of the *Klf9* mRNA.

Another important issue that needs to be addressed that may account for the synergistic regulation of the *Klf9* gene is whether GC or TH plus GC affects the stability or formation of the loops that bridge the enhancer and the promoter. A key

player that is known to facilitate chromosomal looping and interacts with TR and GR during transcriptional regulation is the MED1/TRAP220 subunit of the Mediator complex (Ito and Roeder 2001; Park, Li et al. 2005; Chen and Roeder 2007). In this regard, we need to test if TRAP220 is recruited to the synergy module and if it facilitates the interaction of the *Klf9* synergy module with the promoter in regulating *Klf9* transcription. All these proposed studies will provide a better understanding of the molecular basis behind the transcriptional events that occur at the *Klf9* synergy module.

Using the *Klf9* gene as a model, we can further explore the significance mechanisms of how TR functions as a transcriptional switch and how TR affects the association of other TFs at the synergy module. For example, using a dominant negative form of TR that is not able to bind hormone and therefore is a constitutive repressor, we can determine if the independent and synergistic regulation of *Klf9* by TH and GC is dampened. More importantly, by overexpression of the dominant negative form of TR we can determine by ChIP assay if there are changes in the hormone- dependent association of GR, pol II isoforms and active chromatin marks across the *Klf9* locus. We can also test if the dominant negative TR affects eRNA synthesis and looping.

Functional Role of KLF9 in development

The expression of KLF9 is strongly upregulated during postnatal development of frog and rodent brain (Denver, Ouellet et al. 1999; Denver and Williamson 2009) and it has been shown to play a role in TH-dependent actions on neuronal morphology

(Denver, Ouellet et al. 1999; Cayrou, Denver et al. 2002). Expression of *Klf9* in frog brain and mouse hippocampus and cerebellum parallels the postnatal rise in plasma T_3 concentration and TRβ expression in the brain (Porterfield and Hendrich 1993; Denver, Ouellet et al. 1999; Shi 2000; Morita, Kobayashi et al. 2003; Bagamasbad, Howdeshell et al. 2008; Denver and Williamson 2009). Forced expression of KLF9 in tadpole brain caused an increase in the number of Golgi stained cells (Bonett, Hu et al. 2009). In rodents, deficiency in KLF9 led to a decrease in dendritic branching in the Purkinje cells of the cerebellum (Morita, Kobayashi et al. 2003), delayed neuronal maturation and reduced neurogenesis-dependent LTP in the dentate gyrus (Scobie, Hall et al. 2009) that was accompanied by reduced activity in behavioral tests that define functions of the cerebellum, hippocampus and amygdala (Morita, Kobayashi et al. 2003). The mechanism for how KLF9 functions to regulate neuronal morphology and function is poorly understood.

One of the direct transcriptional targets of KLF9 that we identified in the frog brain is thyroid hormone receptor β (TRβ). The coordinate upregulation of frog *Klf9* and *TRβ* that occurs during tadpole metamorphosis, and the discovery that the *TRβA* promoter has several potential binding sites for KLF9 (Ranjan, Wong et al. 1994) led us to hypothesize that *Klf9*, which is induced by TH with faster kinetics than TRβ, promoted TRβ upregulation by TH (autoinduction). Indeed I found that *Klf9* expression is upregulated earlier than *TRβA* in XTC-2 cells and in the brain of premetamorphic tadpoles treated with TH. More importantly, by ChIP assays I showed that KLF9 associates with the *TRβA* promoter *in vivo* in a TH and developmental stage-dependent manner. Furthermore, forced expression of KLF9 in

XTC-2 cells or tadpole brain *in vivo* accelerated and enhanced TRβA autoinduction (Bagamasbad, Howdeshell et al. 2008), Hu and Denver, unpublished data) supporting our hypothesis that KLF9 functions as an accessory TF necessary for TRβ autoinduction. TRβA autoinduction is hypothesized to be necessary for driving metamorphosis by increasing tissue sensitivity to TH that consequently amplifies gene expression cascades activated by the TH (reviewed in (Bagamasbad and Denver 2011)).

The pattern of TRβ expression in rat brain parallel those seen in the tadpole during metamorphosis where TRβ expression is low at birth and shows a dramatic increase during the first 2 weeks postnatally, that is coincident with rising plasma TH concentrations (Strait, Schwartz et al. 1990). The human *TRβ* promoter has two functional T_3REs that mediate transactivation in transient transfection assays (Suzuki, Miyamoto et al. 1994) but to our knowledge, the occurrence and significance of TRβ autoinduction during mammalian development has not been investigated. Therefore it would be interesting to know if the role of KLF9 in TRβ autoinduction is conserved between frogs and rodents and to investigate the functional significance of TRβ autoinduction in shaping neuronal function and morphology.

The physiological significance for the synergistic action of TH and GC in animal development is best exemplified by amphibian metamorphosis where GC have been shown to synergize with TH in promoting tail morphogenesis through the synergistic effect of TH and GC in regulating TRβ and deiodinase expression (Bonett, Hoopfer et al. 2010). Evidence suggests that GC alone does not regulate TRβ expression but GC can synergize with TH to enhance TRβ expression (Bonett, Hoopfer et al. 2010).

Studies in this thesis have shown that *Klf9* is a direct transcriptional target of TR and GR leading to synergistic levels of *Klf9* expression and that KLF9 functions in TRβ autoinduction. These results when taken together suggest that perhaps the ability of GC to enhance TH-dependent TRβ expression may be, partly, a secondary effect that is mediated by the synergistic expression of *Klf9* by TH and GC. My findings provide another dimension of how TH and GC synergize to accelerate metamorphosis. By creating a positive, feed forward loop where TR and GR synergistically increase *Klf9* expression which consequently enhances TRβ autoinduction, tissue sensitivity to TH can be synergistically amplified to accelerate the metamorphic process (Fig. 1.7).

Glucocorticoids have been found to regulate deiodinase expression in rat liver, kidney and brain *in vivo* (Van der Geyten and Darras 2005). Krüppel like factor 9 was also found to directly upregulate Type I deiodinase activity in mouse hepatocytes (Ohguchi, Tanaka et al. 2008). In tadpole tail, GC and TH synergistically upregulated Type II deiodinase expression (Bonett, Hoopfer et al. 2010). Thus, it is possible that the GC-dependent regulation of deiodinase expression is mediated through KLF9. We can hypothesize that similar to its role in TRβ regulation, KLF9 can regulate deiodinase expression in tadpole tissues and that the synergistic effect of GC and TH in Type II deiodinase expression during tadpole metamorphosis may be an indirect consequence of KLF9 induction. If so, this would further emphasize the functional significance of KLF9 as an intermediate that increases TH sensitivity of target tissue. The developmental consequence of the role of KLF9 as an intermediate of GC and TH transcriptional network can be tested by overexpressing wild type and dominant

negative forms of KLF9 in tadpole brain and determining if this accelerates spontaneous metamorphosis.

There is mounting evidence that KLF9 plays an important role in mediating hormone action in brain development and plasticity (Denver, Ouellet et al. 1999; Cayrou, Denver et al. 2002; Morita, Kobayashi et al. 2003; Lin, Bloodgood et al. 2008; Scobie, Hall et al. 2009). I have established that *Klf9* is also a direct target for GC- dependent induction in the brain. We have yet to determine if KLF9 is a mediator of the GC-dependent changes in neuronal morphology and function. For example, does the KLF9-null mouse exhibit altered response in stress induced changes in neuronal morphology, synaptic plasticity and behavior? We also need to identify other KLF9 target genes so that we can further investigate if neuronal structure and function is differentially influenced by TH, GC or TH plus GC through pathways activated by KLF9.

Results of my microarray analysis showed that there are other genes synergistically regulated by TH and GC involved in shaping cell morphology through reorganization of the cytoskeleton. These results are preliminary but have great potential to better understand the molecular basis for GC and TH action in the hippocampus. We first need to verify if the hormone- regulated genes identified in the microarray exhibit a similar form of regulation *in vivo*. Among genes synergistically regulated by TH and GC, we can conduct extensive bioinformatic analysis to determine if the other genes possess a regulatory region similar to the *Klf9* synergy module. More importantly, we can investigate if these other genes synergistically upregulated by TH and GC also play a role in hormone-dependent changes in

neuronal structure and function, and if there are interactions between these genes required to confer hormone dependent responses. These possibilities can be directly tested by hormone treatment of WT mouse in comparison with KLF9-null mouse and by hormone treatment of *Klf9* siRNA knockdown or overexpression systems in neuronal cultures or tadpole brain. Through these studies we can determine the different changes in neuronal morphology and function that are mediated by the interaction of KLF9 with other hormone-regulated genes. The list of genes that we have generated with the microarray analysis in mouse hippocampal neurons are novel findings and the first study that has looked into the coordinate action of TH and GC in gene regulation in the hippocampus.

Krüppel-like factor 9 has also been shown to play a role in different hormone-dependent physiological functions outside of the nervous system. Krüppel like factor 9 was discovered to directly regulate the expression of peroxisome proliferator-activated receptor ɣ (PPAR ɣ) and mediate PPARɣ- dependent adipocyte differentiation (Pei, Yao et al. 2011). In hepatocytes, KLF9 together with the hepatocyte nuclear factor 4α (HNF4α) and GATA4 synergistically regulates the expression of mouse Type I deiodinase (Ohguchi, Tanaka et al. 2008). In uterine epithelial cells, KLF9 was found to interact with the progesterone receptor (PR) where it enhances progesterone- dependent gene transcription (Zhang, Zhang et al. 2002; Zhang, Zhang et al. 2003). In contrast, KLF9 was found to repress estrogen receptor (ER) expression and consequently inhibit estrogen- dependent signaling in endometrial epithelial cells (Velarde, Zeng et al. 2007). These studies indicate that KLF9 may be an important mediator that integrates estrogen and progesterone

signaling pathways during uterine development. Consistent with its role in progesterone and estrogen signaling, KLF9 deficient female mice exhibit delayed uterine development, reduced embryo implantation, decrease in litter size and delayed parturition (Simmen, Eason et al. 2004; Zeng, Velarde et al. 2008). These findings indicate that KLF9 is involved and may play a central role in several hormone-dependent regulatory pathways during development. Given that estrogen and progesterone also influence brain development and function, it would be interesting to determine if KLF9 functions as an intermediate in the cross- talk between TH-progesterone/estrogen, or GC- progesterone/estrogen in the brain.

Concluding remarks

Hormones, especially stress and thyroid hormone, are powerful signaling molecules that play crucial roles in animal development, particularly development of the nervous system. There is a large body of knowledge that documents the independent effects of TH and GC in the brain but studies that investigate their coordinate actions in neural development is lacking. The studies presented in this thesis describe an evolutionarily conserved mechanism for the synergistic actions of TH and GC in regulation of the *Klf9* gene, which may function as an intermediate that coordinates actions of TH and GC in shaping neuronal morphology and function. Findings in this thesis provide a molecular basis for the synergistic actions of TH and GC in animal development. This recent and novel finding and the discovery of the *Klf9* synergy module suggest that thyroid and stress hormone regulation of *Klf9* arose early in the evolution of the tetrapod vertebrates, and may have been maintained

through evolutionary time because of a critical, adaptive role for KLF9 in promoting hormone-dependent neural development and plasticity.

References

Bagamasbad, P. and R. J. Denver (2011). "Mechanisms and significance of nuclear receptor auto- and cross-regulation." Gen Comp Endocrinol **170**(1): 3-17.

Bagamasbad, P., K. L. Howdeshell, et al. (2008). "A role for basic transcription element-binding protein 1 (BTEB1) in the autoinduction of thyroid hormone receptor beta." J Biol Chem **283**(4): 2275-2285.

Bonett, R. M., E. D. Hoopfer, et al. (2010). "Molecular mechanisms of corticosteroid synergy with thyroid hormone during tadpole metamorphosis." Gen Comp Endocrinol **168**(2): 209-219.

Bonett, R. M., F. Hu, et al. (2009). "Stressor and glucocorticoid-dependent induction of the immediate early gene kruppel-like factor 9: implications for neural development and plasticity." Endocrinology **150**(4): 1757-1765.

Brown, D. D., Z. Wang, et al. (1996). "The thyroid hormone-induced tail resorption program during Xenopus laevis metamorphosis." Proc Natl Acad Sci U S A **93**(5): 1924-1929.

Brown, D. D., Z. Wang, et al. (1995). "Amphibian metamorphosis: a complex program of gene expression changes controlled by the thyroid hormone." Recent Prog Horm Res **50**: 309-315.

Cayrou, C., R. J. Denver, et al. (2002). "Suppression of the basic transcription element-binding protein in brain neuronal cultures inhibits thyroid hormone-induced neurite branching." Endocrinology **143**(6): 2242-2249.

Chen, W. and R. G. Roeder (2007). "The Mediator subunit MED1/TRAP220 is required for optimal glucocorticoid receptor-mediated transcription activation." Nucleic Acids Res **35**(18): 6161-6169.

Courey, A. J. (2001). "Cooperativity in transcriptional control." Curr Biol **11**(7): R250-252.

Denver, R. J., L. Ouellet, et al. (1999). "Basic transcription element-binding protein (BTEB) is a thyroid hormone-regulated gene in the developing central nervous system. Evidence for a role in neurite outgrowth." J Biol Chem **274**(33): 23128-23134.

Denver, R. J., S. Pavgi, et al. (1997). "Thyroid hormone-dependent gene expression program for Xenopus neural development." J Biol Chem **272**(13): 8179-8188.

Denver, R. J. and K. E. Williamson (2009). "Identification of a thyroid hormone response element in the mouse Kruppel-like factor 9 gene to explain its postnatal expression in the brain." Endocrinology **150**(8): 3935-3943.

Furlow, J. D. and A. Kanamori (2002). "The transcription factor basic transcription element-binding protein 1 is a direct thyroid hormone response gene in the frog Xenopus laevis." Endocrinology **143**(9): 3295-3305.

Ho, Y., F. Elefant, et al. (2006). "Locus control region transcription plays an active role in long-range gene activation." Mol Cell **23**(3): 365-375.

Hoopfer, E. D., L. Huang, et al. (2002). "Basic transcription element binding protein is a thyroid hormone-regulated transcription factor expressed during metamorphosis in Xenopus laevis." Dev Growth Differ **44**(5): 365-381.

Ito, M. and R. G. Roeder (2001). "The TRAP/SMCC/Mediator complex and thyroid hormone receptor function." Trends Endocrinol Metab **12**(3): 127-134.

Kim, T. K., M. Hemberg, et al. (2010). "Widespread transcription at neuronal activity-regulated enhancers." Nature **465**(7295): 182-187.

Li, G., M. J. Fullwood, et al. (2010). "ChIA-PET tool for comprehensive chromatin interaction analysis with paired-end tag sequencing." Genome Biol **11**(2): R22.

Lin, Y., B. L. Bloodgood, et al. (2008). "Activity-dependent regulation of inhibitory synapse development by Npas4." Nature **455**(7217): 1198-1204.

Ling, J., L. Ainol, et al. (2004). "HS2 enhancer function is blocked by a transcriptional terminator inserted between the enhancer and the promoter." J Biol Chem **279**(49): 51704-51713.
Mai, W., M. F. Janier, et al. (2004). "Thyroid hormone receptor alpha is a molecular switch of cardiac function between fetal and postnatal life." Proc Natl Acad Sci U S A **101**(28): 10332-10337.
Margaritis, T. and F. C. Holstege (2008). "Poised RNA polymerase II gives pause for thought." Cell **133**(4): 581-584.
Morita, M., A. Kobayashi, et al. (2003). "Functional analysis of basic transcription element binding protein by gene targeting technology." Mol Cell Biol **23**(7): 2489-2500.
Muse, G. W., D. A. Gilchrist, et al. (2007). "RNA polymerase is poised for activation across the genome." Nat Genet **39**(12): 1507-1511.
Ohguchi, H., T. Tanaka, et al. (2008). "Hepatocyte nuclear factor 4alpha contributes to thyroid hormone homeostasis by cooperatively regulating the type 1 iodothyronine deiodinase gene with GATA4 and Kruppel-like transcription factor 9." Mol Cell Biol **28**(12): 3917-3931.
Orom, U. A., T. Derrien, et al. (2010). "Long noncoding RNAs with enhancer-like function in human cells." Cell **143**(1): 46-58.
Park, S. W., G. Li, et al. (2005). "Thyroid hormone-induced juxtaposition of regulatory elements/factors and chromatin remodeling of Crabp1 dependent on MED1/TRAP220." Mol Cell **19**(5): 643-653.
Pei, H., Y. Yao, et al. (2011). "Kruppel-like factor KLF9 regulates PPARgamma transactivation at the middle stage of adipogenesis." Cell Death Differ **18**(2): 315-327.
Porterfield, S. P. and C. E. Hendrich (1993). "The role of thyroid hormones in prenatal and neonatal neurological development--current perspectives." Endocr Rev **14**(1): 94-106.
Ranjan, M., J. Wong, et al. (1994). "Transcriptional repression of Xenopus TR beta gene is mediated by a thyroid hormone response element located near the start site." J Biol Chem **269**(40): 24699-24705.
Rao, N. A., M. T. McCalman, et al. (2011). "Coactivation of GR and NFKB alters the repertoire of their binding sites and target genes." Genome Res **21**(9): 1404-1416.
Scobie, K. N., B. J. Hall, et al. (2009). "Kruppel-like factor 9 is necessary for late-phase neuronal maturation in the developing dentate gyrus and during adult hippocampal neurogenesis." J Neurosci **29**(31): 9875-9887.
Shi, Y.-B. (2000). Amphibian metamorphosis : from morphology to molecular biology. New York, Wiley-Liss.
Shi, Y. B. (2009). "Dual functions of thyroid hormone receptors in vertebrate development: the roles of histone-modifying cofactor complexes." Thyroid **19**(9): 987-999.
Shi, Y. B. and D. D. Brown (1993). "The earliest changes in gene expression in tadpole intestine induced by thyroid hormone." J Biol Chem **268**(27): 20312-20317.
Simmen, R. C., R. R. Eason, et al. (2004). "Subfertility, uterine hypoplasia, and partial progesterone resistance in mice lacking the Kruppel-like factor 9/basic transcription element-binding protein-1 (Bteb1) gene." J Biol Chem **279**(28): 29286-29294.
Strait, K. A., H. L. Schwartz, et al. (1990). "Relationship of c-erbA mRNA content to tissue triiodothyronine nuclear binding capacity and function in developing and adult rats." J Biol Chem **265**(18): 10514-10521.
Suzuki, S., T. Miyamoto, et al. (1994). "Two thyroid hormone response elements are present in the promoter of human thyroid hormone receptor beta 1." Mol Endocrinol **8**(3): 305-314.

Vallabhapurapu, S. and M. Karin (2009). "Regulation and function of NF-kappaB transcription factors in the immune system." Annu Rev Immunol **27**: 693-733.

Van der Geyten, S. and V. M. Darras (2005). "Developmentally defined regulation of thyroid hormone metabolism by glucocorticoids in the rat." J Endocrinol **185**(2): 327-336.

Velarde, M. C., Z. Zeng, et al. (2007). "Kruppel-like factor 9 is a negative regulator of ligand-dependent estrogen receptor alpha signaling in Ishikawa endometrial adenocarcinoma cells." Mol Endocrinol **21**(12): 2988-3001.

Vernimmen, D., M. De Gobbi, et al. (2007). "Long-range chromosomal interactions regulate the timing of the transition between poised and active gene expression." EMBO J **26**(8): 2041-2051.

Wang, Z. and D. D. Brown (1993). "Thyroid hormone-induced gene expression program for amphibian tail resorption." J Biol Chem **268**(22): 16270-16278.

Zeitlinger, J., A. Stark, et al. (2007). "RNA polymerase stalling at developmental control genes in the Drosophila melanogaster embryo." Nat Genet **39**(12): 1512-1516.

Zeng, Z., M. C. Velarde, et al. (2008). "Delayed parturition and altered myometrial progesterone receptor isoform A expression in mice null for Kruppel-like factor 9." Biol Reprod **78**(6): 1029-1037.

Zhang, D., X. L. Zhang, et al. (2002). "Direct interaction of the Kruppel-like family (KLF) member, BTEB1, and PR mediates progesterone-responsive gene expression in endometrial epithelial cells." Endocrinology **143**(1): 62-73.

Zhang, X. L., D. Zhang, et al. (2003). "Selective interactions of Kruppel-like factor 9/basic transcription element-binding protein with progesterone receptor isoforms A and B determine transcriptional activity of progesterone-responsive genes in endometrial epithelial cells." J Biol Chem **278**(24): 21474-21482.

APPENDIX A

Supplemental Methods, Tables and Figures for Chapter 2

Supplemental Materials and Methods

Genomic DNA fragments identified by ChIP-chip assay for MR [35] corresponding to two upstream regions of the human *Klf9* gene (-5139 to -5771 bp and -3875 to -4211 bp) were subcloned into pGL4.23 (Supplemental Table 1) for testing in HEK293-hMR+ cells. As a positive control we used a 626 bp fragment of the upstream region of the human glucocorticoid-induced leucine zipper (GILZ) gene (-1286 to -1912 bp) cloned into pGL4.23; this region of the GILZ gene was previously shown to contain at least two functional GRE/MREs [54]. We cultured and transfected HEK293-hMR+ cells as described previously [35]. We incubated cells for 5 h in the presence or absence of 10 nM ALDO with or without 1 μM of the MR selective antagonist RU26752 (Sigma Chemical Co., St. Louis, MO). The vehicle DMSO was present in all wells at a final concentration of 0.01%. Luciferase activity in cell lysates was analyzed using the Dual Luciferase Reporter Assay (Promega) according to the manufacturer's protocol.

Supplemental Table 2.1. Oligonucleotides used for construction of pGL4.23 promoter plasmids.

PCR primers to amplify promoter fragments cloned into pGL4.23 vector

hKlf9 GRE/MRE-5.5 Fragment1
Forward: 5' acatctcgagGCATGGGGGCCGTACAGAAGGGGGAACT 3'
Reverse: 5' acataagcttCGGCCAGGCTGTGCGGGAGGAGATG 3'

hKlf9 GRE/MRE-4.0 Fragment2
Forward: 5' acagagctcGCCCCTGGGTGTTAGCTGTCATTAT 3'
Reverse: 5' acatctcgagCCAGGCGGGAAGGAAGGAGGAGAAC 3'

hGILZ control -1286 to -1912
Forward: 5' acatctcgagAACATTGGGTTCCACCACATA 3'
Reverse: 5' acataagcttCAGGGAATTCTGATACCAGTTA 3'

Lower case letters represent restriction sites for subcloning into the pGL4.23 vector.

Figures

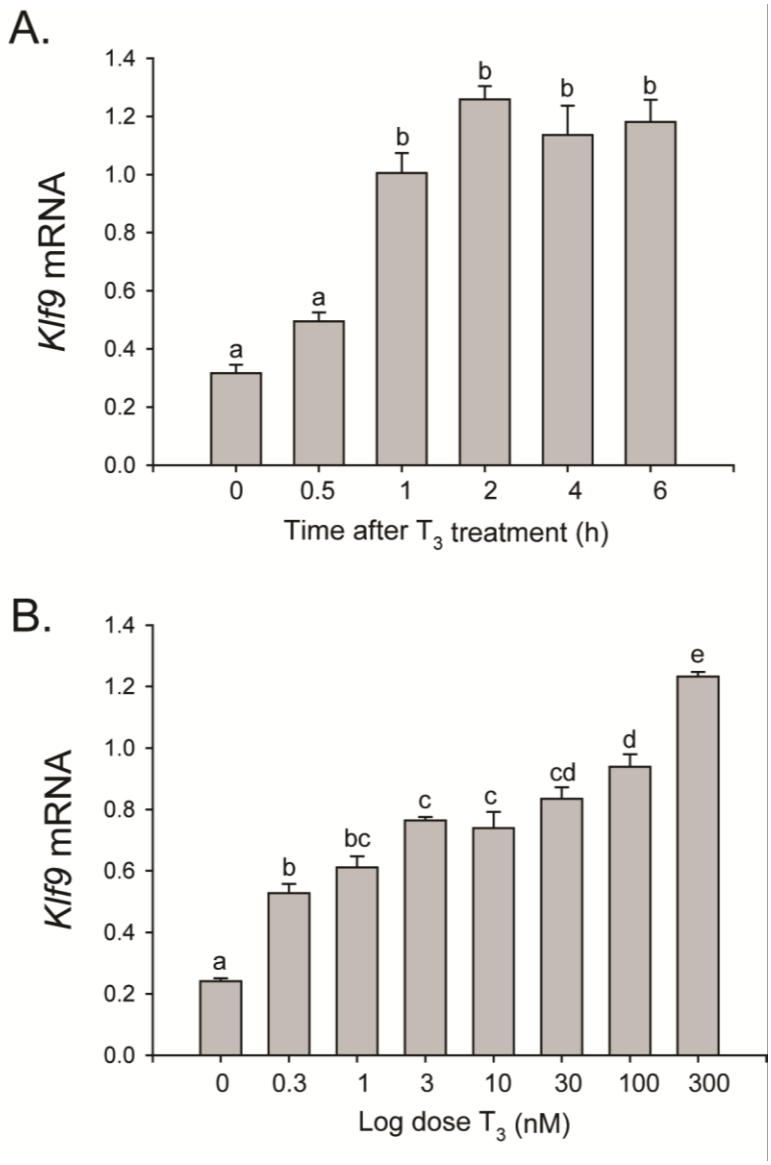

Supplemental Fig 2.1. Treatment with 3,5,3'-triiodothyronine (T_3) caused dose and time-dependent increases in *Klf9* mRNA in HT-22 cells. Cells were treated with 30 nM T_3 for different times **(A;** $F_{(5,23)}$=37.90, p<0.00; ANOVA), or with increasing doses of T_3 for 4 h **(B;** EC50= 1.87 nM; ($F_{(7,31)}$=77.09, p<0.001; ANOVA**)** before harvest and analysis of *Klf9* mRNA. In each experiment cells were treated with the hormone doses for the times indicated before cell harvest, RNA extraction and analysis by RTqPCR. *Klf9* mRNA was normalized to the mRNA level of the housekeeping gene *GAPDH*. Bars represent the mean ± SEM (n=4) and letters above the means indicate significant differences among hormone concentrations or time point (means with the same letter are not significantly different; Tukey's multiple comparison test; P<0.05).

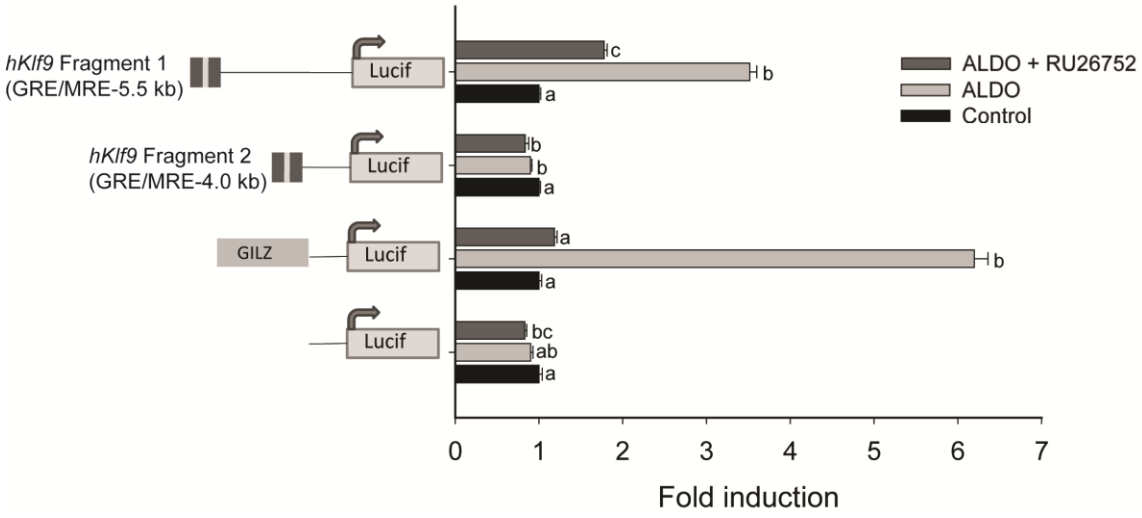

Supplemental Fig 2.2. Identification of an aldosterone-responsive region of the human *Klf9* gene centered at ~-5.5 kb relative to the transcription start site. We co-transfected HEK293-hMR+ cells with promoter-luciferase constructs containing fragments of the human *Klf9* gene and the pRenilla plasmid, and measured luciferase activity after 5 h treatment with 10 nM aldosterone (ALDO) in the presence or absence of 1 μM of the MR-selective antagonist RU26752. Fragment 1 encompassed 632 bp from -5771 to -5139 bp, and fragment 2 encompassed 336 bp from -4211 to -3875 bp upstream of the human *Klf9* transcription start site. A 626 bp fragment of the upstream region the human glucocorticoid-induced leucine zipper gene (GILZ) that contains at least two GRE/MREs served as a positive control for hormone activation, and the pGL4.23 empty vector served as the negative control. Luciferase activity was measured using the Dual Luciferase Reporter Assay. Bars represent the mean $\pm$ SEM (n=8) and letters above the means indicate significant differences among treatments (means with the same letter are not significantly different; fragment 1: $F_{(2,41)}=693.5$, $p<0.001$; fragment 2: $F_{(2,41)}=10.92$, $p<0.05$; GILZ: $F_{(2,41)}=1130$, $p<0.001$; empty vector: $F_{(2,41)}=7.197$, $p<0.01$; ANOVA).

APPENDIX B

Supplemental Figures for Chapter 3

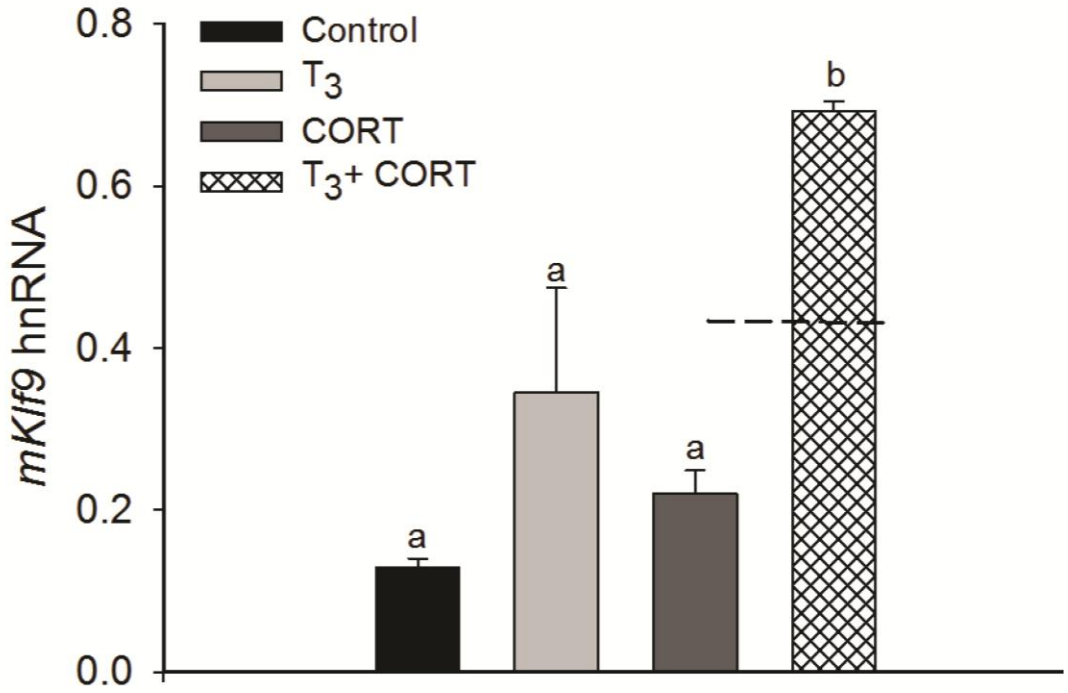

Supplemental Fig. 3.1. **Corticosterone (CORT) synergizes with 3,5,3'-triiodothyronine (T_3) to induce *Klf9* heteronuclear RNA.** HT-22 cells were treated with 30 nM T_3, 100 nM CORT or T_3 plus CORT for different times before harvest and RNA extraction. RNA samples were used to measure *Klf9* heteronuclear RNA (hnRNA) by RTqPCR using Taqman assay targeted against the *Klf9* intronic region. The *Klf9* hnRNA were normalized to the mRNA level of the housekeeping gene *GAPDH*. Bars represent the mean ± SEM and letters above the means indicate significant differences among treatments (means with the same letter are not significantly different; Tukey's multiple comparison test; $P<0.05$). Dashed lines represent the additive effects of T_3 plus CORT **i**n *Klf9* mRNA level

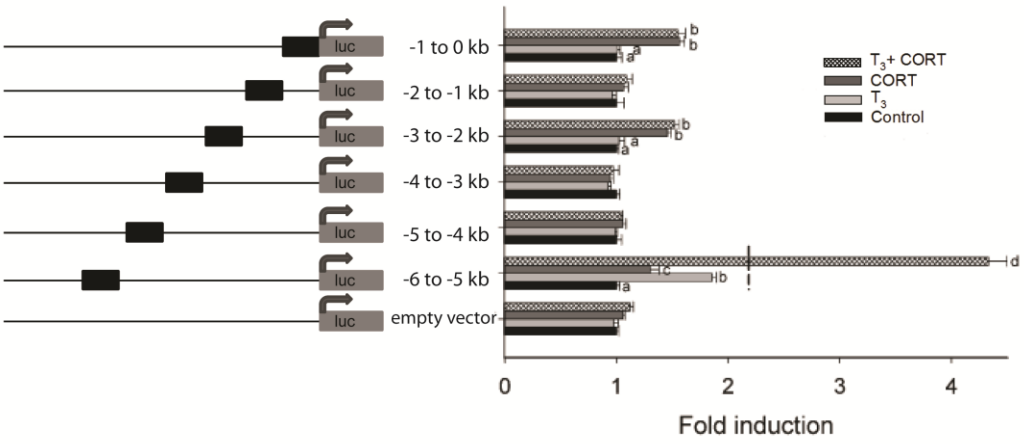

Supplemental Fig. 3.2. The -6 to -5 kb genomic fragment of frog *Klf9* gene shows synergistic transactivation in HT-22 cells. A series of 1 kilobase fragments covering from -7 kb to 0 kb upstream of the *X. tropicalis Klf9* transcription start site were cloned into a luciferase vector and transfected into HT-22 cells. Cells were treated with T_3, CORT or T_3 plus CORT for 4 h before harvest and analysis by dual luciferase assay. Bars represent the mean $\pm$ SEM (n=4-5) fold induction and letters above the means indicate significant differences among hormone concentrations or time point (means with the same letter are not significantly different; Tukey's multiple comparison test; $P<0.05$). Dashed lines represent the additive effects of T_3 plus CORT on luciferase activity.

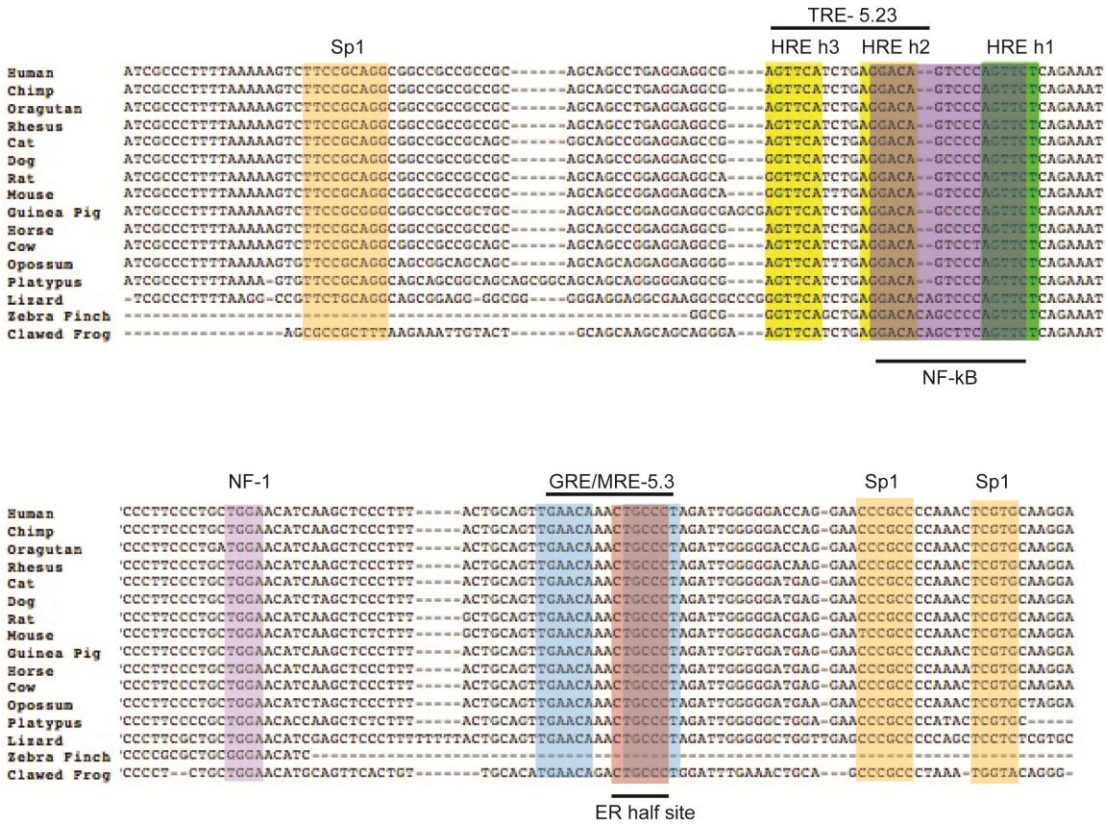

Supplemental Fig. 3.3. Highly conserved transcription factor binding sites within the Klf9 synergy module as identified by TESS and Match. Comparative sequence alignment of the ~180 bp *Klf9* synergy module across several tetrpod species showing conservation of the T_3RE (yellow; HRE h2 and HRE h3), GRE/MRE (blue; mouse GRE/MRE-5.3) and other binding sites for estrogen receptor (ER half site, red), Sp1 (orange), NF-1 (pink) and NFkB as predicted by the the online program TESS using a library of mononucleotide weight matrices from TRANSFAC 6.0 (www.gene-regulation.com)

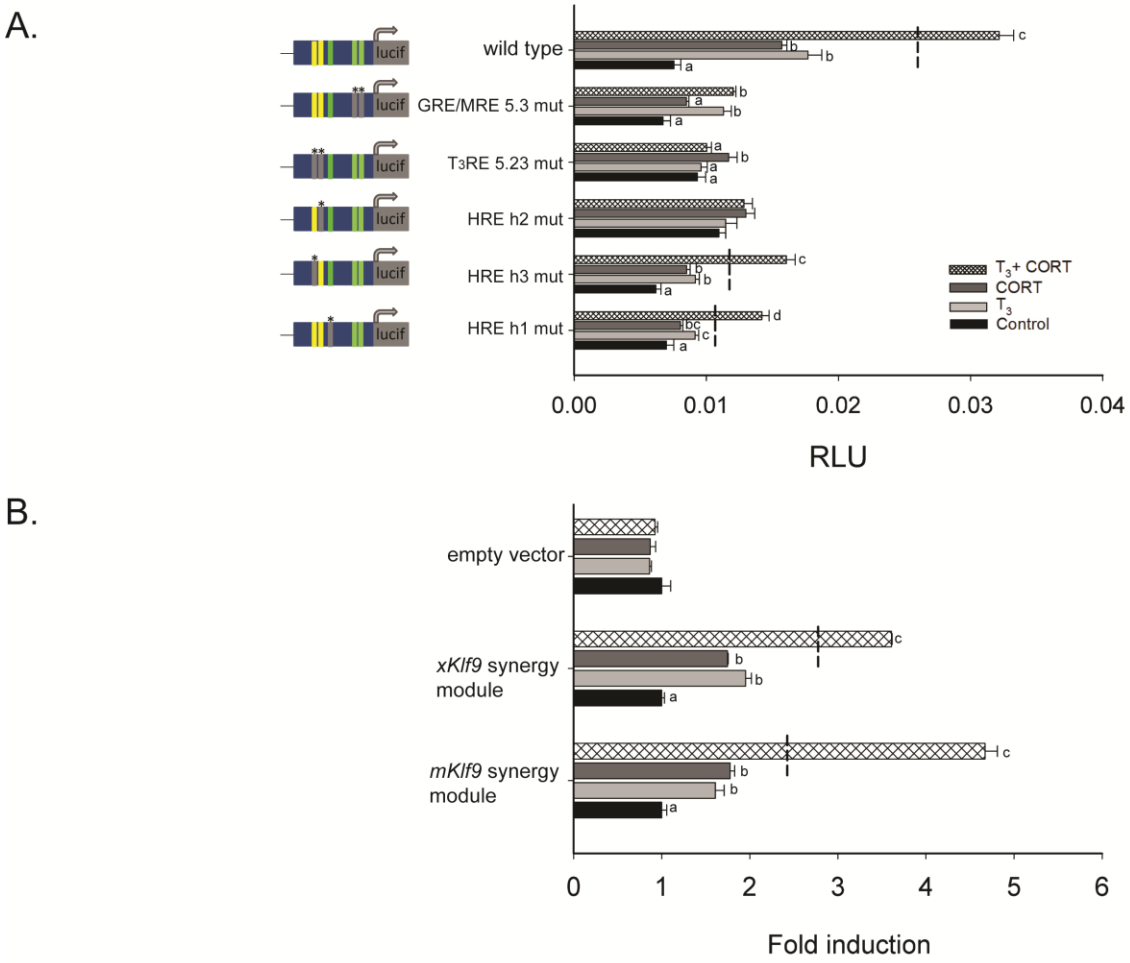

Supplemental Fig. 3.4. Frog and mouse *Klf9* synergy module support synergistic transactivation by T_3 plus CORT in frog and mouse cell lines. (A) HT-22 cells were transfected with promoter luciferase constructs containing the mouse *Klf9* 179 bp synergy module, and corresponding site mutants (*****). Cells were treated with 30 nM T_3, 100 nM CORT or T_3 plus CORT for 4 h before harvest and analysis by dual luciferase assay. Bars represent the mean ± SEM (n=4-5) relative luciferase units. (B) XTC-2 cells were transfected with mouse and frog *Klf9* synergy module promoter- luciferase constructs. Cells were treated with 5 nM T_3, 100 nM CORT or T_3 plus CORT for 4 h before harvest and analysis by dual luciferase assay. Bars represent the mean ± SEM (n=4-5) fold induction and letters above the means indicate significant differences among between hormone treatments (means with the same letter are not significantly different; Tukey's multiple comparison test; $P<0.05$). Dashed lines represent the additive effects of T_3 plus CORT on luciferase activity.

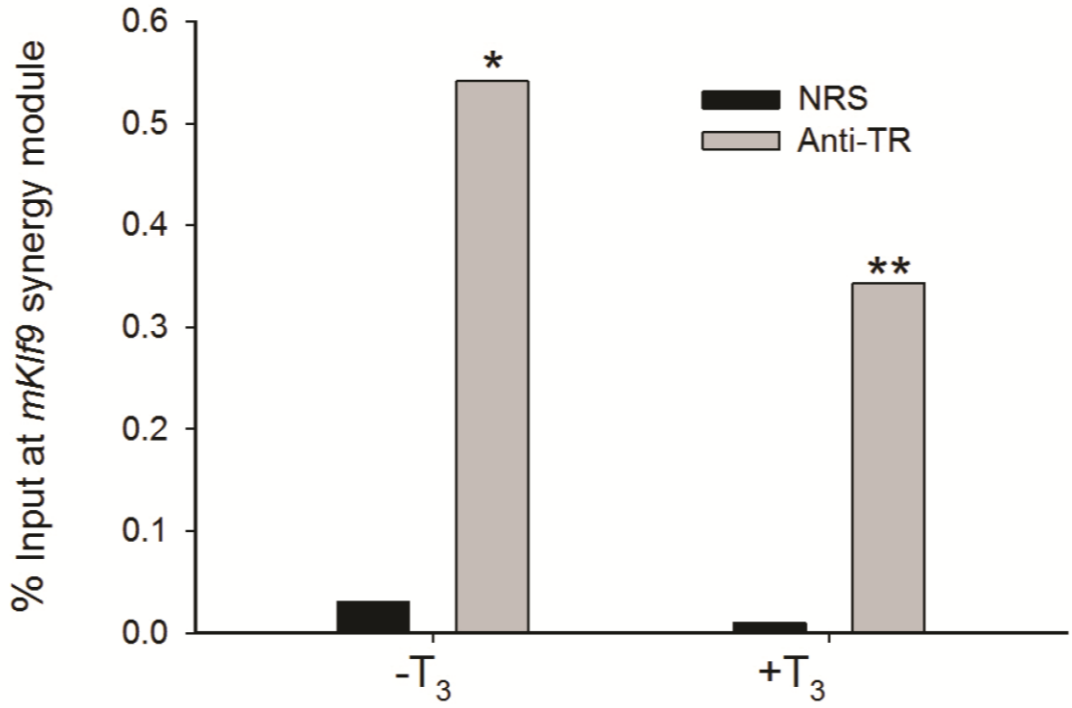

Supplemental Fig 3.5. Thyroid hormone receptor (TR) associates with the synergy module in neuroblastoma cells (N2a[TRβ1]). N2a[TRβ1] cells were treated with or without T_3 (30 nM) for 24 h before harvest for ChIP assay. ChIP samples were analyzed by RTqPCR using TaqMan assays that targeted the synergy module. Bars represent the mean ChIP signals (n=6/ treatment) for TR (anti-TR) and normal rabbit serum (NRS, negative control) expressed as a percentage of the input. Asterisks indicate statistically significant differences between NRS (Control) and TR ChIP signal (*, P<0.05; **, P<0.0001; Student's *t* test).

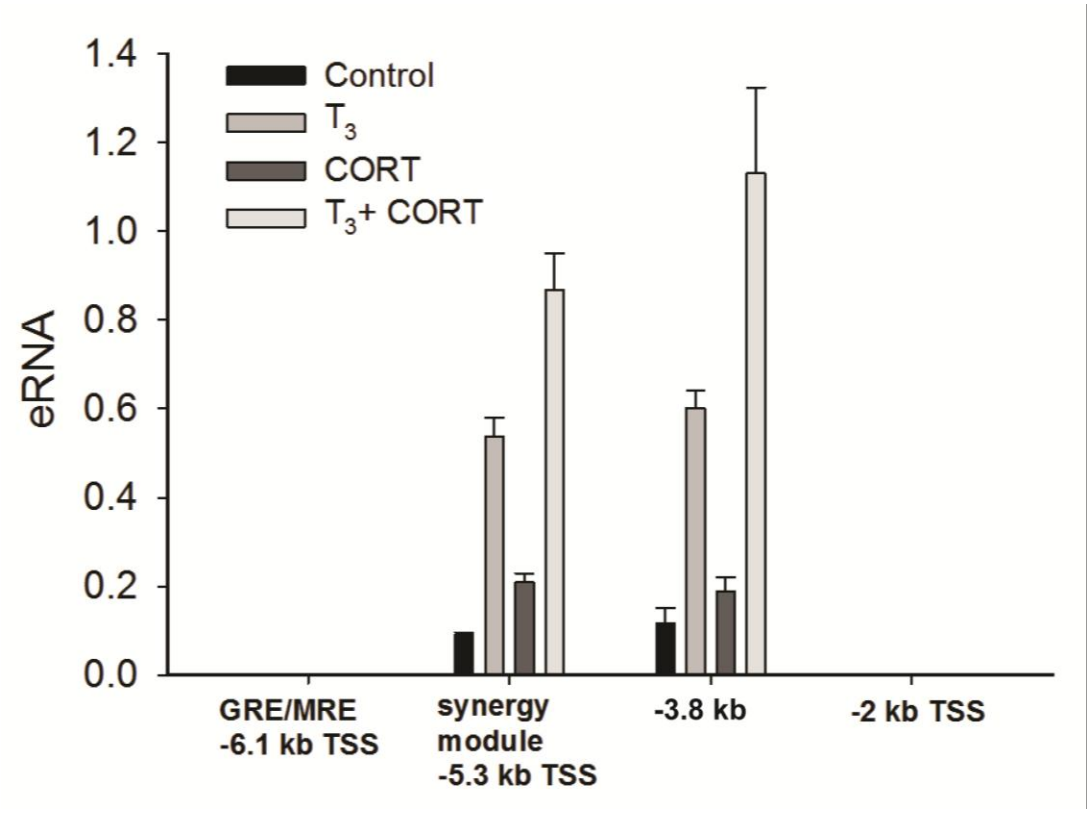

Supplemental Fig. 3.6. (CORT) synergizes with 3,5,3'-triiodothyronine (T_3) to induce transcription at the *Klf9* synergy module and at -3.8 kb TSS. HT-22 cells were treated with 30 nM T_3, 100 nM CORT or T_3 plus CORT for 4h before harvest and RNA extraction. RNA samples were treated with DNAseI and transcripts at the various regions upstream of the TSS were measured by RTqPCR using Taqman assays. RTqPCR without reverse transcriptase was used as a negative control and did not yield any amplicons for any of the assays. RNA transcripts were normalized to the mRNA level of the housekeeping gene *GAPDH*. Bars represent the mean $\pm$ SEM and letters above the means indicate significant differences among treatments (means with the same letter are not significantly different; Tukey's multiple comparison test; $P<0.05$). Dashed lines represent the additive effects of T_3 plus CORT on *Klf9* eRNA levels.

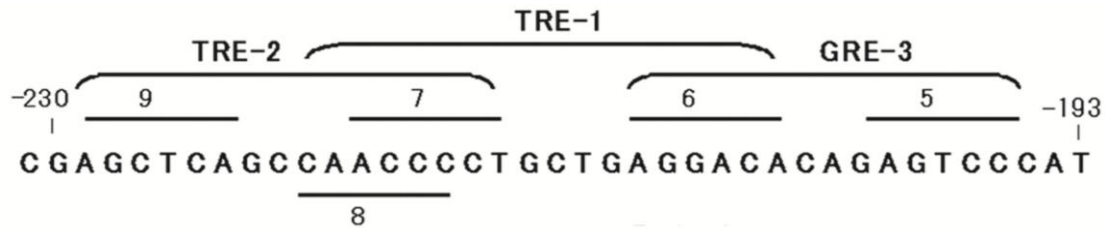

Supplemental Fig. 3.7. **Putative hormone response elements in the 5′-flanking region of the rat GHRH-R gene**. Localizations of putative GREs and TRE in the 5′-flanking region of the rat GHRH-R gene are shown. The hexamer half-sites of hormone response elements are tentatively numbered from 1 through 9 (only 5-9 are shown). GRE-3 (5 and 6) contains 7, 8, or 7 of 12 nucleotides identical to the consensus GRE (GGTACAnnnTGTTCT), respectively. TRE-1, consists of half-sites 6 and 8, appears to be an inverted palindrom-like sequence, and TRE-2 consists of half-sites 7 and 9 appears to be a palindromic TRE. Taken and modified from Nogami H et al. Endocrinology 2002;143:1318-1326.

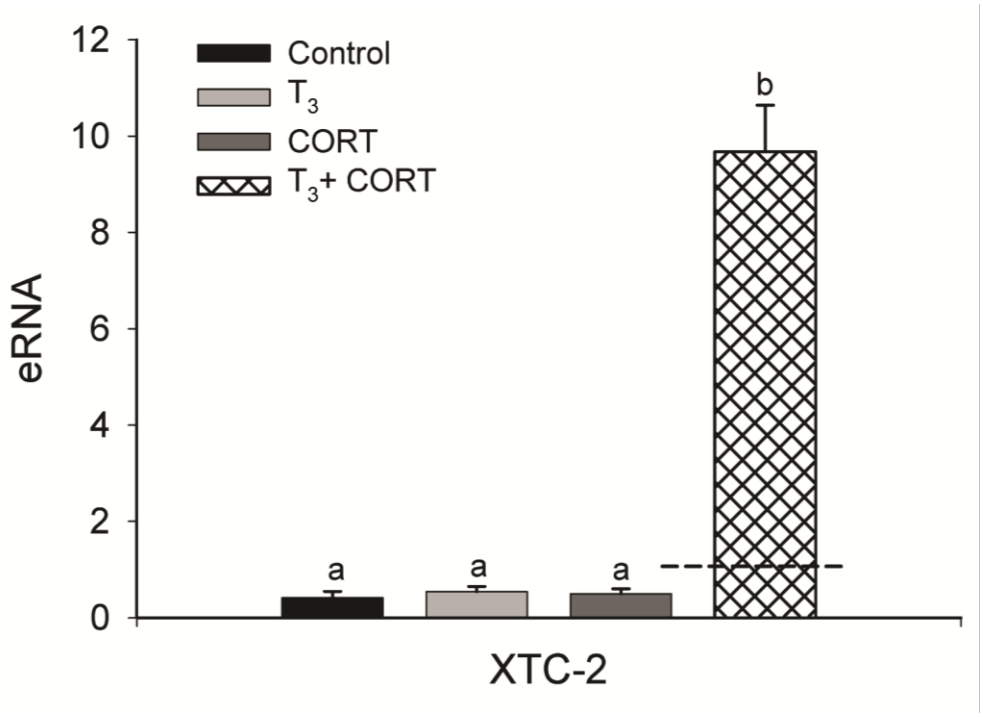

Supplemental Fig. 3.8. Hormone dependent induction of frog *Klf9* eRNA. XTC-2 cells were treated with 5 nM T_3, 100 nM CORT or T_3 plus CORT for 4h before harvest and RNA extraction. RNA samples were treated with DNAseI and transcripts measured by RTqPCR using Taqman assays targeted to the frog *Klf9* synergy module. RTqPCR without reverse transcriptase was used as a negative control and did not yield any amplicons for any of the assays. RNA transcripts were normalized to the mRNA level of the housekeeping gene *rpL8*. Bars represent the mean $\pm$ SEM and letters above the means indicate significant differences among treatments (means with the same letter are not significantly different; Tukey's multiple comparison test; $P<0.05$). Dashed lines represent the additive effects of T_3 plus CORT on frog *Klf9* eRNA l

APPENDIX C

Supplemental Tables for Chapter 4

Supplemental Table 4.1. Complete list of genes upregulated by 4h of T_3 treatment in HT-22 cells.

PROBE ID	SYMBOL	DEFINITION	P value	Fold change
ILMN_1254031	**Klf9**	Mus musculus Kruppel-like factor 9 (Klf9), mRNA.	0	3.09
ILMN_1220280	**Tas1r1**	Mus musculus taste receptor, type 1, member 1 (Tas1r1), mRNA.	0	2.68
ILMN_1232601	**Cyb561**	Mus musculus cytochrome b-561 (Cyb561), mRNA.	0	2.61
ILMN_2430906	**2310051E17Rik**	PREDICTED: Mus musculus RIKEN cDNA 2310051E17 gene (2310051E17Rik), mRNA.	0.00009	2.23
ILMN_1229547	**Spon2**	Mus musculus spondin 2, extracellular matrix protein (Spon2), mRNA.	0	1.93
ILMN_2616226	**Dbp**	Mus musculus D site albumin promoter binding protein (Dbp), mRNA.	0	1.79
ILMN_2484932	**C030002B11Rik**		0	1.74
ILMN_3127391	**Npr3**	Mus musculus natriuretic peptide receptor 3 (Npr3), transcript variant 1, mRNA.	0	1.59
ILMN_1217117	**Cdon**		0	1.51
ILMN_2420341	**9629514_325**		0.02144	1.5
ILMN_2457585	**Trp53inp2**	Mus musculus transformation related protein 53 inducible nuclear protein 2 (Trp53inp2), mRNA.	0	1.49
ILMN_1243564	**Plekha1**	Mus musculus pleckstrin homology domain containing, family A (phosphoinositide binding specific) member 1 (Plekha1), mRNA.	0	1.48
ILMN_1253191	**E230024B12Rik**		0	1.48
ILMN_2708877	**Plekha1**	Mus musculus pleckstrin homology domain containing, family A (phosphoinositide binding specific) member 1 (Plekha1), mRNA.	0	1.47
ILMN_2812215	**Plekhg5**	Mus musculus pleckstrin homology domain containing, family G (with RhoGef domain) member 5 (Plekhg5), mRNA.	0.00009	1.46
ILMN_2918002	**Gbp3**	Mus musculus guanylate nucleotide binding protein 3 (Gbp3), mRNA.	0.00276	1.46
ILMN_1246733	**Gm22**	PREDICTED: Mus musculus gene model 22, (NCBI) (Gm22), mRNA.	0	1.43
ILMN_2517631	**SV40_small_t_Ag_specific**		0.01358	1.42
ILMN_1255967	**B430216N15Rik**		0.01463	1.41
ILMN_2772155	**LOC100045780**	PREDICTED: Mus musculus similar to metalloprotease-disintegrin meltrin beta (LOC100045780), mRNA.	0.005	1.41
ILMN_2966104	**Htra1**	Mus musculus HtrA serine peptidase 1 (Htra1), mRNA.	0	1.38
ILMN_2746738	**Htra1**	Mus musculus HtrA serine peptidase 1 (Htra1), mRNA.	0	1.37

ILMN_2433213	**Klf7**		0	1.37
ILMN_2482756	**Usf2**	Mus musculus upstream transcription factor 2 (Usf2), mRNA.	0.00049	1.36
ILMN_2702193	**Mxra7**	Mus musculus matrix-remodelling associated 7 (Mxra7), mRNA.	0	1.36
ILMN_2833163	**BC064033**	Mus musculus cDNA sequence BC064033 (BC064033), mRNA.	0.01817	1.36
ILMN_1229082	**Klhl21**	Mus musculus kelch-like 21 (Drosophila) (Klhl21), mRNA.	0.00002	1.35
ILMN_2618364	**Flnc**	Mus musculus filamin C, gamma (Flnc), mRNA.	0.00994	1.35
ILMN_2604333	**Npr3**		0	1.34
ILMN_2485408	**9626962_3**		0.00001	1.34
ILMN_1227465	**9628654_5**		0.00509	1.34
ILMN_2976191	**Stat5a**	Mus musculus signal transducer and activator of transcription 5A (Stat5a), mRNA.	0.00005	1.34
ILMN_2433848	**Slco2a1**		0	1.34
ILMN_2685329	**Hspg2**	PREDICTED: Mus musculus perlecan (heparan sulfate proteoglycan 2) (Hspg2), mRNA.	0	1.33
ILMN_2510383	**Tnfrsf25**	Mus musculus tumor necrosis factor receptor superfamily, member 25 (Tnfrsf25), mRNA.	0.00116	1.33
ILMN_1253661	**Plekhg5**	Mus musculus pleckstrin homology domain containing, family G (with RhoGef domain) member 5 (Plekhg5), mRNA.	0.02109	1.32
ILMN_2625920	**Aoc3**	Mus musculus amine oxidase, copper containing 3 (Aoc3), mRNA.	0	1.32
ILMN_2424299	**Tnfrsf12a**	Mus musculus tumor necrosis factor receptor superfamily, member 12a (Tnfrsf12a), mRNA.	0.00263	1.32
ILMN_2422982	**Synpo**		0	1.32
ILMN_1244513	**Gbp3**	Mus musculus guanylate binding protein 3 (Gbp3), mRNA.	0	1.31
ILMN_3091641	**Dab2**	Mus musculus disabled homolog 2 (Drosophila) (Dab2), transcript variant 2, mRNA.	0.00184	1.31
ILMN_2961216	**Slco2a1**	Mus musculus solute carrier organic anion transporter family, member 2a1 (Slco2a1), mRNA.	0.00001	1.31
ILMN_1220443	**LOC381002**	PREDICTED: Mus musculus hypothetical LOC381002 (LOC381002), misc RNA.	0.01517	1.31
ILMN_2834344	**2610029G23Rik**	Mus musculus RIKEN cDNA 2610029G23 gene (2610029G23Rik), mRNA.	0.00842	1.3
ILMN_2420956	**Dysf**	Mus musculus dysferlin (Dysf), transcript variant 1, mRNA.	0	1.29
ILMN_2707308	**Cct5**	Mus musculus chaperonin containing Tcp1, subunit 5 (epsilon) (Cct5), mRNA.	0.0194	1.29
ILMN_3156010	**Pdzrn3**	Mus musculus PDZ domain containing RING finger 3 (Pdzrn3), mRNA.	0.00001	1.29
ILMN_1225880	**Srm**	Mus musculus spermidine synthase (Srm), mRNA.	0.00764	1.29
ILMN_2690122	**Slc27a1**		0.02185	1.29
ILMN_2977903	**BC057627**	Mus musculus cDNA sequence BC057627 (BC057627), mRNA.	0	1.29
ILMN_1230423	**Sh3pxd2b**	Mus musculus SH3 and PX domains 2B (Sh3pxd2b), mRNA.	0.0012	1.29
ILMN_2508910	**Tpst2**		0.00568	1.28
ILMN_2520249	**Hspg2**		0.00556	1.28
ILMN_2602185	**40795**	Mus musculus septin 9 (Sept9), mRNA.	0.00201	1.28

ILMN_2448651	**Ampd3**	Mus musculus adenosine monophosphate deaminase 3 (Ampd3), mRNA.	0.00002	1.28
ILMN_1251426	**Klf7**	Mus musculus Kruppel-like factor 7 (ubiquitous) (Klf7), mRNA.	0	1.27
ILMN_2822579	**Col4a2**	Mus musculus collagen, type IV, alpha 2 (Col4a2), mRNA.	0.03754	1.27
ILMN_2712634	**Nab1**	Mus musculus Ngfi-A binding protein 1 (Nab1), mRNA.	0.026	1.26
ILMN_2466021	**Hivep3**		0.00052	1.26
ILMN_2791272	**Por**	Mus musculus P450 (cytochrome) oxidoreductase (Por), mRNA.	0.00043	1.26
ILMN_2543851	**Sec62**	Mus musculus SEC62 homolog (S. cerevisiae) (Sec62), mRNA.	0.04672	1.26
ILMN_2728118	**Rrp12**	Mus musculus ribosomal RNA processing 12 homolog (S. cerevisiae) (Rrp12), mRNA.	0.02611	1.26
ILMN_3162239	**Prr7**	Mus musculus proline rich 7 (synaptic) (Prr7), mRNA.	0.04194	1.25
ILMN_1242125	**Plekhg5**	Mus musculus pleckstrin homology domain containing, family G (with RhoGef domain) member 5 (Plekhg5), mRNA.	0.00914	1.25
ILMN_1241890	**Klf7**		0.00267	1.25
ILMN_2677921	**Vasn**	Mus musculus vasorin (Vasn), mRNA.	0.00001	1.25
ILMN_2931384	**Lrrc59**	Mus musculus leucine rich repeat containing 59 (Lrrc59), mRNA.	0.00388	1.25
ILMN_2681776	**Mapk6**	Mus musculus mitogen-activated protein kinase 6 (Mapk6), transcript variant 2, mRNA.	0	1.25
ILMN_3031099	**Coq10b**	Mus musculus coenzyme Q10 homolog B (S. cerevisiae) (Coq10b), transcript variant 1, mRNA.	0.00781	1.25
ILMN_2526333	**LOC381284**		0.03845	1.25
ILMN_2886981	**Tm6sf1**	Mus musculus transmembrane 6 superfamily member 1 (Tm6sf1), mRNA.	0.03805	1.25
ILMN_2843782	**Tpst2**	Mus musculus protein-tyrosine sulfotransferase 2 (Tpst2), mRNA.	0.00003	1.24
ILMN_3109360	**Plec1**	Mus musculus plectin 1 (Plec1), transcript variant 11, mRNA.	0	1.24
ILMN_1216597	**Slc25a25**	Mus musculus solute carrier family 25 (mitochondrial carrier, phosphate carrier), member 25 (Slc25a25), nuclear gene encoding mitochondrial protein, mRNA.	0.00026	1.24
ILMN_2496537	**Npr3**	Mus musculus natriuretic peptide receptor 3 (Npr3), transcript variant 2, mRNA.	0.03378	1.24
ILMN_2903351	**Leo1**	Mus musculus Leo1, Paf1/RNA polymerase II complex component, homolog (S. cerevisiae) (Leo1), mRNA.	0.00009	1.24
ILMN_2735118	**Pprc1**	Mus musculus peroxisome proliferative activated receptor, gamma, coactivator-related 1 (Pprc1), mRNA.	0.04014	1.24
ILMN_2714565	**Rrm2**		0.02662	1.24
ILMN_2422014	**LOC100040353**	PREDICTED: Mus musculus similar to splicing coactivator subunit SRm300 (LOC100040353), mRNA.	0.03244	1.24
ILMN_2920200	**Heg1**	Mus musculus HEG homolog 1 (zebrafish) (Heg1), mRNA.	0.0319	1.24
ILMN_2743831	**Pepd**	Mus musculus peptidase D (Pepd), mRNA.	0.04898	1.23
ILMN_1237197	**Nrp1**	Mus musculus neuropilin 1 (Nrp1), mRNA.	0	1.23
ILMN_2669912	**Nrp1**	Mus musculus neuropilin 1 (Nrp1), mRNA.	0.01505	1.23
ILMN_2870487	**Cpne2**	Mus musculus copine II (Cpne2), mRNA.	0.00004	1.23
ILMN_2961221	**Slco2a1**	Mus musculus solute carrier organic anion transporter family, member 2a1 (Slco2a1), mRNA.	0.0012	1.23

ILMN_2920736	**Bbc3**	Mus musculus BCL2 binding component 3 (Bbc3), mRNA.	0.00214	1.23
ILMN_2622983	**Dusp1**	Mus musculus dual specificity phosphatase 1 (Dusp1), mRNA.	0.03329	1.23
ILMN_3023230	**Jmjd3**	Mus musculus jumonji domain containing 3 (Jmjd3), mRNA.	0.04144	1.23
ILMN_2908056	**Tmbim1**	Mus musculus transmembrane BAX inhibitor motif containing 1 (Tmbim1), mRNA.	0.02362	1.23
ILMN_2732317	**Pik3r2**	Mus musculus phosphatidylinositol 3-kinase, regulatory subunit, polypeptide 2 (p85 beta) (Pik3r2), mRNA.	0.02466	1.22
ILMN_2592554	**Rexo1**	Mus musculus REX1, RNA exonuclease 1 homolog (S. cerevisiae) (Rexo1), transcript variant 1, mRNA.	0.03212	1.22
ILMN_2644845	**Trmt6**	Mus musculus tRNA methyltransferase 6 homolog (S. cerevisiae) (Trmt6), mRNA.	0.02571	1.22
ILMN_2987863	**Per2**	Mus musculus period homolog 2 (Drosophila) (Per2), mRNA.	0.01388	1.22
ILMN_1243077	**Peo1**	Mus musculus progressive external ophthalmoplegia 1 (human) (Peo1), mRNA.	0.03554	1.22
ILMN_3095624	**Jmjd3**	Mus musculus jumonji domain containing 3 (Jmjd3), mRNA.	0.00816	1.22
ILMN_2460062	**Atl2**	Mus musculus atlastin GTPase 2 (Atl2), transcript variant 1, mRNA.	0.04075	1.22
ILMN_1255871	**Loxl1**	Mus musculus lysyl oxidase-like 1 (Loxl1), mRNA.	0	1.22
ILMN_2598103	**Emp2**	Mus musculus epithelial membrane protein 2 (Emp2), mRNA.	0	1.22
ILMN_1250969	**LOC100047016**	PREDICTED: Mus musculus similar to GCN1 general control of amino-acid synthesis 1-like 1 (LOC100047016), mRNA.	0.02208	1.22
ILMN_2751072	**Gna11**		0.02043	1.22
ILMN_2714031	**Errfi1**	Mus musculus ERBB receptor feedback inhibitor 1 (Errfi1), mRNA.	0.0324	1.21
ILMN_1258148	**Inppl1**	Mus musculus inositol polyphosphate phosphatase-like 1 (Inppl1), mRNA.	0.02449	1.21
ILMN_1220243	**LOC385644**		0.01038	1.21
ILMN_2554000	**5930429A15Rik**		0.01087	1.21
ILMN_2674822	**Nt5c2**	Mus musculus 5'-nucleotidase, cytosolic II (Nt5c2), mRNA.	0.00835	1.21
ILMN_3147112	**Mapk6**	Mus musculus mitogen-activated protein kinase 6 (Mapk6), transcript variant 2, mRNA.	0.00977	1.21
ILMN_2596278	**Tcfe2a**		0.03226	1.21
ILMN_2772027	**2410016O06Rik**		0.01228	1.21
ILMN_3121255	**Vegfa**	Mus musculus vascular endothelial growth factor A (Vegfa), transcript variant 1, mRNA.	0.00156	1.21
ILMN_2972325	**2410016O06Rik**	Mus musculus RIKEN cDNA 2410016O06 gene (2410016O06Rik), mRNA.	0.0064	1.21
ILMN_2761046	**Slc25a33**	Mus musculus solute carrier family 25, member 33 (Slc25a33), mRNA.	0.01667	1.21
ILMN_2614853	**6720458F09Rik**	Mus musculus RIKEN cDNA 6720458F09 gene (6720458F09Rik), mRNA.	0.00003	1.21
ILMN_2729103	**Adamts2**	Mus musculus a disintegrin-like and metallopeptidase (reprolysin type) with thrombospondin type 1 motif, 2 (Adamts2), mRNA.	0.00034	1.2
ILMN_2701534	**Ampd2**	Mus musculus adenosine monophosphate deaminase 2 (isoform L) (Ampd2), mRNA.	0.00213	1.2
ILMN_3157483	**Ets1**	Mus musculus E26 avian leukemia oncogene 1, 5' domain (Ets1), transcript variant 2, mRNA.	0.02902	1.2

ILMN_2955973	**Smtn**	Mus musculus smoothelin (Smtn), mRNA.	0.00003	1.2

Supplemental Table 4.2. Complete list of genes downregulated by 4h of T_3 treatment in HT-22 cells.

PROBE ID	SYMBOL	DEFINITION	P value	Fold change
ILMN_2606667	**Ddx6**	Mus musculus DEAD (Asp-Glu-Ala-Asp) box polypeptide 6 (Ddx6), mRNA.	0.0318	-1.72
ILMN_2654822	**Chd4**	Mus musculus chromodomain helicase DNA binding protein 4 (Chd4), mRNA.	0.0072	-1.49
ILMN_1230786	**5730588I11Rik**		0.01204	-1.47
ILMN_1253178	**Aldh3a1**	Mus musculus aldehyde dehydrogenase family 3, subfamily A1 (Aldh3a1), mRNA.	0	-1.47
ILMN_2543842	**2810417K24Rik**		0.03291	-1.46
ILMN_1230788	**Tle1**	Mus musculus transducin-like enhancer of split 1, homolog of Drosophila E(spl) (Tle1), mRNA. XM_984202 XM_984240 XM_984277 XM_984316 XM_984359 XM_984397 XM_984426 XM_984456 XM_984492 XM_984530	0	-1.44
ILMN_1237565	**EG626367**	PREDICTED: Mus musculus predicted gene, EG626367 (EG626367), misc RNA.	0	-1.44
ILMN_1256844	**EG668850**	PREDICTED: Mus musculus predicted gene, EG668850 (EG668850), misc RNA.	0	-1.42
ILMN_1235652	**Usp37**	Mus musculus ubiquitin specific peptidase 37 (Usp37), mRNA.	0.00158	-1.41
ILMN_1241320	**Clspn**	Mus musculus claspin homolog (Xenopus laevis) (Clspn), mRNA.	0.00029	-1.41
ILMN_1243988	**LOC269251**		0.00022	-1.41
ILMN_3031781	**Arid5b**	Mus musculus AT rich interactive domain 5B (MRF1-like) (Arid5b), mRNA.	0.01249	-1.39
ILMN_1248733	**Pa2g4**	Mus musculus proliferation-associated 2G4 (Pa2g4), mRNA.	0.03204	-1.36
ILMN_1254307	**1810011O10Rik**	Mus musculus RIKEN cDNA 1810011O10 gene (1810011O10Rik), mRNA.	0.00027	-1.35
ILMN_1219839	**mtDNA_ND6**		0	-1.35
ILMN_2682279	**Gkap1**	Mus musculus G kinase anchoring protein 1 (Gkap1), mRNA.	0.02019	-1.35
ILMN_3038404	**Tcf25**	Mus musculus transcription factor 25 (basic helix-loop-helix) (Tcf25), transcript variant 3, mRNA.	0.0094	-1.34
ILMN_2710678	**Nfic**		0.04947	-1.34
ILMN_1255731	**Dnm3os**	Mus musculus dynamin 3, opposite strand (Dnm3os), non-coding RNA.	0.01697	-1.33
ILMN_2741677	**Bach1**	Mus musculus BTB and CNC homology 1 (Bach1), mRNA.	0.03548	-1.32
ILMN_2874853	**Eef1b2**	Mus musculus eukaryotic translation elongation factor 1 beta 2 (Eef1b2), mRNA.	0.04617	-1.31
ILMN_1259322	**Pdk4**	Mus musculus pyruvate dehydrogenase kinase, isoenzyme 4 (Pdk4), mRNA.	0	-1.31
ILMN_1230726	**5430406J06Rik**		0.01611	-1.31
ILMN_2529519	**LOC230592**		0.02703	-1.3
ILMN_2568488	**A530089A20Rik**		0.0165	-1.3
ILMN_1260447	**LOC100043192**	PREDICTED: Mus musculus similar to ribosomal protein L31 (LOC100043192), mRNA.	0	-1.29

ILMN_1259379	**Pdzd11**	Mus musculus PDZ domain containing 11 (Pdzd11), mRNA.	0.00092	-1.29
ILMN_1234196	**6030458C11 Rik**		0.03797	-1.29
ILMN_1233064	**Cdk2**	Mus musculus cyclin-dependent kinase 2 (Cdk2), transcript variant 1, mRNA.	0.00158	-1.29
ILMN_2819841	**Rpl7a**	Mus musculus ribosomal protein L7a (Rpl7a), mRNA.	0	-1.29
ILMN_2497068	**Zmynd11**	Mus musculus zinc finger, MYND domain containing 11 (Zmynd11), mRNA.	0.01111	-1.28
ILMN_1239542	**Raet1c**	Mus musculus retinoic acid early transcript gamma (Raet1c), mRNA.	0.00022	-1.28
ILMN_1232121	**Zeb2**	Mus musculus zinc finger E-box binding homeobox 2 (Zeb2), transcript variant 2, mRNA.	0.00004	-1.28
ILMN_1229544	**LOC100041569**	PREDICTED: Mus musculus hypothetical protein LOC100041569 (LOC100041569), mRNA.	0.03083	-1.27
ILMN_1246772	**B430305P08 Rik**		0.01052	-1.27
ILMN_1252004	**Itpripl2**	Mus musculus inositol 1,4,5-triphosphate receptor interacting protein-like 2 (Itpripl2), mRNA.	0.00062	-1.27
ILMN_2670271	**Rshl2a**	Mus musculus radial spokehead-like 2A (Rshl2a), mRNA.	0.00247	-1.26
ILMN_1250195	**Ndrg1**	Mus musculus N-myc downstream regulated gene 1 (Ndrg1), mRNA.	0.00828	-1.26
ILMN_1253691	**B430201A12 Rik**	PREDICTED: Mus musculus RIKEN cDNA B430201A12 gene (B430201A12Rik), mRNA.	0.0028	-1.26
ILMN_1218703	**4930402H24 Rik**	Mus musculus RIKEN cDNA 4930402H24 gene (4930402H24Rik), mRNA.	0.00226	-1.26
ILMN_2688728	**Pcyt1a**	Mus musculus phosphate cytidylyltransferase 1, choline, alpha isoform (Pcyt1a), mRNA.	0.0228	-1.26
ILMN_2869623	**6330503C03 Rik**	Mus musculus RIKEN cDNA 6330503C03 gene (6330503C03Rik), mRNA.	0	-1.25
ILMN_1253322	**Tex261**	Mus musculus testis expressed gene 261 (Tex261), mRNA.	0.01516	-1.25
ILMN_2692421	**Ciz1**	Mus musculus CDKN1A interacting zinc finger protein 1 (Ciz1), mRNA.	0.03611	-1.25
ILMN_2645448	**Armcx1**	Mus musculus armadillo repeat containing, X-linked 1 (Armcx1), mRNA.	0.04394	-1.25
ILMN_1220813	**Dtx3l**	Mus musculus deltex 3-like (Drosophila) (Dtx3l), mRNA.	0.00001	-1.25
ILMN_1231686	**Kat2b**	Mus musculus K(lysine) acetyltransferase 2B (Kat2b), mRNA.	0.00415	-1.25
ILMN_2914036	**Zfp607**	Mus musculus zinc finger proten 607 (Zfp607), mRNA.	0.0132	-1.24
ILMN_2543630	**4933439C20 Rik**		0.00504	-1.24
ILMN_2669289	**Htra4**	Mus musculus HtrA serine peptidase 4 (Htra4), mRNA.	0.0145	-1.24
ILMN_2846775	**Cdkn1a**	Mus musculus cyclin-dependent kinase inhibitor 1A (P21) (Cdkn1a), mRNA.	0.00161	-1.24
ILMN_2684909	**Sirt6**	Mus musculus sirtuin 6 (silent mating type information regulation 2, homolog) 6 (S. cerevisiae) (Sirt6), mRNA.	0.03157	-1.24
ILMN_2623112	**Fam168a**	Mus musculus family with sequence similarity 168, member A (Fam168a), mRNA.	0.00487	-1.24
ILMN_2525034	**Cc1**		0.04732	-1.24
ILMN_2936118	**Rpl24**	Mus musculus ribosomal protein L24 (Rpl24), mRNA.	0.00042	-1.24
ILMN_1251984	**C730026J16**		0.00021	-1.24

ILMN_2677065	**4930519N13 Rik**	Mus musculus RIKEN cDNA 4930519N13 gene (4930519N13Rik), mRNA.	0.02432	-1.24
ILMN_1239608	**Arid4a**	Mus musculus AT rich interactive domain 4A (RBP1-like) (Arid4a), mRNA.	0.03768	-1.24
ILMN_1260532	**Jarid1a**	PREDICTED: Mus musculus jumonji, AT rich interactive domain 1A (Rbp2 like), transcript variant 1 (Jarid1a), mRNA.	0.01916	-1.23
ILMN_1245246	**Peg3**	Mus musculus paternally expressed 3 (Peg3), mRNA.	0.00073	-1.23
ILMN_2612238	**2210010L05 Rik**	Mus musculus RIKEN cDNA 2210010L05 gene (2210010L05Rik), transcript variant 1, mRNA.	0.04662	-1.23
ILMN_1228387	**Casp2**		0.03211	-1.22
ILMN_1218543	**2310051N18 Rik**	PREDICTED: Mus musculus RIKEN cDNA 2310051N18 gene, transcript variant 1 (2310051N18Rik), mRNA.	0.03898	-1.22
ILMN_1248357	**LOC100046844**	PREDICTED: Mus musculus similar to transmembrane protein 35 (LOC100046844), mRNA.	0.02197	-1.22
ILMN_2778122	**Pdcd4**	Mus musculus programmed cell death 4 (Pdcd4), mRNA.	0.00041	-1.22
ILMN_2769772	**Pik3ip1**	Mus musculus phosphoinositide-3-kinase interacting protein 1 (Pik3ip1), mRNA.	0.00466	-1.22
ILMN_1212982	**Zfp318**	Mus musculus zinc finger protein 318 (Zfp318), transcript variant 1, mRNA.	0.02129	-1.22
ILMN_2595967	**LOC100039532**	PREDICTED: Mus musculus similar to ribosomal protein L35a (LOC100039532), mRNA.	0.00044	-1.22
ILMN_3158725	**Raet1b**	Mus musculus retinoic acid early transcript beta (Raet1b), mRNA.	0.0278	-1.22
ILMN_1255869	**Catnb**		0.0391	-1.22
ILMN_3112873	**Txnip**	Mus musculus thioredoxin interacting protein (Txnip), transcript variant 1, mRNA.	0	-1.22
ILMN_1225552	**Arsa**	Mus musculus arylsulfatase A (Arsa), mRNA.	0.00019	-1.21
ILMN_2650732	**Taf15**	Mus musculus TAF15 RNA polymerase II, TATA box binding protein (TBP)-associated factor (Taf15), mRNA.	0.00025	-1.21
ILMN_2754253	**Gna13**		0.00001	-1.21
ILMN_2944601	**4933439C20 Rik**	Mus musculus RIKEN cDNA 4933439C20 gene (4933439C20Rik), mRNA.	0.00303	-1.21
ILMN_2717613	**Cdk2**		0.02192	-1.21
ILMN_2662803	**Ptx3**	Mus musculus pentraxin related gene (Ptx3), mRNA.	0.0473	-1.21
ILMN_2718030	**Ank2**	Mus musculus ankyrin 2, brain (Ank2), transcript variant 3, mRNA.	0.01731	-1.21
ILMN_1221341	**LOC100047226**	PREDICTED: Mus musculus hypothetical protein LOC100047226 (LOC100047226), misc RNA.	0.00046	-1.21
ILMN_1253237	**Pdcd4**	Mus musculus programmed cell death 4 (Pdcd4), mRNA.	0.00909	-1.21
ILMN_1256285	**Siat7b**		0.03813	-1.21
ILMN_2481389	**Zfp326**	Mus musculus zinc finger protein 326 (Zfp326), mRNA.	0.00717	-1.21
ILMN_2632940	**Sumo1**		0.00075	-1.2
ILMN_1215661	**Traf2**	Mus musculus Tnf receptor-associated factor 2 (Traf2), mRNA.	0.00525	-1.2
ILMN_2849753	**Erich1**	Mus musculus glutamate-rich 1 (Erich1), mRNA.	0.00044	-1.2
ILMN_2958076	**1110001J03Rik**	Mus musculus RIKEN cDNA 1110001J03 gene (1110001J03Rik), mRNA.	0.00353	-1.2

ILMN_1231586	**Sertad2**	Mus musculus SERTA domain containing 2 (Sertad2), transcript variant 1, mRNA.	0.00316	-1.2

Supplemental Table 4.3. Complete list of genes upregulated by 4h of CORT treatment in HT-22 cells.

PROBE ID	SYMBOL	DEFINITION	P value	Fold change
ILMN_2701664	**Tsc22d3**	Mus musculus TSC22 domain family, member 3 (Tsc22d3), transcript variant 2, mRNA.	0	8.82
ILMN_3150811	**Tsc22d3**	Mus musculus TSC22 domain family, member 3 (Tsc22d3), transcript variant 1, mRNA.	0	5.41
ILMN_1259322	**Pdk4**	Mus musculus pyruvate dehydrogenase kinase, isoenzyme 4 (Pdk4), mRNA.	0	5.02
ILMN_2813484	**Per1**	Mus musculus period homolog 1 (Drosophila) (Per1), mRNA.	0	4.64
ILMN_2588249	**S3-12**	Mus musculus plasma membrane associated protein, S3-12 (S3-12), mRNA.	0	4.48
ILMN_2987862	**Per2**	Mus musculus period homolog 2 (Drosophila) (Per2), mRNA.	0	4.21
ILMN_2770894	**Map3k6**		0	3.82
ILMN_2768972	**Fam107a**	Mus musculus family with sequence similarity 107, member A (Fam107a), mRNA.	0	3.8
ILMN_1232601	**Cyb561**	Mus musculus cytochrome b-561 (Cyb561), mRNA.	0	3.78
ILMN_2712075	**Lcn2**	Mus musculus lipocalin 2 (Lcn2), mRNA.	0	3.74
ILMN_2638923	**Rn18s**	Mus musculus 18S RNA (Rn18s), non-coding RNA.	0	3.69
ILMN_1226935	**Orm1**	Mus musculus orosomucoid 1 (Orm1), mRNA.	0	3.44
ILMN_1219154	**Mt2**	Mus musculus metallothionein 2 (Mt2), mRNA.	0	3.4
ILMN_2654074	**Sesn1**	Mus musculus sestrin 1 (Sesn1), mRNA.	0	3.35
ILMN_1232884	**Sphk1**	Mus musculus sphingosine kinase 1 (Sphk1), transcript variant 1, mRNA.	0	3.24
ILMN_2813487	**Per1**	Mus musculus period homolog 1 (Drosophila) (Per1), mRNA.	0	3.06
ILMN_2987863	**Per2**	Mus musculus period homolog 2 (Drosophila) (Per2), mRNA.	0	3.03
ILMN_2822000	**Slc10a6**	Mus musculus solute carrier family 10 (sodium/bile acid cotransporter family), member 6 (Slc10a6), mRNA.	0	3.03
ILMN_3136744	**Sesn1**	Mus musculus sestrin 1 (Sesn1), mRNA.	0	3.02
ILMN_2622983	**Dusp1**	Mus musculus dual specificity phosphatase 1 (Dusp1), mRNA.	0	3.02
ILMN_2517483	**D15Bwg0759e**		0	2.98
ILMN_1226712	**Ccdc134**	Mus musculus coiled-coil domain containing 134 (Ccdc134), mRNA.	0	2.92
ILMN_2637714	**Rasa3**	Mus musculus RAS p21 protein activator 3 (Rasa3), mRNA.	0	2.87
ILMN_1255287	**Mela**		0	2.71
ILMN_2718266	**Fkbp5**	Mus musculus FK506 binding protein 5 (Fkbp5), mRNA.	0	2.67
ILMN_2793062	**Rasl11b**	Mus musculus RAS-like, family 11, member B (Rasl11b), mRNA.	0	2.54
ILMN_2524986	**Ear3**	Mus musculus eosinophil-associated, ribonuclease A family, member 3 (Ear3), mRNA.	0	2.5
ILMN_1230073	**Rn18s**	Mus musculus 18S RNA (Rn18s), non-coding RNA.	0	2.45
ILMN_2765047	**Chrd**	Mus musculus chordin (Chrd), mRNA.	0	2.43
ILMN_2713055	**Psca**	Mus musculus prostate stem cell antigen (Psca), mRNA.	0	2.41

ILMN_2706819	**Rasl11b**	Mus musculus RAS-like, family 11, member B (Rasl11b), mRNA.	0	2.4
ILMN_2665545	**Rin3**	Mus musculus Ras and Rab interactor 3 (Rin3), mRNA.	0	2.36
ILMN_2738345	**Lims2**	Mus musculus LIM and senescent cell antigen like domains 2 (Lims2), mRNA.	0	2.36
ILMN_3059476	**Sesn1**	Mus musculus sestrin 1 (Sesn1), mRNA.	0	2.35
ILMN_1255766	**Sh3bp2**	Mus musculus SH3-domain binding protein 2 (Sh3bp2), mRNA.	0	2.35
ILMN_1243992	**Ptrf**		0	2.35
ILMN_2979237	**Gsta1**	Mus musculus glutathione S-transferase, alpha 1 (Ya) (Gsta1), mRNA.	0	2.32
ILMN_2445165	**Vdr**	Mus musculus vitamin D receptor (Vdr), mRNA.	0	2.32
ILMN_2947292	**Map3k6**	Mus musculus mitogen-activated protein kinase kinase kinase 6 (Map3k6), mRNA.	0	2.31
ILMN_2776850	**Gas7**	Mus musculus growth arrest specific 7 (Gas7), mRNA.	0	2.28
ILMN_2468473	**B230343A10Rik**		0	2.28
ILMN_1224014	**Tmem100**	Mus musculus transmembrane protein 100 (Tmem100), mRNA.	0	2.28
ILMN_2605645	**Gsn**		0	2.25
ILMN_2452855	**1110003O08Rik**		0	2.23
ILMN_1260061	**D17H6S56E-5**	Mus musculus DNA segment, Chr 17, human D6S56E 5 (D17H6S56E-5), mRNA.	0	2.2
ILMN_2430906	**2310051E17Rik**	PREDICTED: Mus musculus RIKEN cDNA 2310051E17 gene (2310051E17Rik), mRNA.	0	2.19
ILMN_2772410	**Anxa4**		0	2.19
ILMN_2733887	**Mknk2**	Mus musculus MAP kinase-interacting serine/threonine kinase 2 (Mknk2), mRNA.	0	2.18
ILMN_1254031	**Klf9**	Mus musculus Kruppel-like factor 9 (Klf9), mRNA.	0	2.17
ILMN_1252259	**LOC384836**		0	2.16
ILMN_2699621	**Dlk2**	Mus musculus delta-like 2 homolog (Drosophila) (Dlk2), mRNA.	0	2.13
ILMN_2666018	**Mgp**	Mus musculus matrix Gla protein (Mgp), mRNA.	0	2.12
ILMN_2727013	**Nr1h4**	Mus musculus nuclear receptor subfamily 1, group H, member 4 (Nr1h4), mRNA.	0	2.11
ILMN_2447100	**D15Mit260**		0	2.1
ILMN_1259787	**Osr1**	Mus musculus odd-skipped related 1 (Drosophila) (Osr1), mRNA.	0	2.08
ILMN_2676052	**Tef**	Mus musculus thyrotroph embryonic factor (Tef), transcript variant 1, mRNA.	0	2.06
ILMN_2692615	**Tgm2**	Mus musculus transglutaminase 2, C polypeptide (Tgm2), mRNA.	0	2.05
ILMN_2678714	**Id4**	Mus musculus inhibitor of DNA binding 4 (Id4), mRNA.	0	2.05
ILMN_2755008	**Nfkbiz**	Mus musculus nuclear factor of kappa light polypeptide gene enhancer in B-cells inhibitor, zeta (Nfkbiz), mRNA.	0	2.02
ILMN_2450735	**Rn18s**	Mus musculus 18S RNA (Rn18s), non-coding RNA.	0	2.01
ILMN_2445166	**Vdr**	Mus musculus vitamin D receptor (Vdr), mRNA.	0	2.01
ILMN_2846255	**Pgpep1**	Mus musculus pyroglutamyl-peptidase I (Pgpep1), mRNA.	0	2
ILMN_1224336	**Spsb1**	Mus musculus splA/ryanodine receptor domain and SOCS box containing 1 (Spsb1), mRNA.	0	1.99

ILMN_1229315	**Tns1**	PREDICTED: Mus musculus tensin 1 (Tns1), mRNA.	0	1.98
ILMN_2653567	**Rhoj**	Mus musculus ras homolog gene family, member J (Rhoj), mRNA.	0	1.96
ILMN_2636624	**Slc10a6**	Mus musculus solute carrier family 10 (sodium/bile acid cotransporter family), member 6 (Slc10a6), mRNA.	0	1.96
ILMN_2669627	**Vcan**	Mus musculus versican (Vcan), transcript variant 1, mRNA.	0	1.95
ILMN_2473531	**Pik3r1**	Mus musculus phosphatidylinositol 3-kinase, regulatory subunit, polypeptide 1 (p85 alpha) (Pik3r1), transcript variant 1, mRNA.	0	1.95
ILMN_2464474	**9430029L20 Rik**		0	1.93
ILMN_2757617	**Il1rl1**	Mus musculus interleukin 1 receptor-like 1 (Il1rl1), transcript variant 2, mRNA.	0	1.93
ILMN_1231096	**2310036D22 Rik**		0.00271	1.93
ILMN_1213954	**Sgk1**	Mus musculus serum/glucocorticoid regulated kinase 1 (Sgk1), mRNA.	0	1.92
ILMN_2480115	**Rgs2**		0.00001	1.92
ILMN_3162452	**Ppm2c**	Mus musculus protein phosphatase 2C, magnesium dependent, catalytic subunit (Ppm2c), nuclear gene encoding mitochondrial protein, transcript variant 1, mRNA.	0	1.92
ILMN_1246800	**Serpina3n**	Mus musculus serine (or cysteine) peptidase inhibitor, clade A, member 3N (Serpina3n), mRNA.	0	1.91
ILMN_3157399	**Tead4**	Mus musculus TEA domain family member 4 (Tead4), transcript variant 2, mRNA.	0	1.91
ILMN_2776922	**Glrx1**		0.0001	1.91
ILMN_1231997	**Gsta1**	Mus musculus glutathione S-transferase, alpha 1 (Ya) (Gsta1), mRNA.	0	1.91
ILMN_1218981	**Aldh1a7**	Mus musculus aldehyde dehydrogenase family 1, subfamily A7 (Aldh1a7), mRNA.	0	1.9
ILMN_1237939	**Prkrir**	Mus musculus protein-kinase, interferon-inducible double stranded RNA dependent inhibitor, repressor of (P58 repressor) (Prkrir), mRNA.	0	1.9
ILMN_1230440	**1700041B20 Rik**		0	1.89
ILMN_2702039	**Cblb**	Mus musculus Casitas B-lineage lymphoma b (Cblb), mRNA. XM_001003462 XM_001003472 XM_001003476 XM_001003639 XM_001003649 XM_156257 XM_902056 XM_902058 XM_917535 XM_924994 XM_924996	0	1.89
ILMN_1215275	**Add1**	Mus musculus adducin 1 (alpha) (Add1), transcript variant 1, mRNA.	0	1.89
ILMN_2942674	**Lims2**	Mus musculus LIM and senescent cell antigen like domains 2 (Lims2), mRNA.	0	1.89
ILMN_3114641	**Pik3r1**	Mus musculus phosphatidylinositol 3-kinase, regulatory subunit, polypeptide 1 (p85 alpha) (Pik3r1), transcript variant 2, mRNA.	0	1.89
ILMN_2588337	**D930015E0 6Rik**		0	1.87
ILMN_3009521	**Foxred2**	Mus musculus FAD-dependent oxidoreductase domain containing 2 (Foxred2), mRNA.	0	1.87
ILMN_1257117	**Nol14**	Mus musculus nucleolar protein 14 (Nol14), mRNA.	0	1.87
ILMN_2622605	**Srr**	Mus musculus serine racemase (Srr), mRNA.	0.00087	1.87
ILMN_2737713	**Edn1**	Mus musculus endothelin 1 (Edn1), mRNA.	0	1.86

ILMN_2666622	**Rgs2**		0	1.86
ILMN_2657636	**Gsta1**		0	1.86
ILMN_1216522	**Nfatc1**	Mus musculus nuclear factor of activated T-cells, cytoplasmic, calcineurin-dependent 1 (Nfatc1), transcript variant 2, mRNA.	0	1.86
ILMN_1247996	**LOC673501**	PREDICTED: Mus musculus hypothetical protein LOC673501 (LOC673501), mRNA.	0	1.85
ILMN_1226587	**EG668300**	PREDICTED: Mus musculus predicted gene, EG668300 (EG668300), mRNA.	0	1.85
ILMN_2763679	**Sipa1l1**	Mus musculus signal-induced proliferation-associated 1 like 1 (Sipa1l1), mRNA.	0	1.85
ILMN_1225994	**Vav2**	Mus musculus vav 2 oncogene (Vav2), mRNA.	0	1.85
ILMN_2675922	**2310047A01 Rik**	PREDICTED: Mus musculus RIKEN cDNA 2310047A01 gene (2310047A01Rik), mRNA.	0	1.84
ILMN_1224842	**LOC385068**		0	1.84
ILMN_2766930	**Faah**	Mus musculus fatty acid amide hydrolase (Faah), mRNA.	0	1.83
ILMN_2473620	**Rsn**		0	1.81
ILMN_2810645	**Ehd2**	Mus musculus EH-domain containing 2 (Ehd2), mRNA.	0	1.79
ILMN_2645208	**Arhgef3**	Mus musculus Rho guanine nucleotide exchange factor (GEF) 3 (Arhgef3), mRNA.	0	1.79
ILMN_2611180	**Ccdc3**		0	1.79
ILMN_2836749	**Rasl12**	Mus musculus RAS-like, family 12 (Rasl12), mRNA.	0	1.79
ILMN_2772632	**Saa3**	Mus musculus serum amyloid A 3 (Saa3), mRNA.	0	1.79
ILMN_1221805	**Dtna**	Mus musculus dystrobrevin alpha (Dtna), transcript variant 2, mRNA.	0	1.79
ILMN_2641816	**Slurp1**	Mus musculus secreted Ly6/Plaur domain containing 1 (Slurp1), mRNA.	0	1.78
ILMN_2602821	**Cdk5rap1**	Mus musculus CDK5 regulatory subunit associated protein 1 (Cdk5rap1), mRNA.	0	1.78
ILMN_2544674	**2310045K21 Rik**		0	1.78
ILMN_2777535	**LOC666053**	PREDICTED: Mus musculus similar to protein tyrosine phosphatase-like protein PTPLB (LOC666053), misc RNA.	0	1.77
ILMN_2491125	**Tbl1xr1**	Mus musculus transducin (beta)-like 1X-linked receptor 1 (Tbl1xr1), mRNA.	0	1.77
ILMN_2619697	**B3gnt9**	Mus musculus UDP-GlcNAc:betaGal beta-1,3-N-acetylglucosaminyltransferase 9 (B3gnt9), mRNA.	0	1.77
ILMN_2599986	**Tead4**	Mus musculus TEA domain family member 4 (Tead4), transcript variant 2, mRNA.	0	1.77
ILMN_1249378	**Bhlhb2**	Mus musculus basic helix-loop-helix domain containing, class B2 (Bhlhb2), mRNA.	0	1.76
ILMN_2885277	**Nnmt**	Mus musculus nicotinamide N-methyltransferase (Nnmt), mRNA.	0	1.76
ILMN_1252450	**LOC380707**		0	1.75
ILMN_2515081	**Trim59**	Mus musculus tripartite motif-containing 59 (Trim59), mRNA.	0	1.75
ILMN_2868480	**Ear4**	Mus musculus eosinophil-associated, ribonuclease A family, member 4 (Ear4), mRNA.	0.00001	1.75
ILMN_2924831	**Gas7**	Mus musculus growth arrest specific 7 (Gas7), mRNA.	0	1.75
ILMN_2420341	**9629514_32 5**		0	1.74

ILMN_2548664	**Loxl4**	Mus musculus lysyl oxidase-like 4 (Loxl4), mRNA.	0	1.74
ILMN_1228919	**St13**	Mus musculus suppression of tumorigenicity 13 (St13), mRNA.	0	1.74
ILMN_2873750	**Gldc**	Mus musculus glycine decarboxylase (Gldc), mRNA.	0	1.73
ILMN_3083163	**Cp**	Mus musculus ceruloplasmin (Cp), transcript variant 2, mRNA.	0	1.73
ILMN_1235932	**Pdgfra**	Mus musculus platelet derived growth factor receptor, alpha polypeptide (Pdgfra), transcript variant 1, mRNA.	0	1.72
ILMN_1218206	**Klf13**	Mus musculus Kruppel-like factor 13 (Klf13), mRNA.	0	1.72
ILMN_1241610	**Adrb2**	Mus musculus adrenergic receptor, beta 2 (Adrb2), mRNA.	0	1.71
ILMN_1258759	**Col6a2**		0	1.71
ILMN_2672190	**Id1**	Mus musculus inhibitor of DNA binding 1 (Id1), mRNA.	0	1.71
ILMN_1232396	**Ear2**	Mus musculus eosinophil-associated, ribonuclease A family, member 2 (Ear2), mRNA.	0.00001	1.71
ILMN_2909782	**Rras2**	Mus musculus related RAS viral (r-ras) oncogene homolog 2 (Rras2), mRNA.	0	1.71
ILMN_2533916	**LOC380655**		0	1.71
ILMN_1248849	**Gsta2**	Mus musculus glutathione S-transferase, alpha 2 (Yc2) (Gsta2), mRNA.	0	1.71
ILMN_2618745	**Supv3l1**	Mus musculus suppressor of var1, 3-like 1 (S. cerevisiae) (Supv3l1), mRNA.	0	1.7
ILMN_2554000	**5930429A15 Rik**		0	1.69
ILMN_1220063	**EG666668**	PREDICTED: Mus musculus predicted gene, EG666668 (EG666668), mRNA.	0	1.69
ILMN_1227951	**Gcnt2**	Mus musculus glucosaminyl (N-acetyl) transferase 2, I-branching enzyme (Gcnt2), transcript variant 3, mRNA.	0	1.69
ILMN_2638299	**Slc29a1**		0	1.69
ILMN_2687032	**Fbxo31**	Mus musculus F-box protein 31 (Fbxo31), mRNA.	0	1.69
ILMN_2707452	**Ebf1**	Mus musculus early B-cell factor 1 (Ebf1), mRNA.	0.00079	1.69
ILMN_1222069	**Bbx**		0.0089	1.69
ILMN_2734142	**Snta1**	Mus musculus syntrophin, acidic 1 (Snta1), mRNA.	0.00043	1.68
ILMN_1247916	**Lims2**	Mus musculus LIM and senescent cell antigen like domains 2 (Lims2), mRNA.	0	1.68
ILMN_2440059	**scl0001533.1_63**		0	1.68
ILMN_1250550	**scl0001259.1_60**		0	1.68
ILMN_1241854	**Lrrc59**	Mus musculus leucine rich repeat containing 59 (Lrrc59), mRNA.	0	1.68
ILMN_2965903	**Hdc**	Mus musculus histidine decarboxylase (Hdc), mRNA.	0	1.68
ILMN_2459899	**Adamtsl4**	Mus musculus ADAMTS-like 4 (Adamtsl4), mRNA.	0	1.68
ILMN_1236037	**LOC627317**	PREDICTED: Mus musculus similar to ribosomal protein L11 (LOC627317), misc RNA.	0	1.68
ILMN_3134632	**Adam22**	Mus musculus a disintegrin and metallopeptidase domain 22 (Adam22), transcript variant 1, mRNA.	0	1.68
ILMN_1220173	**Ppm2c**	Mus musculus protein phosphatase 2C, magnesium dependent, catalytic subunit (Ppm2c), nuclear gene encoding mitochondrial protein, transcript variant 1, mRNA.	0	1.67
ILMN_1254630	**Ptpre**	Mus musculus protein tyrosine phosphatase, receptor type,	0	1.67

		E (Ptpre), mRNA.		
ILMN_1260112	**2400003C14 Rik**	Mus musculus RIKEN cDNA 2400003C14 gene (2400003C14Rik), mRNA.	0.00002	1.67
ILMN_2764143	**Scap**	Mus musculus SREBF chaperone (Scap), mRNA.	0	1.67
ILMN_2724469	**4732473B16 Rik**	Mus musculus RIKEN cDNA 4732473B16 gene (4732473B16Rik), mRNA.	0	1.67
ILMN_1225995	**Morc2a**	Mus musculus microrchidia 2A (Morc2a), mRNA.	0	1.66
ILMN_1220530	**Smc1a**	Mus musculus structural maintenance of chromosomes 1A (Smc1a), mRNA.	0.00003	1.66
ILMN_1223428	**Eif3s8**		0	1.66
ILMN_2655336	**Vcan**	Mus musculus versican (Vcan), transcript variant 1, mRNA.	0	1.65
ILMN_1235435	**LOC666621**	PREDICTED: Mus musculus similar to 40S ribosomal protein S2 (LOC666621), mRNA.	0	1.65
ILMN_2993334	**Plekhf1**	Mus musculus pleckstrin homology domain containing, family F (with FYVE domain) member 1 (Plekhf1), mRNA.	0	1.65
ILMN_2693019	**Acpp**	Mus musculus acid phosphatase, prostate (Acpp), transcript variant 1, mRNA.	0	1.65
ILMN_2762326	**Kif22**	Mus musculus kinesin family member 22 (Kif22), mRNA.	0	1.64
ILMN_2671601	**Selk**		0	1.64
ILMN_2712731	**Phf10**	Mus musculus PHD finger protein 10 (Phf10), mRNA.	0.00005	1.64
ILMN_1377923	**Actb**	Mus musculus actin, beta (Actb), mRNA.	0	1.64
ILMN_1232596	**Pom121**	Mus musculus nuclear pore membrane protein 121 (Pom121), mRNA.	0	1.64
ILMN_2663230	**Slco3a1**	Mus musculus solute carrier organic anion transporter family, member 3a1 (Slco3a1), transcript variant 1, mRNA.	0	1.64
ILMN_2945551	**Ptplb**	Mus musculus protein tyrosine phosphatase-like (proline instead of catalytic arginine), member b (Ptplb), mRNA.	0	1.64
ILMN_2520239	**Cp**		0	1.64
ILMN_2698430	**Bcl2l1**	Mus musculus BCL2-like 1 (Bcl2l1), nuclear gene encoding mitochondrial protein, mRNA.	0.00005	1.64
ILMN_2629191	**Cpm**	PREDICTED: Mus musculus carboxypeptidase M (Cpm), mRNA.	0.00019	1.63
ILMN_2439341	**Vars**	Mus musculus valyl-tRNA synthetase (Vars), nuclear gene encoding mitochondrial protein, mRNA.	0	1.63
ILMN_2619594	**Il11ra1**	Mus musculus interleukin 11 receptor, alpha chain 1 (Il11ra1), mRNA.	0	1.63
ILMN_1222071	**C920004C0 8Rik**		0	1.63
ILMN_1243179	**Sec24d**	Mus musculus Sec24 related gene family, member D (S. cerevisiae) (Sec24d), mRNA.	0.00031	1.63
ILMN_2542885	**Wdr89**	PREDICTED: Mus musculus WD repeat domain 89, transcript variant 2 (Wdr89), mRNA.	0	1.63
ILMN_2683958	**Col3a1**	Mus musculus collagen, type III, alpha 1 (Col3a1), mRNA.	0.00027	1.63
ILMN_1216689	**Aplp2**	Mus musculus amyloid beta (A4) precursor-like protein 2 (Aplp2), transcript variant 3, mRNA.	0	1.62
ILMN_2677567	**Galt**	Mus musculus galactose-1-phosphate uridyl transferase (Galt), mRNA.	0	1.62
ILMN_2961005	**Ier5l**	Mus musculus immediate early response 5-like (Ier5l), mRNA.	0	1.62
ILMN_1222872	**Wbscr16**	Mus musculus Williams-Beuren syndrome chromosome region 16 homolog (human) (Wbscr16), mRNA.	0	1.62

ILMN_2534090	**LOC216443**		0	1.61
ILMN_2594714	**Ets2**	Mus musculus E26 avian leukemia oncogene 2, 3' domain (Ets2), mRNA.	0	1.61
ILMN_2659062	**Add1**		0	1.61
ILMN_2789239	**Tgfbr3**	Mus musculus transforming growth factor, beta receptor III (Tgfbr3), mRNA.	0	1.61
ILMN_1250956	**6330414G02 Rik**		0	1.61
ILMN_1228942	**Cd59a**	Mus musculus CD59a antigen (Cd59a), mRNA.	0	1.61
ILMN_2773540	**Thap4**	Mus musculus THAP domain containing 4 (Thap4), mRNA.	0	1.61
ILMN_1238597	**Omd**	Mus musculus osteomodulin (Omd), mRNA.	0.00002	1.61
ILMN_3159720	**Rin2**	Mus musculus Ras and Rab interactor 2 (Rin2), mRNA.	0	1.61
ILMN_1214120	**1500005N04 Rik**		0	1.6
ILMN_2971479	**Trp53inp1**	Mus musculus transformation related protein 53 inducible nuclear protein 1 (Trp53inp1), mRNA.	0.00239	1.6
ILMN_2846254	**Pgpep1**	Mus musculus pyroglutamyl-peptidase I (Pgpep1), mRNA.	0	1.6
ILMN_1220305	**D19Bwg1357e**	Mus musculus DNA segment, Chr 19, Brigham & Women's Genetics 1357 expressed (D19Bwg1357e), mRNA.	0	1.6
ILMN_2785454	**Hist2h2ab**	Mus musculus histone cluster 2, H2ab (Hist2h2ab), mRNA.	0	1.6
ILMN_2659063	**Add1**	Mus musculus adducin 1 (alpha) (Add1), transcript variant 2, mRNA.	0.00001	1.6
ILMN_2892441	**Gsta4**	Mus musculus glutathione S-transferase, alpha 4 (Gsta4), mRNA.	0	1.59
ILMN_1232416	**Idb4**		0.00002	1.59
ILMN_1215969	**Rcor1**	Mus musculus REST corepressor 1 (Rcor1), mRNA.	0	1.59
ILMN_2728729	**Sdc4**	Mus musculus syndecan 4 (Sdc4), mRNA.	0	1.59
ILMN_2953277	**EG433182**	Mus musculus predicted gene, EG433182 (EG433182), mRNA.	0	1.59
ILMN_2595732	**LOC100046232**	PREDICTED: Mus musculus similar to NFIL3/E4BP4 transcription factor (LOC100046232), mRNA.	0	1.59
ILMN_2704619	**Cc2d2a**	Mus musculus coiled-coil and C2 domain containing 2A (Cc2d2a), mRNA.	0.00008	1.59
ILMN_2611767	**Gprc5b**	Mus musculus G protein-coupled receptor, family C, group 5, member B (Gprc5b), mRNA.	0	1.59
ILMN_2678019	**Psmd8**	Mus musculus proteasome (prosome, macropain) 26S subunit, non-ATPase, 8 (Psmd8), mRNA. XM_001002011	0	1.59
ILMN_2448651	**Ampd3**	Mus musculus adenosine monophosphate deaminase 3 (Ampd3), mRNA.	0.00017	1.59
ILMN_2723639	**Pacs1**		0	1.59
ILMN_1244096	**Fam171a1**	Mus musculus family with sequence similarity 171, member A1 (Fam171a1), mRNA.	0	1.58
ILMN_1254927	**Ly6c1**	Mus musculus lymphocyte antigen 6 complex, locus C1 (Ly6c1), mRNA.	0.00001	1.58
ILMN_2598420	**Rbm16**	PREDICTED: Mus musculus RNA binding motif protein 16, transcript variant 1 (Rbm16), mRNA.	0.00011	1.58
ILMN_2637165	**2310001H17 Rik**		0	1.58
ILMN_2422333	**Trap1**	Mus musculus TNF receptor-associated protein 1 (Trap1), mRNA.	0	1.58

ILMN_1225544	**Slc19a1**	Mus musculus solute carrier family 19 (sodium/hydrogen exchanger), member 1 (Slc19a1), mRNA.	0	1.58
ILMN_2655577	**Pold1**	Mus musculus polymerase (DNA directed), delta 1, catalytic subunit (Pold1), mRNA.	0	1.58
ILMN_2825144	**Fndc7**	Mus musculus fibronectin type III domain containing 7 (Fndc7), mRNA.	0	1.58
ILMN_2791272	**Por**	Mus musculus P450 (cytochrome) oxidoreductase (Por), mRNA.	0	1.58
ILMN_2631098	**Msh6**	Mus musculus mutS homolog 6 (E. coli) (Msh6), mRNA.	0.00478	1.58
ILMN_2728088	**Cda**	Mus musculus cytidine deaminase (Cda), mRNA.	0	1.57
ILMN_2733091	**Baiap2**	Mus musculus brain-specific angiogenesis inhibitor 1-associated protein 2 (Baiap2), transcript variant 2, mRNA.	0	1.57
ILMN_2881263	**Aifm1**	Mus musculus apoptosis-inducing factor, mitochondrion-associated 1 (Aifm1), nuclear gene encoding mitochondrial protein, mRNA.	0	1.57
ILMN_2781458	**Tlcd1**	Mus musculus TLC domain containing 1 (Tlcd1), mRNA.	0	1.57
ILMN_1223807	**EG382843**	PREDICTED: Mus musculus predicted gene, EG382843 (EG382843), mRNA.	0	1.57
ILMN_1229082	**Klhl21**	Mus musculus kelch-like 21 (Drosophila) (Klhl21), mRNA.	0	1.57
ILMN_2815506	**Gamt**	Mus musculus guanidinoacetate methyltransferase (Gamt), mRNA.	0	1.57
ILMN_2766455	**Lrrc8d**	Mus musculus leucine rich repeat containing 8D (Lrrc8d), mRNA.	0	1.57
ILMN_2764309	**Dusp14**	Mus musculus dual specificity phosphatase 14 (Dusp14), mRNA.	0	1.57
ILMN_2842366	**Mrpl2**	Mus musculus mitochondrial ribosomal protein L2 (Mrpl2), nuclear gene encoding mitochondrial protein, mRNA.	0	1.57
ILMN_2502623	**Zhx3**	Mus musculus zinc fingers and homeoboxes 3 (Zhx3), mRNA.	0	1.57
ILMN_2714360	**Cd34**	Mus musculus CD34 antigen (Cd34), mRNA.	0.00004	1.57
ILMN_1254655	**Casp4**	Mus musculus caspase 4, apoptosis-related cysteine peptidase (Casp4), mRNA.	0	1.56
ILMN_2651715	**Axl**	Mus musculus AXL receptor tyrosine kinase (Axl), mRNA.	0	1.56
ILMN_2538852	**LOC384307**		0	1.56
ILMN_1230788	**Tle1**	Mus musculus transducin-like enhancer of split 1, homolog of Drosophila E(spl) (Tle1), mRNA. XM_984202 XM_984240 XM_984277 XM_984316 XM_984359 XM_984397 XM_984426 XM_984456 XM_984492 XM_984530	0.00009	1.56
ILMN_1259355	**Ccdc117**	Mus musculus coiled-coil domain containing 117 (Ccdc117), mRNA.	0	1.56
ILMN_1222356	**1110067D22 Rik**	Mus musculus RIKEN cDNA 1110067D22 gene (1110067D22Rik), mRNA.	0	1.56
ILMN_2525049	**Fstl**		0	1.56
ILMN_2622089	**5430432N15 Rik**	PREDICTED: Mus musculus RIKEN cDNA 5430432N15 gene (5430432N15Rik), mRNA.	0	1.56
ILMN_2496817	**Ulk2**	Mus musculus Unc-51 like kinase 2 (C. elegans) (Ulk2), mRNA.	0	1.55
ILMN_2757682	**Leng9**	Mus musculus leukocyte receptor cluster (LRC) member 9 (Leng9), mRNA.	0	1.55
ILMN_2631097	**Msh6**	Mus musculus mutS homolog 6 (E. coli) (Msh6), mRNA.	0	1.55
ILMN_2498851	**2310075M1 5Rik**		0.00002	1.55

ILMN_1232447	**Por**	Mus musculus P450 (cytochrome) oxidoreductase (Por), mRNA.	0	1.55
ILMN_2774646	**Myd88**		0	1.55
ILMN_2981550	**Capn1**	Mus musculus calpain 1 (Capn1), mRNA.	0	1.55
ILMN_2733778	**Il4i1**	Mus musculus interleukin 4 induced 1 (Il4i1), mRNA.	0	1.54
ILMN_1257552	**Tars**	Mus musculus threonyl-tRNA synthetase (Tars), mRNA.	0.00008	1.54
ILMN_2585112	**1200008A14 Rik**		0	1.54
ILMN_2428113	**scl0001379. 1_70**		0	1.54
ILMN_1233129	**Zbtb22**	Mus musculus zinc finger and BTB domain containing 22 (Zbtb22), mRNA.	0	1.54
ILMN_1224768	**Ehd4**	Mus musculus EH-domain containing 4 (Ehd4), mRNA.	0	1.54
ILMN_1242767	**Dok1**	Mus musculus docking protein 1 (Dok1), mRNA.	0	1.54
ILMN_1227465	**9628654_5**		0	1.53
ILMN_2761169	**3110050N22 Rik**		0.00003	1.53
ILMN_2842357	**Ryr1**	Mus musculus ryanodine receptor 1, skeletal muscle (Ryr1), mRNA.	0.00007	1.53
ILMN_1255236	**2510003E04 Rik**	Mus musculus RIKEN cDNA 2510003E04 gene (2510003E04Rik), mRNA.	0.00024	1.53
ILMN_2811705	**Fbxo18**	Mus musculus F-box protein 18 (Fbxo18), mRNA.	0	1.53
ILMN_1233283	**P2rx5**	Mus musculus purinergic receptor P2X, ligand-gated ion channel, 5 (P2rx5), mRNA.	0.00004	1.53
ILMN_2669782	**Phca**	Mus musculus phytoceramidase, alkaline (Phca), mRNA.	0	1.53
ILMN_2664548	**Pgls**	Mus musculus 6-phosphogluconolactonase (Pgls), mRNA.	0	1.53
ILMN_2674407	**Arpp19**	Mus musculus cAMP-regulated phosphoprotein 19 (Arpp19), mRNA.	0	1.52
ILMN_2599018	**Clic4**	Mus musculus chloride intracellular channel 4 (mitochondrial) (Clic4), nuclear gene encoding mitochondrial protein, mRNA.	0.00001	1.52
ILMN_2742426	**LOC100044 204**	PREDICTED: Mus musculus hypothetical protein LOC100044204 (LOC100044204), mRNA.	0.00164	1.52
ILMN_2744380	**Npc2**	Mus musculus Niemann Pick type C2 (Npc2), mRNA.	0	1.52
ILMN_1246108	**Hist1h2ah**	Mus musculus histone cluster 1, H2ah (Hist1h2ah), mRNA.	0.0004	1.52
ILMN_1256817	**Slpi**	Mus musculus secretory leukocyte peptidase inhibitor (Slpi), mRNA.	0.00001	1.52
ILMN_2428961	**Xpnpep1**	Mus musculus X-prolyl aminopeptidase (aminopeptidase P) 1, soluble (Xpnpep1), mRNA.	0	1.52
ILMN_2526572	**LOC545369**	PREDICTED: Mus musculus similar to ribosomal protein L4 (LOC545369), misc RNA.	0	1.52
ILMN_2604029	**Klf2**	Mus musculus Kruppel-like factor 2 (lung) (Klf2), mRNA.	0	1.52
ILMN_2638558	**Pes1**	Mus musculus pescadillo homolog 1, containing BRCT domain (zebrafish) (Pes1), mRNA.	0	1.52
ILMN_1238179	**Ipmk**	Mus musculus inositol polyphosphate multikinase (Ipmk), mRNA.	0	1.52
ILMN_2589181	**Eef2**	Mus musculus eukaryotic translation elongation factor 2 (Eef2), mRNA.	0	1.51
ILMN_2819679	**Tmem50a**	Mus musculus transmembrane protein 50A (Tmem50a), mRNA.	0	1.51
ILMN_2474887	**Whsc2**	Mus musculus Wolf-Hirschhorn syndrome candidate 2 (human) (Whsc2), mRNA.	0	1.51

ILMN_2531581	**LOC381215**		0.00014	1.51
ILMN_2669690	**Mpst**	Mus musculus mercaptopyruvate sulfurtransferase (Mpst), nuclear gene encoding mitochondrial protein, mRNA.	0	1.51
ILMN_2687612	**4831426I19 Rik**	Mus musculus RIKEN cDNA 4831426I19 gene (4831426I19Rik), transcript variant 1, mRNA.	0.00014	1.51
ILMN_2881272	**Aifm1**	Mus musculus apoptosis-inducing factor, mitochondrion-associated 1 (Aifm1), nuclear gene encoding mitochondrial protein, mRNA.	0.00051	1.51
ILMN_1240471	**Retsat**	Mus musculus retinol saturase (all trans retinol 13,14 reductase) (Retsat), mRNA.	0	1.51
ILMN_1249269	**5830457O10 Rik**	Mus musculus RIKEN cDNA 5830457O10 gene (5830457O10Rik), mRNA.	0	1.51
ILMN_2647885	**Bcl2l1**	Mus musculus BCL2-like 1 (Bcl2l1), nuclear gene encoding mitochondrial protein, mRNA.	0.00381	1.51
ILMN_2521620	**Phf15**	Mus musculus PHD finger protein 15 (Phf15), mRNA.	0.00133	1.5
ILMN_2628629	**Cdh1**	Mus musculus cadherin 1 (Cdh1), mRNA.	0	1.5
ILMN_3008068	**Scara5**	Mus musculus scavenger receptor class A, member 5 (putative) (Scara5), mRNA.	0.00006	1.5
ILMN_2759484	**C3**		0.00002	1.5
ILMN_1241955	**Dnali1**		0	1.5
ILMN_2982200	**Mrpl13**	Mus musculus mitochondrial ribosomal protein L13 (Mrpl13), mRNA.	0.0064	1.5
ILMN_2641278	**Mfn2**	Mus musculus mitofusin 2 (Mfn2), nuclear gene encoding mitochondrial protein, mRNA. XM_919144 XM_919157 XM_919164	0	1.5
ILMN_2748499	**Fshprh1**		0	1.5
ILMN_3111575	**Mef2b**	Mus musculus myocyte enhancer factor 2B (Mef2b), transcript variant 2, mRNA.	0.00048	1.5
ILMN_2536649	**LOC665235**	PREDICTED: Mus musculus similar to hCG1642689 (LOC665235), misc RNA.	0.00001	1.5
ILMN_2637742	**Padi1**	Mus musculus peptidyl arginine deiminase, type I (Padi1), mRNA.	0.00072	1.5

Supplemental Table 4.4. Complete list of genes downregulated by 4h of CORT treatment in HT-22 cells.

PROBE ID	SYMBOL	DEFINITION	Pvalue	Fold change
ILMN_2710253	**Cyr61**	Mus musculus cysteine rich protein 61 (Cyr61), mRNA.	0	-3.17
ILMN_2754985	**Phlda1**	Mus musculus pleckstrin homology-like domain, family A, member 1 (Phlda1), mRNA.	0	-3.09
ILMN_2662926	**Egr1**	Mus musculus early growth response 1 (Egr1), mRNA.	0	-2.91
ILMN_2794645	**Cyr61**	Mus musculus cysteine rich protein 61 (Cyr61), mRNA.	0	-2.88
ILMN_2483786	**1110004P21Rik**		0	-2.43
ILMN_1251193	**A630084D02Rik**		0	-2.42
ILMN_2937596	**Ngfb**	Mus musculus nerve growth factor, beta (Ngfb), mRNA.	0	-2.36
ILMN_2660233	**Ngfb**	Mus musculus nerve growth factor, beta (Ngfb), mRNA.	0	-2.34
ILMN_1229745	**Sertad4**	Mus musculus SERTA domain containing 4 (Sertad4), mRNA.	0	-2.34
ILMN_2959272	**Rnu6**	Mus musculus U6 small nuclear RNA (Rnu6), non-coding RNA.	0	-2.33

ILMN_2752569	**Paip1**	Mus musculus polyadenylate binding protein-interacting protein 1 (Paip1), transcript variant 1, mRNA.	0	-2.17
ILMN_1235571	**Cyr61**	Mus musculus cysteine rich protein 61 (Cyr61), mRNA.	0	-2.16
ILMN_1253178	**Aldh3a1**	Mus musculus aldehyde dehydrogenase family 3, subfamily A1 (Aldh3a1), mRNA.	0	-2.01
ILMN_2551741	**0610010I05Rik**		0	-1.98
ILMN_2868220	**Inhba**	Mus musculus inhibin beta-A (Inhba), mRNA.	0	-1.92
ILMN_2833706	**Fgf7**	Mus musculus fibroblast growth factor 7 (Fgf7), mRNA.	0	-1.91
ILMN_2937735	**Irak2**	Mus musculus interleukin-1 receptor-associated kinase 2 (Irak2), mRNA.	0	-1.87
ILMN_2451115	**1500001E21Rik**		0	-1.83
ILMN_2684563	**Cldnd1**	Mus musculus claudin domain containing 1 (Cldnd1), mRNA.	0	-1.8
ILMN_2507810	**mtDNA_ND5**		0	-1.79
ILMN_2988299	**Srf**	Mus musculus serum response factor (Srf), mRNA.	0	-1.79
ILMN_2683593	**Fubp1**		0	-1.79
ILMN_2778655	**Vcam1**	Mus musculus vascular cell adhesion molecule 1 (Vcam1), mRNA.	0	-1.77
ILMN_2550570	**Fibp**		0.00095	-1.76
ILMN_2937738	**Irak2**	Mus musculus interleukin-1 receptor-associated kinase 2 (Irak2), mRNA.	0	-1.75
ILMN_2726371	**Nqo1**	Mus musculus NAD(P)H dehydrogenase, quinone 1 (Nqo1), mRNA.	0	-1.75
ILMN_2695412	**AI451617**	Mus musculus expressed sequence AI451617 (AI451617), mRNA.	0	-1.74
ILMN_1232741	**Fdps**		0.00041	-1.73
ILMN_1216764	**Ier3**	Mus musculus immediate early response 3 (Ier3), mRNA.	0	-1.72
ILMN_2416218	**5530400B01Rik**		0	-1.72
ILMN_2840091	**Ugcg**	Mus musculus UDP-glucose ceramide glucosyltransferase (Ugcg), mRNA.	0	-1.72
ILMN_2479290	**Fas**	Mus musculus Fas (TNF receptor superfamily member 6) (Fas), mRNA.	0	-1.71
ILMN_1247823	**Lrp8**	Mus musculus low density lipoprotein receptor-related protein 8, apolipoprotein e receptor (Lrp8), transcript variant 2, mRNA.	0	-1.71
ILMN_1252479	**LOC100041567**	PREDICTED: Mus musculus similar to p47 protein (LOC100041567), mRNA.	0	-1.71
ILMN_1212848	**Rybp**	Mus musculus RING1 and YY1 binding protein (Rybp), mRNA.	0	-1.71
ILMN_2771176	**Ccl7**		0	-1.7
ILMN_3163340	**Rbm45**	Mus musculus RNA binding motif protein 45 (Rbm45), mRNA.	0	-1.69
ILMN_2434853	**mtDNA_ND2**		0	-1.68
ILMN_2623867	**Ostm1**	Mus musculus osteopetrosis associated transmembrane protein 1 (Ostm1), mRNA.	0	-1.67
ILMN_2511089	**Ugcg**		0	-1.66
ILMN_1236308	**LOC268730**		0	-1.65
ILMN_2629582	**Plau**	Mus musculus plasminogen activator, urokinase (Plau), mRNA.	0	-1.65
ILMN_2606210	**Dpt**	Mus musculus dermatopontin (Dpt), mRNA.	0	-1.65

ILMN_3131887	**Spag9**	Mus musculus sperm associated antigen 9 (Spag9), transcript variant 4, mRNA.	0	-1.65
ILMN_3127066	**Mark2**	Mus musculus MAP/microtubule affinity-regulating kinase 2 (Mark2), transcript variant 1, mRNA.	0	-1.64
ILMN_2557387	**E430005I09Rik**		0	-1.64
ILMN_2860804	**Tfrc**	Mus musculus transferrin receptor (Tfrc), mRNA.	0	-1.63
ILMN_2605031	**E330018D03Rik**	Mus musculus RIKEN cDNA E330018D03 gene (E330018D03Rik), mRNA.	0	-1.63
ILMN_1232716	**Cyp1b1**	Mus musculus cytochrome P450, family 1, subfamily b, polypeptide 1 (Cyp1b1), mRNA.	0	-1.63
ILMN_2965660	**Apcdd1**	Mus musculus adenomatosis polyposis coli down-regulated 1 (Apcdd1), mRNA.	0.00012	-1.62
ILMN_2904641	**Snora65**	Mus musculus small nucleolar RNA, H/ACA box 65 (Snora65) on chromosome 2.	0	-1.62
ILMN_2902979	**Fas**	Mus musculus Fas (TNF receptor superfamily member 6) (Fas), mRNA.	0	-1.62
ILMN_2664129	**Hist1h4h**	Mus musculus histone cluster 1, H4h (Hist1h4h), mRNA.	0	-1.62
ILMN_2592093	**Ift20**	Mus musculus intraflagellar transport 20 homolog (Chlamydomonas) (Ift20), mRNA.	0	-1.62
ILMN_3122961	**Gbp2**	Mus musculus guanylate binding protein 2 (Gbp2), mRNA.	0	-1.62
ILMN_2640862	**Lrig1**	Mus musculus leucine-rich repeats and immunoglobulin-like domains 1 (Lrig1), mRNA.	0	-1.61
ILMN_1257107	**LOC100043821**	PREDICTED: Mus musculus hypothetical protein LOC100043821 (LOC100043821), mRNA.	0	-1.61
ILMN_1245710	**Ccl2**	Mus musculus chemokine (C-C motif) ligand 2 (Ccl2), mRNA.	0	-1.61
ILMN_2672528	**Pabpn1**	Mus musculus poly(A) binding protein, nuclear 1 (Pabpn1), mRNA.	0	-1.61
ILMN_2734755	**Col4a5**		0	-1.61
ILMN_2960700	**Prf1**	Mus musculus perforin 1 (pore forming protein) (Prf1), mRNA.	0.00054	-1.61
ILMN_2835117	**Ccl7**	Mus musculus chemokine (C-C motif) ligand 7 (Ccl7), mRNA.	0	-1.61
ILMN_1240346	**Socs5**	Mus musculus suppressor of cytokine signaling 5 (Socs5), mRNA.	0	-1.6
ILMN_2763245	**Cxcl1**	Mus musculus chemokine (C-X-C motif) ligand 1 (Cxcl1), mRNA.	0	-1.6
ILMN_1245733	**Ddx49**	Mus musculus DEAD (Asp-Glu-Ala-Asp) box polypeptide 49 (Ddx49), mRNA.	0	-1.59
ILMN_2726837	**Nppb**	Mus musculus natriuretic peptide precursor type B (Nppb), mRNA.	0	-1.59
ILMN_1230375	**LOC383125**		0	-1.58
ILMN_1250815	**Wsb1**	Mus musculus WD repeat and SOCS box-containing 1 (Wsb1), transcript variant 2, mRNA.	0	-1.58
ILMN_2760514	**Agps**	Mus musculus alkylglycerone phosphate synthase (Agps), mRNA.	0	-1.57
ILMN_2619848	**Tfrc**	Mus musculus transferrin receptor (Tfrc), mRNA.	0	-1.57
ILMN_2491831	**D11Bwg0414e**		0	-1.57
ILMN_3149024	**Scoc**	Mus musculus short coiled-coil protein (Scoc), transcript variant 2, mRNA.	0	-1.57
ILMN_1215167	**Ddx5**	Mus musculus DEAD (Asp-Glu-Ala-Asp) box polypeptide 5 (Ddx5), mRNA.	0.00001	-1.57
ILMN_2657911	**Cnot4**	Mus musculus CCR4-NOT transcription complex, subunit 4 (Cnot4), mRNA.	0	-1.56

ILMN_1259905	**Sfrs11**	Mus musculus splicing factor, arginine/serine-rich 11 (Sfrs11), transcript variant 1, mRNA.	0	-1.56
ILMN_1239677	**2010107E04Rik**	Mus musculus RIKEN cDNA 2010107E04 gene (2010107E04Rik), mRNA.	0	-1.56
ILMN_2747923	**Slc40a1**	Mus musculus solute carrier family 40 (iron-regulated transporter), member 1 (Slc40a1), mRNA.	0.00254	-1.56
ILMN_1255925	**Col8a1**		0	-1.56
ILMN_2625451	**Ankrd1**	Mus musculus ankyrin repeat domain 1 (cardiac muscle) (Ankrd1), mRNA.	0	-1.56
ILMN_2758073	**Dmtf1**	Mus musculus cyclin D binding myb-like transcription factor 1 (Dmtf1), mRNA.	0	-1.55
ILMN_1229193	**Msn**		0	-1.55
ILMN_2683374	**Asna1**	Mus musculus arsA arsenite transporter, ATP-binding, homolog 1 (bacterial) (Asna1), mRNA.	0	-1.55
ILMN_1234412	**LOC674427**	PREDICTED: Mus musculus similar to ribosomal protein L7a (LOC674427), misc RNA.	0	-1.55
ILMN_2972478	**Nlgn2**	Mus musculus neuroligin 2 (Nlgn2), mRNA.	0	-1.55
ILMN_2825803	**Parp14**	Mus musculus poly (ADP-ribose) polymerase family, member 14 (Parp14), mRNA. XM_901644 XM_916789 XM_924484 XM_924488	0	-1.55
ILMN_2974069	**Slc35a3**	Mus musculus solute carrier family 35 (UDP-N-acetylglucosamine (UDP-GlcNAc) transporter), member 3 (Slc35a3), mRNA.	0	-1.55
ILMN_2710354	**Acta2**	Mus musculus actin, alpha 2, smooth muscle, aorta (Acta2), mRNA.	0	-1.55
ILMN_2848463	**Mthfsd**	Mus musculus methenyltetrahydrofolate synthetase domain containing (Mthfsd), mRNA.	0.00001	-1.55
ILMN_1255317	**Arnt**		0	-1.55
ILMN_2585738	**A730086L23Rik**		0	-1.54
ILMN_2479681	**Mex3a**	Mus musculus mex3 homolog A (C. elegans) (Mex3a), mRNA.	0	-1.54
ILMN_2972585	**Pvr**	Mus musculus poliovirus receptor (Pvr), mRNA.	0.00007	-1.54
ILMN_3147112	**Mapk6**	Mus musculus mitogen-activated protein kinase 6 (Mapk6), transcript variant 2, mRNA.	0	-1.54
ILMN_1231803	**Dmtf1**	Mus musculus cyclin D binding myb-like transcription factor 1 (Dmtf1), mRNA.	0	-1.53
ILMN_1238820	**LOC332788**		0	-1.53
ILMN_1240420	**Arid1b**	Mus musculus AT rich interactive domain 1B (SWI-like) (Arid1b), mRNA.	0	-1.53
ILMN_2830661	**Top2a**	Mus musculus topoisomerase (DNA) II alpha (Top2a), mRNA.	0	-1.53
ILMN_1213322	**Chd2**	Mus musculus chromodomain helicase DNA binding protein 2 (Chd2), mRNA.	0.00001	-1.53
ILMN_3153753	**Cacnb3**	Mus musculus calcium channel, voltage-dependent, beta 3 subunit (Cacnb3), transcript variant 1, mRNA.	0	-1.53
ILMN_2659644	**Map2k3**	Mus musculus mitogen activated protein kinase kinase 3 (Map2k3), mRNA.	0	-1.53
ILMN_1220813	**Dtx3l**	Mus musculus deltex 3-like (Drosophila) (Dtx3l), mRNA.	0	-1.53
ILMN_1239921	**Man1b1**	Mus musculus mannosidase, alpha, class 1B, member 1 (Man1b1), mRNA.	0	-1.53
ILMN_3144289	**Traf3**	Mus musculus Tnf receptor-associated factor 3 (Traf3), transcript variant 1, mRNA.	0	-1.52
ILMN_2737867	**Mtap1b**	Mus musculus microtubule-associated protein 1 B (Mtap1b), mRNA.	0.00102	-1.52

ILMN_1230278	**LOC100044702**	PREDICTED: Mus musculus similar to LPS-induced CXC chemokine (LOC100044702), mRNA.	0.00186	-1.52
ILMN_1248039	**mtDNA_COXII**		0	-1.52
ILMN_1214412	**Antxr2**	Mus musculus anthrax toxin receptor 2 (Antxr2), mRNA.	0	-1.52
ILMN_2794796	**E2f4**	Mus musculus E2F transcription factor 4 (E2f4), mRNA.	0	-1.52
ILMN_3157483	**Ets1**	Mus musculus E26 avian leukemia oncogene 1, 5' domain (Ets1), transcript variant 2, mRNA.	0	-1.52
ILMN_2776603	**Ccl9**	Mus musculus chemokine (C-C motif) ligand 9 (Ccl9), mRNA.	0	-1.52
ILMN_3093089	**Tardbp**	Mus musculus TAR DNA binding protein (Tardbp), transcript variant 2, mRNA.	0	-1.51
ILMN_2757489	**Ppp1r11**	Mus musculus protein phosphatase 1, regulatory (inhibitor) subunit 11 (Ppp1r11), mRNA.	0	-1.51
ILMN_2612407	**Wdsub1**	Mus musculus WD repeat, SAM and U-box domain containing 1 (Wdsub1), mRNA.	0	-1.51
ILMN_2742599	**Nfix**	Mus musculus nuclear factor I/X (Nfix), transcript variant 2, mRNA. XM_921228 XM_921240 XM_921250 XM_921261 XM_921270 XM_921288 XM_921293 XM_921299 XM_921300 XM_921307	0	-1.51
ILMN_2849753	**Erich1**	Mus musculus glutamate-rich 1 (Erich1), mRNA.	0	-1.51
ILMN_1246153	**Erdr1**	Mus musculus erythroid differentiation regulator 1 (Erdr1), mRNA.	0.01121	-1.51
ILMN_2742675	**Rock1**	Mus musculus Rho-associated coiled-coil containing protein kinase 1 (Rock1), mRNA.	0	-1.51
ILMN_1222584	**Sfrs11**	Mus musculus splicing factor, arginine/serine-rich 11 (Sfrs11), transcript variant 1, mRNA.	0.00204	-1.51
ILMN_1258330	**LOC384348**		0	-1.51
ILMN_1213026	**9630058J23Rik**	Mus musculus RIKEN cDNA 9630058J23 gene (9630058J23Rik), mRNA.	0	-1.51
ILMN_2942989	**Mtpn**	Mus musculus myotrophin (Mtpn), mRNA.	0	-1.51
ILMN_3158725	**Raet1b**	Mus musculus retinoic acid early transcript beta (Raet1b), mRNA.	0	-1.51
ILMN_1227458	**Nuak1**	Mus musculus NUAK family, SNF1-like kinase, 1 (Nuak1), mRNA.	0	-1.51
ILMN_1259340	**1810073M12Rik**		0	-1.5
ILMN_2497068	**Zmynd11**	Mus musculus zinc finger, MYND domain containing 11 (Zmynd11), mRNA.	0	-1.5
ILMN_2552490	**6720463L11Rik**		0	-1.5
ILMN_2657338	**D930038J03Rik**		0	-1.5
ILMN_2761662	**Samd4b**	Mus musculus sterile alpha motif domain containing 4B (Samd4b), mRNA.	0	-1.5
ILMN_2974945	**Cog6**	Mus musculus component of oligomeric golgi complex 6 (Cog6), mRNA.	0	-1.5
ILMN_3031099	**Coq10b**	Mus musculus coenzyme Q10 homolog B (S. cerevisiae) (Coq10b), transcript variant 1, mRNA.	0	-1.5
ILMN_2768053	**Supt16h**	Mus musculus suppressor of Ty 16 homolog (S. cerevisiae) (Supt16h), mRNA.	0.00014	-1.5
ILMN_1253539	**LOC432554**	PREDICTED: Mus musculus similar to Ddx5 protein (LOC432554), misc RNA.	0	-1.5

Supplemental Table 4.5. Complete list of genes upregulated by 4h of T_3 plus CORT treatment in HT-22 cells.

PROBE ID	SYMBOL	DEFINITION	P value	Fold change
ILMN_1232601	**Cyb561**	Mus musculus cytochrome b-561 (Cyb561), mRNA.	0	10.52
ILMN_2701664	**Tsc22d3**	Mus musculus TSC22 domain family, member 3 (Tsc22d3), transcript variant 2, mRNA.	0	7.25
ILMN_1254031	**Klf9**	Mus musculus Kruppel-like factor 9 (Klf9), mRNA.	0	5.518
ILMN_2430906	**2310051E17Rik**	PREDICTED: Mus musculus RIKEN cDNA 2310051E17 gene (2310051E17Rik), mRNA.	0	5.245
ILMN_1259322	**Pdk4**	Mus musculus pyruvate dehydrogenase kinase, isoenzyme 4 (Pdk4), mRNA.	0	4.71
ILMN_3150811	**Tsc22d3**	Mus musculus TSC22 domain family, member 3 (Tsc22d3), transcript variant 1, mRNA.	0	4.506
ILMN_2813484	**Per1**	Mus musculus period homolog 1 (Drosophila) (Per1), mRNA.	0	4.291
ILMN_2987862	**Per2**	Mus musculus period homolog 2 (Drosophila) (Per2), mRNA.	0	3.917
ILMN_2524986	**Ear3**	Mus musculus eosinophil-associated, ribonuclease A family, member 3 (Ear3), mRNA.	0	3.793
ILMN_2638923	**Rn18s**	Mus musculus 18S RNA (Rn18s), non-coding RNA.	0	3.65
ILMN_1220280	**Tas1r1**	Mus musculus taste receptor, type 1, member 1 (Tas1r1), mRNA.	0	3.196
ILMN_2770894	**Map3k6**		0	3.102
ILMN_2822000	**Slc10a6**	Mus musculus solute carrier family 10 (sodium/bile acid cotransporter family), member 6 (Slc10a6), mRNA.	0	3.064
ILMN_2813487	**Per1**	Mus musculus period homolog 1 (Drosophila) (Per1), mRNA.	0	3.008
ILMN_2622983	**Dusp1**	Mus musculus dual specificity phosphatase 1 (Dusp1), mRNA.	0	2.93
ILMN_2738345	**Lims2**	Mus musculus LIM and senescent cell antigen like domains 2 (Lims2), mRNA.	0	2.913
ILMN_2712075	**Lcn2**	Mus musculus lipocalin 2 (Lcn2), mRNA.	0	2.821
ILMN_2588249	**S3-12**	Mus musculus plasma membrane associated protein, S3-12 (S3-12), mRNA.	0	2.805
ILMN_2768972	**Fam107a**	Mus musculus family with sequence similarity 107, member A (Fam107a), mRNA.	0	2.783
ILMN_2654074	**Sesn1**	Mus musculus sestrin 1 (Sesn1), mRNA.	0	2.765
ILMN_2637714	**Rasa3**	Mus musculus RAS p21 protein activator 3 (Rasa3), mRNA.	0	2.758
ILMN_2987863	**Per2**	Mus musculus period homolog 2 (Drosophila) (Per2), mRNA.	0	2.683
ILMN_1219154	**Mt2**	Mus musculus metallothionein 2 (Mt2), mRNA.	0	2.571
ILMN_2517483	**D15Bwg0759e**		0	2.552
ILMN_1226935	**Orm1**	Mus musculus orosomucoid 1 (Orm1), mRNA.	0	2.541
ILMN_2616226	**Dbp**	Mus musculus D site albumin promoter binding protein (Dbp), mRNA.	0	2.516
ILMN_2718266	**Fkbp5**	Mus musculus FK506 binding protein 5 (Fkbp5), mRNA.	0	2.466
ILMN_3136744	**Sesn1**	Mus musculus sestrin 1 (Sesn1), mRNA.	0	2.44
ILMN_1255287	**Mela**		0	2.437

ILMN_1230073	**Rn18s**	Mus musculus 18S RNA (Rn18s), non-coding RNA.	0	2.427
ILMN_2942674	**Lims2**	Mus musculus LIM and senescent cell antigen like domains 2 (Lims2), mRNA.	0	2.373
ILMN_1260061	**D17H6S56E-5**	Mus musculus DNA segment, Chr 17, human D6S56E 5 (D17H6S56E-5), mRNA.	0	2.368
ILMN_1253191	**E230024B12Rik**		0	2.281
ILMN_1232884	**Sphk1**	Mus musculus sphingosine kinase 1 (Sphk1), transcript variant 1, mRNA.	0	2.273
ILMN_2727013	**Nr1h4**	Mus musculus nuclear receptor subfamily 1, group H, member 4 (Nr1h4), mRNA.	0	2.261
ILMN_1255766	**Sh3bp2**	Mus musculus SH3-domain binding protein 2 (Sh3bp2), mRNA.	0	2.225
ILMN_2868480	**Ear4**	Mus musculus eosinophil-associated, ribonuclease A family, member 4 (Ear4), mRNA.	0	2.214
ILMN_1243992	**Ptrf**		0	2.19
ILMN_2605645	**Gsn**		0	2.184
ILMN_3059476	**Sesn1**	Mus musculus sestrin 1 (Sesn1), mRNA.	0	2.144
ILMN_1247996	**LOC673501**	PREDICTED: Mus musculus hypothetical protein LOC673501 (LOC673501), mRNA.	0	2.133
ILMN_2714031	**Errfi1**	Mus musculus ERBB receptor feedback inhibitor 1 (Errfi1), mRNA.	0	2.103
ILMN_2665545	**Rin3**	Mus musculus Ras and Rab interactor 3 (Rin3), mRNA.	0	2.08
ILMN_1224842	**LOC385068**		0	2.076
ILMN_1229082	**Klhl21**	Mus musculus kelch-like 21 (Drosophila) (Klhl21), mRNA.	0	2.053
ILMN_2452855	**1110003O08Rik**		0	2.029
ILMN_2619697	**B3gnt9**	Mus musculus UDP-GlcNAc:betaGal beta-1,3-N-acetylglucosaminyltransferase 9 (B3gnt9), mRNA.	0	2.026
ILMN_1255967	**B430216N15Rik**		0	2.022
ILMN_1232396	**Ear2**	Mus musculus eosinophil-associated, ribonuclease A family, member 2 (Ear2), mRNA.	0	2.022
ILMN_2793062	**Rasl11b**	Mus musculus RAS-like, family 11, member B (Rasl11b), mRNA.	0	2.022
ILMN_2733887	**Mknk2**	Mus musculus MAP kinase-interacting serine/threonine kinase 2 (Mknk2), mRNA.	0	2.02
ILMN_1260112	**2400003C14Rik**	Mus musculus RIKEN cDNA 2400003C14 gene (2400003C14Rik), mRNA.	0	2.004
ILMN_2450735	**Rn18s**	Mus musculus 18S RNA (Rn18s), non-coding RNA.	0	1.998
ILMN_2947292	**Map3k6**	Mus musculus mitogen-activated protein kinase kinase kinase 6 (Map3k6), mRNA.	0	1.996
ILMN_2699621	**Dlk2**	Mus musculus delta-like 2 homolog (Drosophila) (Dlk2), mRNA.	0	1.992
ILMN_2420341	**9629514_325**		0	1.987
ILMN_2765047	**Chrd**	Mus musculus chordin (Chrd), mRNA.	0	1.975
ILMN_2791272	**Por**	Mus musculus P450 (cytochrome) oxidoreductase (Por), mRNA.	0	1.964
ILMN_2706819	**Rasl11b**	Mus musculus RAS-like, family 11, member B (Rasl11b), mRNA.	0	1.949
ILMN_2763679	**Sipa1l1**	Mus musculus signal-induced proliferation-associated 1 like 1 (Sipa1l1), mRNA.	0	1.944
ILMN_2772410	**Anxa4**		0.00009	1.942

ILMN_2445165	**Vdr**	Mus musculus vitamin D receptor (Vdr), mRNA.	0	1.941
ILMN_1218981	**Aldh1a7**	Mus musculus aldehyde dehydrogenase family 1, subfamily A7 (Aldh1a7), mRNA.	0.00001	1.937
ILMN_1252259	**LOC384836**		0	1.927
ILMN_1232447	**Por**	Mus musculus P450 (cytochrome) oxidoreductase (Por), mRNA.	0	1.926
ILMN_2473531	**Pik3r1**	Mus musculus phosphatidylinositol 3-kinase, regulatory subunit, polypeptide 1 (p85 alpha) (Pik3r1), transcript variant 1, mRNA.	0	1.916
ILMN_1213954	**Sgk1**	Mus musculus serum/glucocorticoid regulated kinase 1 (Sgk1), mRNA.	0	1.916
ILMN_2676052	**Tef**	Mus musculus thyrotroph embryonic factor (Tef), transcript variant 1, mRNA.	0	1.887
ILMN_2653567	**Rhoj**	Mus musculus ras homolog gene family, member J (Rhoj), mRNA.	0	1.878
ILMN_1237939	**Prkrir**	Mus musculus protein-kinase, interferon-inducible double stranded RNA dependent inhibitor, repressor of (P58 repressor) (Prkrir), mRNA.	0	1.875
ILMN_2692615	**Tgm2**	Mus musculus transglutaminase 2, C polypeptide (Tgm2), mRNA.	0	1.87
ILMN_2447100	**D15Mit260**		0	1.865
ILMN_2671601	**Selk**		0	1.85
ILMN_2509988	**Lbr**		0	1.849
ILMN_2464474	**9430029L20Rik**		0	1.846
ILMN_1227465	**9628654_5**		0	1.845
ILMN_1247916	**Lims2**	Mus musculus LIM and senescent cell antigen like domains 2 (Lims2), mRNA.	0	1.827
ILMN_2737713	**Edn1**	Mus musculus endothelin 1 (Edn1), mRNA.	0	1.825
ILMN_2909782	**Rras2**	Mus musculus related RAS viral (r-ras) oncogene homolog 2 (Rras2), mRNA.	0	1.814
ILMN_2491125	**Tbl1xr1**	Mus musculus transducin (beta)-like 1X-linked receptor 1 (Tbl1xr1), mRNA.	0	1.807
ILMN_2544674	**2310045K21Rik**		0	1.804
ILMN_2979237	**Gsta1**	Mus musculus glutathione S-transferase, alpha 1 (Ya) (Gsta1), mRNA.	0	1.79
ILMN_2445166	**Vdr**	Mus musculus vitamin D receptor (Vdr), mRNA.	0	1.771
ILMN_2611180	**Ccdc3**		0	1.768
ILMN_1241854	**Lrrc59**	Mus musculus leucine rich repeat containing 59 (Lrrc59), mRNA.	0	1.765
ILMN_2675922	**2310047A01Rik**	PREDICTED: Mus musculus RIKEN cDNA 2310047A01 gene (2310047A01Rik), mRNA.	0	1.763
ILMN_1215275	**Add1**	Mus musculus adducin 1 (alpha) (Add1), transcript variant 1, mRNA.	0	1.763
ILMN_1256943	**Ear3**	Mus musculus eosinophil-associated, ribonuclease A family, member 3 (Ear3), mRNA.	0.00098	1.759
ILMN_1231096	**2310036D22Rik**		0.00064	1.755
ILMN_2772632	**Saa3**	Mus musculus serum amyloid A 3 (Saa3), mRNA.	0	1.749
ILMN_3114641	**Pik3r1**	Mus musculus phosphatidylinositol 3-kinase, regulatory subunit, polypeptide 1 (p85 alpha) (Pik3r1), transcript variant 2, mRNA.	0	1.747
ILMN_1221494	**Ubtd2**	Mus musculus ubiquitin domain containing 2 (Ubtd2), mRNA.	0.00252	1.737

ILMN_1226587	**EG668300**	PREDICTED: Mus musculus predicted gene, EG668300 (EG668300), mRNA.	0.00001	1.736
ILMN_2602597	**Sh3rf1**	Mus musculus SH3 domain containing ring finger 1 (Sh3rf1), mRNA.	0	1.733
ILMN_2595359	**Slc3a2**	Mus musculus solute carrier family 3 (activators of dibasic and neutral amino acid transport), member 2 (Slc3a2), mRNA.	0.00005	1.727
ILMN_2485408	**9626962_3**		0	1.727
ILMN_2702039	**Cblb**	Mus musculus Casitas B-lineage lymphoma b (Cblb), mRNA. XM_001003462 XM_001003472 XM_001003476 XM_001003639 XM_001003649 XM_156257 XM_902056 XM_902058 XM_917535 XM_924994 XM_924996	0	1.722
ILMN_1226712	**Ccdc134**	Mus musculus coiled-coil domain containing 134 (Ccdc134), mRNA.	0	1.718
ILMN_1224336	**Spsb1**	Mus musculus splA/ryanodine receptor domain and SOCS box containing 1 (Spsb1), mRNA.	0	1.714
ILMN_1216689	**Aplp2**	Mus musculus amyloid beta (A4) precursor-like protein 2 (Aplp2), transcript variant 3, mRNA.	0	1.706
ILMN_2742426	**LOC100044204**	PREDICTED: Mus musculus hypothetical protein LOC100044204 (LOC100044204), mRNA.	0.00001	1.699
ILMN_1259787	**Osr1**	Mus musculus odd-skipped related 1 (Drosophila) (Osr1), mRNA.	0	1.697
ILMN_2655577	**Pold1**	Mus musculus polymerase (DNA directed), delta 1, catalytic subunit (Pold1), mRNA.	0	1.69
ILMN_3009521	**Foxred2**	Mus musculus FAD-dependent oxidoreductase domain containing 2 (Foxred2), mRNA.	0	1.689
ILMN_1259355	**Ccdc117**	Mus musculus coiled-coil domain containing 117 (Ccdc117), mRNA.	0	1.687
ILMN_2881272	**Aifm1**	Mus musculus apoptosis-inducing factor, mitochondrion-associated 1 (Aifm1), nuclear gene encoding mitochondrial protein, mRNA.	0.00212	1.684
ILMN_2669627	**Vcan**	Mus musculus versican (Vcan), transcript variant 1, mRNA.	0	1.683
ILMN_2766455	**Lrrc8d**	Mus musculus leucine rich repeat containing 8D (Lrrc8d), mRNA.	0	1.681
ILMN_2672190	**Id1**	Mus musculus inhibitor of DNA binding 1 (Id1), mRNA.	0	1.68
ILMN_1246800	**Serpina3n**	Mus musculus serine (or cysteine) peptidase inhibitor, clade A, member 3N (Serpina3n), mRNA.	0	1.678
ILMN_2776922	**Glrx1**		0	1.674
ILMN_2659063	**Add1**	Mus musculus adducin 1 (alpha) (Add1), transcript variant 2, mRNA.	0	1.672
ILMN_1254630	**Ptpre**	Mus musculus protein tyrosine phosphatase, receptor type, E (Ptpre), mRNA.	0	1.671
ILMN_2712731	**Phf10**	Mus musculus PHD finger protein 10 (Phf10), mRNA.	0	1.671
ILMN_2636624	**Slc10a6**	Mus musculus solute carrier family 10 (sodium/bile acid cotransporter family), member 6 (Slc10a6), mRNA.	0.00003	1.669
ILMN_1223428	**Eif3s8**		0	1.668
ILMN_1215969	**Rcor1**	Mus musculus REST corepressor 1 (Rcor1), mRNA.	0	1.664
ILMN_1220173	**Ppm2c**	Mus musculus protein phosphatase 2C, magnesium dependent, catalytic subunit (Ppm2c), nuclear gene encoding mitochondrial protein, transcript variant 1, mRNA.	0	1.664
ILMN_2663230	**Slco3a1**	Mus musculus solute carrier organic anion	0	1.658

		transporter family, member 3a1 (Slco3a1), transcript variant 1, mRNA.		
ILMN_1236037	**LOC627317**	PREDICTED: Mus musculus similar to ribosomal protein L11 (LOC627317), misc RNA.	0.00003	1.657
ILMN_2764143	**Scap**	Mus musculus SREBF chaperone (Scap), mRNA.	0	1.655
ILMN_1225994	**Vav2**	Mus musculus vav 2 oncogene (Vav2), mRNA.	0	1.652
ILMN_2752010	**Mcm4**	Mus musculus minichromosome maintenance deficient 4 homolog (S. cerevisiae) (Mcm4), mRNA.	0	1.652
ILMN_2502623	**Zhx3**	Mus musculus zinc fingers and homeoboxes 3 (Zhx3), mRNA.	0	1.649
ILMN_3157399	**Tead4**	Mus musculus TEA domain family member 4 (Tead4), transcript variant 2, mRNA.	0	1.649
ILMN_1215803	**Slc38a4**	Mus musculus solute carrier family 38, member 4 (Slc38a4), mRNA.	0.01414	1.649
ILMN_2622605	**Srr**	Mus musculus serine racemase (Srr), mRNA.	0.00715	1.647
ILMN_1228919	**St13**	Mus musculus suppression of tumorigenicity 13 (St13), mRNA.	0	1.644
ILMN_2748499	**Fshprh1**		0	1.643
ILMN_2618745	**Supv3l1**	Mus musculus suppressor of var1, 3-like 1 (S. cerevisiae) (Supv3l1), mRNA.	0	1.639
ILMN_1225995	**Morc2a**	Mus musculus microrchidia 2A (Morc2a), mRNA.	0	1.639
ILMN_2842366	**Mrpl2**	Mus musculus mitochondrial ribosomal protein L2 (Mrpl2), nuclear gene encoding mitochondrial protein, mRNA.	0	1.638
ILMN_1229416	**1110034A24Rik**		0.00006	1.637
ILMN_2854943	**Gprc5a**	Mus musculus G protein-coupled receptor, family C, group 5, member A (Gprc5a), mRNA.	0	1.634
ILMN_2682945	**Psmd2**	Mus musculus proteasome (prosome, macropain) 26S subunit, non-ATPase, 2 (Psmd2), mRNA.	0	1.633
ILMN_2777535	**LOC666053**	PREDICTED: Mus musculus similar to protein tyrosine phosphatase-like protein PTPLB (LOC666053), misc RNA.	0	1.631
ILMN_1233813	**Ss18**	Mus musculus synovial sarcoma translocation, Chromosome 18 (Ss18), mRNA.	0	1.629
ILMN_1228942	**Cd59a**	Mus musculus CD59a antigen (Cd59a), mRNA.	0.00023	1.625
ILMN_2633777	**Rab34**	Mus musculus RAB34, member of RAS oncogene family (Rab34), mRNA.	0	1.621
ILMN_1240471	**Retsat**	Mus musculus retinol saturase (all trans retinol 13,14 reductase) (Retsat), mRNA.	0	1.618
ILMN_2885277	**Nnmt**	Mus musculus nicotinamide N-methyltransferase (Nnmt), mRNA.	0	1.614
ILMN_1233129	**Zbtb22**	Mus musculus zinc finger and BTB domain containing 22 (Zbtb22), mRNA.	0	1.61
ILMN_1222071	**C920004C08Rik**		0	1.608
ILMN_1221805	**Dtna**	Mus musculus dystrobrevin alpha (Dtna), transcript variant 2, mRNA.	0	1.607
ILMN_2713055	**Psca**	Mus musculus prostate stem cell antigen (Psca), mRNA.	0	1.607
ILMN_1218206	**Klf13**	Mus musculus Kruppel-like factor 13 (Klf13), mRNA.	0	1.607
ILMN_1230422	**BC018507**	PREDICTED: Mus musculus cDNA sequence BC018507, transcript variant 5 (BC018507), mRNA.	0	1.596
ILMN_1257772	**BC026590**	Mus musculus cDNA sequence BC026590 (BC026590), mRNA.	0	1.596

ILMN_3160881	**Vrk3**	Mus musculus vaccinia related kinase 3 (Vrk3), mRNA.	0	1.595
ILMN_1232055	**9330175B01Rik**		0	1.595
ILMN_2971479	**Trp53inp1**	Mus musculus transformation related protein 53 inducible nuclear protein 1 (Trp53inp1), mRNA.	0.00004	1.594
ILMN_2766930	**Faah**	Mus musculus fatty acid amide hydrolase (Faah), mRNA.	0	1.594
ILMN_2588337	**D930015E06Rik**		0.00001	1.593
ILMN_1220063	**EG666668**	PREDICTED: Mus musculus predicted gene, EG666668 (EG666668), mRNA.	0	1.593
ILMN_1230788	**Tle1**	Mus musculus transducin-like enhancer of split 1, homolog of Drosophila E(spl) (Tle1), mRNA. XM_984202 XM_984240 XM_984277 XM_984316 XM_984359 XM_984397 XM_984426 XM_984456 XM_984492 XM_984530	0	1.593
ILMN_1224014	**Tmem100**	Mus musculus transmembrane protein 100 (Tmem100), mRNA.	0	1.591
ILMN_1224250	**B230342M21Rik**	Mus musculus RIKEN cDNA B230342M21 gene (B230342M21Rik), mRNA.	0	1.591
ILMN_1228557	**Id2**	Mus musculus inhibitor of DNA binding 2 (Id2), mRNA.	0.00003	1.59
ILMN_2648937	**Pdzrn3**	Mus musculus PDZ domain containing RING finger 3 (Pdzrn3), mRNA.	0.00092	1.589
ILMN_2602821	**Cdk5rap1**	Mus musculus CDK5 regulatory subunit associated protein 1 (Cdk5rap1), mRNA.	0	1.582
ILMN_2682947	**Psmd2**	Mus musculus proteasome (prosome, macropain) 26S subunit, non-ATPase, 2 (Psmd2), mRNA.	0	1.582
ILMN_2533916	**LOC380655**		0	1.581
ILMN_2595732	**LOC100046232**	PREDICTED: Mus musculus similar to NFIL3/E4BP4 transcription factor (LOC100046232), mRNA.	0	1.581
ILMN_2707452	**Ebf1**	Mus musculus early B-cell factor 1 (Ebf1), mRNA.	0	1.579
ILMN_1228245	**Prickle1**	Mus musculus prickle like 1 (Drosophila) (Prickle1), mRNA.	0	1.578
ILMN_2944646	**Cope**	Mus musculus coatomer protein complex, subunit epsilon (Cope), mRNA.	0	1.578
ILMN_2619594	**Il11ra1**	Mus musculus interleukin 11 receptor, alpha chain 1 (Il11ra1), mRNA.	0	1.577
ILMN_2515081	**Trim59**	Mus musculus tripartite motif-containing 59 (Trim59), mRNA.	0	1.576
ILMN_1243908	**Sh3gl1**	Mus musculus SH3-domain GRB2-like 1 (Sh3gl1), mRNA.	0	1.576
ILMN_2698430	**Bcl2l1**	Mus musculus BCL2-like 1 (Bcl2l1), nuclear gene encoding mitochondrial protein, mRNA.	0	1.575
ILMN_2490548	**Tspan4**	Mus musculus tetraspanin 4 (Tspan4), mRNA.	0	1.574
ILMN_2881263	**Aifm1**	Mus musculus apoptosis-inducing factor, mitochondrion-associated 1 (Aifm1), nuclear gene encoding mitochondrial protein, mRNA.	0	1.573
ILMN_2955806	**Arfip2**	Mus musculus ADP-ribosylation factor interacting protein 2 (Arfip2), mRNA.	0	1.572
ILMN_2461582	**4732460K03Rik**	PREDICTED: Mus musculus RIKEN cDNA 4732460K03 gene, transcript variant 1 (4732460K03Rik), mRNA.	0	1.571
ILMN_2704619	**Cc2d2a**	Mus musculus coiled-coil and C2 domain containing 2A (Cc2d2a), mRNA.	0	1.571
ILMN_1226366	**Uck1**	Mus musculus uridine-cytidine kinase 1 (Uck1), mRNA.	0	1.57

ILMN_2636832	**Cyb5r3**	Mus musculus cytochrome b5 reductase 3 (Cyb5r3), mRNA.	0	1.57
ILMN_2774646	**Myd88**		0	1.569
ILMN_2644845	**Trmt6**	Mus musculus tRNA methyltransferase 6 homolog (S. cerevisiae) (Trmt6), mRNA.	0	1.569
ILMN_2631097	**Msh6**	Mus musculus mutS homolog 6 (E. coli) (Msh6), mRNA.	0	1.568
ILMN_2687032	**Fbxo31**	Mus musculus F-box protein 31 (Fbxo31), mRNA.	0	1.567
ILMN_2811705	**Fbxo18**	Mus musculus F-box protein 18 (Fbxo18), mRNA.	0.00018	1.567
ILMN_2776585	**Slc1a5**	Mus musculus solute carrier family 1 (neutral amino acid transporter), member 5 (Slc1a5), mRNA.	0.00002	1.564
ILMN_2511971	**Whsc1l1**	Mus musculus Wolf-Hirschhorn syndrome candidate 1-like 1 (human) (Whsc1l1), transcript variant 1, mRNA.	0	1.563
ILMN_2517631	**SV40_small_t_Ag_specific**		0	1.563
ILMN_1257501	**Pet112l**	Mus musculus PET112-like (yeast) (Pet112l), mRNA.	0.00002	1.559
ILMN_2982200	**Mrpl13**	Mus musculus mitochondrial ribosomal protein L13 (Mrpl13), mRNA.	0	1.559
ILMN_2473620	**Rsn**		0	1.558
ILMN_2764205	**Tor1a**	Mus musculus torsin family 1, member A (torsin A) (Tor1a), mRNA.	0	1.557
ILMN_2644920	**Plekhf1**	Mus musculus pleckstrin homology domain containing, family F (with FYVE domain) member 1 (Plekhf1), mRNA.	0	1.556
ILMN_2489314	**2500002G23Rik**		0	1.555
ILMN_3134632	**Adam22**	Mus musculus a disintegrin and metallopeptidase domain 22 (Adam22), transcript variant 1, mRNA.	0	1.553
ILMN_2448651	**Ampd3**	Mus musculus adenosine monophosphate deaminase 3 (Ampd3), mRNA.	0	1.551
ILMN_2762326	**Kif22**	Mus musculus kinesin family member 22 (Kif22), mRNA.	0	1.551
ILMN_1250036	**Tmem201**	Mus musculus transmembrane protein 201 (Tmem201), transcript variant 1, mRNA.	0	1.549
ILMN_3162452	**Ppm2c**	Mus musculus protein phosphatase 2C, magnesium dependent, catalytic subunit (Ppm2c), nuclear gene encoding mitochondrial protein, transcript variant 1, mRNA.	0	1.548
ILMN_2819530	**D15Ertd682e**	Mus musculus DNA segment, Chr 15, ERATO Doi 682, expressed (D15Ertd682e), mRNA.	0	1.548
ILMN_2547078	**Zc3h13**	Mus musculus zinc finger CCCH type containing 13 (Zc3h13), mRNA.	0.00001	1.547
ILMN_2845839	**1700065O13Rik**	Mus musculus RIKEN cDNA 1700065O13 gene (1700065O13Rik), mRNA.	0.00053	1.547
ILMN_3156010	**Pdzrn3**	Mus musculus PDZ domain containing RING finger 3 (Pdzrn3), mRNA.	0	1.545
ILMN_1254927	**Ly6c1**	Mus musculus lymphocyte antigen 6 complex, locus C1 (Ly6c1), mRNA.	0	1.544
ILMN_3023230	**Jmjd3**	Mus musculus jumonji domain containing 3 (Jmjd3), mRNA.	0	1.544
ILMN_2631098	**Msh6**	Mus musculus mutS homolog 6 (E. coli) (Msh6), mRNA.	0	1.543
ILMN_2861176	**Calr**	Mus musculus calreticulin (Calr), mRNA.	0	1.542
ILMN_1224768	**Ehd4**	Mus musculus EH-domain containing 4 (Ehd4), mRNA.	0	1.542

ILMN_2496817	**Ulk2**	Mus musculus Unc-51 like kinase 2 (C. elegans) (Ulk2), mRNA.	0	1.539
ILMN_1222872	**Wbscr16**	Mus musculus Williams-Beuren syndrome chromosome region 16 homolog (human) (Wbscr16), mRNA.	0	1.539
ILMN_2631192	**Vps26b**	Mus musculus vacuolar protein sorting 26 homolog B (yeast) (Vps26b), mRNA.	0	1.539
ILMN_1222356	**1110067D22Rik**	Mus musculus RIKEN cDNA 1110067D22 gene (1110067D22Rik), mRNA.	0	1.538
ILMN_1243564	**Plekha1**	Mus musculus pleckstrin homology domain containing, family A (phosphoinositide binding specific) member 1 (Plekha1), mRNA.	0	1.538
ILMN_2455637	**Top1mt**	Mus musculus DNA topoisomerase 1, mitochondrial (Top1mt), nuclear gene encoding mitochondrial protein, mRNA.	0	1.538
ILMN_2709681	**Hdlbp**	Mus musculus high density lipoprotein (HDL) binding protein (Hdlbp), mRNA.	0	1.537
ILMN_1238179	**Ipmk**	Mus musculus inositol polyphosphate multikinase (Ipmk), mRNA.	0	1.537
ILMN_2422333	**Trap1**	Mus musculus TNF receptor-associated protein 1 (Trap1), mRNA.	0.00029	1.537
ILMN_2971721	**2410025L10Rik**	Mus musculus RIKEN cDNA 2410025L10 gene (2410025L10Rik), mRNA.	0	1.535
ILMN_1216116	**Smarcd2**	Mus musculus SWI/SNF related, matrix associated, actin dependent regulator of chromatin, subfamily d, member 2 (Smarcd2), mRNA.	0	1.533
ILMN_3051252	**BC026590**	Mus musculus cDNA sequence BC026590 (BC026590), mRNA.	0	1.533
ILMN_1233283	**P2rx5**	Mus musculus purinergic receptor P2X, ligand-gated ion channel, 5 (P2rx5), mRNA.	0	1.533
ILMN_1217144	**Tbc1d5**	Mus musculus TBC1 domain family, member 5 (Tbc1d5), mRNA.	0	1.532
ILMN_2599412	**Kti12**	Mus musculus KTI12 homolog, chromatin associated (S. cerevisiae) (Kti12), mRNA.	0	1.531
ILMN_2933399	**Ppp1r10**	Mus musculus protein phosphatase 1, regulatory subunit 10 (Ppp1r10), mRNA.	0	1.53
ILMN_1228501	**Tob2**	Mus musculus transducer of ERBB2, 2 (Tob2), mRNA.	0	1.526
ILMN_2497581	**Uhrf1**	Mus musculus ubiquitin-like, containing PHD and RING finger domains, 1 (Uhrf1), mRNA.	0.0001	1.526
ILMN_2439341	**Vars**	Mus musculus valyl-tRNA synthetase (Vars), nuclear gene encoding mitochondrial protein, mRNA.	0	1.526
ILMN_2647885	**Bcl2l1**	Mus musculus BCL2-like 1 (Bcl2l1), nuclear gene encoding mitochondrial protein, mRNA.	0.00001	1.524
ILMN_1243179	**Sec24d**	Mus musculus Sec24 related gene family, member D (S. cerevisiae) (Sec24d), mRNA.	0	1.523
ILMN_1234112	**Tomm70a**	Mus musculus translocase of outer mitochondrial membrane 70 homolog A (yeast) (Tomm70a), mRNA.	0	1.523
ILMN_1214918	**LOC546015**	PREDICTED: Mus musculus similar to ribosomal protein S9 (LOC546015), misc RNA.	0	1.522
ILMN_2678714	**Id4**	Mus musculus inhibitor of DNA binding 4 (Id4), mRNA.	0.00015	1.52
ILMN_2443831	**Uba1**	Mus musculus ubiquitin-like modifier activating enzyme 1 (Uba1), mRNA.	0.00003	1.519
ILMN_1252450	**LOC380707**		0	1.519
ILMN_2727309	**LOC100044204**	PREDICTED: Mus musculus hypothetical protein LOC100044204 (LOC100044204), mRNA.	0.00017	1.515

ILMN_2677567	**Galt**	Mus musculus galactose-1-phosphate uridyl transferase (Galt), mRNA.	0	1.514
ILMN_2599018	**Clic4**	Mus musculus chloride intracellular channel 4 (mitochondrial) (Clic4), nuclear gene encoding mitochondrial protein, mRNA.	0	1.513
ILMN_2820379	**Rnf135**	Mus musculus ring finger protein 135 (Rnf135), mRNA.	0	1.511
ILMN_1249269	**5830457O10Rik**	Mus musculus RIKEN cDNA 5830457O10 gene (5830457O10Rik), mRNA.	0	1.511
ILMN_2985111	**Chfr**	Mus musculus checkpoint with forkhead and ring finger domains (Chfr), mRNA.	0	1.51
ILMN_1243679	**Cep55**	Mus musculus centrosomal protein 55 (Cep55), mRNA.	0.00004	1.51
ILMN_2746328	**BC003993**	Mus musculus cDNA sequence BC003993 (BC003993), mRNA.	0.00044	1.509
ILMN_2789239	**Tgfbr3**	Mus musculus transforming growth factor, beta receptor III (Tgfbr3), mRNA.	0	1.509
ILMN_2773862	**C730025P13Rik**	Mus musculus RIKEN cDNA C730025P13 gene (C730025P13Rik), mRNA.	0	1.509
ILMN_2794686	**Fam152b**	Mus musculus family with sequence similarity 152, member B (Fam152b), mRNA.	0	1.509
ILMN_2761169	**3110050N22Rik**		0.00048	1.508
ILMN_2589181	**Eef2**	Mus musculus eukaryotic translation elongation factor 2 (Eef2), mRNA.	0	1.508
ILMN_2515982	**Ugt1a6b**	Mus musculus UDP glucuronosyltransferase 1 family, polypeptide A6B (Ugt1a6b), mRNA.	0	1.508
ILMN_1225363	**E430025E21Rik**	Mus musculus RIKEN cDNA E430025E21 gene (E430025E21Rik), mRNA.	0	1.507
ILMN_2695150	**Smc5l1**		0.00235	1.505
ILMN_1223015	**Dedd2**	Mus musculus death effector domain-containing DNA binding protein 2 (Dedd2), mRNA.	0	1.504
ILMN_2678019	**Psmd8**	Mus musculus proteasome (prosome, macropain) 26S subunit, non-ATPase, 8 (Psmd8), mRNA. XM_001002011	0	1.504
ILMN_1257117	**Nol14**	Mus musculus nucleolar protein 14 (Nol14), mRNA.	0	1.504
ILMN_2773540	**Thap4**	Mus musculus THAP domain containing 4 (Thap4), mRNA.	0	1.501
ILMN_2724469	**4732473B16Rik**	Mus musculus RIKEN cDNA 4732473B16 gene (4732473B16Rik), mRNA.	0.0001	1.501
ILMN_2480463	**Trim25**	Mus musculus tripartite motif-containing 25 (Trim25), mRNA.	0	1.5

Supplemental Table 4.6. Complete list of genes downregulated by 4h of T_3 plus CORT treatment in HT-22 cells.

PROBE ID	SYMBOL	DEFINITION	P value	Fold change
ILMN_2754985	**Phlda1**	Mus musculus pleckstrin homology-like domain, family A, member 1 (Phlda1), mRNA.	0	-2.883
ILMN_2835117	**Ccl7**	Mus musculus chemokine (C-C motif) ligand 7 (Ccl7), mRNA.	0	-2.716
ILMN_2771176	**Ccl7**		0	-2.687
ILMN_1229745	**Sertad4**	Mus musculus SERTA domain containing 4 (Sertad4), mRNA.	0	-2.673
ILMN_2660233	**Ngfb**	Mus musculus nerve growth factor, beta (Ngfb), mRNA.	0	-2.653
ILMN_2937596	**Ngfb**	Mus musculus nerve growth factor, beta (Ngfb), mRNA.	0	-2.427
ILMN_1251193	**A630084D02 Rik**		0	-2.259
ILMN_1253178	**Aldh3a1**	Mus musculus aldehyde dehydrogenase family 3, subfamily A1 (Aldh3a1), mRNA.	0	-2.244
ILMN_2662926	**Egr1**	Mus musculus early growth response 1 (Egr1), mRNA.	0	-2.137
ILMN_2833706	**Fgf7**	Mus musculus fibroblast growth factor 7 (Fgf7), mRNA.	0	-2.124
ILMN_2778655	**Vcam1**	Mus musculus vascular cell adhesion molecule 1 (Vcam1), mRNA.	0	-2.122
ILMN_2759365	**Angptl4**	Mus musculus angiopoietin-like 4 (Angptl4), mRNA.	0	-2.099
ILMN_2752569	**Paip1**	Mus musculus polyadenylate binding protein-interacting protein 1 (Paip1), transcript variant 1, mRNA.	0	-2.068
ILMN_2794645	**Cyr61**	Mus musculus cysteine rich protein 61 (Cyr61), mRNA.	0.00002	-2.044
ILMN_2479290	**Fas**	Mus musculus Fas (TNF receptor superfamily member 6) (Fas), mRNA.	0	-2.014
ILMN_2959272	**Rnu6**	Mus musculus U6 small nuclear RNA (Rnu6), non-coding RNA.	0	-2.011
ILMN_1245710	**Ccl2**	Mus musculus chemokine (C-C motif) ligand 2 (Ccl2), mRNA.	0	-2.003
ILMN_2606210	**Dpt**	Mus musculus dermatopontin (Dpt), mRNA.	0	-2.002
ILMN_2483786	**1110004P21 Rik**		0.00001	-1.993
ILMN_2695412	**AI451617**	Mus musculus expressed sequence AI451617 (AI451617), mRNA.	0	-1.974
ILMN_2710253	**Cyr61**	Mus musculus cysteine rich protein 61 (Cyr61), mRNA.	0	-1.94
ILMN_2776603	**Ccl9**	Mus musculus chemokine (C-C motif) ligand 9 (Ccl9), mRNA.	0	-1.898
ILMN_2902979	**Fas**	Mus musculus Fas (TNF receptor superfamily member 6) (Fas), mRNA.	0	-1.89
ILMN_2996648	**Prl2c4**	Mus musculus prolactin family 2, subfamily c, member 4 (Prl2c4), mRNA.	0	-1.823
ILMN_2623793	**Zfhx3**	Mus musculus zinc finger homeobox 3 (Zfhx3), mRNA.	0	-1.821
ILMN_1255925	**Col8a1**		0	-1.813
ILMN_2741096	**Timp3**	Mus musculus tissue inhibitor of metalloproteinase 3 (Timp3), mRNA.	0	-1.791
ILMN_2506727	**9430052C07 Rik**		0	-1.783
ILMN_2511089	**Ugcg**		0	-1.776
ILMN_2875585	**Prl2c3**	Mus musculus prolactin family 2, subfamily c, member 3 (Prl2c3), mRNA.	0	-1.756

ILMN_2840091	**Ugcg**	Mus musculus UDP-glucose ceramide glucosyltransferase (Ugcg), mRNA.	0	-1.746
ILMN_2416218	**5530400B01 Rik**		0	-1.736
ILMN_2625451	**Ankrd1**	Mus musculus ankyrin repeat domain 1 (cardiac muscle) (Ankrd1), mRNA.	0	-1.736
ILMN_1232716	**Cyp1b1**	Mus musculus cytochrome P450, family 1, subfamily b, polypeptide 1 (Cyp1b1), mRNA.	0	-1.735
ILMN_2683593	**Fubp1**		0	-1.731
ILMN_2734755	**Col4a5**		0	-1.724
ILMN_2937136	**Tceal1**	Mus musculus transcription elongation factor A (SII)-like 1 (Tceal1), mRNA.	0	-1.72
ILMN_1240346	**Socs5**	Mus musculus suppressor of cytokine signaling 5 (Socs5), mRNA.	0	-1.71
ILMN_1230278	**LOC100044702**	PREDICTED: Mus musculus similar to LPS-induced CXC chemokine (LOC100044702), mRNA.	0.00038	-1.705
ILMN_2451115	**1500001E21 Rik**		0.00002	-1.689
ILMN_2479681	**Mex3a**	Mus musculus mex3 homolog A (C. elegans) (Mex3a), mRNA.	0	-1.682
ILMN_2434853	**mtDNA_ND2**		0	-1.68
ILMN_1217489	**LOC671878**	PREDICTED: Mus musculus similar to spermine synthase (LOC671878), mRNA.	0	-1.678
ILMN_1259982	**LOC100046616**	PREDICTED: Mus musculus similar to aquaporin 5 (LOC100046616), mRNA.	0	-1.677
ILMN_2672528	**Pabpn1**	Mus musculus poly(A) binding protein, nuclear 1 (Pabpn1), mRNA.	0	-1.67
ILMN_1220813	**Dtx3l**	Mus musculus deltex 3-like (Drosophila) (Dtx3l), mRNA.	0	-1.661
ILMN_3115472	**Aqp5**	Mus musculus aquaporin 5 (Aqp5), mRNA.	0	-1.659
ILMN_1222584	**Sfrs11**	Mus musculus splicing factor, arginine/serine-rich 11 (Sfrs11), transcript variant 1, mRNA.	0	-1.658
ILMN_1252479	**LOC100041567**	PREDICTED: Mus musculus similar to p47 protein (LOC100041567), mRNA.	0	-1.656
ILMN_3158725	**Raet1b**	Mus musculus retinoic acid early transcript beta (Raet1b), mRNA.	0	-1.655
ILMN_2763245	**Cxcl1**	Mus musculus chemokine (C-X-C motif) ligand 1 (Cxcl1), mRNA.	0	-1.654
ILMN_2657911	**Cnot4**	Mus musculus CCR4-NOT transcription complex, subunit 4 (Cnot4), mRNA.	0	-1.652
ILMN_2816180	**Lbh**	Mus musculus limb-bud and heart (Lbh), mRNA.	0	-1.649
ILMN_2550570	**Fibp**		0.00365	-1.647
ILMN_2868220	**Inhba**	Mus musculus inhibin beta-A (Inhba), mRNA.	0	-1.647
ILMN_2742599	**Nfix**	Mus musculus nuclear factor I/X (Nfix), transcript variant 2, mRNA. XM_921228 XM_921240 XM_921250 XM_921261 XM_921270 XM_921288 XM_921293 XM_921299 XM_921300 XM_921307	0	-1.644
ILMN_2806159	**Tmsb4x**	Mus musculus thymosin, beta 4, X chromosome (Tmsb4x), mRNA.	0	-1.64
ILMN_2557387	**E430005I09Rik**		0	-1.64
ILMN_3122961	**Gbp2**	Mus musculus guanylate binding protein 2 (Gbp2), mRNA.	0	-1.638
ILMN_2474666	**4933411D12 Rik**		0.00001	-1.635

ILMN_3007428	**Sox9**	Mus musculus SRY-box containing gene 9 (Sox9), mRNA.	0	-1.635
ILMN_2507810	**mtDNA_ND5**		0	-1.635
ILMN_1212848	**Rybp**	Mus musculus RING1 and YY1 binding protein (Rybp), mRNA.	0	-1.631
ILMN_1240420	**Arid1b**	Mus musculus AT rich interactive domain 1B (SWI-like) (Arid1b), mRNA.	0	-1.628
ILMN_2551741	**0610010I05Rik**		0	-1.626
ILMN_2775937	**Plat**		0	-1.624
ILMN_2617996	**Prl2c2**	Mus musculus prolactin family 2, subfamily c, member 2 (Prl2c2), mRNA.	0.00003	-1.624
ILMN_2640862	**Lrig1**	Mus musculus leucine-rich repeats and immunoglobulin-like domains 1 (Lrig1), mRNA.	0	-1.622
ILMN_1232741	**Fdps**		0.00235	-1.621
ILMN_1236123	**Tomm6**	Mus musculus translocase of outer mitochondrial membrane 6 homolog (yeast) (Tomm6), nuclear gene encoding mitochondrial protein, mRNA.	0	-1.62
ILMN_2972478	**Nlgn2**	Mus musculus neuroligin 2 (Nlgn2), mRNA.	0	-1.62
ILMN_2643241	**Accn2**	Mus musculus amiloride-sensitive cation channel 2, neuronal (Accn2), mRNA.	0	-1.62
ILMN_2696592	**C77080**		0	-1.619
ILMN_2848463	**Mthfsd**	Mus musculus methenyltetrahydrofolate synthetase domain containing (Mthfsd), mRNA.	0.00004	-1.619
ILMN_1230152	**Adamts4**		0	-1.618
ILMN_1250075	**Dpysl3**	Mus musculus dihydropyrimidinase-like 3 (Dpysl3), mRNA.	0	-1.618
ILMN_1259905	**Sfrs11**	Mus musculus splicing factor, arginine/serine-rich 11 (Sfrs11), transcript variant 1, mRNA.	0	-1.615
ILMN_2726371	**Nqo1**	Mus musculus NAD(P)H dehydrogenase, quinone 1 (Nqo1), mRNA.	0	-1.605
ILMN_2965660	**Apcdd1**	Mus musculus adenomatosis polyposis coli down-regulated 1 (Apcdd1), mRNA.	0	-1.601
ILMN_2653207	**Tead2**	Mus musculus TEA domain family member 2 (Tead2), mRNA.	0	-1.6
ILMN_1222565	**A930002H24Rik**	PREDICTED: Mus musculus RIKEN cDNA A930002H24 gene (A930002H24Rik), mRNA.	0	-1.599
ILMN_2760979	**Tgfbr2**	Mus musculus transforming growth factor, beta receptor II (Tgfbr2), transcript variant 1, mRNA.	0	-1.597
ILMN_2684563	**Cldnd1**	Mus musculus claudin domain containing 1 (Cldnd1), mRNA.	0	-1.597
ILMN_1216381	**Nfic**	Mus musculus nuclear factor I/C (Nfic), transcript variant 2, mRNA.	0	-1.596
ILMN_2841720	**Ttc3**	Mus musculus tetratricopeptide repeat domain 3 (Ttc3), mRNA.	0	-1.591
ILMN_2623776	**Eps8**	Mus musculus epidermal growth factor receptor pathway substrate 8 (Eps8), mRNA.	0	-1.59
ILMN_2726837	**Nppb**	Mus musculus natriuretic peptide precursor type B (Nppb), mRNA.	0	-1.589
ILMN_1228031	**Dusp8**	Mus musculus dual specificity phosphatase 8 (Dusp8), mRNA.	0	-1.588
ILMN_1213376	**Cfl1**	Mus musculus cofilin 1, non-muscle (Cfl1), mRNA.	0	-1.586
ILMN_1255731	**Dnm3os**	Mus musculus dynamin 3, opposite strand (Dnm3os), non-coding RNA.	0	-1.584
ILMN_1257107	**LOC1000438**	PREDICTED: Mus musculus hypothetical protein	0	-1.583

	21	LOC100043821 (LOC100043821), mRNA.		
ILMN_3163340	**Rbm45**	Mus musculus RNA binding motif protein 45 (Rbm45), mRNA.	0	-1.582
ILMN_1213322	**Chd2**	Mus musculus chromodomain helicase DNA binding protein 2 (Chd2), mRNA.	0	-1.58
ILMN_3131887	**Spag9**	Mus musculus sperm associated antigen 9 (Spag9), transcript variant 4, mRNA.	0	-1.573
ILMN_1244343	**B230369L08 Rik**		0	-1.572
ILMN_2819841	**Rpl7a**	Mus musculus ribosomal protein L7a (Rpl7a), mRNA.	0	-1.57
ILMN_1229193	**Msn**		0	-1.569
ILMN_2495703	**Clip2**	Mus musculus CAP-GLY domain containing linker protein 2 (Clip2), transcript variant 2, mRNA.	0	-1.568
ILMN_1238838	**LOC100045005**	PREDICTED: Mus musculus similar to Deltex3 (LOC100045005), misc RNA.	0	-1.568
ILMN_1234412	**LOC674427**	PREDICTED: Mus musculus similar to ribosomal protein L7a (LOC674427), misc RNA.	0	-1.566
ILMN_2942989	**Mtpn**	Mus musculus myotrophin (Mtpn), mRNA.	0	-1.566
ILMN_2828916	**Frmd6**	Mus musculus FERM domain containing 6 (Frmd6), mRNA.	0	-1.564
ILMN_1246841	**Relb**	Mus musculus avian reticuloendotheliosis viral (v-rel) oncogene related B (Relb), mRNA.	0	-1.562
ILMN_1239921	**Man1b1**	Mus musculus mannosidase, alpha, class 1B, member 1 (Man1b1), mRNA.	0	-1.557
ILMN_2617265	**Ipo13**	Mus musculus importin 13 (Ipo13), mRNA.	0	-1.555
ILMN_2710354	**Acta2**	Mus musculus actin, alpha 2, smooth muscle, aorta (Acta2), mRNA.	0	-1.553
ILMN_2757870	**Psmb10**	Mus musculus proteasome (prosome, macropain) subunit, beta type 10 (Psmb10), mRNA.	0	-1.55
ILMN_2642913	**Emp1**	Mus musculus epithelial membrane protein 1 (Emp1), mRNA.	0	-1.55
ILMN_1219807	**Hoxd4**	Mus musculus homeo box D4 (Hoxd4), mRNA.	0.00081	-1.548
ILMN_1223697	**Cd44**	Mus musculus CD44 antigen (Cd44), transcript variant 2, mRNA.	0	-1.545
ILMN_1227131	**Ehbp1l1**	Mus musculus EH domain binding protein 1-like 1 (Ehbp1l1), mRNA.	0	-1.545
ILMN_2747381	**Ddx24**	Mus musculus DEAD (Asp-Glu-Ala-Asp) box polypeptide 24 (Ddx24), mRNA.	0	-1.542
ILMN_1235173	**LOC386218**		0	-1.54
ILMN_1213200	**Med16**	Mus musculus mediator complex subunit 16 (Med16), mRNA.	0	-1.538
ILMN_1225835	**Mfap5**	Mus musculus microfibrillar associated protein 5 (Mfap5), mRNA.	0	-1.535
ILMN_3153753	**Cacnb3**	Mus musculus calcium channel, voltage-dependent, beta 3 subunit (Cacnb3), transcript variant 1, mRNA.	0	-1.534
ILMN_2449019	**Tnk2**	Mus musculus tyrosine kinase, non-receptor, 2 (Tnk2), mRNA.	0	-1.533
ILMN_3160416	**2900024O10 Rik**	Mus musculus RIKEN cDNA 2900024O10 gene (2900024O10Rik), mRNA.	0	-1.53
ILMN_2758073	**Dmtf1**	Mus musculus cyclin D binding myb-like transcription factor 1 (Dmtf1), mRNA.	0	-1.53
ILMN_2625351	**Sh3bgrl3**	Mus musculus SH3 domain binding glutamic acid-rich protein-like 3 (Sh3bgrl3), mRNA.	0	-1.529
ILMN_2440530	**Vat1**	Mus musculus vesicle amine transport protein 1 homolog (T californica) (Vat1), mRNA.	0	-1.526

ILMN_2760254	**Mrgprf**	Mus musculus MAS-related GPR, member F (Mrgprf), mRNA.	0	-1.526
ILMN_1216764	**Ier3**	Mus musculus immediate early response 3 (Ier3), mRNA.	0	-1.526
ILMN_1249547	**Zfp292**	PREDICTED: Mus musculus zinc finger protein 292, transcript variant 4 (Zfp292), mRNA.	0	-1.525
ILMN_3161105	**Ahnak2**	Mus musculus AHNAK nucleoprotein 2 (Ahnak2), mRNA.	0	-1.524
ILMN_2656422	**BC028528**	Mus musculus cDNA sequence BC028528 (BC028528), mRNA.	0	-1.523
ILMN_1238535	**4832420L08 Rik**		0.00001	-1.523
ILMN_2974720	**Igf2bp2**	Mus musculus insulin-like growth factor 2 mRNA binding protein 2 (Igf2bp2), mRNA.	0	-1.523
ILMN_2629601	**Slc4a7**		0	-1.521
ILMN_2937735	**Irak2**	Mus musculus interleukin-1 receptor-associated kinase 2 (Irak2), mRNA.	0	-1.521
ILMN_2520249	**Hspg2**		0	-1.52
ILMN_1246153	**Erdr1**	Mus musculus erythroid differentiation regulator 1 (Erdr1), mRNA.	0.01773	-1.52
ILMN_2441921	**Trim56**	Mus musculus tripartite motif-containing 56 (Trim56), mRNA.	0	-1.52
ILMN_1259610	**Cd276**	Mus musculus CD276 antigen (Cd276), mRNA.	0	-1.519
ILMN_2768053	**Supt16h**	Mus musculus suppressor of Ty 16 homolog (S. cerevisiae) (Supt16h), mRNA.	0.0001	-1.518
ILMN_1252222	**Hectd2**	Mus musculus HECT domain containing 2 (Hectd2), mRNA.	0	-1.518
ILMN_2424299	**Tnfrsf12a**	Mus musculus tumor necrosis factor receptor superfamily, member 12a (Tnfrsf12a), mRNA.	0	-1.517
ILMN_1235732	**Cdsn**	Mus musculus corneodesmosin (Cdsn), mRNA.	0	-1.514
ILMN_1247823	**Lrp8**	Mus musculus low density lipoprotein receptor-related protein 8, apolipoprotein e receptor (Lrp8), transcript variant 2, mRNA.	0	-1.514
ILMN_2825803	**Parp14**	Mus musculus poly (ADP-ribose) polymerase family, member 14 (Parp14), mRNA. XM_901644 XM_916789 XM_924484 XM_924488	0	-1.513
ILMN_2658815	**Tmem98**	Mus musculus transmembrane protein 98 (Tmem98), mRNA.	0	-1.513
ILMN_1228441	**C230043G09 Rik**		0	-1.51
ILMN_1229547	**Spon2**	Mus musculus spondin 2, extracellular matrix protein (Spon2), mRNA.	0	-1.507
ILMN_2778151	**Sox9**		0	-1.506
ILMN_1225373	**C1qbp**	Mus musculus complement component 1, q subcomponent binding protein (C1qbp), nuclear gene encoding mitochondrial protein, mRNA.	0	-1.505
ILMN_2737867	**Mtap1b**	Mus musculus microtubule-associated protein 1 B (Mtap1b), mRNA.	0	-1.505
ILMN_2689307	**Spnb2**	Mus musculus spectrin beta 2 (Spnb2), transcript variant 2, mRNA.	0	-1.504
ILMN_2731057	**Psme2**	Mus musculus proteasome (prosome, macropain) 28 subunit, beta (Psme2), transcript variant 1, mRNA.	0	-1.504
ILMN_1259967	**Prl2c2**	Mus musculus prolactin family 2, subfamily c, member 2 (Prl2c2), mRNA.	0.00309	-1.502

Supplemental Table 4.7. T_3 regulated genes that are found in the thyroid hormone and thyroid hormone receptor interaction pathway generated by the Ingenuity knowledge base (Illimuna)

PROBE ID	SYMBOL	DEFINITION	P value	Fold change
ILMN_2654822	**Chd4**	Mus musculus chromodomain helicase DNA binding protein 4 (Chd4), mRNA.	0.0072	-1.49
ILMN_1259322	**Pdk4**	Mus musculus pyruvate dehydrogenase kinase, isoenzyme 4 (Pdk4), mRNA.	0	-1.31
ILMN_1233064	**Cdk2**	Mus musculus cyclin-dependent kinase 2 (Cdk2), transcript variant 1, mRNA.	0.00158	-1.29
ILMN_2819841	**Rpl7a**	Mus musculus ribosomal protein L7a (Rpl7a), mRNA.	0	-1.29
ILMN_1231686	**Kat2b**	Mus musculus K(lysine) acetyltransferase 2B (Kat2b), mRNA.	0.00415	-1.25
ILMN_2846775	**Cdkn1a**	Mus musculus cyclin-dependent kinase inhibitor 1A (P21) (Cdkn1a), mRNA.	0.00161	-1.24
ILMN_1241890	**Klf7**		0.00267	1.25
ILMN_2791272	**Por**	Mus musculus P450 (cytochrome) oxidoreductase (Por), mRNA.	0.00043	1.26
ILMN_2976191	**Stat5a**	Mus musculus signal transducer and activator of transcription 5A (Stat5a), mRNA.	0.00005	1.34
ILMN_1254031	**Klf9**	Mus musculus Kruppel-like factor 9 (Klf9), mRNA.	0	3.09

Supplemental Table 4.8. CORT regulated genes that are found in the glucocorticoid and glucocorticoid receptor interaction pathway generated by the Ingenuity knowledge base (Illimuna).

PROBE ID	SYMBOL	DEFINITION	Pvalue	Fold change
ILMN_2937596	**Ngfb**	Mus musculus nerve growth factor, beta (Ngfb), mRNA.	0	-2.36
ILMN_1253178	**Aldh3a1**	Mus musculus aldehyde dehydrogenase family 3, subfamily A1 (Aldh3a1), mRNA.	0	-2.01
ILMN_2840091	**Ugcg**	Mus musculus UDP-glucose ceramide glucosyltransferase (Ugcg), mRNA.	0	-1.72
ILMN_2479290	**Fas**	Mus musculus Fas (TNF receptor superfamily member 6) (Fas), mRNA.	0	-1.71
ILMN_3122961	**Gbp2**	Mus musculus guanylate binding protein 2 (Gbp2), mRNA.	0	-1.62
ILMN_2993334	**Plekhf1**	Mus musculus pleckstrin homology domain containing, family F (with FYVE domain) member 1 (Plekhf1), mRNA.	0	1.65
ILMN_2764143	**Scap**	Mus musculus SREBF chaperone (Scap), mRNA.	0	1.67
ILMN_1241610	**Adrb2**	Mus musculus adrenergic receptor, beta 2 (Adrb2), mRNA.	0	1.71
ILMN_1228919	**St13**	Mus musculus suppression of tumorigenicity 13 (St13), mRNA.	0	1.74
ILMN_2737713	**Edn1**	Mus musculus endothelin 1 (Edn1), mRNA.	0	1.86
ILMN_1213954	**Sgk1**	Mus musculus serum/glucocorticoid regulated kinase 1 (Sgk1), mRNA.	0	1.92
ILMN_2733887	**Mknk2**	Mus musculus MAP kinase-interacting serine/threonine kinase 2 (Mknk2), mRNA.	0	2.18
ILMN_2718266	**Fkbp5**	Mus musculus FK506 binding protein 5 (Fkbp5), mRNA.	0	2.67
ILMN_2622983	**Dusp1**	Mus musculus dual specificity phosphatase 1 (Dusp1), mRNA.	0	3.02
ILMN_2987863	**Per2**	Mus musculus period homolog 2 (Drosophila) (Per2), mRNA.	0	3.03
ILMN_2813487	**Per1**	Mus musculus period homolog 1 (Drosophila) (Per1), mRNA.	0	3.06
ILMN_1219154	**Mt2**	Mus musculus metallothionein 2 (Mt2), mRNA.	0	3.4
ILMN_1226935	**Orm1**	Mus musculus orosomucoid 1 (Orm1), mRNA.	0	3.44

APPENDIX D

Supplemental Table 5.1. The *X. laevis Tr*βA promoter divided into seven segments for analysis, and location of GC-rich sequences.

A) -1138/-823 Three GC boxes (-1029/-1024; -1020/-1015; -973/-968)

C agtggagtaactaccaggggagcaggggtgcgattgggccagggcctgcaccccgtcagggcctcgcgcgccattgacttctttgtaattct
gggcgtacggaggggGGCGGGgggCCCGCCctcctctagttacgttactgtctgcctaggttgcaaagataGGCGGGgggg
tggtgctgtgcaggtacttaacatttgtctgcctacccctagtctatgctctcttgctcctgctgcct
ctttcctcagttgtgcctgcttgcttgctaccccgtgcacacaacatcatacagtagtgcaggcatgtgtacc

B) -841/-604 Two GC boxes (-767/-762; -720/-715)

tagtgcaggcatgtgtacccacagggggaggtgaggtggccggccggtttgcctagggtgccaggtcagcttggCCCGCCtattatagttt
agaaagtgggccctcagcctaaggttttctGGCGGGgccctgttatcccagtctgacactgccgacctcg
aactcttcttcgcgggtggcgtcaaatgccggcttctgacttctgggttcgtcttttatagatgctgcacctgctcg

C) -622/-414 One GC box (-538/-533)

Tagatgctgcacctgctcgccccatccctttgtgacttcatcagcggcacaggtctataaaagcaacctggcagtcggatgcg
GGCGGGcgcgggctaaggtaagcccgggttagggtcggggaaataccaacctgcacatcactaccggactggcaatct
gtgggttctggcatatgccagagaggctgctgtaacatgccatagtc

D) -432/-266 No GC box

gctgtaacatgccatagtcattatttagtgggctggtggggagctgagtgggtccttgtgtacttggaatgccagggcctattttga
atcccagtccagacctgcagacacacacaaacccccaatcctgcaactgccccacagcccttatgggtcttcactcaggc

E) -283/-92 No GC box

atgggtcttcactcaggctcttattttcctgcagattctgtttagttgttactgaataagccctgctgcttccaagctgcactctccctgtgtgactgaaga
ggcgcaggctggctgagttaatatagtgaataaagtacccccctcttgtaaaatataaggatattataagttaccga
ggagtttcatgacc

F) -109/+182 No GC box

ccgaggagtttcatgaccatataaaaacacgaggccgaaggccgagtgtttttatacaggtcatggaactccgaggtaact
tctaatatcctcgtattttacaactggg**G**gtactttattaattataatacacacatttcagtgagtcatgtgacagaaattacatcactactcaccgtttata
actgatgacatcactactcaccgtttataaggatataatttacaggatattcatggcttttgtgtattatatatatgtatgtatacagtaagctgcctgtgtct
ata

G) +164/+366 One GC box (+231/+236)

taagctgcctgtgtctatactgatgggatgggaagcagaggctgcccgacccctcctcttgattctccCCGCCCcccctatccttgttcgtcct
ccctaggc**aggtca**tttc**aggaca**gcccagcgccctggtgcacgatcagctgtagatctccctgtctgtgtcgctgctgccgctgctacttcagttc
ctctgactgtcag

GC boxes are indicated in boldtype capitals. TRE half sites are boldtype lowercase underlined. The transcription start site is the capital, boldtype, shaded 'G' in fragment F (based on 58). Genbank Accession # U04675.